# Development of the Human Fovea after Preterm Birth measured using Hand Held Spectral Domain Optical Coherence Tomography (HH SD-OCT)

Thesis submitted for the degree of

Doctor of Philosophy

at

The University of Leicester

by

**S Anwar MSc., FRCOphth.**

Ulverscroft Eye Unit

Department of Neuroscience, Psychology and Behaviour

University of Leicester

December 2019

# Abstract

Development of the Human Fovea after Preterm Birth measured using Hand Held Spectral Domain Optical Coherence Tomography (HH SD-OCT).

Author: S Anwar

## Background

Much remains unknown about the influence of severity of prematurity and presence of retinopathy of prematurity (ROP) on the development of the fovea after preterm birth during the perinatal period from postmenstrual age (PMA) 30 to 44 weeks.

## Aims

Measures of foveal morphology, individual retinal layers and foveal oedema (CME), with and without ROP using HH-OCT, adjusting for gestational age (GA) and birthweight (BW).

## Methods

Prospective mixed cross-sectional and longitudinal study of infants (23 to 36 weeks GA). Foveal width, area, depth, central foveal thickness (CFT), individual retinal layers and CME severity were analysed. Infants with ROP were included until they underwent treatment.

## Results

HH SD-OCT images (n=344) from n= 112 infants were suitable for analysis (n=278 foveal morphology, retinal layers; n=66 CME). A significant interaction between ROP and PMA independent of GA or BW ($p<0.001$), was due to increasing foveal width with PMA for ROP and decreasing in the non-ROP group. This correlated with significantly increased outer retinal layers in early PMA ($p<0.001$).

Severity of GA and BW correlated with foveal area ($p<0.005$) and depth ($p\leq0.001$); CFT ($p=0.007$) correlated only with GA. In the perinatal period, the thicker fovea observed

in early GA compared to later born infants is due to an increased INL (p=0.005).

CME was present in 22% of all infants. CME severity may relate to presence or absence of the external limiting membrane (ELM).

## Conclusions

Dynamic differences exist between foveal parameters and retinal layers during the perinatal period depending on the severity of prematurity and presence of ROP. Independent of GA and BW, foveal width has potential as a marker that distinguishes between infants with and without ROP in early screening using HH SD-OCT. The severity of CME may relate to ELM disruption; further study would aid understanding of any adverse future outcomes.

# Contents

# Acknowledgements

Thanks are due to Professor Irene Gottlob for supervising and facilitating the opportunity to complete this research. Sincere gratitude to Dr Frank Proudlock for his support and guidance over seven years, and to Dr Mintu Nath for his unique statistical expertise and teaching. I am grateful to all the Ophthalmology Group colleagues, in particular Dr Aarti Patel, Dr Helena Lee, Miss Seema Teli and Dr Rebecca McLean.

I would like to acknowledge the Ulverscroft Foundation and the Medical Research Council for supporting this work conducted in collaboration with the Ophthalmology Group at the University of Leicester.

Many thanks also to Samantha Brown, Hima Thanki and the Staff of the Neonatal Service at the University Hospitals of Leicester NHS Trust. This work would not have been possible without the generosity of all the Parents and their beautiful babies.

I am indebted to Miss Nagini Sarvananthan, Miss Sarit Lesnik-Oberstein, Miss Teresa Sandinha and Mr Straton Tyradellis, Consultant Ophthalmologists for their patience and encouragement. I am obliged to Professor Alexander Foss and Miss Lucy Butler Consultant Ophthalmologists for the stimulating discussions concerning the retina, infants and retinopathy of prematurity.

Finally, to RSB, MA-U-H, IKA and the precious three, thank you for always making everything so straightforward *[F41:53] [A6:97].*

*Remembering Semmelweis.*

# LIST OF TABLES

# LIST OF FIGURES

| LIST OF ABBREVIATIONS | |
|---|---|
| BW | birth weight |
| CFT | central foveal thickness |
| CME | cystoid macular edema |
| CMT | central macular thickness |
| ELM | external limiting membrane |
| EM | electron microscopy |
| EZ | ellipsoid zone |
| FFA | fundus fluorescein angiography |
| GA | gestational age at birth |
| GCL | ganglion cell layer |
| HH | hand held |
| LPC | laser photocoagulation |
| ILM | inner limiting membrane |
| INL | inner nuclear layer |
| IPL | inner plexiform layer |
| IVT | intra-vitreal treatment |
| OCT | optical coherence tomography |
| OIR | oxygen induced retinopathy |
| ONL | outer nuclear layer |
| OPL | outer plexiform layer |

| | |
|---|---|
| PMA | postmenstrual age |
| PRC | photoreceptor complex |
| PRT | parafoveal retinal thickness |
| PCA | pure cone area |
| ROP | retinopathy of prematurity |
| RNFL | retinal nerve fibre layer |
| RPE | retinal pigment epithelium |
| RT | retinal thickness |
| SD-OCT | spectral domain optical coherence tomography |
| VEGF | vascular endothelial growth factor |

# Chapter 1 Introduction and Background

## 1.1 Introduction

It is estimated that globally, 285 million people are defined as visually impaired, of which 39 million people are blind (Pascolini and Mariotti 2012). Children between 0-15 years constitute around 4% (19 million) of worldwide blindness, and a leading cause of preventable childhood visual impairment is retinopathy of prematurity (ROP) (Kong et al. 2012; Blencowe et al. 2013). ROP is exclusively associated with preterm (also known as premature) birth, and the lower the gestational age (GA) and birthweight (BW), the greater the severity of ROP (Gallo et al. 1991; Gunn, Cartwright, and Gole 2012).

An estimated 11.1% of all live births worldwide are preterm (Blencowe et al. 2012), of which 5.2% are less than 28 weeks GA, and 10.4% are between 28-31 weeks GA (Blencowe et al. 2013) making this a substantial health concern. Consequently, improving early detection of sight threatening ROP during infant screening in the preterm period is a major objective in the management of ROP. An additional goal has been to determine the impact of prematurity itself on visual development.

It is known that treated and severe ROP affects visual function and ocular development (Robinson and O'Keefe 1993; O'Connor et al. 2002; Fulton et al. 2009; Wu et al. 2012; Holmstrom et al. 2014; Fielder et al. 2015; Siatkowski et al. 2013). However, premature birth is also associated with visual deficit or delay unrelated to treated or severe ROP (Sebris, V., and E. 1984; Madan, Jan, and Good 2005; Dowdeswell et al. 1995; Larsson, Rydberg, and Holmstrom 2005) even though the central retina often appears grossly normal on fundoscopy (Isenberg 1986).

The use of portable optical coherence tomography (HH-OCT) to image the central retina is increasingly being used to visualise both the effects of ROP and changes that may be associated with factors of prematurity such as GA and BW. Large prospective studies in older children and adults report conflicting results regarding the increased

central retinal thickness observed using OCT in premature individuals with visual acuity (Hellgren et al. 2016; Balasubramanian et al. 2018).

There is a paucity of information on central age-related retinal change measured with OCT and normal visual development in childhood. In the premature group, there is a lack of prospective longitudinal studies using OCT plus vision assessment, and comparison with normal visual development.

The aim of the study was to investigate central retinal development in preterm infants during the perinatal period from 30 to 44 weeks postmenstrual age (PMA), specifically at the fovea, measured using HH-OCT. The underlying purpose was to determine if the observed changes were secondary to the effect of ROP or factors associated with prematurity, namely GA, BW.

## 1.2 Background

### 1.21 Prematurity (preterm birth) and Retinopathy of Prematurity (ROP)

The International Classification of Diseases definition of 'term' delivery is between 37 weeks 0 days until 41 weeks and 6 days GA (Spong 2013). The World Health Organisation definition of preterm birth (also known as premature birth and used interchangeably from here on) is any birth before 37 weeks completed gestation (World Health Organization 1970). Subgroups of premature birth based on GA exist, including extreme preterm (less than 28 weeks), very preterm (28-32 weeks) and moderate to late preterm (32 to 37 weeks) (World Health Organization 2018).

Although prematurity is considered a continuum, there are varying GA and BW specific outcomes depending on the degree of prematurity (Raju 2013; Walsh et al. 2017). Very low birth weight (VLBW) (less than 1500 grams) (Malan AF 1975) and extreme/very preterm infants are particularly vulnerable to complications such as delayed growth and psychomotor development (Vohr et al. 2000; Lin, Lin, and Lin 2011; Pierrat et al. 2017) and ROP, a potentially treatable, sight threatening vaso-proliferative disorder of immature intra-retinal vasculature.

A decade ago it was estimated that 50,000 children worldwide suffered blindness from ROP (Gilbert 2008) and in 2010, that an estimated 184,700 preterm infants developed ROP, of which 65% were born in middle income economies such as in Latin America, South East Asia and the Middle East (Blencowe et al. 2013). More recently, almost 1 in 10 of live births globally (around 12 million infants) are reported as preterm births in high income countries and at risk of the visual complications of ROP and prematurity (Blencowe et al. 2013).

Whilst the prevalence of ROP has remained stable in the United States (Quinn et al. 2016) the survival rates of extreme preterm infants at the 'threshold of viability'

(defined by the Royal College of Obstetrics and Gynaecologists as 23 weeks + 0 days to 24 weeks + 6 days GA) (RCOG 2014) have increased. Consequently, it is expected that the incidence of severe ROP will also increase.

Additionally, in emerging economies with less regulated neonatal intensive care units, the prevalence of ROP is estimated to be up to 30% in all preterm infants (Gergely and Gerinec 2010) while ROP develops in heavier older preterm infants (Gilbert et al. 2005) reducing the usefulness of ROP screening recommendations for these countries based on GA (ETROP 2003) or emerging predictive risk algorithms based on BW (Hellstrom et al. 2009; Binenbaum G et al. 2012; Lofqvist et al. 2006). Furthermore, identifying the infants that benefit most from ROP intervention is based currently on subjective assessment of the retinal appearance and can vary between specialists (Chiang et al. 2007; Wallace et al. 2008; Slidsborg et al. 2012).

As a result, there has been a drive to investigate newer methods of assessment through imaging modalities such as fluorescein angiography (Zepeda-Romero et al. 2013; Klufas et al. 2015; Ng, Lannigan, and O'Keefe 2006), ultra-wide field imaging of the retina (Patel et al. 2013), digital colour fundus photography (Biten et al. 2018) and OCT (Maldonado et al. 2014; Chavala et al. 2009) in order to improve management and identification of preterm infants that develop treatment warranted ROP (also known as Type 1 ROP, TW-ROP). The primary objective has been to both reduce unnecessary screening, and to maximise treatment outcome from judicious intervention without missing infants that require treatment.

A number of prospective studies indicate that preterm children and adults and have reduced visual acuity in comparison to term born peers (Larsson, Rydberg, and Holmstrom 2005; Holmstrom and Larsson 2008; Hellgren et al. 2016; Balasubramanian et al. 2018). Therefore, another research area has been to describe the impact of prematurity and ROP on foveal structure in preterm individuals through visualisation of the central retina (Vinekar et al. 2011; Vajzovic et al. 2015; Lee, Kim, and Yu 2010; Park and Oh 2012).

## 1.22 Anatomical development of the fovea and retinal layers using human microscopy studies

The developed central retina contains the macula (lutea) in which lies the fovea (centralis). The fovea is an important structure for precise daytime vision in humans (Figure 1.1).

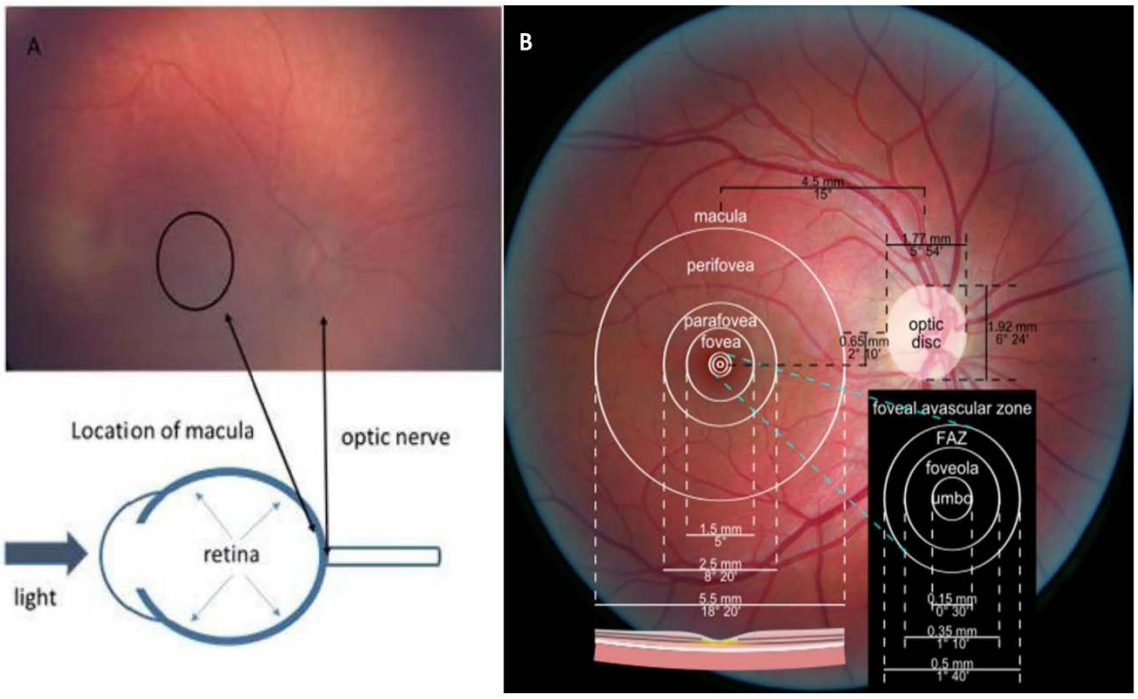


**Figure 1.1 A Colour image of the central retina with corresponding locations on the eye schematic below**. **B** Subdivisions of the macula. Foveola (centre of the foveal depression, 0.35mm diameter). Fovea (rod free depression in central macula, 1.5mm diameter), parafovea and perifovea *(B is taken with permission from https://commons.wikimedia.org/wiki/File:Macula.svg accessed Mar 2019. Photograph: Danny Hope from Brighton & Hove, UK. Diagram: User: Zyxwv99)*

Figure 1.1A shows the location of the macula with respect to the optic nerve in the right eye. The retina is located on the inner surface of the eye shown on the schematic below the colour image. Figure 1.1B illustrates the subdivisions of the macula. The corresponding locations and width in millimetres (mm) are shown with the central depression below.

The mature retina consists of 10 layers further subdivided into the inner retina and outer retina. The inner retina refers to the retinal layers that are closest to the centre of the eye, and the outer retina refers to the layers closest to the outer portion of the

eye. The layers are illustrated in Figure 1.2. The neural retina consists of all layers except the retinal pigment epithelium (RPE).

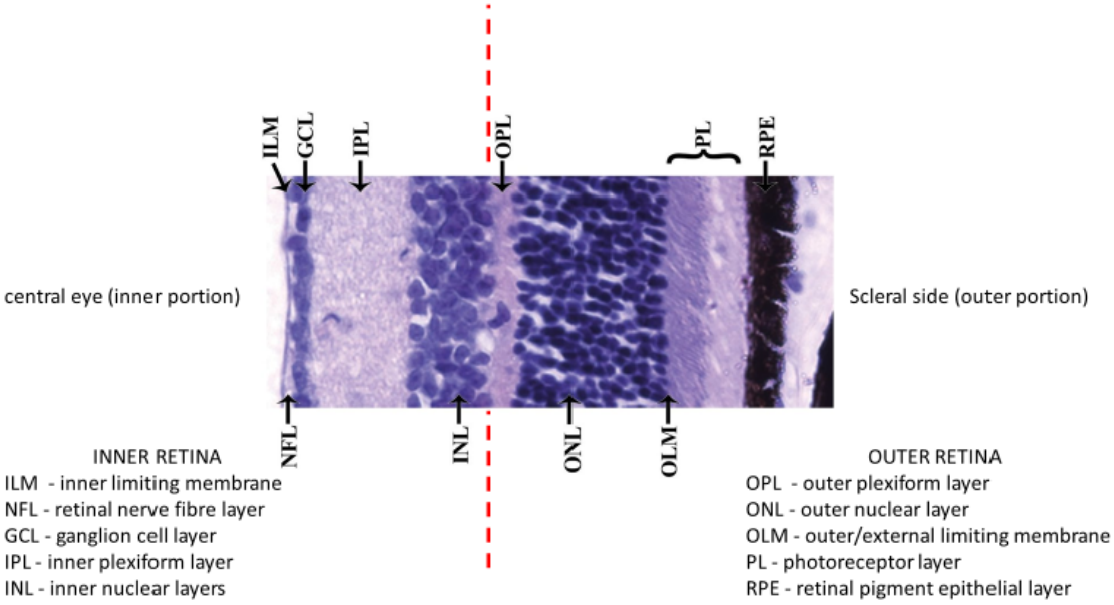


**Figure 1.2 Retinal layers of the mature eye.** Constructed from an image taken with permission (license CC BY 3.0 https://creativecommons.org/licenses/by/3.0/) accessed October 2018.

Retinal development commences from week 6 of gestation when the neuroepithelium is recognisable histologically arising through the differentiation of retinal progenitor cells to form the neural retina (Bach and Seefelder 1914; Mann 1950; Barishak 2001; Barber 1955). Figure 1.3 illustrates the neuroepithelium using monoclonal Pax 6 gene anti-body in the developing human eye. The neuroepithelium separates into inner and outer neuroblastic zones.

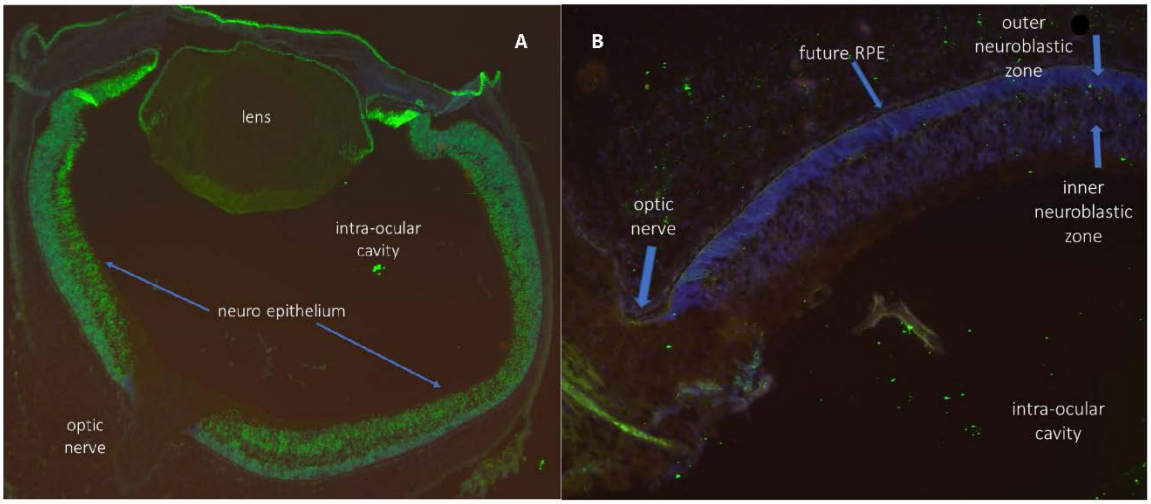


**Figure 1.3 A Human embryo 8 weeks gestation**, immunochemical photomicrograph of **ocular section** stained with monoclonal rabbit anti-Pax6 antibody. Green indicates the location of Pax 6 which appears especially in the neuroepithelium at this stage. **B** H**uman embryo 10 weeks** gestation immunochemical photomicrograph of **ocular section** showing inner and outer neuroblastic zones. [S Anwar, MSc Dissertation 2010: Gene Expression Patterns and the Developing Human Retina. Brunel University & Institute of Ophthalmology (Professor Marcus Fruttiger), London].

In the central retina, by 10 - 11 weeks gestation, photoreceptor cone precursors are detected as a monolayer adjacent to the developing retinal pigment epithelium (RPE) (O'Brien, Schulte, and Hendrickson 2003; Linberg and Fisher 2009; Xiao and Hendrickson 2000). This cone monolayer has been described as the future fovea (Mann 1950) and the edge of this region demonstrates early rod photoreceptors (Hendrickson et al. 2008).

At this time point, there is differentiation of Müller cells and the outer plexiform layer (OPL) which contains differentiating cone pedicles. The inner plexiform layer (IPL) and a developing inner nuclear layer (INL), which contains early cells similar to horizontal and bipolar cells, are already present. (Nag and Wadhwa 2006; Linberg and Fisher 2009).

By the 6$^{th}$ month of gestation (22-26 weeks GA), the macula appears as a bulge. The photoreceptors continue differentiation and maturation, in particular the cones. There is also a thickened ganglion cell layer (GCL) (Hendrickson and Yuodelis 1984). The

primitive photoreceptor outer segments and inner segments may only be demonstrated using electron microscopy (EM) (Yamada and Ishikawa 1965; Narayanan and Wadhwa 1998).

By the beginning of the seventh month of gestation (26-30 weeks GA) the foveal depression is evident histologically and the main retinal layer components are all present (Hendrickson and Yuodelis 1984) (Figure 1.4).

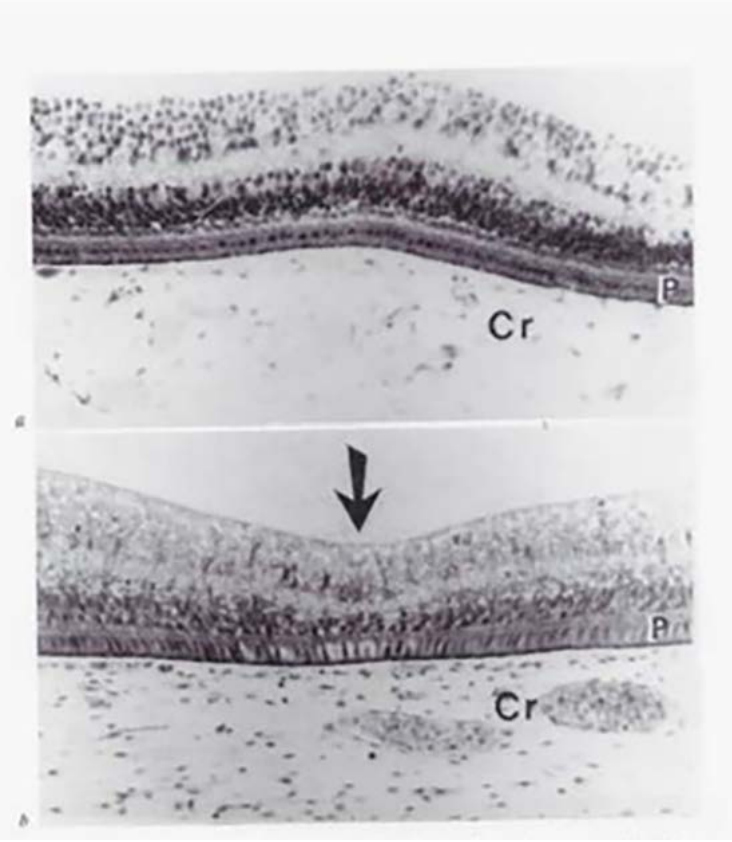


**Figure 1.4**. **Human fetus 7 months gestation**, histological section of central retina showing location of **foveal depression (arrow)**. Image of original from Hendrickson and Yuodelis 1984 (Barishak 2001) *[permission granted (STM permissions guidelines), Ophthalmology copyright]*.

Although the cone layer is still only one cell thick, there is elongation of the inner segment and cone axons (which form the future Henle fibre layer). Outer segment photoreceptor discs are seen at 28 weeks onwards using EM and histochemical studies (Yamada and Ishikawa 1965; Johnson et al. 1985).

The mature fovea is a depression within the retina characterised by the absence of retinal vessels and rod photoreceptors, and is sometimes referred to as the pure cone area (PCA). It contains the highest density of cone photoreceptor packing where the longest and thinnest cones are present (Curcio et al. 1987; Polyak 1941; Hogan, Alvarado, and Weddell 1971; Osterberg 1935). During fovea maturation, the fovea deepens, the number of cone photoreceptors increases below the foveal base (foveola) and the diameter of the fovea reduces.

The increased deepening of the foveal depression is accomplished by central thinning of the inner retinal layers due to outward movement or migration of the GCL and INL, and an inward movement of outer retina cone photoreceptors (Yuodelis and Hendrickson 1986; Provis, Diaz, and Dreher 1998). This inner movement of the cones results in the increased packing and subsequent elongation (thinning) of the cone photoreceptors cells, a process that begins before the outward migration of inner retina (Diaz-Araya and Provis 1992).

Maturation also increases the length and width of cone photoreceptor inner and outer segments reflected in increased vertical width of the outer retina between the external limiting membrane (ELM) and the retinal pigment layer (RPE), which is maximum beneath the foveola. Cone photoreceptor axons also lengthen and become angulated around the foveola to form the fibres of Henle. This increases the width of the outer plexiform layer (OPL) adjacent to the foveal centre (Hendrickson et al. 2012).

As the photoreceptors mature, the cone cells continue tight packing and elongation at the fovea, consequently the diameter of the PCA decreases from infancy until early childhood (Yuodelis and Hendrickson 1986). By the 5$^{th}$ year of childhood, the fovea is similar to the adult except in the length of the fibres of Henle, being longer and thinner in mature adulthood (Hendrickson and Yuodelis 1984; Yuodelis and Hendrickson 1986).

The limitation of histological studies is that the information does not observe dynamic change and the timing and mechanism of foveal deepening due to preterm birth is not well understood.

### 1.23 Optical coherence tomography (OCT) of the central retina.

Optical coherence tomography (OCT) is a real time non-invasive *in vivo* method of imaging which permits high resolution visualisation and dynamic evaluation of human tissue such as the retina in normal and pathologic states (Drexler and Fujimoto 2008). This has been achieved through correlation and validation of histological tissue with the corresponding sections on the OCT images of adults (Srinivasan et al. 2008; Drexler et al. 2001; Spaide and Curcio 2011; Staurenghi et al. 2014; Pons and Garcia-Valenzuela 2005; Chen et al. 2006).

The use of OCT in retinal assessment is now a routine investigation during the management of ocular disease but limited to patients who are co-operative or those that can sit upright at the instrument. However, the development of portable non-contact hand held spectral domain OCT (HH SD-OCT) devices have enabled imaging of young children and infants.

Similar to histology, OCT has revealed significant differences between the OCT images of the central retina (macula and fovea) in adults, children and infants. Even between normal adults, OCT has shown variations in foveal morphology which depend on race and sex (Tick et al. 2011; Wagner-Schuman et al. 2011), while variations have also been observed in otherwise normal children (Noval et al. 2014).

Portable OCT imaging has revealed central retinal structure in infants and young children that is not visualised with conventional examination. Findings such as sub-foveal fluid in normal newborns are described (Cabrera et al. 2012) that are not apparent by early childhood (Lee et al. 2015).

Cross-sectional OCT reports of central retina maturation at various ages have helped to show the differences between immature and mature central retina (Maldonado et al. 2011; Vajzovic et al. 2012; Yanni et al. 2013; Rothman, Sevilla, Freedman, et al. 2015; Dubis et al. 2012), but there are few longitudinal studies of retinal structure using OCT (Lee et al. 2015; Alabduljalil et al. 2018).

Differences on OCT imaging of the retina in children also exist between preterm and term individuals (Ecsedy et al. 2007; Tariq, Burlutsky, and Mitchell 2012; Tariq et al. 2011; Akerblom et al. 2012; Akerblom et al. 2011; Molnar et al. 2017; Park and Oh 2012; Fieβ et al. 2017; Bowl et al. 2016; Wang et al. 2012b; Rosen et al. 2015) and in individuals with a history of ROP (treated and untreated) (Recchia and Recchia 2007; Hammer et al. 2008; Lee, Kim, and Yu 2010; Wu et al. 2012; Villegas et al. 2014; Yanni et al. 2012; Pueyo et al. 2015; Park and Oh 2015; Vinekar et al. 2011; Jayadev et al. 2017; Vajzovic et al. 2015; do Lago et al. 2007; Erol et al. 2014; Gursoy et al. 2016; Vogel et al. 2018; Wang et al. 2012b; Rosen et al. 2015).

Table 1.1 summarises a number of studies investigating prematurity and ROP on visual acuity, central retinal structure in children and infants using either OCT or portable/HH-OCT and discussed further below.

**Table 1.1. Central retinal imaging studies in children and infants using optical coherence tomography (OCT)** or portable OCT. *VA – visual acuity; CFT/CMT - central foveal/macular thickness; RNFL – retinal nerve fibre layer; CME – cystoid macular edema; EZ - ellipsoid zone (formerly known as the photoreceptor inner/ outer junction).*

| Study | Type | Portable OCT | Includes children <5 years | Total number preterms born<32 weeks | Untreated ROP number | Includes treated ROP | Compares term born individuals | Outcome measure | Statistics | Findings |
|---|---|---|---|---|---|---|---|---|---|---|
| Recchia 2007 *small numbers* | Retrospective observation | No | No | 12 | 8 | Yes | No | CFT, VA, foveal contour | Descriptive Medians *small numbers* | Preservation inner layers, abnormal foveal contour, CFT greater than 220um |
| Ecsedy 2007 *small numbers stats questionable* | Prospective case control | No | No | 30 | 10 | Yes | Yes | CFT, VA, axial length | Non -parametric difference of means, longitudinal analysis of categorical data | Preterm thicker CFT vs term |
| Hammer 2008 *small numbers* | Cross sectional descriptive observational | No | No | 5 | 5 | No | Yes | CFT, retinal layers, foveal depth | Unclear | CFT thicker in ROP Fovea deeper in terms, wider and shallower in ROP |
| Lee 2010 | Retrospective observational descriptive | No | No | 4 | 1 | Yes | No | VA clinical description | none | Macula change after laser |
| Wang 2012 *stats analysis small numbers* | retrospective | No | No | 26 | 17 | Yes | Yes | CFT, Retinal layers, shape size foveal pit | means between ROP and terms bilinear/logistic model CFT and GA Between preterm and terms *assumes no difference in variance no adjustment treated or untreated ROP* | Increased CFT in ROP Increased mean thickness retinal layers in ROP Thicker CFT GA <28 weeks Reduced Foveal slope and depth in ROP <28 weeks Vs >29 weeks |

| Study | Type | Portable OCT | Includes children <5 years | Total number preterms born<32 weeks | Untreated ROP number | Includes treated ROP | Compares term born individuals | Outcome measure | Statistics | Findings |
|---|---|---|---|---|---|---|---|---|---|---|
| Wu 2012<br>*Omissions in stats analysis* | Prospective case control | No | No | 86 | 18 | Yes | Yes | CFT, refractive error, VA,<br>Anterior chamber depth and lens thickness | Descriptive, p values between 4 means, Multiple linear regression for GA and CFT, did not include ROP | CFT thickest in early GA |
| Villegas 2014<br>*questionable stats analysis*<br>*children under 5 years* | Retrospective cohort | No | Yes | 44 | 8 | Yes | No | CFT, VA | Chi square, t test<br>Correlation CFT and VA<br>Clinical observation<br>Age and VA – p value<br>inappropriate application of statistics, categorical data | Percentage Foveal depression absence and vision above or below 20/40<br>No correlation between CFT and GA |
| Yanni 2012<br>*small numbers of untreated ROP*<br>*no adjustment for ROP (treated, untreated, None)* | Cross-sectional descriptive | No | No | 24 | 5 | Yes | Yes | CFT, VA<br>Retinal layers, Fovea diameter, depth, slope | descriptive<br>t tests for means<br>Linear correlation | Shallow less steep fovea in preterms vs terms<br>CFT thicker preterms vs terms<br>Reduced VA means preterms vs terms<br>Thicker inner retina preterms vs terms |
| Pueyo 2015<br>*small numbers, children under 5 years* | Retrospective cohort | No | Yes | 27 | 17 | Yes | Yes | VA<br>Retinal layers, CMT | Multiple regression models<br>ANOVA<br>*no details, no coefficients* | Retinal structure is no different in preterms vs terms<br>Only treated ROP changed structure |
| Park 2015<br>*children under 5 years*<br>*treated ROP not adjusted* | Cross sectional observational | No | Yes | 50 | 30 | Yes | Yes | Retinal layers<br>RNFL thickness<br>VA | Correlation<br>Multivariate model<br>GA, BW, ROP stage, (not treatment), age at exam | Smaller average RNFL between preterm vs term significantly different<br>ROP stage inverse correlation with nasal RNFL<br>VA poorer in preterms vs terms |

| Study | Type | Portable OCT | Includes children <5 years | Total number preterms born<32 weeks | Untreated ROP number | Includes treated ROP | Compares term born individuals | Outcome measure | Statistics | Findings |
|---|---|---|---|---|---|---|---|---|---|---|
| Bowl 2016 | Cross sectional observational | No | No | 150 | 50 | No | Yes | CFT, retinal layers thickness | Linear regression ANOVA | GA, BW both correlates inversely with CFT and retinal layers |
| Rosen 2015 *small numbers, no adjustment for treated ROP* | Cross sectional observational | No | No | 40 | 10 | Yes | Yes | Foveal depth, retinal layers thickness | t test for means, correlation | Reduced foveal depth <27 weeks |
| Vinekar 2011 *older heavier preterms*<br><br>*19 infants at 52 weeks PMA follow up* | observational case series | No | infants | 74 | 54 ROP<br>Stage 1 = 27 eyes<br>Stage 2 = 79 eyes<br><br>20 infants nonROP | No | No | Presence or absence of cystic changes<br><br>observation of CME pattern<br><br>CFT<br>Stage of ROP | difference of means for CFT between stage 1, 2 and nonROP<br><br>Post hoc test then performed for stage of ROP | Stage 1 & non ROP showed no cystic changes<br><br>CFT in preterms significant to stage 2 ROP<br><br>Normalisation at 52 weeks PMA (19 eyes) |
| Jayadev 2017 *small numbers in each group so 't test' questionable no adjustment for GA or ROP* | Retrospective observational | Yes | Yes | 32 | 22 nonROP<br>10 ROP | No | No | Teller acuity test age groups in months (3-6 n= 17; 6-9 n=8; 9-12 n=7) presence absence of ELM, IRL, EZ, OS-RPE at fovea | Correlation<br><br>Comparison of means (t test) | VA correlates with changes in foveal IRL ELM, EZ layers depending on age group |

| Study | Type | Portable OCT | Includes children <5 years | Total number preterms born<32 weeks | Untreated ROP number | Includes treated ROP | Compares term born individuals | Outcome measure | Statistics | Findings |
|---|---|---|---|---|---|---|---|---|---|---|
| Vajzovic 2015 Comparison of preterm with term assumes no difference of variance; *Unclear treated ROP numbers* | Prospective observational | Yes | infants | 64 | 7 non ROP; treated unclear | Yes | Yes | EZ (presence absence); EZ distance means from foveal centre; CME foveal cystic changes | Non-parametric means; Correlation; Linear regression adjusted GA, BW, PMA | EZ absence higher in preterms and greater with CME; Increased proximity to foveal centre with terms vs preterms; Foveal contour present with CME in terms |
| do Lago 2007 | Case series descriptive | No | infants | 12 | 12 | No | No | Description of foveal depression | percentages | No foveal depression in 80 % |
| Erol 2014 *no regression analysis on CFT* | Retrospective | Yes | infants | 179 | 58 | Yes | No | CFT, CME and grading of cysts | Comparison of means; non-parametric correlation | CME significant with ROP and with stage; CFT correlated with GA, BW |
| Gursoy 2016 *small numbers no linear regression or adjustment for treated ROP, GA, BW or PMA* acknowledge that ROP vs prematurity not possible to differentiate in study | Prospective cross-sectional mixed observation | Yes | infants | 72 | 18 nonROP 15 ROP 21 pre-treatment ROP 18 treated ROP | Yes | No | CFT, fovea depression (yes/no), CME (yes/no) | ANCOVA for GA, BW<br>Means ANOVA with post-test to identify the group that was different<br>Presence/absence Chi test | No foveal depression 40% when ROP absent 85% in severe ROP;<br>CFT thicker in severe untreated ROP; GA, BW on CFT not significant;<br>CME significant with ROP |

| Study | Type | Portable OCT | Includes children <5 years | Total number preterms born<32 weeks | Untreated ROP number | Includes treated ROP | Compares term born individuals | Outcome measure | Statistics | Findings |
|---|---|---|---|---|---|---|---|---|---|---|
| Tariq 2012<br>*ROP history unknown,*<br>*BW excluded from linear model* | Cross -sectional observational retrospective | No | No | 148 | Not known | No | Yes | VA, CMT | Multivariate linear<br>BW excluded from analysis | GA before 32 weeks thicker CMT<br>VA worse than term |
| Akerblom 2011 | Cross -sectional | No | No | 65 | 22 | Yes | Yes | CFT<br>VA | Multiple regression analysis<br>ANOVA<br>t test | Prematurity (GA, only not BW) without ROP has thicker CFT<br>No correlation between VA and CFT |
| Vogel 2018<br>Study of treated ROP only | Observational Case series | Yes | infants | 131 | 0 | Yes | No | RT inner and outer | Linear mixed models<br>GA, BW, sex, race, PMA | Outer retina thickening in IVT vs LPC where EZ is delayed |
| Akerblom 2012 | Cross-sectional | No | No | 62 | 20 | Yes | Yes | RNFL | ANCOVA<br>Bivariate correlation for RNFL and GA | RNFL thickness and quadrants increased with increased BW not GA |
| Molnar 2017 | Cross-sectional analysis of prospective population study | No | No | 134 | 80 | Yes | Yes | CMT | t test<br>Multiple linear mixed model | Increase CFT with GA (adjust for ROP & males)<br><br>ROP, males not VA had thicker CMT |
| Fieβ 2017<br>Children under 5 years | Prospective cross sectional | No | Yes | 173 | 34 | Yes | Yes | Retinal layers thickness<br>GA, ROP, VA | Multiple linear regression<br>No adjustment for BW<br>No adjustment for treated ROP | CFT thicker in lower GA independent of ROP |

# Chapter 2 Review of the Literature

### 2.1 Infant OCT studies of macular development, prematurity and ROP.

A case of a premature infant with severe advanced ROP that required retinal surgery was first reported using a non-portable Stratus OCT 3000 machine while the infant was anaesthetised (Patel 2006). The OCT findings revealed a macular detachment with microcystic changes in inner retina that could not be detected clinically, which changed the surgical approach to the management of the infant. The author suggested that OCT imaging of infants could provide an objective method of management in advanced ROP.

However, the practicalities of using a non-portable device for infants outside of the operating room precluded routine use of OCT in this group. Despite this, do Lago and colleagues (do Lago et al. 2007) successfully imaged 12 preterm infants awake during the ROP screening exam using a Stratus OCT device from between 32 weeks to 41 weeks PMA. The authors reported the macular morphology in the presence of ROP from mild to severe (Stages 1-3). Their main finding was that the foveal depression was 'easily recognizable' in only 25% and that the OCT features correlated with the known histological descriptions of immature retina, concluding that OCT could be used to follow macular development in preterm infants.

With the advent of a portable OCT device, Chavala and colleagues (Chavala et al. 2009) described portable HH SD-OCT imaging in 3 premature infants with advanced ROP while under anaesthesia which demonstrated sub-clinical retinoschisis, a shallow retinal detachment and pre-retinal lesions. This was also not detected with either direct visualisation or using the RetCam ocular contact colour imaging system (Clarity Medical Systems, Pleasanton, CA).

Similar reports in preterm infants supported these findings (Muni et al. 2010; Joshi, Trese, and Capone 2006) but it was not until Lee et al (Lee et al. 2011), that an evaluation of the use of HH SD-OCT without anaesthesia in neonates during ROP screening in the neonatal intensive unit (NNU) was described more fully.

The conclusion of Lee and colleagues' study (Lee et al. 2011) was that portable HH SD-OCT imaging could be used as an adjunct to ROP screening but it could not replace conventional ophthalmoscope examination. Although retinal architecture elucidated by HH SD-OCT imaging might explain poor outcomes from advanced ROP, the device did not indicate the presence or absence of 'Plus' disease during screening. 'Plus' disease is a severe clinical feature that determines the need for treatment by subjective assessment of the vascular appearances in the retina of infants with ROP.

Maldonado et al (Maldonado et al. 2014) developed a grading system using portable HH SD-OCT in infants with ROP to describe vascular anomalies in an attempt to describe 'Plus' disease but the findings were not consistent enough to be used in routine ROP screening with HH SD-OCT.

When portable HH SD-OCT was optimised to account for the smaller preterm eye's axial length according to age (Maldonado et al. 2010), customisation of scans improved the quality and reliability of infant image acquisition. Studies of the developing macula were now able to elucidate dynamic foveal features, quantify retinal layers in preterm and post term infants and children and correlate HH SD-OCT images with histologic findings (Vajzovic et al. 2012; Vajzovic et al. 2015; Dubis et al. 2012; Maldonado et al. 2011; Dubis et al. 2013).

These HH SD-OCT imaging studies confirmed earlier histologic reports of an immature retina in preterm and term infants and revealed a thicker inner retina in comparison

with the outer retina which gradually reversed with maturity. This is shown in figure 2.1.

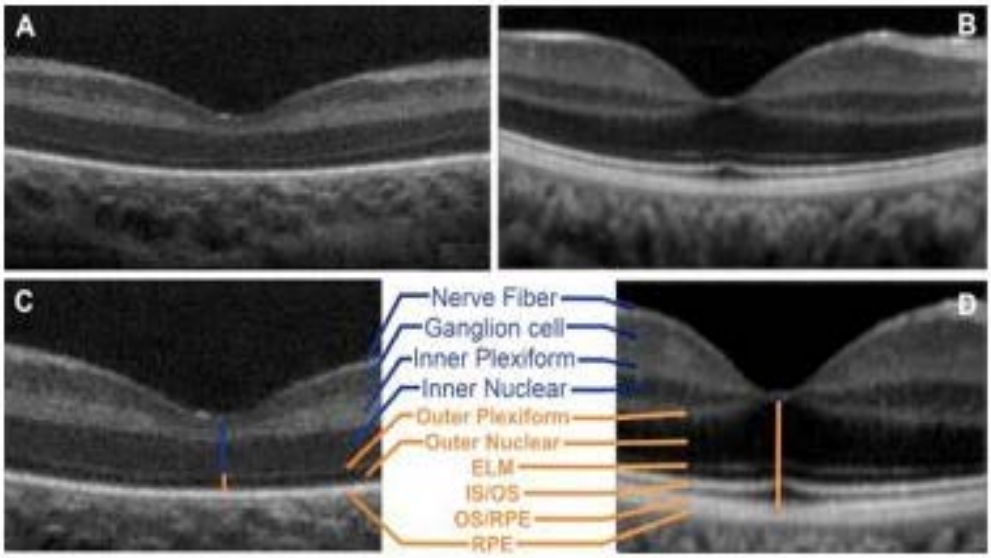


**Figure 2.1. The immature preterm retina (A) is compared with a mature adult retina (B)** showing the changes in inner retina and outer retina at the fovea with maturity, on spectral domain OCT. Taken from Maldonado et al (Maldonado et al. 2011) *[permission granted (STM permissions guidelines), Ophthalmology copyright]*.

The foveal depression was shallow with continuation of inner layers across the foveal depression and a thin photoreceptor layer in infancy. Dynamic HH SD-OCT also revealed inner retinal migration in conjunction with deepening of the foveal depression with age.

Maldonado and colleagues concluded that inner retinal migration occurred primarily between 31 and 42 weeks (Maldonado et al. 2011). However, their study described the macular findings of 13 preterm infants with untreated ROP (excluding Stage 3 or treated infants) and the impact of ROP on dynamic foveal changes was unclear.

Dubis et al (Dubis et al. 2012) investigated the outer retina using age matched human histology (35 and 41 weeks PMA), macaque histology and HH SD-OCT images in 16 preterm infants from 30 weeks PMA that included stage 2 ROP in the group. Despite this the authors state that *'the foveal region seems to follow a developmental time course similar to that associated with in utero maturation in premature infants who do not develop retinopathy of prematurity'*.

During foveal maturation, correlation of SD-OCT bands with retinal layer histology show the absence of photoreceptor bands even by term birth, appearing to mature by 24 months of age (Vajzovic et al. 2012). The changes in the retinal layers according age are shown in figure 2.2.

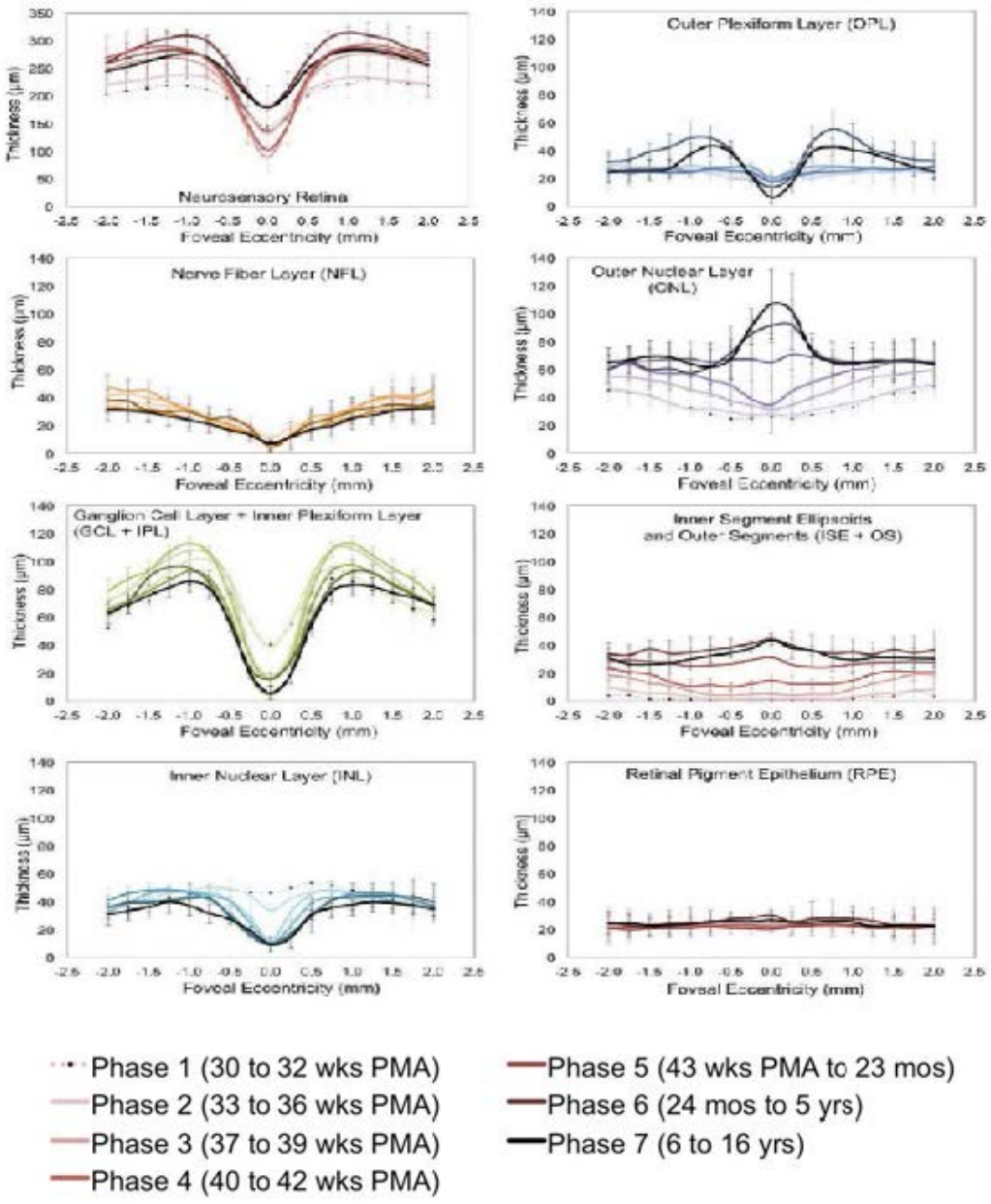


**Figure 2.2 Retinal layers according to age (phases) and location from the fovea.** Neurosensory retina, NFL- nerve fibre layer, GCL+IPL- ganglion cell layer plus inner plexiform layer, INL- inner nuclear layer, OPL-PSL- outer plexiform layer and photoreceptor synapse, ONL +HFL- outer nuclear layer and Henle fibre layer, IS+OS – inner and outer photoreceptor segments, RPE- retinal pigment epithelium (Vajzovic et al. 2012), *[permission granted (STM permissions guidelines), American Journal of Ophthalmology copyright]*.

The study has unclear details regarding the presence or absence of ROP in the preterm groups or an adjustment for the severity of prematurity. This makes it uncertain if either ROP or gestation age impacts retinal layers at the fovea.

A study by the same group, of photoreceptor development (appearance of the EZ at the fovea) between preterm infants and term born infants, reported a delay in the preterm group (Vajzovic et al. 2015) as shown in figure 2.3. The authors measured the mean distance to the foveal centre of the EZ band as a measure of photoreceptor delay.

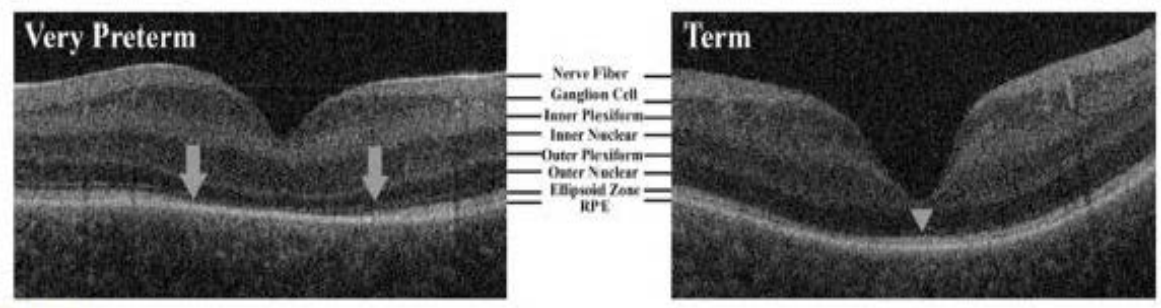


**Figure 2.3. The distance between the two ends of the ellipsoid zone (EZ)** which represents the appearance of photoreceptor segments at the fovea, thereby illustrating the gap in the preterm infant image on the left. By contrast the term infant has a complete EZ band across the fovea. Taken from Vajzovic (Vajzovic et al. 2015) *(permission granted November 2019, Association for Research in Vision and Ophthalmology copyright)*

Figure 2.3 shows the delay in the appearance of the ellipsoid zone (previously known as the inner segment/outer segment band) on HH SD-OCT in the preterm infant image in comparison to the term infant. Both images were acquired at 39 weeks PMA.

The authors state that *'the incidence of the EZ did not significantly differ by sex, race, nor any measure of ROP severity'.* In this study nineteen infants had received ROP treatment and only seven preterm infants without ROP. The statistical analysis of ROP severity consisted of a comparison between the mean EZ foveal distances in the ROP groups while the linear regression model of GA, BW and PMA, did not include ROP. Both limit the analysis conclusions regarding either GA, BW, or ROP on the appearance of the EZ band in preterm infants. Secondly, the assumption that term infants and preterm infant development prior to 37 weeks was similar enough to permit a direct

comparison between the two groups at 39 weeks PMA is questionable since clearly both are not from the same population of infants born before 40 weeks gestation.

Vinekar et al (Vinekar et al. 2011) studied acute mild ROP in preterm infants using OCT. Their group converted a table top SD-OCT device to image 146 eyes from 74 Asian Indian infants with a mean GA of between 30-32 weeks and imaged at a mean PMA of 37 weeks. The cohort was divided into three groups according to the stage of ROP (stage 1, stage 2 or none).

The mean macular retinal thickness (CMT) was compared between the groups and found to be significantly higher in Stage 2 ROP but not Stage 1, versus no ROP. Since there was no difference between the GA, BW and PMA between the 3 groups, no adjustment was deemed necessary in comparing the mean CMT of the 3 groups. However, 29% of the Stage 2 group showed cystic change at the fovea on a retrospective review, with distortion of CMT, which was not accounted for in the original analysis. This raises questions about the author conclusions regarding the significance of severity of ROP and CMT. The cystic eyes were further analysed and 10 infants re-imaged 1 year later, when the authors reported resolution of the cystic changes noted originally.

Erol et al (Erol et al. 2014) also reported increasing central foveal retinal thickness (CFT) with increased severity of ROP but the authors made no adjustment for either GA or BW, the means of which differed between the four groups (no ROP, stages 1, 2 and 3 ROP) by up to 5 weeks of GA and 45% of BW.

In another large study investigating the effect of ROP on preterm foveal retinal thickness, Gursoy and colleagues (Gursoy et al. 2016) analysed 131 portable SD-OCT images prospectively acquired from 72 preterm infants which were then divided into 4 groups as shown in Table 2.1.

| | Group 1 (no ROP) | Group 2 (mild to moderate ROP) | Group 3 (pre-treatment ROP) | Group 4 (Laser treated ROP) |
|---|---|---|---|---|
| number of eyes | 30 | 30 | 40 | 31 |
| number of infants | 18 | 15 | 21 | 18 |
| mean PMA at image acquisition (weeks) | 40.3 | 37.9 | 37.2 | 45.72 |
| (range) | (26-44) | (34-40) | (32-43) | (39-60) |
| mean GA (weeks) | 33.7 | 31.3 | 28.4 | 28.4 |
| (range) | (30-36) | (26-33) | (25-33) | (24-32) |
| mean BW (grams) | 2112 | 1447 | 1097 | 1231 |
| (range) | (1200-1700) | (1090-2010) | (680-1560) | (480-1700) |

**Table 2.1 Preterm infant group characteristics from Gursoy** (Gursoy et al. 2016). *PMA – postmenstrual age, GA – gestational age, BW – birthweight, ROP – retinopathy of prematurity*

The authors examined the mean CFT between the groups, the number of eyes with a formed foveal depression in each group, and the mean PMA in each group when cystic changes at the fovea were documented. They further subdivided their results according to right or left eyes.

In their analysis, the authors did not find a significant difference between GA or BW on the mean CFT for the cohort and therefore the CFT measurements were analysed for each group without adjustment.

Their findings were as follows:

- The mean CFT between the 4 groups significantly increased from group 1 (no ROP) to group 4 (treated ROP)
- The mean CFT was significantly greater between Group 1 and Groups 3 and 4 (severe and treated ROP) but not between Group 1 and Group 2 (no ROP versus mild to moderate ROP)
- There was no difference in mean CFT between right and left eyes
- The percentage of eyes (right/left) with a 'well-formed foveal pit' was greatest in infants with no ROP: 60 (67%) in Group 1, 33 (20%) in Group 2, 14 (16%) in Group 3, but 40 (31%) in Group 4.

- The percentage of cystic changes found in Group 1 [0 (0%), mean PMA 40.3 weeks], Group 2 [7 (13%), mean PMA 37.9 weeks], Group 3 [29 (21%), mean PMA 37.2 weeks] Group 4 [13 (13%), mean PMA 45.7 weeks].

  The main conclusions were that CFT increased with only either severe pre- treatment ROP or treated ROP and that a well-formed foveal depression was most likely in preterm infants with no ROP.

  A major limitation in the analysis is lack of adjustment for the mean PMA at which the imaging was acquired (see table 3.1). This is important since it is evident from the previous literature that the foveal depression changes with time.

  Although the authors attempt to address this by tabulating the mean GA at various PMA's with the number of images that show a well-formed foveal depression, this was not correlated with either ROP or treated ROP. The authors do admit that their study was not able to differentiate between ROP and prematurity in their analysis of CFT.

  Furthermore, the definition of a well-formed foveal depression in the study is also unclear particularly since the presence of a foveal depression (shallow or otherwise) has been reported to be universally present using HH SD-OCT to image the retina in preterm infants (Maldonado et al. 2011).

**2.2 Optical coherence findings of cystic change in the macula**

In their study of dynamic foveal development, Maldonado et al (Maldonado et al. 2011) described foveal distortion by cystic spaces located in the inner retina especially the inner nuclear layer (INL) in 58% of the preterm group. This was labelled 'cystic macular edema' (CME) due to its similar appearances in mature retina known to show oedema but unlike mature retina, it was clinically undetectable.

Several infant studies using HH SD-OCT in infants report CME (Vinekar et al. 2011; Maldonado et al. 2012; Erol et al. 2014; Gursoy et al. 2016; Lee et al. 2011; Dubis et al. 2013; Cabrera et al. 2012). The natural history of CME is not known although several

authors report resolution of the appearances at the fovea from between 4 and 52 weeks after detection. Some of the reports include infants that have been treated with either laser or intra-vitreal injection for ROP which adds further complexity to the conclusions.

In an effort to better understand CME in infants, investigators have graded CME according to distortion of foveal contour (yes/no) (Erol et al. 2014), single or multiple spaces (Vinekar et al. 2011; Dubis et al. 2013; Maldonado et al. 2012), and degree of ROP severity. It is currently unclear if ROP and ROP severity is associated with CME (Vinekar et al. 2011; Erol et al. 2014) or not (Maldonado et al. 2012; Dubis et al. 2013; Erol et al. 2016) with conflicting conclusions regarding either. However, given that CME and sub-foveal fluid has also been reported in healthy newborns (Cabrera et al. 2012), the exact aetiology of CME in infants still remains unexplained.

Table 2.2 summarises of studies investigating cystoid macular oedema (CME) on central retinal structure in children and infants using either OCT or portable/HH-OCT.

**Table 2.2 Cystoid macular oedema studies using optical coherence tomography in infants**. *CME – cystoid macular oedema, CFT-central foveal thickness, RT – retinal thickness, ROP – retinopathy of prematurity, GA – gestational age, BW- birthweight, EZ – ellipsoid zone, IVT – intra-vitreal treatment, LPC – laser photocoagulation*

| Study | type | portable OCT | CME | number preterms | untreated ROP infants | includes treated ROP | term born individuals | outcome measure | statistics | other findings |
|---|---|---|---|---|---|---|---|---|---|---|
| Patel 2006 | Case study | no | Intraretinal cystic change | 1 | 0 | yes | no | Observation of OCT image | none | macular detachment |
| Chavala 2009 | Prospective observational case series | yes | Intraretinal cystic change | 3 | 0 | yes | no | Observation of OCT image | none | retinoschisis, pre-retinal structures, retinal detachment |
| Muni 2010 | Retrospective case series | yes | Intraretinal cystic change | 3 | 0 | yes | no | Observation of OCT image | none | Retinoschisis, intra-retinal cystic changes |
| Maldonado 2011 | Observational | yes | CME 58% | 31 | 31 | no | no | Observation of OCT image | percentages | timeline of retinal layers |
| Lee 2011 | Prospective observational case series | yes | CME 39% | 38 | 27 ROP<br>11 nonROP | no | no | 39 eyes of 23 infants (61%) CME | none | 32% epiretinal membrane;<br>54% optic nerve hyaloid remnants; subclinical macular detachment |
| Vinekar 2011<br>*older heavier preterms*<br>*19 infants at 52 weeks PMA follow up* | observational case series | no | CME 29%<br>In stage 2 ROP only | 74<br>Mean GA<br>stage 1 = 32 weeks<br>stage 2 = 30 weeks<br>nonROP = 31 weeks | 54 ROP<br>Stage 1 = 27 eyes<br>Stage 2 = 79 eyes<br>20 infants nonROP | no | no | Presence or absence of cystic changes<br>observation of CME pattern<br>CFT<br>Stage of ROP | difference of means for CFT between stage 1, 2 and nonROP<br>Post hoc test then performed for stage of ROP | Stage 1 & non ROP showed no cystic changes;<br>CFT in preterms significant to stage 2 ROP;<br>Normalisation at 52 weeks PMA (19 eyes) |

| Study | type | portable OCT | CME | number preterms | untreated ROP infants | includes treated ROP | term born individuals | outcome measure | statistics | other findings |
|---|---|---|---|---|---|---|---|---|---|---|
| Maldonado 2012 *small numbers stats do not adjust for ROP/GA/PMA and CFT pre-plus is subjective* | Prospective observational case series | yes | CME 50% | 42 | 30 | Yes<br>n=12 progressed to treatment | no | CME severity (CFT) ROP outcomes (laser yes/no, stage, severity plus/no plus/pre-plus) | Comparison of means CFT in groups<br>linear regression for CME and systemic factors | Outcome ROP and systemic factors not significant;<br>CFT significant if stage 3 or laser or plus disease |
| Cabrera 2012 | Prospective observational case series | yes | CME 2.5% | 0 | 0 | no | yes<br>n= 39 | observation | percentages | 15% sub-foveal fluid (SRF) also found |
| Dubis 2013 *No adjustment for treated ROP or GA in linear regression model for CME and risk factors* | Prospective observational case series | yes | CME 56% | 46 | 34<br>8 progressed to laser<br>4 IVT | yes | no | Severity of CME; persistence of inner layers | Percentages; comparison of CFT means<br>No linear regression | CME not related to ROP stage;<br>Younger GA in CME group;<br>Persistence of inner layers irrespective of ROP stage |
| Cabrera 2013 Study of racial differences in term born infants | Prospective observational case series | yes | CME 10% | 0 | 0 | no | Yes<br>n=20 | Observation of OCT image<br>CFT | Percentages<br>Non-parametric comparison of mean CFT | Resolution by 3 months.<br>SRF also seen (10%) |
| Erol 2014 *no regression analysis on CFT* | Retrospective | yes | CME ROP 54% vs CME 31% nonROP | 179 | 58 | yes | no | CFT, CME and grading of cysts | Comparison of means;<br>non-parametric correlation | CME significant with ROP and with stage;<br>CFT correlated with GA, BW |
| Vajzovic 2015 *Comparison of preterm with term assumes no difference of variance; Unclear treated ROP numbers* | Prospective observational | yes | CME 72% preterm<br>CME 6% term | 64 | 7 non ROP; treated unclear | yes | yes | EZ (presence absence);<br>EZ distance means from foveal centre;<br>CME foveal cystic changes | Non-parametric means;<br>Correlation;<br>Linear regression adjusted GA, BW, PMA | EZ absence higher in preterms and greater with CME;<br>Increased proximity to foveal centre with terms vs preterms; Foveal contour present with CME in terms |

| Study | type | portable OCT | CME | number preterms | untreated ROP infants | includes treated ROP | term born individuals | outcome measure | statistics | other findings |
|---|---|---|---|---|---|---|---|---|---|---|
| Rothman 2015 *No adjustment for ROP treatment or effect of IVT ROP treatment* | Cohort | yes | CME 58.5% | 53 | Images taken before treatment | Treated infants in study at 18-24 months corrected age | no | Bayley cognitive language and motor scales at 18-24 months corrected age | Chi Square and t testing of means, correlation least squares regression | CME preterms had lower cognitive scales vs non-CME |
| Vinekar 2015 *no adjustment for ROP, GA small numbers* | Prospective observational | yes | ROP CME group n=11 vs no CME ROP n= 16 vs nonROP no CME n= 17 | 44 | 44 | no | no | Visual acuity Refraction at age 3, 6, 9 12 months | Comparison of means depending on parametric/non-parametric testing | Reduced visual acuity in CME group but only significant at 3 months, not by 12 months Increased hyperopia in CME group but at 3 months only |
| Erol 2016 | Prospective observational | yes | 51.5% | 80 | 80 | no | no | Sub-foveal choroidal thickness | report of means comparison only no details of repeated measures | Thinner choroid with higher stage of ROP Choroid thickness correlated with BW not GA |
| Gursoy 2016 *small numbers no linear regression or adjustment for treated ROP, GA, BW or PMA* Authors acknowledge that ROP vs prematurity not possible to differentiate in study | Prospective cross-sectional mixed observation | yes | CME 29% right eyes, 21% left eyes | 72 | 18 nonROP 15 ROP 21 pre- treatment ROP 18 treated ROP | yes | no | CFT, fovea depression (yes/no), CME (yes/no) | ANCOVA for GA, BW<br>Means ANOVA with post-test to identify the group that was different<br>Presence/absence Chi test | No foveal depression 40% when ROP absent 85% in severe ROP;<br>CFT thicker in severe untreated ROP; GA, BW on CFT not significant;<br>CME significant with ROP |

| Study | type | portable OCT | CME | number preterms | untreated ROP infants | includes treated ROP | term born individuals | outcome measure | statistics | other findings |
|---|---|---|---|---|---|---|---|---|---|---|
| Vogel 2018 Study of treated ROP *Small numbers of LPC and IVT eyes* | Observational case series | yes | 53% | 131 | 108 | Yes n=23 | no | Weekly change foveal RT inner and outer & at nasal/temporal foveal rim EZ, CME | Linear mixed models GA, BW, sex, race, PMA, treated and untreated eyes | Outer retina thickening greater in treated eyes with IVT vs untreated EZ delayed in LPC vs untreated eyes |

### 2.3 OCT studies in ex-premature children with and without ROP

Several earlier non-portable OCT studies reported central retinal anomalies in older ex-premature children with and without a history of ROP, including individuals who had also received ROP treatment.

Ecsedy and colleagues (Ecsedy et al. 2007) examined a prospective cohort of 40 ex-preterm children aged 7-14 years defined by gestational age at birth of less than 32 weeks and birth weight less than 1501 grams. The cohort was divided into 3 groups – children who had received treatment for ROP, children in whom ROP had spontaneously regressed, and those with no ROP at any time. The control group consisted of 10 age matched term children. OCT measurements were taken using a Stratus OCT3 device (Carl Zeiss Meditec). The authors found:

- A thicker foveal centre was seen in the premature group compared with controls and this was due to the continuation of the inner retina at the fovea in the ex-preterm children.
- Children with a history of ROP treatment had greater mean values of retinal thickness compared with ex-preterm children with no history of ROP but this was not statistically significant.
- Premature children with no ROP had mean foveal central retinal thicknesses similar to controls.
- The total macular volume was similar in all premature and control groups; however, no statistical difference was detected in the mean outer retinal thickness between the groups.

The authors concluded that the presence of ROP (treated and untreated) modified the development of the central retina i.e. macula, through persistence of the inner retinal

layers at the fovea. However, the analysis did not adjust for the severity of prematurity i.e. gestational age of the participants as a possible confounder.

Thicker inner layers at the macula were also reported in addition to an abnormal foveal contour by Recchia et al (Recchia and Recchia 2007) in 12 ex-preterm individuals aged 8 to 38 years using a Stratus OCT. Here, the authors describe features as a percentage of the whole group, without distinguishing any relationships between those that had received ROP treatment with those that had not, in their final conclusion on regressed ROP and foveal anomalies.

A number of studies report increased CFT or CMT using OCT imaging of retina in ex - preterm children either with or without a history of ROP and in comparison, with term born individuals (see Table 1.1).

A few have significant limitations such as small numbers of children (Yanni et al. 2012; Hammer et al. 2008; Rosen et al. 2015) or questions regarding the analysis (Wu et al. 2012) or inclusion of children under 5 years (Villegas et al. 2014; Pueyo et al. 2015; Park and Oh 2015; Jayadev et al. 2017; Fieβ et al. 2017), where no adjustment has been made for development of the retina.

However, where adjustment for ROP is made, early GA was the only risk factor found for increasing CFT in comparison with term born children (Akerblom et al. 2011; Molnar et al. 2017). Severe ROP and BW appears to result in a thinner mean retinal nerve fibre layer (RNFL) (Akerblom et al. 2012) but others suggest that only GA and BW are risk factors for increased mean individual retinal layer thickness at the fovea (Bowl et al. 2016). The mean papillomacular bundle RNFL in very preterm infants is also significantly reduced compared with term infants using HH SD-OCT (Rothman et al. 2015).

There remains a paucity of current literature reporting dynamic longitudinal measures of foveal morphology parameters in preterm infants using HH-OCT.

# Chapter 3 Research Objectives and Aims

The study objective was to visualise and measure the development of the specialised area of central retina known as the fovea and parafovea in preterm infants with and without ROP and prior to treatment for ROP. This would be achieved by acquiring and analysing HH SD-OCT images of preterm infants from 30 – 44 weeks of postmenstrual age recruited from the University Hospitals of Leicester NHS Hospital's neonatal and maternity service.

The research aims were:

1. To determine the effect of gestational age, birthweight and ROP on the trajectory of foveal morphology with postmenstrual age for preterm infants without foveal cystic changes. This is presented in Chapter 5.

2. To examine the relationship of individual retinal layers at the fovea and parafovea with gestational age, birthweight and ROP diagnosis after adjusting for postmenstrual age in preterm infants without foveal cystic changes. This is presented in Chapter 6.

3. To describe the foveal cystic changes observed in preterm infants and examine possible associations between gestational age, birthweight and other factors such as ethnicity and multiplicity of birth. This is presented in Chapter 7.

# Chapter 4 Methods

## 4.1 Recruitment of Participants

*4.11 Introduction*

The study was conducted in accordance with the tenets of the Declaration of Helsinki and granted approval by an independent Local Ethics Committee (NRES committee, Nottingham, East Midlands, United Kingdom). The principal investigators all completed and maintained certificates of Good Clinical Practice throughout the study and research period.

Patients were recruited from the Leicester Royal Infirmary neonatal and maternity unit, United Kingdom (NNU). All preterm babies from 31 to 44 weeks PMA who required ROP screening were eligible for inclusion in the study. Screening was performed according to UK recommendations (RCOphth, RCPCH, and BAPM 2008) where premature babies with gestational age up to 31 weeks and 6 days and/or birthweight under 1501 grams were included for ROP screening.

Infant eyes were instilled with topical dilating drops (Cyclomydril® = cyclopentolate hydrochloride 0.2 % and phenylephrine hydrochloride 1%) and examined while awake, using a lid speculum. Binocular indirect ophthalmoscopy (BIO) was used in order to establish the presence or absence of ROP. Documentation of demographic and clinical parameters for each preterm infant included: PMA, GA and BW, presence or absence of ROP, the stage of ROP if present, single or multiple birth, sex, eye (right or left) and ethnicity (Caucasian or Non-Caucasian). Non-Caucasian patients included South Asian and non-South Asian ethnicity. The number of infants who switched from no ROP to ROP and vice versa where ROP regressed spontaneously during the course of imaging, was also documented.

An abnormal ocular examination other than diagnosis of ROP, and treated ROP, were exclusion criteria. Premature infants who were born under 37 weeks GA (Spong 2013) but did not require ROP screening were also recruited to the study.

ROP staging criteria were in accordance with the international guidelines (ICROP 2005). For the purpose of the study, ROP was defined as stages 1-3 using the UK guidelines (stages 4 or 5: partial or total retinal detachment, respectively, were excluded from the study) (RCOphth, RCPCH, and BAPM 2008). At the time of imaging no infants had received treatment for ROP and the highest classification of ROP was stage 3 in zone 2. Data from infants requiring treatment was included up until treatment was performed.

A neonatal research nurse assisted with recruitment by identifying babies suitable for inclusion and by approaching parents initially. Recruitment consisted of informing parents, who were given a leaflet outlining details of the study aims and objectives. Informed consent was subsequently obtained from parents/guardians of all participants prior to commencement of ocular imaging.

Case Report Forms (CRF) for each participant including consent were kept confidential and filed in the Investigator Site File and all documents were stored in a locked and designated space within the University of Leicester, Ophthalmology group premises.

*4.12 Population*

The Leicester Royal Infirmary NNU covers Leicester City and Leicestershire County. Leicester City is an ethnically diverse population of an estimated 330,000 people with a high proportion of citizens from non-White British ethnic groups (42%). The County of Leicestershire has an additional 620 000 persons with a predominantly White British population (90%).

There is wide socioeconomic variation with 20% of City residents claiming benefits and Leicester is the 25$^{th}$ most deprived local authority in the United Kingdom according to the 2009 Index of Multiple Deprivation. While 25% of City local authorities are in the 10% most deprived in the United Kingdom, 1% of the County local authorities are in the worst 10% indicating higher socio economic status in the County (Statistics 2012; Council 2011; City Council 2012).

The study population demographics are relevant given that maternal ethnicity and socioeconomic inequality has been described as a risk factor in the incidence of very low birth weight preterm birth and ROP severity (Aralikatti et al. 2010; Husain et al. 2013; Smith et al. 2007).

One hundred and seventy-four preterm infants were successfully recruited over from April 2012 until October 2015 to the study. Infants in whom foveal cystic changes were observed were analysed separately and discussed in Chapter 7.

## 4.2 Equipment and acquisition of data

### *4.21 Introduction*

The study was as a collaboration between members of the Ophthalmology Group and the Neonatal Service. Recruitment of participants was undertaken by a research neonatal nurse (S Brown, SB), a research ophthalmologist (Dr A Patel, AP) and the author (SA). Acquisition of images for the study was conducted by the author (SA) and AP from 2012 to 2015. Facilitation of access to preterm infants and their parents was achieved through co-ordination by the Neonatal Department (Head of Service Dr Jonathan Cusack, Dr Joe Fawkes and Deputy Sister Hima Thanki).

Over 1000 raw OCT foveal image data were reviewed and images selected by SA for analysis in JPEG format for segmentation. Segmentation macros and 'difference of gaussian' foveal width measurement tools were developed by Dr Proudlock, images were segmented and analysed by SA (further details to follow) and masked observers included two ophthalmologists (AP and Dr H Lee, HL).

Data were stored on Microsoft Excel workbooks, cleaned and grouped by SA. The exploratory statistical analysis was undertaken by SA and discussed with Dr Proudlock and Dr Nath (Senior Biostatistician). Linear mixed regression modelling was developed by Dr Nath through a collaboration with the SA over a period of four years and resulted from regular discussion regarding the preliminary statistical analysis and clinical

interpretation by SA for all three research aims. Dr Proudlock developed the foveal movie (https://www.dropbox.com/s/z2vo8qdl0t5blli/video%201%20.avi?dl=0) (video1) and guided SA on the process for composition of moving schematic images from the data using Microsoft® Excel.

*4.22 General principles of OCT*

Optical coherence tomography (OCT) of the retina permits in vivo visualisation of the retinal layers possible through the use of computer algorithms. The technology is based on the principle of interferometry (Schmitt 1999).

Interference is a physical phenomenon in which energy in the form of two waves collide with one another. The resultant wave of greater or lower amplitude forms a pattern where energy levels (intensity) reach a minimum or a maximum and anything in between. If the waves come from the same energy source or have similar wavelengths the interaction of the waves may be described as coherent or incoherent depending on the interaction.

Constructive interference occurs when the maximum of one wave meets the maximum of another wave, and the displacement of the two maxima is the sum of the individual waves at the same point. Destructive interference is the opposite when the maximum of one wave collides with the minimum of the second wave so that the combined displacement is zero.

The difference between constructive and destructive interference depends on the difference between the waves and these differences are known as phases. The pattern/intensity of interference can map out the difference in the phase between the two waves.

Instruments that use this principle essentially transmit light (known as the sample light) on to the object of interest e.g. retina, and measure the interference when the sample light is reflected back towards a reference light. The 'back scattering' of the light will vary according to the difference in structure of the tissue sample, since each tissue component will demonstrate varying optical properties. As a result of this, the time taken for the light to backscatter will also vary and the differences in the time for

structures, known as a delay or echo, may then be measured, giving an outline for the structure of interest.

The reflected sample light and the reference light must have similar light paths or optical lengths determined by the wavelength of the light being used otherwise a sufficiently useful interference pattern is not produced. This is known as the coherence length, or distance between which the two waves may interact, in order that interference is produced. The coherence length of light is indicative of the bandwidth of the light source. OCT devices state the bandwidth of their light sources so that the resolution capability may be specified.

Resolution depends on the coherence or the wavelength/bandwidth of light being used because if there is a larger difference travelled by the different arms of reflected light than the wavelength of the light used, interference will be poor or absent. A high-bandwidth light source has a very low-coherence length, and a low-bandwidth light source has a very high coherence length (Fujimoto et al. 2000).

High or broad bandwidth light with low coherence length, typically near-infrared, is preferred in OCT. The longitudinal resolution, governed by the coherence length, is inversely proportional to the optical bandwidth of the light source so that as the coherence length decreases, smaller spaces and higher axial resolution is possible. Tissue that reflects back a lot of light will create greater interference (more intensity) than areas that do not. This appears bright on OCT images, such as retinal nuclear layers while fibre layers such as the plexiform layers appear less bright.

This reflectivity profile or axial depth scan, called an A-scan, contains information about the spatial dimensions and location of structures within the tissue of interest. A cross-sectional tomograph known as a B-scan may be achieved by laterally combining a series of axial depth A scans. This is shown in Figure 4.1 which illustrates the orientation of A-scans, stacked against each other to create the B-scan. The B-scan represents a cross-section of the fovea. The en-face view is also shown in Figure 4.1.

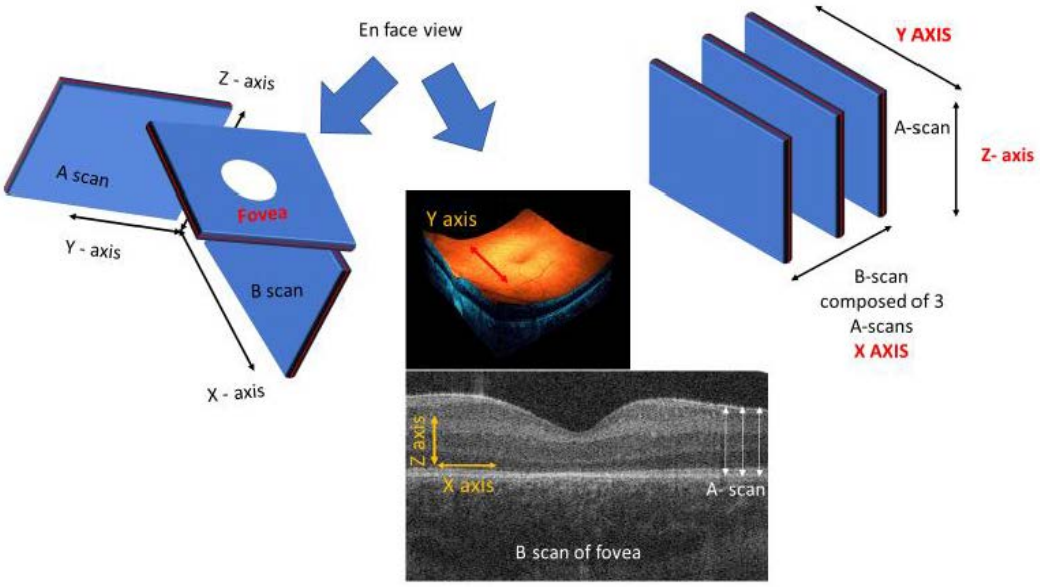


**Figure 4.1 Schematic with original infant OCT image showing orientation of A-scans, B scans and en-face view of foveal depression**. 3-D foveal image courtesy of Dr M Thomas and Prof Gottlob.

Spectroscopy is the technique of separating different components of electromagnetic emissions and measuring the intensity of those components e.g. different wavelengths in light source such as white light or light from a torch or from crystals etc. Monochromatic spectroscopy is where one wavelength at a time is measured by blocking all the others. This can be time consuming.

In spectral domain (SD) OCT, different wavelengths are used to obtain as much detail as possible about the tissue using the various wavelengths to produce multiple interference intensities.

In order to detect the many wavelengths, Fourier analysis is used. A Fourier Transform is a mathematical method of analysing different components of a sinusoidal wave so that individual components may be isolated and decomposed into an algebraic equation. Points in the signal are now simpler to remove or detect which is particularly useful where a waveform is complex such as a high bandwidth light wave that contains many sinusoidal forms/wavelengths similar to that used in SD OCT.

*4.23 Hand-held OCT device and image acquisition*

Imaging was performed at 1 to 2 weekly intervals after dilation of pupils in preterm infants recruited from the weekly ROP screening ward round as described above. Imaging of the supine preterm infant participants in the study was performed using a portable (hand-held, HH) non-contact SD-OCT device, the Envisu™ C-Class OCT (Leica Microsystems). The device is shown in Figure 4.2. The hand- held probe is positioned vertically over the supine infant's eye, while the en-face view and cross-sectional B-scan images are seen on the device screen.

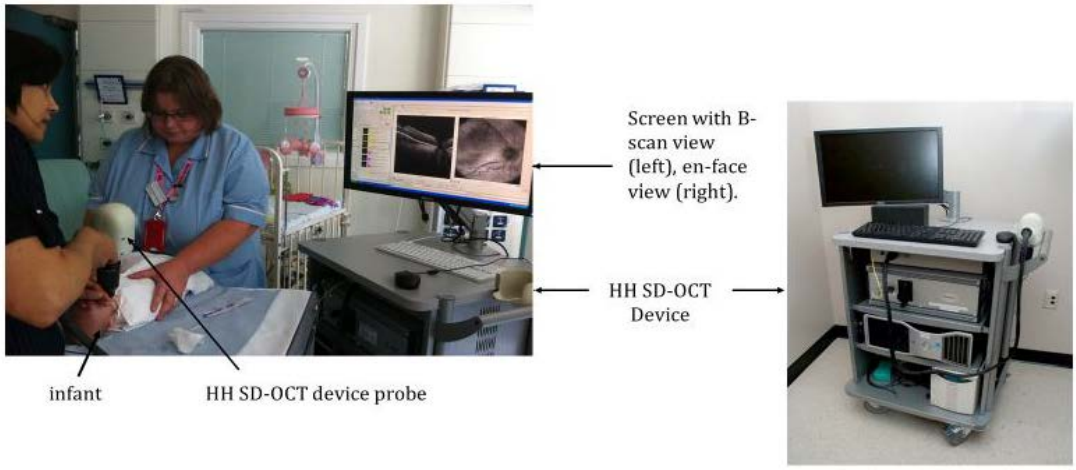


**Figure 4.2. Envisu C-class portable hand-held spectral domain optical coherence system** (Leica Microsystems). The infant is swaddled by research nurse (SB) while the probe is directed vertically over the infant's eye by the operator (SA). The desired image is viewed on the device screen before capture.

The Envisu C2300-VHR (very high resolution of 3-5µm) OCT has a 2.5mm imaging depth in tissue. VHR has a broad optical bandwidth and the broader/higher the bandwidth, the greater the resolution achieved. As discussed earlier, this is due to the reduced coherence length, because as coherence length decreases, smaller spaces are visible and more detail is captured on the image.

The HH SD-OCT may be customised for use depending on the requirements for imaging. It has a supine and upright facility; supine settings were used for infant imaging as shown in Figure 4.2 where the infant is being imaged in the supine position.

Optimisation of B scan quality is a balance between speed of acquisition and the number of A scans acquired per B scan. Therefore, scans were customised for imaging the macula to obtain a single high-quality scan at the central retina. This sequence was chosen because it has a high B-scan density with the aim of getting the best central foveal scan.

The rectangular (raster volume) scan consisted of a series of parallel B scans with 500 A scans (each A-scan having a width of 25µm) for each B scan, and 100 B scans (each having a width of 50µm) over a 5.0 mm x 10.0 mm area (see Figure 4.1 to review orientation of B-scan and A-scans). The total scan time was 2.9 seconds (or 5.8 milliseconds per B scan).

The width of 10 mm allowed the optic nerve to be captured in order to use it as a landmark to locate the fovea particularly in very young infants where the location of the fovea was not always evident on the B-scan view while acquiring the image. This was useful where the foveal depression was shallow and the imaging time was brief. En-face views aided in centering the B-scan capture.

A reference arm on the HH SD-OCT device allowed adjustments according to a Standard Reference Table as described by Maldonado and colleagues (Maldonado et al. 2010). The lateral distance settings (defined for adults on the machine) were corrected to account for the smaller axial lengths in the infant population using a conversion table according to PMA and GA from the data presented by the study authors. The authors recommended optimising scans with respect to the paediatric eye due to the impact of refractive error and axial length on magnification and field of view when using HH SD-OCT. This was based on the calculated optical parameters (refraction, axial length) as functions of age for infants by analysing the literature on eye growth in this group and developing a theoretical eye model for preterm infants.

*4.24 Challenges with image acquisition*

In the main, images became easier to acquire after an initial learning curve which involved the operator becoming familiar with the weight of the probe, the distance that the probe was held above the infant eye and recognizing the central ocular landmarks of the optic nerve and adjacent central retina.

A number of challenges in image acquisition were encountered initially at the commencement of the study which are detailed below. This resulted in a greater number of participant images being excluded due to image quality in the early months of the study. Subsequently, solutions were developed to maximise image acquisition which gradually became less problematic with recognition and the number of successful images increased in the first year of the study period:

- A time of 10 minutes per eye was set to limit the stress of handling for each baby and to enable the ROP ward round to continue smoothly. In the initial 6 – 12 months this resulted in less images being acquired per ward round but image acquisition became faster with practice.
- Access to the infant – a significant number of infants were kept in incubators and were too frail to be moved on to a table top. This limited access to the infant due to the weight and size of the probe. However, with practice holding and using the probe, this became negligible.
- Access to the eye - intubated babies or babies on supplemental oxygen use continuous positive airway pressure (CPAP). This is shown in Figure 4.3 below. CPAP interfered with maintaining the probe upright. In addition, the water vapour created by this airway method needed constant wiping of the probe lens during image acquisition. This further lengthened the time necessary to complete imaging which was particularly difficult for the smaller sicker infants who were unstable. However, CPAP also interferes with ocular examination during ROP screening and the CPAP mask may be angled laterally without interfering in oxygen delivery during ocular examination. Similarly, this was found to be an effective strategy in OCT image acquisition with the

aid of an assistant who lubricated the ocular surface and wiped the probe lens prior to image capture.

- Movement of the eyes or head - Despite the speed of image acquisition, rapid or frequent movements of either the eyes or head resulted in poor quality scans or prolonged times in image acquisition, which in some cases had to be abandoned. Thirty-six percent of all participant's images were unsuitable for analysis due to poor quality or inaccuracy.

**Figure 4.3 Preterm infant with continuous positive airway pressure (CPAP)** mask. University Hospitals of Leicester NHS Trust, England.

### 4.3 Image processing and analysis

*4.31 Images*

Captured images were saved as raw spectral data (OCT files) from which processed files could be loaded for viewing using ImageJ software with customised macros supplied by the manufacturer. We aimed to acquire five HH-OCT images per infant per eye. Repeated longitudinal images from each infant from 31 till 44 weeks PMA were included in the study and analysis.

Using HH OCT, in premature infants, the outer retina is poorly developed but the inner retina is proportionally thicker and forms a continuous band across the foveal location (Maldonado et al. 2011). A foveal depression may be identified on close inspection,

and successful identification of the fovea was achieved by examining 5 uninterrupted B scan images on either side of the B -scan image with the deepest point in the central retina (Lee et al. 2013) as shown in Figure 4.4.

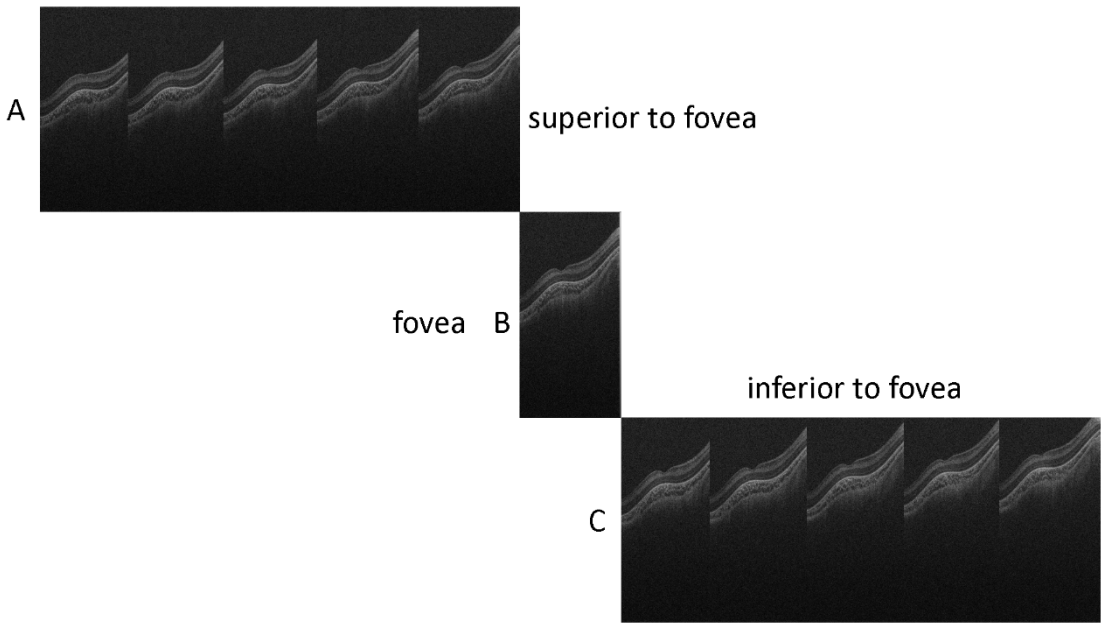


**Figure 4.4 Sequence of 11 uninterrupted B-scans**. A – superior to fovea, B- Fovea (deepest depression, scan chosen for analysis), C – inferior to fovea.

Figure 4.4 shows five sequential images superior to the fovea (panel A), deepening of the foveal depression to maximum (panel B) and 5 images with decreasing foveal depression (panel C) as the sequence moves inferior to the fovea.

From the HH-OCT scans acquired for each infant, those with the brightest and clearest components on retinal scanning were chosen for analysis. The most suitable images were saved as JPEGs and each image was labeled with a unique identifier including the date of acquisition, the laterality (right or left) and PMA. This was done so that original raw unprocessed spectral image data could be identified from a JPEG if further evaluation or repeated review was necessary.

*4.32 Image Segmentation*

Analysis of the JEPG images was performed using ImageJ software (U.S. National Institutes of Health, Bethesda, MD) and customised layer segmentation macros after flattening of JPEG images using Bruch's basement membrane as a reference line and translating individual A-scans vertically.

Figure 4.5 shows a B- scan image (A) which has been flattened (B) prior to analysis. The boundaries include the foveal contour (ILM), the individual retinal layers and the junction between the retinal pigment epithelium (RPE) and the choroid. An example of the results of segmentation of the image is shown in schematic form (C).

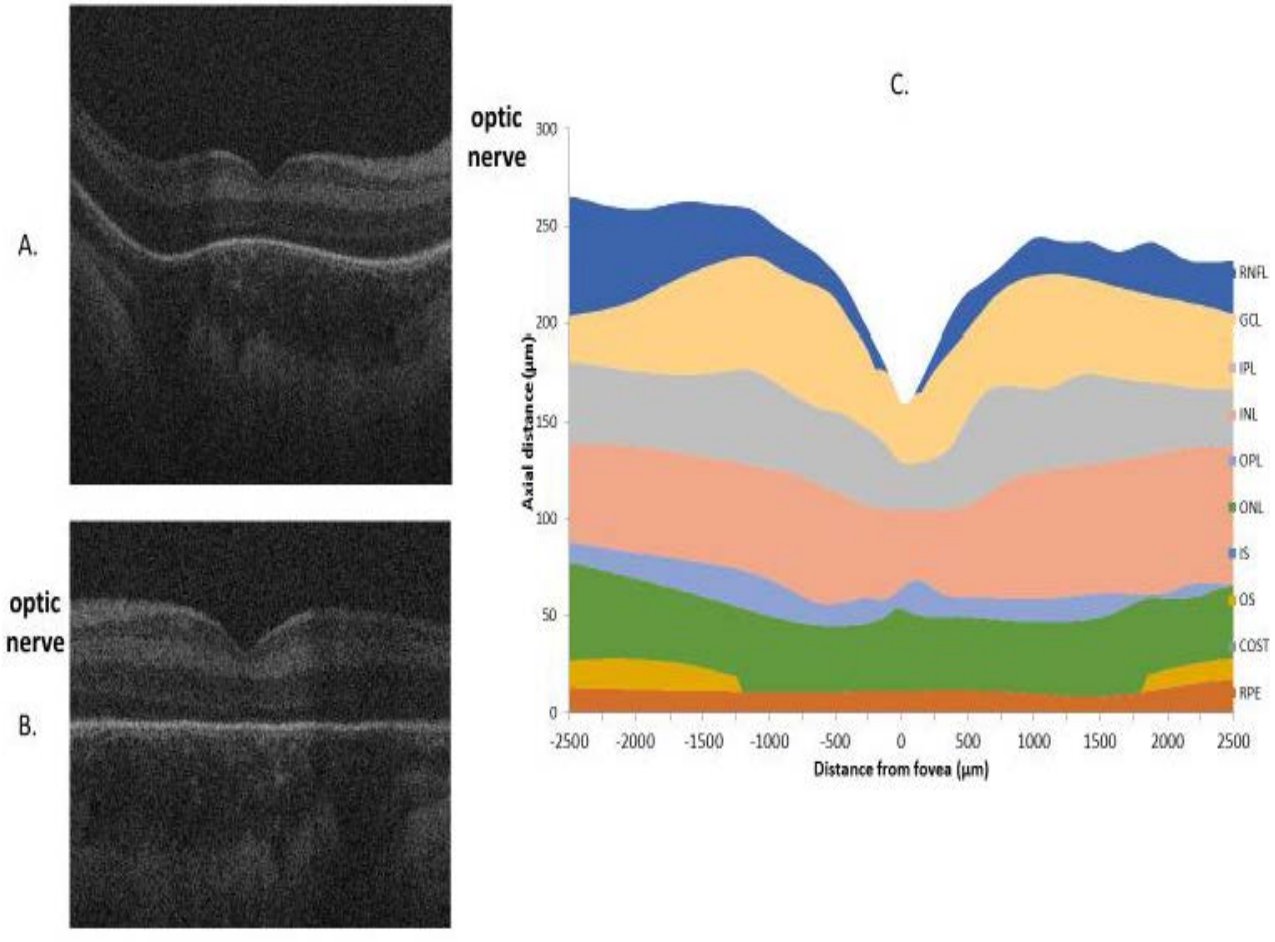


**Figure 4.5. A. Original optical coherence tomograph B- scan of the right foveal depression**. **B** shows the same scan after flattening of the image. The image has been flipped horizontally so that the optic nerve is now located on the left. **C** depicts a schematic of individual retinal layers after image segmentation with each layer identified on the right vertical axis, the axial distance or thickness in microns of each layer on the left vertical axis. The location of each layer as a distance on either side of the fovea in microns is shown on the horizontal axis. Nasal is left and temporal is right of the fovea.

Boundary detection of the ILM was performed using semi-automatic segmentation where automated detection utilised the ImageJ plugin 'ABSnake' for the ILM and other border layer edges were identified using a manual process locating points on the border which were fitted with a cubic spline. Fine adjustment of the fitted line was used to generate the final segmentation.

As mentioned above, the lateral scaling of each image was estimated using previously reported pediatric axial length data due to the change in axial length from 32 to 40 weeks postmenstrual age (15.44 to 16.84 mm respectively) (Maldonado et al. 2010) and based on information provided by the manufacturer.

Manual segmentation defined layers according to the reported literature (Toth et al. 1997; Pons and Garcia-Valenzuela 2005; Srinivasan et al. 2008; Spaide and Curcio 2011; Dubis et al. 2012; Vajzovic et al. 2012; Kafieh, Rabbani, and Kermani 2013; Staurenghi et al. 2014). Individual layer thicknesses were calculated between border edges using ImageJ and Excel macros.

Details of the retinal layer border definitions used in the study analysis are shown in Table 4.1.

| | | |
|---|---|---|
| Retinal Pigment Epithelium | RPE | Upper RPE border to lower RPE border |
| Retinal thickness | RT | Internal limiting membrane (ILM) to upper RPE border |
| Retinal nerve fibre layer | RNFL | ILM border to upper GCL border |
| Ganglion cell layer | GCL | Lower RNFL border to upper IPL border |
| Inner plexiform layer | IPL | Lower GCL border to upper INL border |
| Inner nuclear layer | INL | Lower IPL border to upper OPL border |
| Outer plexiform layer | OPL | Lower INL border to lower border of OPL |
| Photoreceptor complex | PRC | Lower border of OPL to upper border of RPE |
| Inner retinal thickness | RT Inner | RNFL+GCL+IPL+INL |
| Outer retinal thickness | RT Outer | OPL+PRC |

**Table 4.1 Retinal layer borders and definitions** used in the study.

The choroid was identified and segmented from the outer border of the RPE to the inner scleral border/outer border of the choroid (Spaide, Koizumi, and Pozzoni 2008; Moren et al. 2013; Bidaut-Garnier et al. 2014). The choroid is more visible in infants, due to the decreased density of the pigment in the RPE during development (Robb 1985).

*4.33 Difficulties with Segmentation - the developing outer retina*

Previous reports using HH SD-OCT describe that the inner retinal layers are generally present across the central retina in preterm infants from 30 weeks' postmenstrual age (Maldonado et al. 2011; Dubis et al. 2012; Vajzovic et al. 2012). Good quality images were considered to be those where the inner retinal borders were detected. Images where the inner retinal borders could not be defined were therefore discarded.

In the developing outer retina, a border was labelled absent if it was not present where the image was of good quality. Borders were labelled as missing where an edge was present but uneven or incomplete.

Outer retinal borders including the external limiting membrane, ELM (also known as the outer limiting membrane), and the previously labelled IS/OS (inner /outer segment), now called the ellipsoid zone (EZ) (Staurenghi et al. 2014) were challenging to detect. This was partly due to the delayed maturation of the photoreceptor layer in very preterm infants (Vajzovic et al. 2015) and partly because the outer retina is rudimentary before term and in early infancy (Yuodelis and Hendrickson 1986; Dubis et al. 2012; Vajzovic et al. 2012; Lee et al. 2015).

Defining the lower border of the outer nuclear layer depends on the detection /presence of the ELM border. In many early gestation infants compared with later born infants, the ELM was absent. An example is shown in Figure 4.6 below.

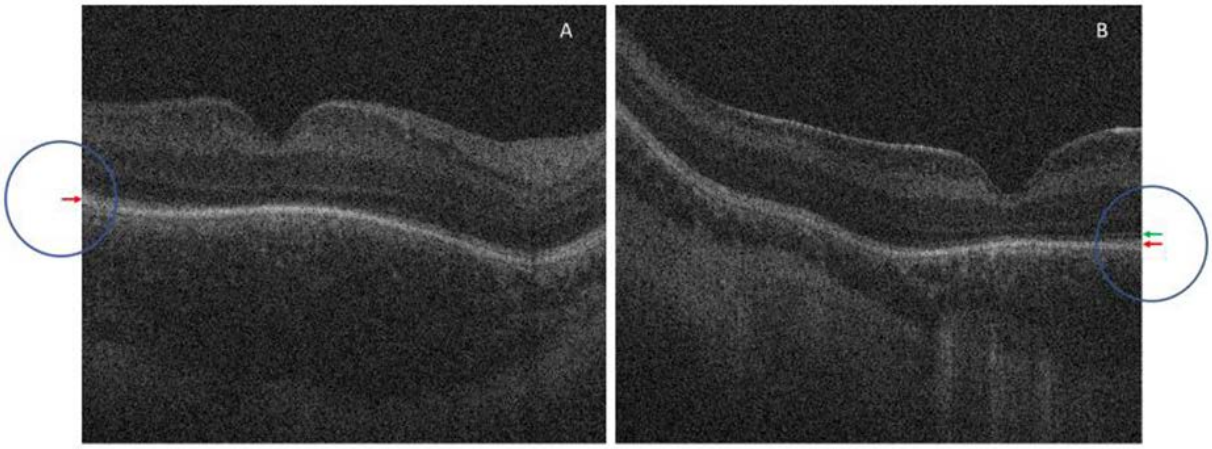


**Figure 4.6. Hand-held optical coherence images of two separate preterm infants acquired at mean postmenstrual age 36 weeks.** The green arrow denotes the external limiting membrane, the red arrow points to the location of the photoreceptor layer. The ELM is not visualised on image A. *GA – gestational age*, *ROP – retinopathy of prematurity*

Figure 4.6 illustrates that the ELM is not always visualised in OCT images of preterm infants in the preterm period. The outer nuclear layer (ONL) is defined from the lower border of the OPL to the upper border of the ELM, but where the ELM is missing, it is not possible to define the ONL. As a result, analysis of ONL thickness, and individual photoreceptor borders was not possible. Furthermore, the OS could not be identified in images taken before 42 weeks PMA, and the IS was variably absent centrally. Therefore, the outer retina to the upper border of the RPE but not including the OPL was collectively labelled as the Photoreceptor Receptor Complex (PRC) as defined in Table 4.1. In addition, the presence of a hyperreflective band at the location of the OPL could be an artifact in the developing retina so the outer retina (OPL+PRC) was used in the analysis.

*4.34 Difficulties with Segmentation – the developing retinal layers*

In normal adult retina, automated and manual segmentation has been shown to be comparable (Bagci et al. 2008), but developing boundaries such as in the premature retina pose a particular challenge for fully automated edge detection segmentation tools. Therefore, manual segmentation was used in assessment of retinal layers in this study. Due to the variation in layer definition especially of the developing outer layers,

images were inspected for differences between preterm infants by 2 independent masked observers. Scans were numbered and observers were unaware of the details of the infant for each image [gender, GA, PMA, and Diagnosis (presence or absence of ROP)]. The masked observers described integrity of contours for each layer particularly at the fovea. A binary system of grading was utilised where a change of contour was recorded as being present or absent, with any additional comments by the observer.

*4.35 Examples of the developing fovea and layers with postmenstrual age*

The following figures demonstrate the change in visibility of layers with PMA on B-scan OCT images during development.

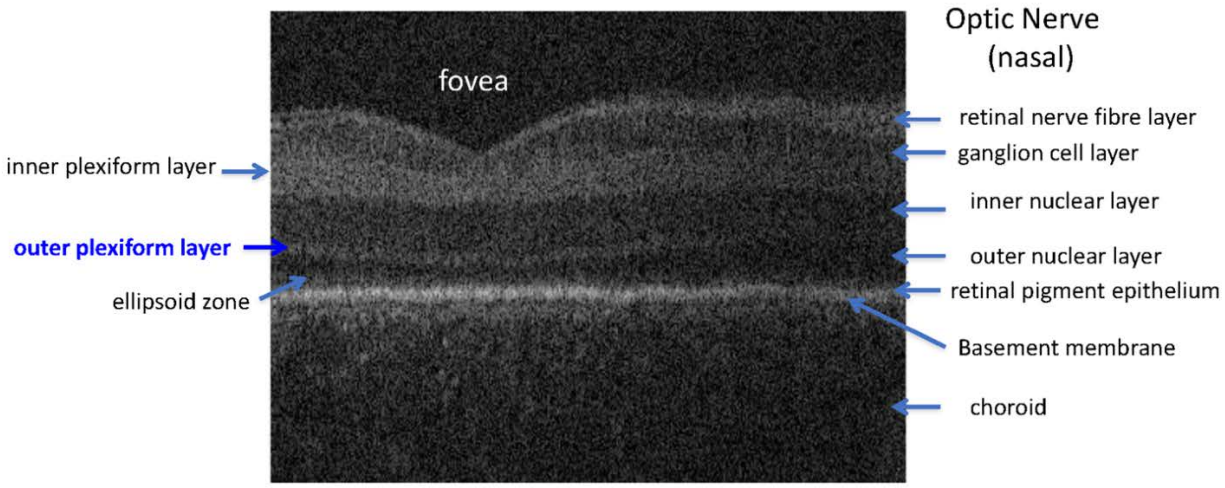


**Figure 4.7. Early postmenstrual age (PMA) flattened HH SD-OCT B -scan of right fovea**. Image acquired at **31 weeks PMA** from preterm infant born at 29 weeks gestational age.

Figure 4.7 shows an immature central retina with shallow foveal depression where the inner retinal layers cross the fovea. The outer retina is thinner than the inner retina. The ellipsoid zone (EZ) is just becoming visible peripheral to the fovea but the ELM is absent on this image. Note that the hyperreflective band labelled as outer plexiform layer' could be an artifact in the early preterm developing retina.

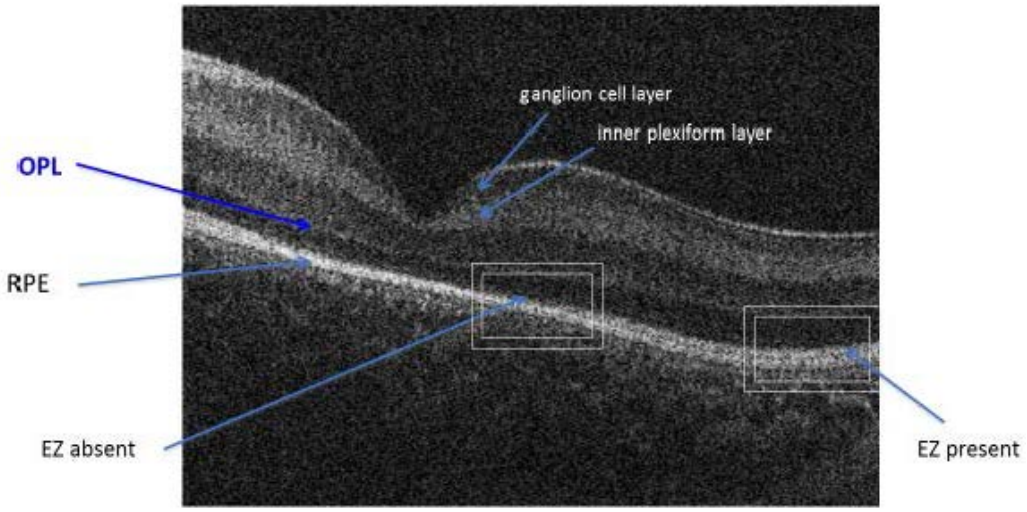


**Figure 4.8 Mean postmenstrual age (PMA) flattened HH SD-OCT B -scan of left fovea**. Image acquired at **36 weeks PMA** from preterm infant born at 26 weeks gestation age. *OPL - outer plexiform layer, EZ – ellipsoid zone, RPE – retinal pigment epithelium.*

In Figure 4.8, the fovea is deepening while the GCL thins centrally. The outer retina is becoming more distinct as shown by the appearance of the EZ peripherally (white box) where a hyper-reflective bright layer appears above the RPE, but remains invisible centrally (white box). This indicates that central photoreceptors, particularly cones which are located at the fovea, remain rudimentary. A dark line between the EZ and the RPE in the periphery indicates the appearance of early photoreceptor outer segments. The ELM is present above the EZ peripherally (not marked).

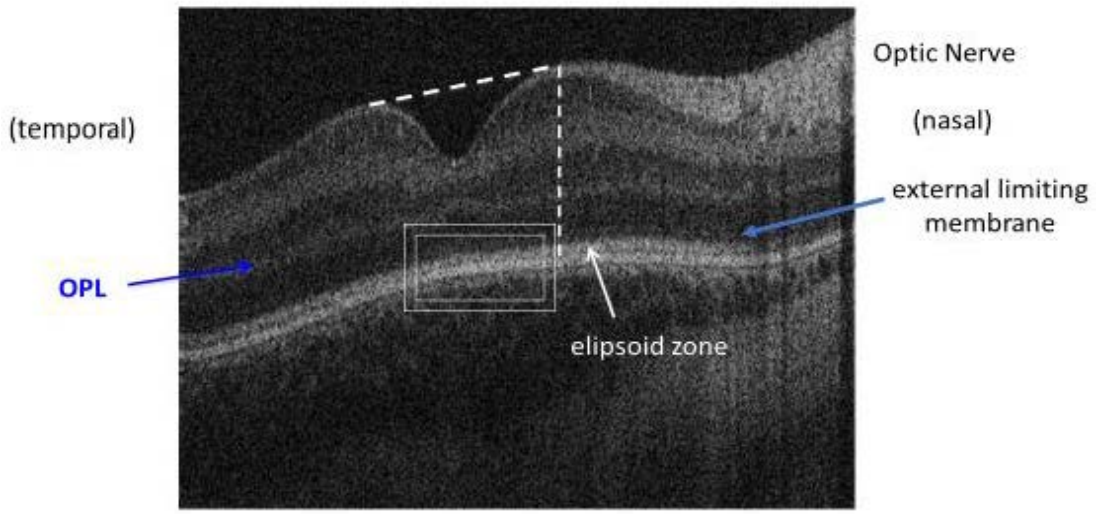


**Figure 4.9 Late postmenstrual age (PMA) flattened HH SD-OCT B -scan of right fovea**. Image acquired at **42 weeks PMA** from preterm infant born at 26 weeks gestation age. *OPL - outer plexiform layer.*

In Figure 4.9 the most notable feature is the presence of a continuous bright band centrally in the outer retina which correlates to the EZ (double white box) i.e. cone photoreceptors are now detectable. Note also that the total retinal thickness (RT) nasal and temporal to the fovea is increased (vertical dotted line shows the nasal RT). The thickness of the outer retina and inner retina is similar and the central cone photoreceptor outer segments appear centrally as a hypo-reflective band sandwiched between the EZ and RPE hyper-reflective bands. The ELM is now visible across the fovea.

The figures above show the changes at the fovea with PMA but do not indicate if there are differences between infants born at different gestational ages, birthweights or if presence or absence of the diagnosis if ROP influences the layers or foveal depression. This will be explored further in the following chapters.

*4.36 Foveal morphology measurement*

There is currently no standard methodology regarding the measurement of foveal shape dimensions but mathematical models have been described utilising a principle known as 'Difference of Gaussians' (DoG) (Basu 2002).

The fovea was modelled using a DoG customized fit based on previous literature (Dubis, McAllister, and Carroll 2009; Liu et al. 2016) and analysis of the images was performed using customized layer segmentation macros written in ImageJ software (United States National Institutes of Health, Bethesda, MD, https://imagej.nih.gov/ij/, downloaded on December 2013). Foveal parameters included width, area and depth, central foveal thickness, steepest slope of the foveal wall and parafoveal retinal thickness (see Figure 4.12 below, p67).

Foveal shape dimensions were analyzed using an enhanced model based on the model described by Dubis et al (Dubis, McAllister, and Carroll 2009). Using DoG methodology, the authors assumed a symmetrical foveal diameter (rim to rim) but recognised that there can be differences in height between the nasal and temporal rim. Foveal shape varies with age, race and gender (Nesmith et al. 2014; Wagner-Schuman et al. 2011;

Shin et al. 2015) and asymmetry of measurements has been shown in population-based studies of young children (Huynh et al. 2007). Liu et al (Liu et al. 2016) described a flexible piecemeal Gaussian fit to improve accuracy where foveal pit asymmetry exists while Scheibe et al (Scheibe et al. 2014; Scheibe et al. 2016) developed a 3-dimensional one-sided fovea contour fit in order to model asymmetric foveal shape. In an effort to overcome the variations in foveal shape, Moore et al (Moore et al. 2016) presented an algorithm called 'FOVEA' to quantify variations in foveal slope, width and depth using images (histology or OCT) in order to study comparative dimensions between vertebrates.

Since the fovea is asymmetric as reported by Liu (Liu et al. 2016) we modelled the nasal and temporal aspects of the fovea separately. The DoG fits were calculated using Solver, an add-in tool in Excel, (Microsoft Corporation, Seattle, USA). The aim of the Solver Tool was to reduce the root sum of squares of the differences between the actual and fitted values by adjusting the height and width terms of the Gaussians. An additional term was added to reduce the error between the bottom of the foveal pit values and the nasal and temporal fit. The starting points approximate to typical foveal profile consisting of a narrower inverted Gaussian which mainly fits the pit and a wider non-inverted Gaussian which mainly fits the parafovea. For consistency, this method was used on all images including those where the parafovea was fitted with a non-inverted Gaussian.

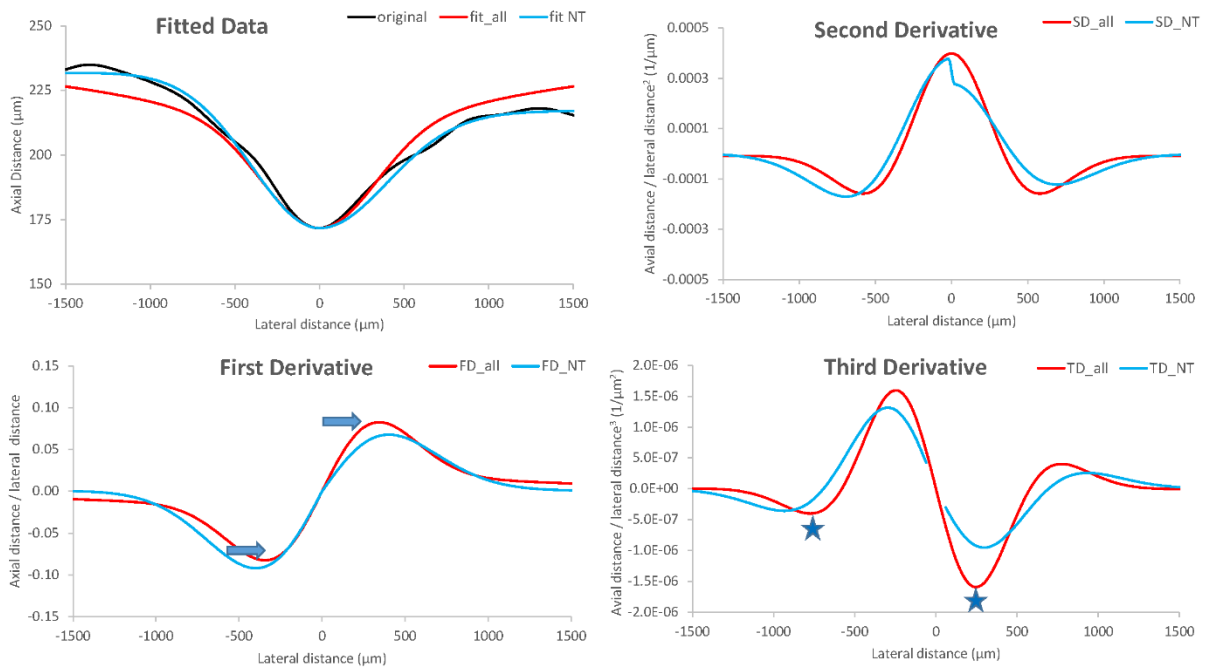


**Figure 4.10 Difference of Gaussians using Solver tool.** Fitted data graph shows 3 foveal internal limiting membrane (ILM) contours. The original is grey and superimposed is the assumed symmetric Gaussian (fit all, in red) and the asymmetric nasal - temporal fit (fit NT, in blue). The first derivative graph illustrates the maximum rate of change (blue arrows) using symmetric and asymmetric fitting technique, the third derivative graph indicates the points where the rate of change in contour was minimal (blue stars).

The model we developed used two halves of the foveal shape (nasal and temporal) through modelling the nasal and temporal retina separately (flipping the profile of each around the foveal centre by 180 degrees).

In the model by Liu (Liu et al. 2016), the two rim points that determine the maximum diameter of the foveal depression were taken to be at the highest points on the two sides of the pit. This was determined from points of inflection where the direction of the ILM changes direction. However, in many preterm infant images, the foveal contour continues to increase beyond the foveal rim. An example is shown in Figure 4.11.

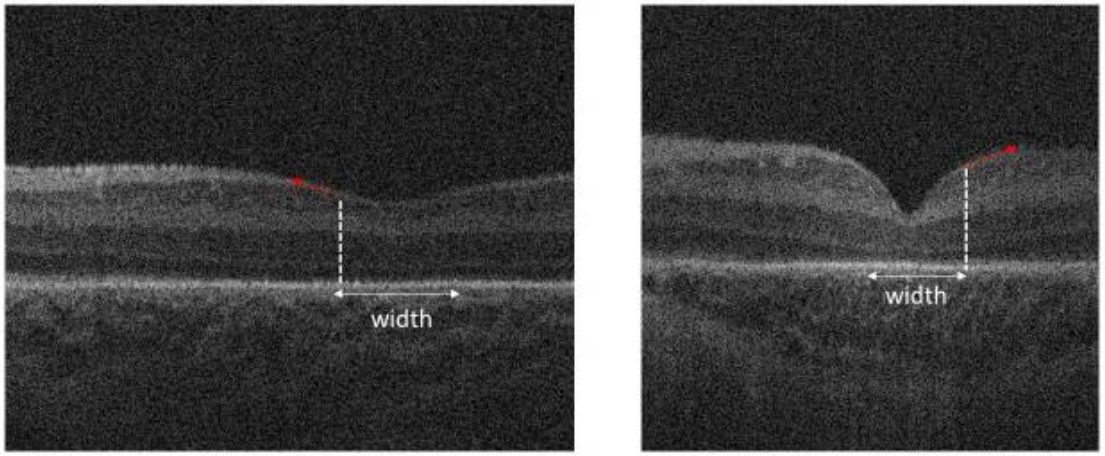


**Figure 4.11 Example of preterm infant flattened HH SD-OCT images of the foveal pit showing continuation of internal limiting membrane (ILM) beyond width edge**. The image on the left is at 34 weeks PMA, and on the right at 36 weeks PMA. The ILM contour continues to rise (red arrows) beyond the measured width which ends at the vertical dotted line.

Therefore, in the developing retina, the inverted Gaussian has an upper constraint on width since the wider Gaussian fitting of the parafovea, which extends beyond the edges of the fovea, can also follow an inverted profile in contrast to adult retina.

A calculation of the rate of change of the foveal slope using the changes in the ILM contour was used. A rate of change is known as the first derivative and where the ILM contour (i.e. slope) change is minimal is a good approximation of where the foveal rim begins. This is seen in Figure 4.12 which illustrates the equivalent 1$^{st}$ derivative of the foveal ILM.

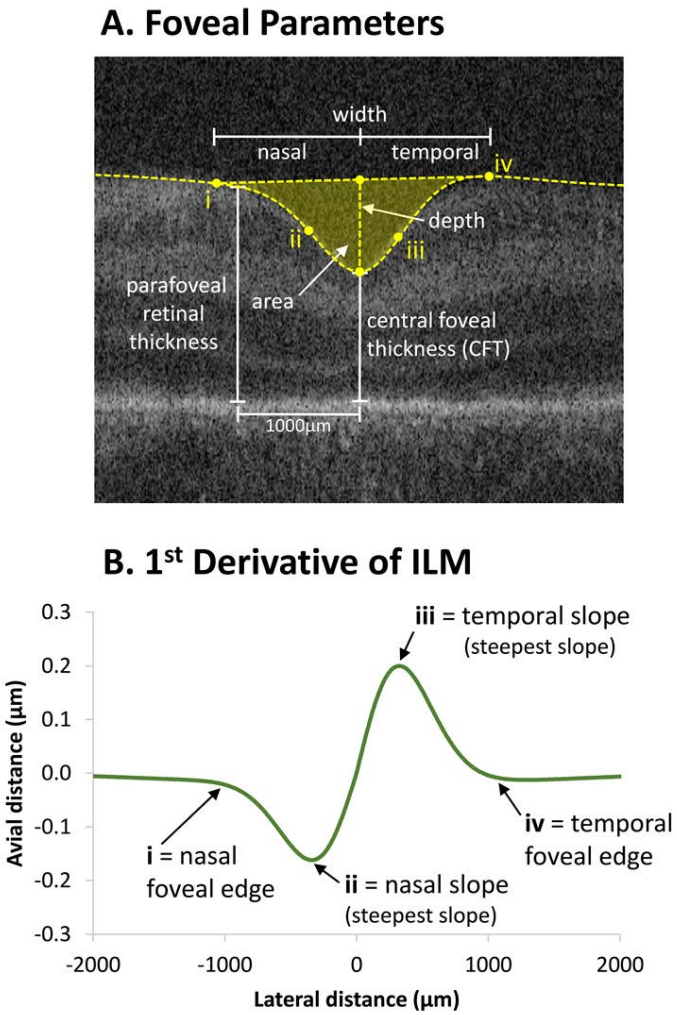


**Figure 4.12** (A) **Foveal parameters are shown with respect to an original optical coherence tomography B- scan image.** The nasal and temporal edges of the foveal depression are indicated by (i) and (iv), and the steepest foveal slope by (ii) and (iii), respectively. Parameters (i-iv) are defined using first, second and third derivatives of the internal limiting membrane (ILM). These are shown in (B) with respect to the first derivative of the ILM.

In our model, the rim width measurement using the horizontal lateral scale was the maximum of the 3rd derivative of the ILM profile. This is the earliest indication of the falling away (minimal slope change) of the ILM to form the foveal pit. This equates to the points on the first derivative graph where the rate of change in slope is minimal. Note that these points located nasally and temporally are not identical further illustrating the asymmetry of the foveal depression.

The blue arrows on figure 4.10 show the maximum nasal (negative) and temporal (positive) curves which represents the steepest slope angles nasally and temporally in the foveal pit (Wang et al. 2012b).

The parafovea is located 1000µm from the foveal centre. The maximum angle of slope was identified at the point of maximum steepness (blue arrows on figure 4.10). Area (nasal and temporal) was also calculated.

## 4.4 Statistics Analysis

### *4.41 Study design and sample size*

This was an observational study (Mann 2003; Mathes and Pieper 2017) with mixed cross-sectional and longitudinal data conducted from 2012 until 2015. A number of individuals had only a single observation and others had repeated measurements. Dynamic changes were described using this approach which is comparable to previous studies (Maldonado et al. 2011). The analysis of repeated measures required a predictive model to adjust for both between subject differences, e.g. gestational age, birthweight, but also within subject variance such as repeated time intervals or right and left eyes. This is discussed in further detail below.

A provisional sample size was based on detecting a 15% difference in macular thickness between infants with and without ROP using an online calculator (https://www.stat.ubc.ca/) using data provided from 62 prematurely born neonates by Maldonado et al (Maldonado et al. 2011). A sample size of at least 29 infants in each group (with and without ROP) will be sufficient to detect a 15% difference in macular thickness (mean thickness 127µm, estimated standard deviation 22µm in patients without macular oedema) in each of the groups at a power of 90%.

### *4.42 Approach to data analysis*

The analysis of data was broadly split into:

- Descriptive - charts, tests of normality, decision regarding distribution and univariate analysis (SA).
- Exploratory – bivariate analysis (strengths of association), multivariate analysis adjusting for covariates (SA)

- Predictive and inferential modelling - repeated measures and between/ within subject variation (SA and Dr Nath).

Descriptive and exploratory analysis was performed by SA using IBM® SPSS Statistics V22 software (SPSS, Inc Chicago, IL USA), fractional polynomial analysis utilised STATA® software. Predictive and inferential models were generated by Dr Nath using R software version 3.4.

Descriptive analyses included summaries of counts/percentages for categorical data and frequency tables. Tables of groups according to diagnosis of ROP, ethnicity, eye (right/left), multiplicity of birth, sex, presence or absence of foveal oedema, numbers of repeated images were used to inform further analysis accordingly.

Univariate analysis consisted of measures of location included the mean/median, standard deviation, z-score or inter quartile range (IQR) for continuous data. Histograms, bar charts, box plots and scatter graphs were utilised to visualise the data initially. Gestational age, birthweight and postmenstrual age were continuous data for each group, with postmenstrual age repeated measures. For example, Figure 7.3 (see Chapter 7, p129) plotted presence and absence of foveal oedema for each continuous variable using stacked histograms. This allowed an estimate of the sample spread and distance from the centre of the data.

Similarly, for example, the means for individual retinal layers at the fovea were used to investigate comparisons between the layers between ROP and non-ROP at the fovea or between the fovea and locations eccentric to the fovea. Initially this was performed for each PMA (30 to 44 weeks) to explore the changes across PMA for individual layers, or foveal depth, width, area, central foveal thickness for infants with or without oedema.

The choice of further analysis testing was based on distribution (normal parametric, or non-parametric) after initial inspection of the descriptive data determining the likelihood of normality. An example of how this was calculated is shown below in Table 4.2 which depicts a table of calculations exploring the normality of distribution for

mean foveal thickness of the PRC between ROP and non-ROP infants.

| | variable | mean (SD) | median | mean-median | %diff | skewness (SE) | critical value 1 skewness/SE | kurtosis (SE) | critical value 2 kurtosis/SE | 2 Standard Deviations | Estimate 95% range mean '+/-' 2SD |
|---|---|---|---|---|---|---|---|---|---|---|---|
| PRC | ROP | 40.28 (13.39) | 38.52 | 1.76 | 4.37 | 2.35 (0.236) | 9.99 | 8.39 (0.467) | 17.96 | 26.78 | 13.5 to 67.06 |
| | nROP | 34.22 (8.9) | 32.98 | 1.24 | 3.67 | 0.609 (0.185) | 3.29 | 0.596 (0.368) | 1.61 | 17.8 | 16.42 to 50.02 |

| | Normal yes or no? | | | | | | | | | | |
|---|---|---|---|---|---|---|---|---|---|---|---|
| PRC | mean-median | mean +/- 2SD | skewness | kurtosis | critical value 1 | critical value 2 | K-S/S-W tests | plots | Decision | t test | |
| ROP | low | maybe | skewed | abnormal | >3 N | >3N | sig | | not normal | Mann-Whitney U test | asymp 2 tailed |
| nROP | low | yes | skewed | moderate | >3N | >1 moderate | sig | | not normal | | 0.00 |

**Table 4.2. Mean and median central foveal thickness of the PRC between infants with and without retinopathy of prematurity (ROP, nROP respectively)**. Calculations include the percentage difference between the mean and median (%diff), magnitude of skew, kurtosis and the estimated 95% range (mean ± 2 standard deviations). *PRC – photoreceptor complex, ROP – retinopathy of prematurity*

Table 4.2 illustrates the criteria regarding how a decision was made regarding the use of either a student's t-test or non-parametric Mann - Whitney U to compare two independent samples of mean foveal thickness of the PRC for ROP and non-ROP infants.

The criteria were based on the estimated 95% range, degree of skew and kurtosis and the Shapiro-Wilk test of normality plots. Similarly, the means or medians for various parameters (central foveal thickness, depth, width, area, all individual retinal layers, oedema types) were analysed for each group e.g. sex, ethnicity, right or left eyes. The conclusion for the above example was that the mean foveal PRC was not normally distributed for either group. This approach was used throughout when assessing group comparisons.

Exploratory statistics comprised bivariate and multi-variate analyses. Bivariate analysis for continuous data consisted of comparisons between two variables i.e. Student's t-test for normally distributed continuous independent sample means or Mann-Whitney U test for non- parametric data. An example of this approach is the comparison of central foveal thickness between two groups with foveal oedema discussed in Chapter 7 and shown in Table 7.4 (see p131). Scatterplots were also used to visualise data to inspect for possibilities of linear or quadratic trajectories. In the preliminary analysis, linear relationships were assumed by the author (SA).

Correlation was utilised to measure the strength of association between two continuous variables e.g. GA and PMA, or BW and PMA reported by Pearson's (normal distribution) or Spearman's coefficient depended on sample size. Kendall rank correlation was used for non-parametric continuous data. An example of correlation calculations between gestational age and the foveal mean thickness of individual retinal layers is shown in Figure 4.13.

| CORRELATION | | retinal nerve fibre layer (RNFL) FOVEA | gestational age (weeks) |
|---|---|---|---|
| retinal nerve fibre layer (RNFL) FOVEA | Pearson Correlation | 1 | -.083 |
| | Sig. (2-tailed) | | .168 |
| | N | 278 | 278 |
| gestational age (weeks) | Pearson Correlation | -.083 | 1 |
| | Sig. (2-tailed) | .168 | |
| | N | 278 | 278 |

| CORRELATION | | ganglion cell layer (GCL) FOVEA | gestational age (weeks) |
|---|---|---|---|
| ganglion cell layer (GCL) FOVEA | Pearson Correlation | 1 | -.308** |
| | Sig. (2-tailed) | | .000 |
| | N | 278 | 278 |
| gestational age (weeks) | Pearson Correlation | -.308** | 1 |
| | Sig. (2-tailed) | .000 | |
| | N | 278 | 278 |

**. Correlation is significant at the 0.01 level (2-tailed).

| CORRELATION | | inner nuclear layer (INL) FOVEA | gestational age (weeks) |
|---|---|---|---|
| inner nuclear layer (INL) FOVEA | Pearson Correlation | 1 | -.269** |
| | Sig. (2-tailed) | | .000 |
| | N | 278 | 278 |
| gestational age (weeks) | Pearson Correlation | -.269** | 1 |
| | Sig. (2-tailed) | .000 | |
| | N | 278 | 278 |

| CORRELATION | | inner plexiform layer (IPL) FOVEA | gestational age (weeks) |
|---|---|---|---|
| inner plexiform layer (IPL) FOVEA | Pearson Correlation | 1 | -.027 |
| | Sig. (2-tailed) | | .651 |
| | N | 278 | 278 |
| gestational age (weeks) | Pearson Correlation | -.027 | 1 |
| | Sig. (2-tailed) | .651 | |
| | N | 278 | 278 |

**. Correlation is significant at the 0.01 level (2-tailed).

**Figure 4.13. Example of correlation calculations** between gestational age and mean foveal thickness for inner retinal layers.

The results of correlation were used to inform simple regression models e.g. correlation results shown in figure 4.13 shows that the GCL and INL are candidates in investigating of the effect of GA and individual mean retinal layer thickness at the fovea.

For categorical data, Fishers' exact test of independence or Chi-square test (depending on sample size) was applied to the data when comparing two groups such as sex (male/female), eye (right/left), birth multiplicity (singleton/multiple), ethnicity (Caucasian/Non-Caucasian) and diagnosis (ROP/nonROP). For example, this approach was used to explore the presence and absence of foveal oedema between groups where initial bar charts visualised differences in percentages between groups (see

Chapter 7, Figure 7.4, p133).

*4.43 Multivariate analysis*

A one-way repeated measures ANOVA e.g. comparison of the mean retinal layer thicknesses between categorical factors such as ROP and non-ROP was complicated by variances between and within subjects such as the time points between measurements. These were not fixed and identical for all subjects and data with missing records could not be analysed by repeated measures ANOVA. This then reduced the overall number of images for analysis effectively reducing the sample size. In addition, the difference between individuals was not the only random effect structure for the data, with several other levels, for example, eyes within each subject. This was not handled well by repeated measures ANOVA.

A simple binary logistic regression was utilised by SA to investigate fixed effects e.g. BW or GA effect on a dichotomous categorical variable such as foveal oedema type, or presence or absence of foveal oedema. The simple regression model could not adjust for other variables such as repeated measures with PMA. However, the results were used by SA to explore and discuss with Dr Nath possible predictor variables, informing multilevel statistical modelling that adjusted for multiple continuous and categorical variables.

*4.44 Statistical modelling*

The choice of model (s) was determined by a number of problems encountered in predictive modelling of the data as follows:

- Potential for non-linear change in retinal parameters with time (PMA).
- Comparison of three or more groups that may not follow the same time course dynamics.
- Several retinal layers measured at multiple locations from the fovea resulting in the issue of multiple comparisons and increased false positives or Type 1 error. To

account for multiple comparisons of means, the Bonferroni correction method was employed so that the overall type 1 error (α) was less than 0.05.

- Visibility of retina layers dependent on development i.e. age at birth and time for image acquisition of retinal layer (GA, PMA)
- Co-linearity e.g. BW and GA (Tariq et al. 2011)
- Mixed analysis, i.e. categorical and continuous data
- Repeated measures data within the same individual e.g. different eyes, time points and locations.
- The data were also clustered where responses are measured for each subject but the subject is part of a group / cluster e.g. presence or absence of ROP within a group of singletons or for sex.
- Fixed effects e.g. BW, GW and random effects such number of right and left eyes, or the effect of each individual on the dependent variable (random slope).
- Assumptions of homogeneity of variance (Levene's test), homogeneity of regression slopes and normal distribution of continuous variables for each categorical factor. The accuracy of a given model are reduced when these assumptions are not met and increase the likelihood of an incorrect statistical significance.

Fractional polynomial modelling was considered initially by SA based on a model developed by Dr Helena Lee (personal correspondence).

This was adapted for use in the analysis where layers were initially absent and then appeared e.g. PRC at the fovea. An example of mean retinal thickness between ROP and non-ROP is shown below in Figure 4.14 using this approach.

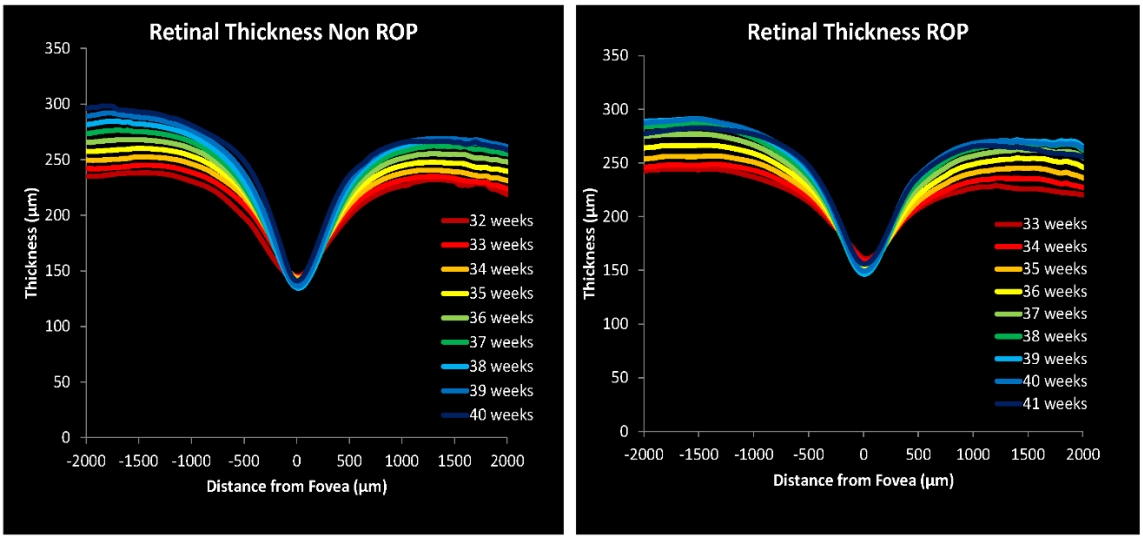


**Figure 4.14. Results of a fractional polynomial statistical model illustrating mean retinal thickness between non-ROP and ROP for preterm infants** at the fovea and eccentric to the fovea for increasing postmenstrual age between 32 to 41 weeks. The fovea is location '0', negative is nasal and positive is temporal. *ROP - retinopathy of prematurity*

However, the presence of several mixed continuous and categorical variables resulted in some difficulties in interpretation of the relationship between the dependent and explanatory variables. The fractional model also did not adjust for repeated multiple observations nor was it possible to determine the effect of gestational age or birthweight while adjusting for both diagnosis of ROP and postmenstrual age.

The author (SA) collaborated with Dr Nath in developing a multilevel linear mixed regression analysis. This required a joint approach whereby specific questions relating to the research aims which had arisen from the literature, along with the data analysis explored by SA were discussed with Dr Nath. Models were developed accordingly over time and estimated the effect of a single variable following adjustment of other variables e.g. effect of GA adjusting for PMA, repeated measures, and diagnosis of ROP on foveal parameters or individual retinal layers for multiple locations. The result was that multivariate linear mixed models were used for foveal data, and generalised additive mixed models were used for retinal data. The difference in model approach reflected the greater flexibility required to fit the data better in the retinal analysis which comprised data across many locations from the foveal centre.

# Chapter 5 Foveal Morphology

Chapter 5 addresses the first research aim which was to investigate the effect of gestational age, birthweight and ROP on foveal shape as measured by the foveal depth, thickness, width and area.

To recap, earlier HH - OCT studies in preterm infants' report persistence of inner retinal layers across the foveal depression, increased thickness of the inner retina, shallow foveae and reduced depth (Maldonado et al. 2011; Vajzovic et al. 2012; Dubis et al. 2012; Gursoy et al. 2016). However, since GA, BW and ROP are all strongly correlated, the relationship between foveal changes observed on OCT with severity of prematurity and changes associated with ROP remains unclear (Pueyo et al. 2015).

Figure 5.1 shows actual HH SD-OCT right eye images of preterm infants where the images have been acquired at postmenstrual ages (PMA) 31, 33, 35, 37 and 40 weeks. The images are flipped horizontally and flattened. For each PMA, two infant images are shown, each infant has a different gestational age (GA). A number of the infants also have ROP present or absent (nROP) at the time of image acquisition.

Inspection of the images suggests that the foveal depth and central foveal thickness is increased and decreased respectively in premature infants who are born later compared with those born earlier. However, it is not apparent regarding the effect of ROP on the foveal differences between preterm infants of different GA at similar PMA from this figure. Some the infants may well have resolved ROP (nROP) by the time the image was acquired, while others have developed ROP having initially not had any.

It is also not apparent from the figure which retinal layers account for these differences and that is the subject of investigation presented in the next chapter.

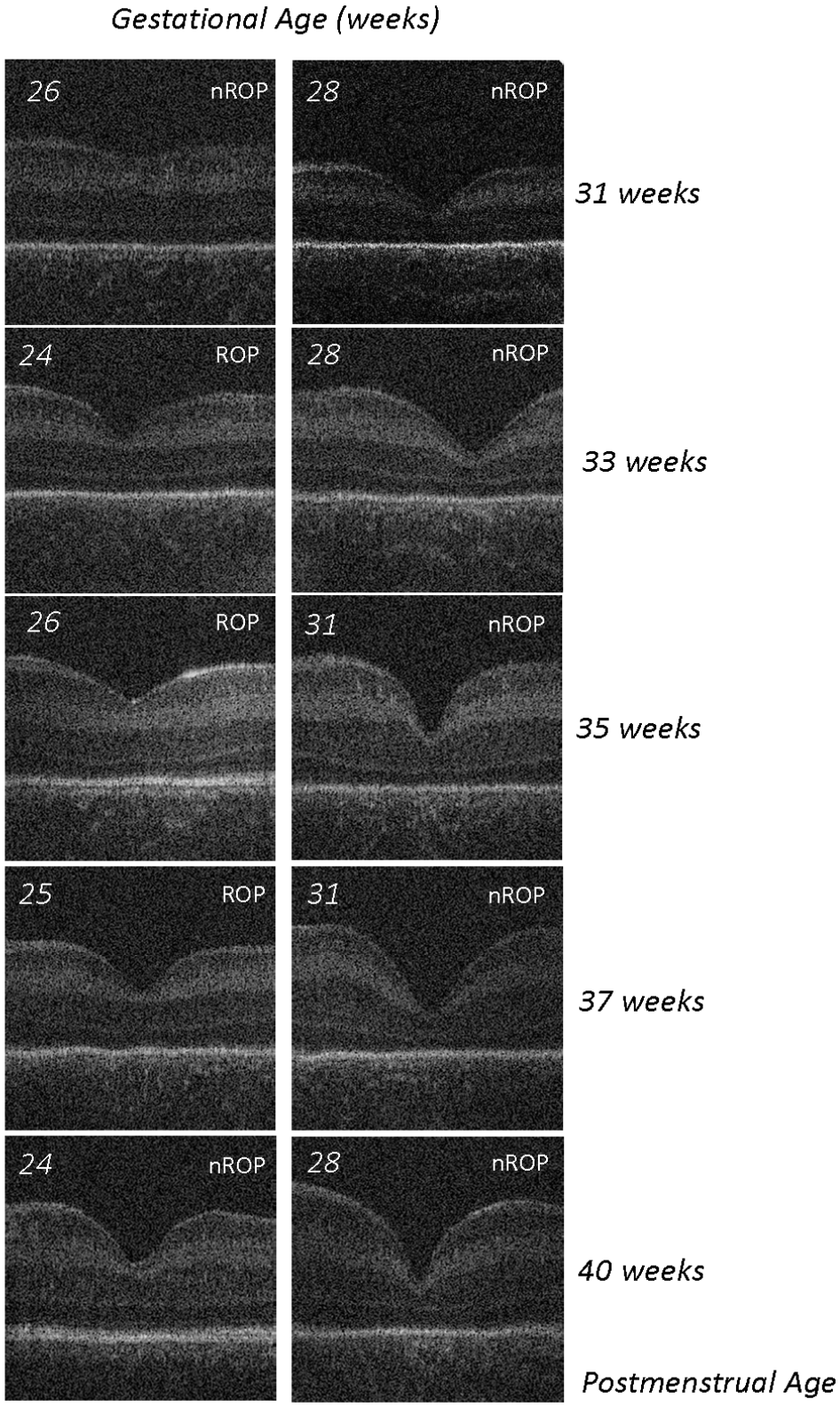


**Figure 5.1. Original hand-held spectral domain optical coherence images of infants** acquired at postmenstrual ages (PMA) 31,33,35,37 and 40 weeks. For each PMA, two images of infants with separate gestational age are shown. Only right eyes are shown, images have been flipped and flattened. *ROP – retinopathy of prematurity, nROP – no ROP present*

### 5.1 Methods

The measurement of foveal parameters was as described earlier in Chapter 4 Methods and illustrated in Figure 4.12A, p 67. As stated earlier, due to the variation of the developing outer layers, images were inspected for differences between preterm infants by 2 independent masked observers with 94.6% inter observer agreement.

Multivariate mixed models were generated to investigate the effect of diagnosis of ROP on foveal parameters described above with PMA, adjusting for the degree of prematurity (GA and BW) as well as other potential factors that may influence foveal morphology. Due to the close relationship of GA and BW in our infants with and without ROP where we found a high correlation coefficient between GA and BW (r=0.70, standard error=0.08) , we fitted separate models for all response variables incorporating either GA or BW as a predictor to adjust for the effects of GA or BW (Tariq et al. 2011).

Statistical multivariate models were generated to model changes in foveal parameters with PMA and to identify significant differences made by the absence or presence of ROP in each infant. To explore the influence of different predictor variables on the foveal morphology (response variable), we employed a separate linear mixed model for each of the following foveal variables: (i) width, (ii) area, (iii) depth, (iv) central foveal thickness (CFT, defined as the distance between the internal limiting membrane at the deepest point of the foveal depression and the upper border of the retinal pigment epithelium), (v) slope (maximum slope nasally and temporally), as well as, (vi) retinal thickness (RT) at the parafovea (1000 µm from the foveal centre). We also investigated the statistical effect of nasal and temporal location on all foveal variables except for foveal depth.

Additional predictor variables for the model were: sex (male and female), ethnicity (Caucasian and Non-Caucasian), multiple birth (yes or no), and eye (right or left). Our rationale for choosing these additional factors was based on the reported literature describing differences between the sexes in prematurity and incidences of ROP in ethnic groups and in multiple births (Ingemarsson 2003; Aralikatti et al. 2010; Friling et al. 2007). Foveal asymmetry was also explored by comparing nasal and temporal measures of steepest slope of the foveal wall and parafoveal retinal thickness.

All continuous variables, GA, BW and PMA, were centred by taking the deviation from the mean (mean GA=27.55 weeks, mean BW=1083.18g, mean PMA=36.20 weeks). In order to determine the separate influence of diagnosis of ROP, prematurity (GA, BW) or PMA on foveal morphology, two-way interactions were also investigated.

All models included a random intercept and random time-specific slope for each infant thereby accounting for random effects. The overall statistical significance of a categorical or continuous variable in a linear mixed model was assessed using the F-statistic where the denominator degree of freedom was calculated using the Kenward and Roger method (Kenward and Roger 1997). To determine the statistical significance of a predictor or interaction term, we considered type 1 error rate as less than 0.05 ($p<0.05$). All statistical analyses were carried out using the R software, version 3.4 with appropriate packages (lme4, lmerTest, multcomp, ggplot2) (R Core Team, 2017).

### 5.2 Results

One hundred and seventy-four preterm infants were recruited to the study over 42 months (91 males, 83 females). Poor quality images for both eyes were discarded with the result that data could not be analyzed for 62 participants (36%) (31 males, 31 females). A further 25 infants (14%) developed cystic appearances (identical to cystoid macular edema) of the central retina (Maldonado et al. 2011; Vinekar et al. 2011; Lee et al. 2011; Maldonado et al. 2012; Dubis et al. 2012; Erol et al. 2014) distorting foveal structure and these infants were also excluded from the foveal morphology analysis. Details are shown in table 5.1.

| | Recruited | Included | Excluded | Cystic Change |
|---|---|---|---|---|
| Total | 174 | 87 (50%) | 62 (36%) | 25 (14%) |
| Sex M/F | 91/83 | 47/40 | 31/31 | 13/12 |

**Table 5.1** Recruited participant details.

The remaining 87 participants (47 males, 40 females) and 278 images were analysed in the study. Fifty-seven infants (65%) never had ROP at any imaging session, while

nineteen infants (22%) had ROP recorded at every imaging session and eleven infants (13%) had ROP on at least one imaging session. In this last group (mixed ROP/no ROP), seven infants developed ROP in one eye, whereas one infant developed ROP in both eyes. In two infants the ROP regressed spontaneously and another infant initially had no ROP recorded which then developed into ROP and then subsequently spontaneously regressed. Details of the infant cohort are shown in table 5.2.

| | **Always had ROP** | **Never had ROP** | **Mixed (ROP or no ROP)** |
|---|---|---|---|
| **Number of children** | | | |
| Total 87 (100%) | 19 (22%) | 57 (65%) | 11 (13%) |
| Male | 7 | 33 | 7 |
| Female | 12 | 24 | 4 |
| Caucasian | 9 | 29 | 4 |
| Non-Caucasian | 10 | 28 | 7 |
| Single birth | 14 | 52 | 9 |
| Multiple birth | 5 | 5 | 2 |
| **Mean (± SD) *GA, BW, PMA** | | | |
| GA (weeks) | 26.1±1.98 | 28.6±2.43 | 26.6±1.79 |
| BW (grams) | 807±170 | 1154±423 | 864±179 |
| PMA (weeks) | 36.5±2.63 | 36.1±2.45 | 36.0±3.18 |
| **Number of images** | | | |
| Total 278 (100%) | 73 (26%) | 156 (55%) | 49(18%) |
| stage 1 | 12 | - | 11 |
| stage 2 | 57 | - | 17 |
| stage 3 | 4 | - | 2 |
| Right eye | 40 | 73 | 12 ROP<br>10 no ROP |
| Left eye | 33 | 83 | 18 ROP<br>9 no ROP |

**Table 5.2** Participant and image characteristics.*GA – gestational age, BW – birthweight, PMA – postmenstrual age*

Further summary details of (i) number of successfully analyzed repeated images and (ii) details of ethnicity, multiplicity and sex and (iii) characteristics according to BW and GA are shown in tables 5.3, 5.4 and 5.5 respectively.

| Imaging sessions | Number of infants | Number of images |
|---|---|---|
| 1 | 19 | 19 |
| 2 | 25 | 50 |
| 3 | 12 | 36 |
| 4 | 11 | 44 |
| 5 | 5 | 25 |
| 6 | 7 | 42 |
| 7 | 2 | 14 |
| 8 | 6 | 48 |
| Total | 87 | 278 |

**Table 5.3** Number of infants and imaging sessions.

**Ethnicity**

| | PMA at Exam (weeks) | | GA at Birth (weeks) | | Birth Weight (grams) | |
|---|---|---|---|---|---|---|
| | Non-caucasian | Caucasian | Non-caucasian | Caucasian | Non-caucasian | Caucasian |
| *Total* | 46 | 41 | 46 | 41 | 46 | 41 |
| *minimum* | 31.29 | 31.57 | 23.43 | 24.00 | 635.00 | 500.00 |
| *maximum* | 41.85 | 41.85 | 35.71 | 34.00 | 3540.00 | 1750.00 |
| *mean* | 35.73 | 36.25 | 27.84 | 28.59 | 1076.52 | 1090.66 |
| *SD* | 2.76 | 2.47 | 2.70 | 2.48 | 498.32 | 341.39 |
| *median* | 35.71 | 36.85 | 27.93 | 28.71 | 970.00 | 1100.00 |
| *p value* | p=0.36 | | p=0.18 | | p=0.88 | |

**Multiplicity of birth**

| | PMA at Exam (weeks) | | GA at Birth (weeks) | | Birth Weight (grams) | |
|---|---|---|---|---|---|---|
| | single birth | multiple birth | single birth | multiple birth | single birth | multiple birth |
| *Total* | 75 | 12 | 75 | 12 | 75 | 12 |
| *minimum* | 31.29 | 31.57 | 23.43 | 24.43 | 500.00 | 555.00 |
| *maximum* | 41.85 | 40.00 | 35.71 | 29.57 | 3540.00 | 1370.00 |
| *mean* | 35.99 | 35.86 | 28.32 | 27.42 | 1093.23 | 1020.42 |
| *SD* | 2.54 | 3.26 | 2.72 | 1.67 | 449.78 | 272.30 |
| *median* | 36.43 | 35.71 | 28.57 | 27.21 | 1042.00 | 1025.00 |
| *p value* | p=0.89 | | p=0.13 | | p=0.45 | |

**Sex**

| | PMA at Exam (weeks) | | | GA at Birth (weeks) | | | Birth Weight (grams) | | |
|---|---|---|---|---|---|---|---|---|---|
| | All infants | Female | Male | All infants | Female | Male | All infants | Female | Male |
| *total* | 87 | 40 | 47 | 87 | 40 | 47 | 87 | 40 | 47 |
| *minimum* | 31.00 | 31.57 | 31.29 | 23.43 | 23.43 | 24.29 | 500.00 | 555.00 | 500.00 |
| *maximum* | 43.85 | 39.57 | 41.85 | 35.71 | 34.71 | 35.71 | 3540.00 | 3540.00 | 2430.00 |
| *mean* | 36.20 | 35.63 | 36.36 | 28.19 | 27.84 | 28.49 | 1083.18 | 1037.67 | 1121.91 |
| *SD* | 2.64 | 2.33 | 2.85 | 2.61 | 2.73 | 2.49 | 429.18 | 509.79 | 347.41 |
| *median* | 36.00 | 35.78 | 36.71 | 28.43 | 28.29 | 28.71 | 1042.00 | 915.00 | 1120.00 |
| *p value* | | p=0.27 | | | p=0.25 | | | p=0.38 | |

**Table 5.4 Summary statistics on preterm infants** according to ethnicity, multiplicity of birth and sex. PMA = postmenstrual age, GA = gestational age, SD = standard deviation.

| | Total | Never ROP | Always ROP | Mixed |
|---|---|---|---|---|
| | 87 | 57 | 19 | 11 |
| **Birthweight** | | | | |
| less than 1000 g | 40 | 16 | 18 | 7 |
| 1000 – 1499 g | 37 | 31 | 1 | 4 |
| more than 1500 g | 10 | 10 | 0 | 0 |
| **Gestational age** | | | | |
| less than 28 weeks | 37 | 13 | 17 | 8 |
| 28 – 32 weeks | 46 | 40 | 2 | 3 |
| more than 32 weeks | 4 | 4 | 0 | 0 |

**Table 5.5 Characteristics of preterm infants according to birthweight and gestational age**. ROP – retinopathy of prematurity. Mixed – infants with ROP that regressed or infants with no ROP that developed subsequently. *g - grams*

Figure 5.2 shows predicted mean fits (with 95% confidence intervals) of statistical models adjusted for GA for: (i) foveal width (figure 5.2B), (ii) area (figure 5.2C), (iii) depth (figure 5.2D) and (iv) central foveal thickness (CFT, figure 5.2E), and figure 5.3 for: (v) steepest slope of the foveal wall (figure 5.3B) and (vi) parafoveal retinal thickness (figure 5.3C).

Separate plots are provided where statistical models demonstrate a factor that significantly affects the foveal parameter (e.g. presence or absence of ROP for foveal width, figure 5.2B).

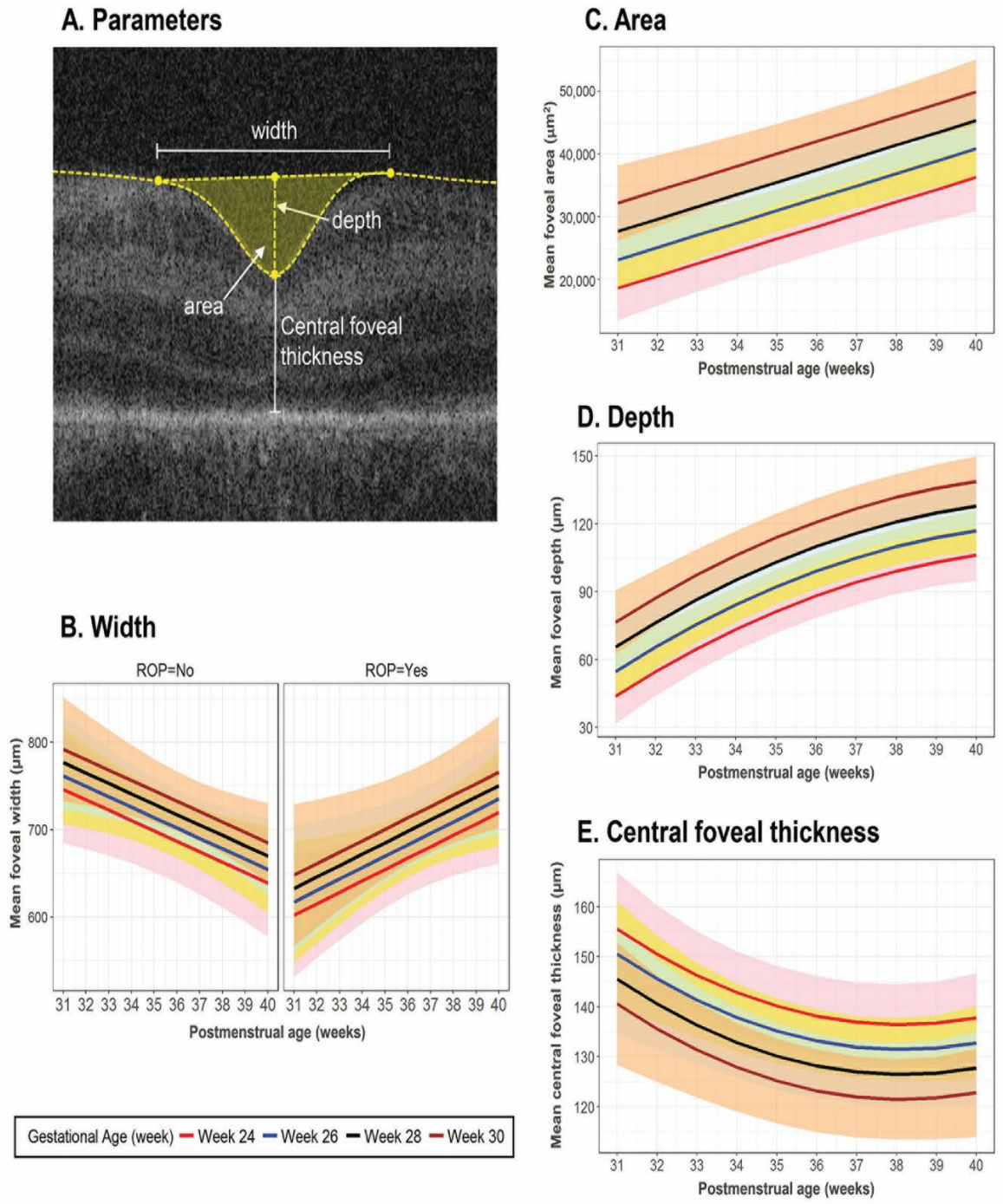


**Figure 5.2. Foveal parameters** (A), predicted mean fits (with 95% confidence intervals) of statistical models adjusted for gestational age (GA) for change with postmenstrual age (PMA): (B) **foveal width**, (C) **area,** (D) **depth**, and (E) **central foveal thickness**. Predicted mean fits are displayed for GA 24, 26, 28 and 30 weeks illustrated using coloured lines, with matching shaded regions representing 95% confidence intervals of the mean. Absence / presence of ROP was only significant for foveal width and hence plots for these two conditions are displayed in (B).

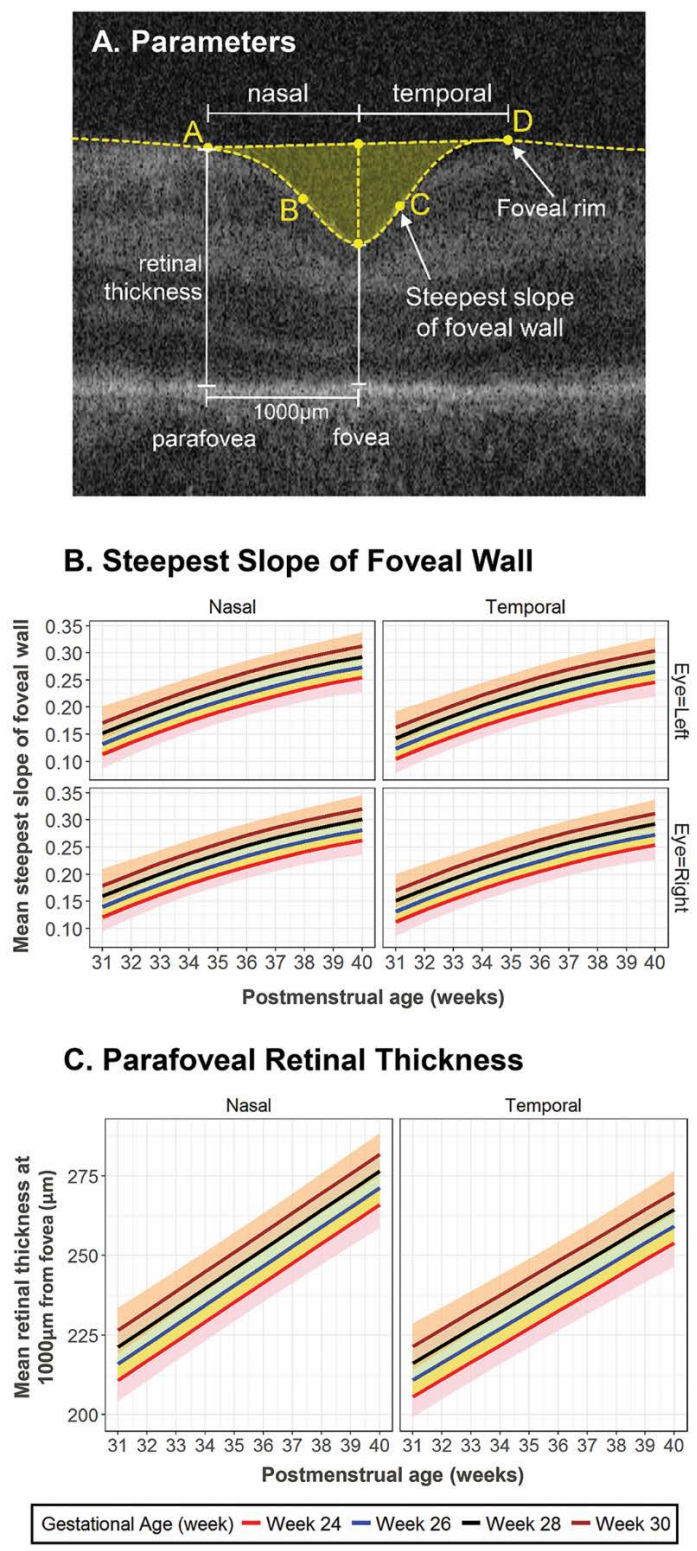


**Figure 5.3 Foveal parameters** (A), predicted mean fits (with 95% confidence intervals) of statistical models adjusted for gestational age (GA) for change with postmenstrual age (PMA): (B) **steepest slope of the foveal wall**, and (C) **parafoveal retinal thickness**. The predicted effect of GA on the mean difference in the parameter is illustrated using coloured lines for GA 24, 26, 28 and 30 weeks, with matching shaded regions representing 95% confidence intervals of the mean. There was a significant difference for temporal and nasal aspects for both steepest slope and parafoveal retinal thickness. Eye (right or left) was also a significant factor for steepest slope.

### 5.3 Differences between ROP and non-ROP infants

Figure 5.4 (see also figure 5.2B) shows the results of multivariate modelling for GA and BW on foveal width, with predicted mean fits (with 95% confidence intervals) shown in Figures 4B and 4D, respectively, and results of statistical modelling shown in Figures 4C and 4E, respectively. Similar formats are used for foveal area (see figure 5.5), foveal depth (see figure 5.6), central foveal thickness (CFT) (see figure 5.7), steepest slope of foveal wall (slope) (see figure 5.8) and parafoveal retinal thickness (pRT) (see figure 5.9) respectively.

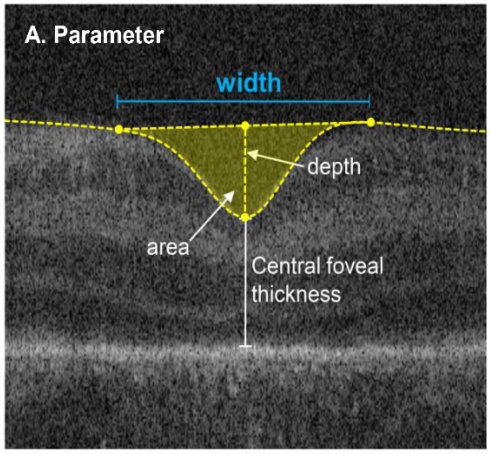


**Change in FOVEAL WIDTH with Postmenstrual Age showing the effect of GESTATIONAL AGE at Birth**

***B. Predicted mean fits (with 95% CI)***

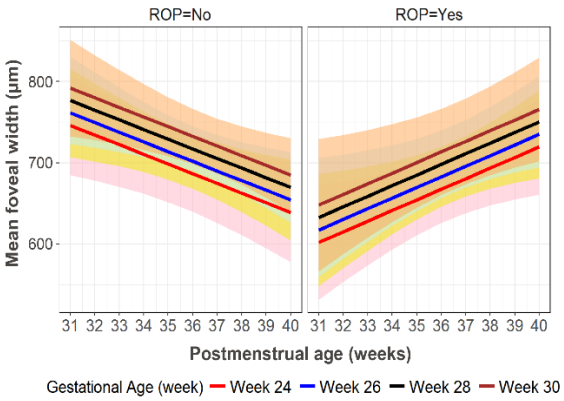


***C. Statistical modelling***

| **Change in Foveal Width with Postmenstrual Age (PMA)** | |
|---|---|
| Change per week of PMA with **ROP ABSENT** | -11.18 ± 4.46 µm |
| Change per week of PMA with **ROP PRESENT** | 24.96 ± 6.92 µm |
| *P values* | |
| Change with PMA | $p$=0.01 |
| Interaction between PMA and ROP diagnosis | $p$<0.001 |

| **Effect of Gestational Age at Birth (GA) on Foveal Width** | |
|---|---|
| Change per week of Gestational Age | 7.66 ± 4.86 µm |
| *P* value | $p$=0.11 |

**Change in FOVEAL WIDTH with Postmenstrual Age showing the effect of BIRTH WEIGHT**

***D. Predicted mean fits (with 95% CI)***

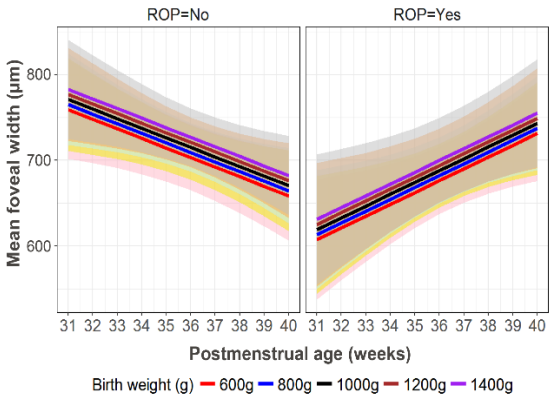


***E. Statistical modelling***

| **Change in Foveal Width with Postmenstrual Age (PMA)** | |
|---|---|
| Change per week of PMA with **ROP ABSENT** | -11.18 ± 4.46 µm |
| Change per week of PMA with **ROP PRESENT** | 24.96 ± 6.88 µm |
| *P values* | |
| Change with PMA | $p$=0.01 |
| Interaction between PMA and ROP diagnosis | $p$<0.001 |

| **Effect of Birth Weight on Foveal Width** | |
|---|---|
| Change per 100g of Birth Weight | 2.96 ± 2.87 µm |
| *P* value | $p$=0.31 |

**Figure 5.4 Foveal width** (A), predicted mean fits (with 95% confidence intervals) and results of statistical models of change in foveal width with postmenstrual age (PMA), **adjusted for gestational age (GA) and birth weight (BW).** In (B) the predicted effect of GA on the mean difference in the foveal width is illustrated using coloured lines for gestational ages 24, 26, 28 and 30 weeks, with matching shaded regions representing 95% confidence intervals of the mean. Similarly, this is shown in (D) for BW 600, 800, 1000, 1200 and 1400 grams. Results of the statistical models are shown in (C) and (E), respectively. Absence / presence of ROP had a significant effect on foveal width and hence plots for these two conditions are displayed in (B) and (D).

Foveal width was the only parameter where diagnosis of ROP had a significant effect, with a highly significant interaction between absence / presence of ROP and PMA ($p<0.001$). Foveal width decreased when ROP was absent, at a mean (± SEM) rate of -11.18 ± 4.46µm per week, but increased when ROP was present at a rate of -24.96 ± 6.92µm per week (Figure 4B and 4C). This interaction was independent of GA and BW, neither of which were correlated with foveal width ($p=0.11$, $p=0.30$). Exceptions to this trend were observed in 14.3% of infants without ROP (where foveal width increased ≥5% per week) and 18.2% of infants with ROP (where foveal width decreased ≥5% per week). For the three infants where ROP regressed, one infant showed an increase in foveal width (i.e. ≥5% per week between 32-37 weeks PMA), whereas two infants remained the same (<5% change per week).

The difference in trajectories with ROP absent and present resulted in a significant difference for the earliest PMA. On average, when ROP was present foveal width was 76% of the value when ROP was absent at 32 weeks PMA (mean± SE: 1203.6 ± 84.40µm compared to 1584.9 ± 77.25µm, respectively).

The results for the other foveal parameters as described above are shown (see figures 5.5, 5.6, 5.7, 5.8 and 5.9, respectively) (see also figures 5.2 and 5.3 to directly compare changes in parameters with PMA). In contrast to foveal width, absence or presence of ROP had no statistically significant effect on other parameters.

**5.4 Parameters significantly correlated with GA and BW**

Both GA and BW were significantly correlated with increasing foveal area ($p<0.001$, $p=0.004$) (see figure 5.5), depth ($p<0.001$, $p=0.001$) (see figure 5.6), slope ($p<0.001$, $p=009$) (see figure 5.8) and pRT ($p<0.001$, $p=0.013$) (see figure 5.9). However only GA was a significant predictor for CFT ($p<0.001$) (see figure 5.7) which decreased with increasing GA.

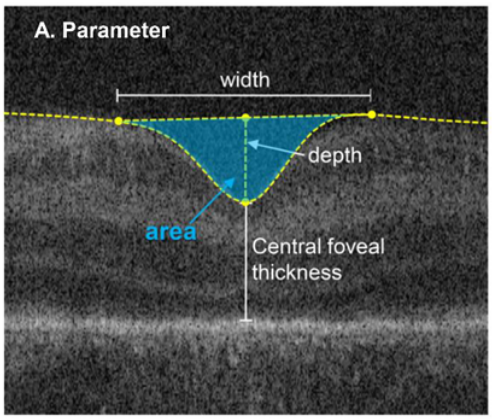


**Change in FOVEAL AREA with Postmenstrual Age showing the effect of GESTATIONAL AGE at Birth**

***B. Predicted mean fits (with 95% CI)***

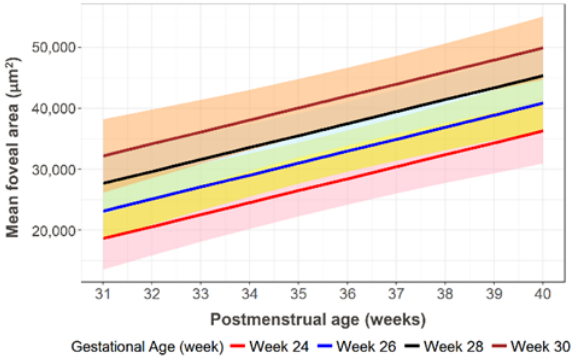


***C. Statistical modelling***

| Change in Foveal Area with Postmenstrual Age (PMA) | |
|---|---|
| Change per week of PMA | 1968.0 ± 355.4 µm² |
| *P* value | *p*<0.001 |

| Effect of Gestational Age at Birth (GA) on Foveal Area | |
|---|---|
| Change per week of Gestational Age | 2266.5 ± 499.5 µm² |
| *P value* | *p*<0.001 |

**Change in FOVEAL AREA with Postmenstrual Age showing the effect of BIRTH WEIGHT**

***D. Predicted mean fits (with 95% CI)***

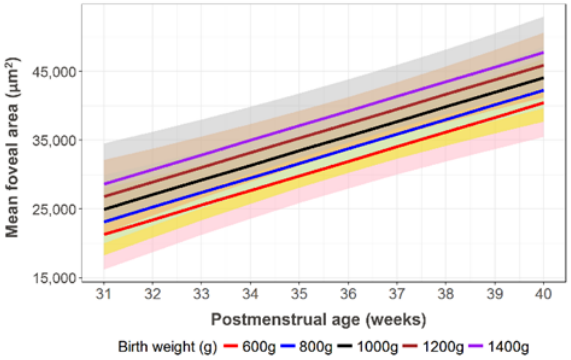


***E. Statistical modelling***

| Change in Foveal Area with Postmenstrual Age (PMA) | |
|---|---|
| Change per week of PMA | 2121.4 ± 358.8 µm² |
| *P* value | *p*<0.001 |

| Effect of Birth Weight on Foveal Area | |
|---|---|
| Change per 100g of Birth Weight | 911.9 ± 313.3 µm² |
| *P value* | *p*=0.004 |

**Figure 5.5 Foveal area** (A), predicted mean fits (with 95% confidence intervals) and results of statistical models of change in foveal area with postmenstrual age (PMA), **adjusted for gestational age (GA) and birth weight (BW)**. In (B) the predicted effect of gestational age on the mean difference in the foveal area is illustrated using colored lines for gestational ages 24, 26, 28 and 30 weeks, with matching shaded regions representing 95% confidence intervals of the mean. Similarly, this is shown in **(D)** for birth weights 600, 800, 1000, 1200 and1400 grams. Results of the statistical models are shown in **(C)** and **(E)**, respectively.

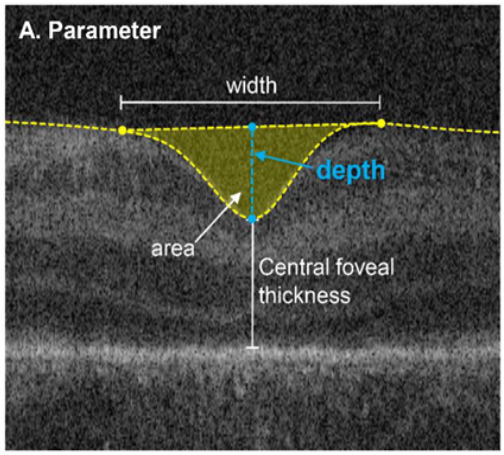


**Change in FOVEAL DEPTH with Postmenstrual Age showing the effect of GESTATIONAL AGE at Birth**

***B. Predicted mean fits (with 95% CI)***

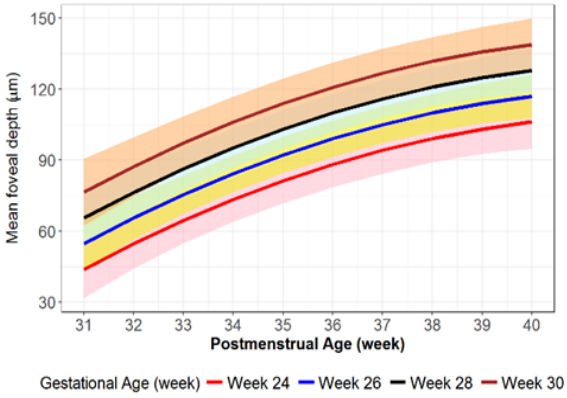


***C. Statistical modelling***

| Change in Foveal Depth with Postmenstrual Age (PMA) | |
|---|---|
| Linear change per week of PMA | 6.24 ± 0.56 µm |
| *P* value | *p*<0.001 |
| Non-linear change per week of PMA | -0.49 ± 1.6 µm |
| *P* value | *p*=0.003 |

| Effect of Gestational Age at Birth (GA) on Foveal Depth | |
|---|---|
| Change per week of Gestational Age | 5.43 ± 1.12 µm |
| *P value* | *p*<0.001 |

**Change in FOVEAL DEPTH with Postmenstrual Age showing the effect of BIRTH WEIGHT**

***D. Predicted mean fits (with 95% CI)***

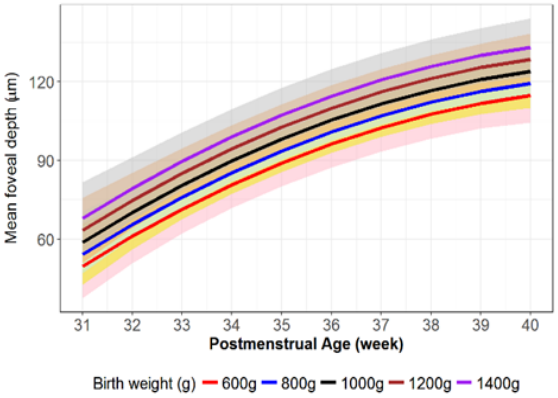


***E. Statistical modelling***

| Change in Foveal Depth with Postmenstrual Age (PMA) | |
|---|---|
| Linear change per week of PMA | 6.51 ± 0.57 µm |
| *P* value | *p*<0.001 |
| Non-linear change per week of PMA | -0.52 ± 1.6 µm |
| *P* value | *p*=0.002 |

| Effect of Birth Weight on Foveal Depth | |
|---|---|
| Change per 100g of Birth Weight | 2.28 ± 0.71 µm |
| *P value* | *p*=0.001 |

**Figure 5.6 Foveal depth** (A), predicted mean fits (with 95% confidence intervals) and results of statistical models of change in foveal depth with postmenstrual age (PMA), **adjusted for gestational age (GA) and birth weight (BW)**. In (B) the predicted effect of gestational age on the mean difference in the foveal depth is illustrated using colored lines for gestational ages 24, 26, 28 and 30 weeks, with matching shaded regions representing 95% confidence intervals of the mean. Similarly, this is shown in **(D)** for birth weights 600, 800, 1000, 1200 and1400 grams. Results of the statistical models are shown in **(C)** and **(E)**, respectively.

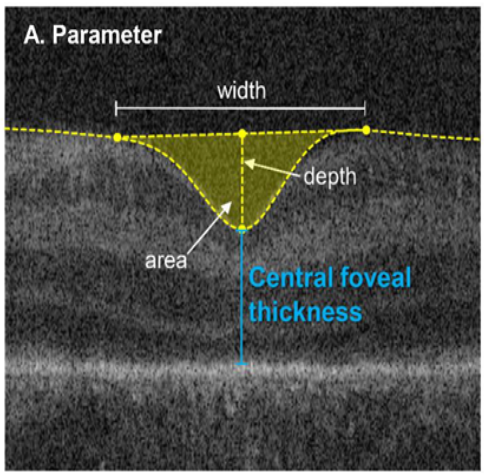


**Change in CENTRAL FOVEAL THICKNESS with Postmenstrual Age showing the effect of GESTATIONAL AGE at Birth**

***B. Predicted mean fits (with 95% CI)***

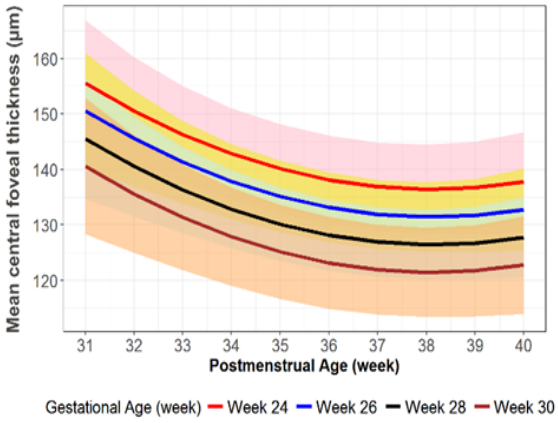


***C. Statistical modelling***

| Change in Central Foveal Thickness with Postmenstrual Age (PMA) | |
|---|---|
| Linear change per week of PMA | -1.45 ± 0.53 µm |
| *P* value | *p*=0.009 |
| Non-linear change per week of PMA | +0.38 ± 1.3 µm |
| *P* value | *p*=0.006 |

| Effect of Gestational Age at Birth (GA) on Central Foveal Thickness | |
|---|---|
| Change per week of Gestational Age | -2.49 ± 0.91 µm |
| *P value* | *p*=0.007 |

**Change in CENTRAL FOVEAL THICKNESS with Postmenstrual Age showing the effect of BIRTH WEIGHT**

***D. Predicted mean fits (with 95% CI)***

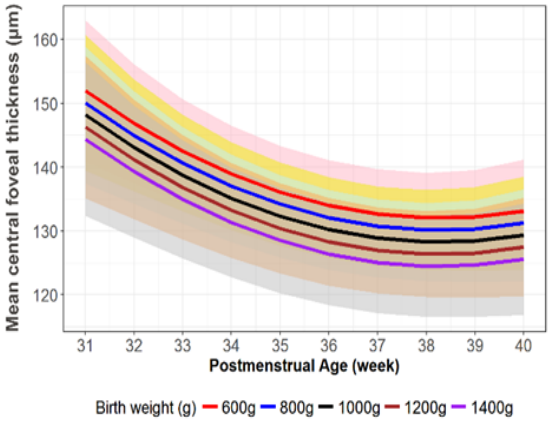


***E. Statistical modelling***

| Change in Central Foveal Thickness with Postmenstrual Age (PMA) | |
|---|---|
| Linear change per week of PMA | -1.56 ± 0.53 µm |
| *P* value | *p*=0.005 |
| Non-linear change per week of PMA | +0.38 ± 1.3 µm |
| *P* value | *p*=0.006 |

| Effect of Birth Weight on Central Foveal Thickness | |
|---|---|
| Change per 100g of Birth Weight | -0.948 ± 0.553 µm |
| *P value* | *p*=0.09 |

**Figure 5.7 Central foveal thickness (CFT)** (A), predicted mean fits (with 95% confidence intervals) and results of statistical models of change in CFT with postmenstrual age (PMA), **adjusted for gestational age (GA) and birth weight (BW)**. In (B) the predicted effect of gestational age on the mean difference in the CFT is illustrated using colored lines for gestational ages 24, 26, 28 and 30 weeks, with matching shaded regions representing 95% confidence intervals of the mean. Similarly, this is shown in **(D)** for birth weights 600, 800, 1000, 1200 and1400 grams. Results of the statistical models are shown in **(C)** and **(E)**, respectively.

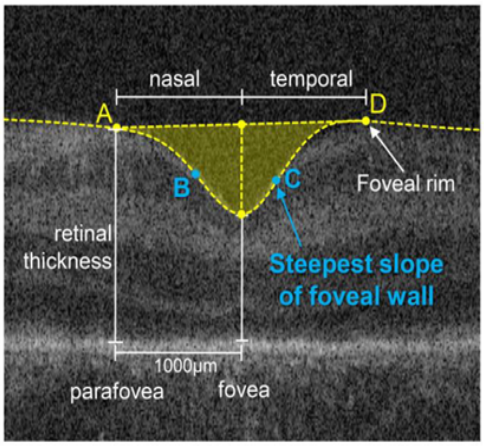


**Change in STEEPEST SLOPE OF FOVEAL WALL with Postmenstrual Age showing the effect of GESTATIONAL AGE at Birth**

***B. Predicted mean fits (with 95% CI)***

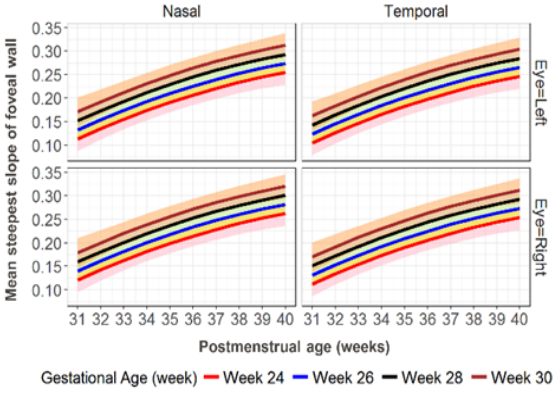


***C. Statistical modelling***

| Change in Steepest Slope of Foveal Wall with Postmenstrual Age (PMA) | |
|---|---|
| Linear change per week of PMA | 0.015 ± 0.00 |
| *P* value | *p*<0.001 |
| Non-linear change per week of PMA | -0.0007 ± 0.0003 |
| *P* value | *p*=0.04 |

| Effect of Gestational Age at Birth (GA) on Steepest Slope of Foveal Wall | |
|---|---|
| Change per week of Gestational Age | 0.009 ± 0.002 |
| *P* value | *p*<0.001 |

| Other predictors | |
|---|---|
| Nasal > temporal | 0.009 ± 0.003 |
| P value | *p*=0.001 |
| Right eye > Left eye | 0.007 ± 0.003 |
| P value | *p*=0.005 |

**Change in STEEPEST SLOPE OF FOVEAL WALL with Postmenstrual Age showing the effect of BIRTH WEIGHT**

***D. Predicted mean fits (with 95% CI)***

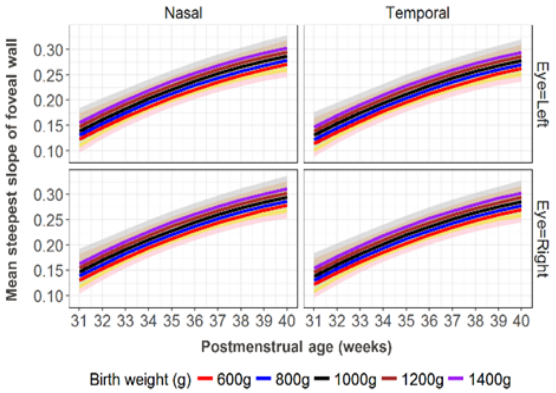


***E. Statistical modelling***

| Change in Steepest Slope of Foveal Wall with Postmenstrual Age (PMA) | |
|---|---|
| Linear change per week of PMA | 0.02 ± 0.00° |
| *P* value | *p*<0.001 |
| Non-linear change per week of PMA | -0.0008 ± 0.0003 |
| *P* value | *p*=0.02 |

| Effect of Birth Weight on Steepest Slope of Foveal Wall | |
|---|---|
| Change per 100g of Birth Weight | 0.004 ± 0.002 |
| *P* value | *p*=0.009 |

| Other predictors | |
|---|---|
| Nasal > temporal | 0.009 ± 0.002 |
| P value | *p*=0.001 |
| Right eye > Left eye | 0.007 ± 0.003 |
| P value | *p*=0.009 |

**Figure 5.8 Steepest slope of foveal wall (slope)**, predicted mean fits (with 95% confidence intervals) and results of statistical models of change in slope with postmenstrual age (PMA), **adjusted for gestational age (GA) and birth weight (BW)**. In (B) the predicted effect of gestational age on the mean difference in the slope is illustrated using colored lines for gestational ages 24, 26, 28 and 30 weeks, with matching shaded regions representing 95% confidence intervals of the mean. Similarly, this is shown in **(D)** for birth weights 600, 800, 1000, 1200 and1400 grams. Results of the statistical models are shown in **(C)** and **(E)**, respectively. There was a temporal nasal asymmetry with the nasal wall being steeper. The slope in the right eye was also significantly greater than that in the left.

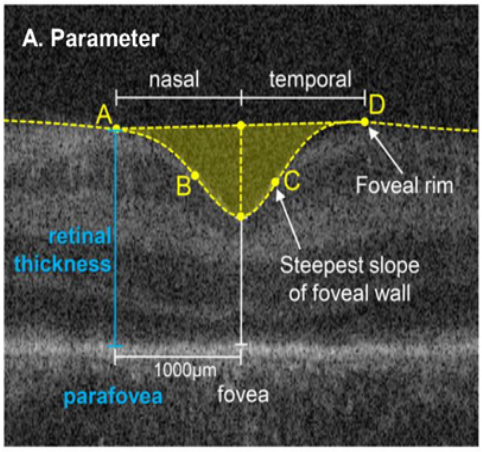


**Change in PARAFOVEAL RETINAL THICKNESS with Postmenstrual Age showing the effect of GESTATIONAL AGE at Birth**

***B. Predicted mean fits (with 95% CI)***

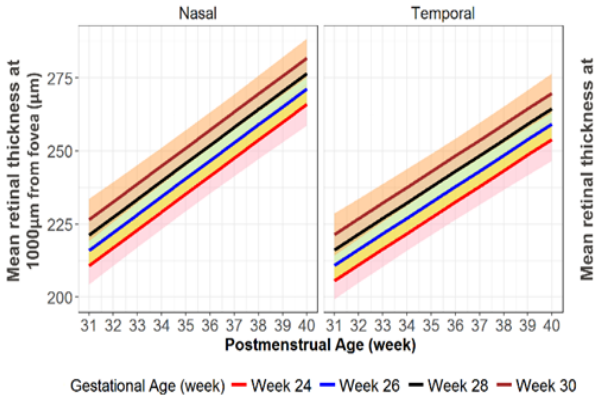


***C. Statistical modelling***

| Change in Foveal Thickness 1000µm from the Fovea with Postmenstrual Age (PMA) | |
|---|---|
| Linear change per week of PMA | 6.14 ± 0.39 µm |
| *P* value | *p*<0.001 |
| **Effect of Gestational Age at Birth (GA) on Foveal Thickness 1000µm from the Fovea** | |
| Change per week of Gestational Age | 2.63 ± 0.70 µm |
| *P* value | *p*<0.001 |
| **Other predictors** | |
| Nasal > temporal | 9.07 ± 0.64 µm |
| P value | *p*<0.0001 |
| Difference in slope (nasal > temporal) | 0.78 ± 0.24 µm |
| Interaction between PMA and nasal / temporal location | *p*<0.001 |

**Change in PARAFOVEAL RETINAL THICKNESS with Postmenstrual Age showing the effect of BIRTH WEIGHT**

***D. Predicted mean fits (with 95% CI)***

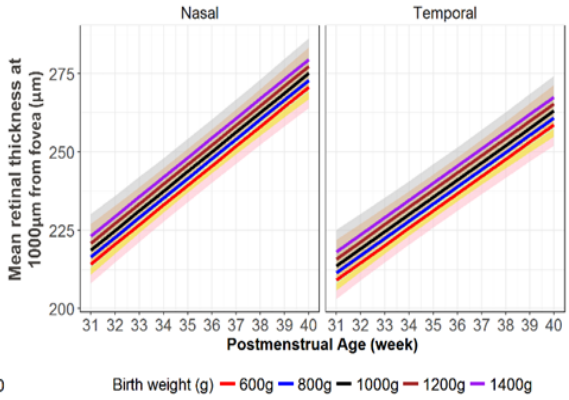


***E. Statistical modelling***

| Change in Foveal Thickness 1000µm from the Fovea with Postmenstrual Age (PMA) | |
|---|---|
| Linear change per week of PMA | 6.26 ± 0.40 µm |
| *P* value | *p*<0.001 |
| **Effect of Birth Weight on Foveal Thickness 1000µm from the Fovea** | |
| Change per 100g of Birth Weight | 1.107 ± 0.44 µm |
| *P* value | *p*=0.013 |
| **Other predictors** | |
| Nasal > temporal | 9.01 ± 0.64 µm |
| P value | *p*<0.0001 |
| Difference in slope (nasal > temporal) | 0.78 ± 0.24 µm |
| Interaction between PMA and nasal / temporal location | *p*=0.001 |

**Figure 5.9 Parafoveal retinal thickness (pRT)** (A), predicted mean fits (with 95% confidence intervals) and results of statistical models of change in pRT with postmenstrual age (PMA), **adjusted for gestational age (GA) and birth weight (BW)**. In (B) the predicted effect of gestational age on the mean difference in the pRT is illustrated using colored lines for gestational ages 24, 26, 28 and 30 weeks, with matching shaded regions representing 95% confidence intervals of the mean. Similarly, this is shown in **(D)** for birth weights 600, 800, 1000, 1200 and1400 grams. Results of the statistical models are shown in **(C)** and **(E)**, respectively. There was a temporal nasal asymmetry with the nasal wall being steeper. There was temporal nasal asymmetry with nasal parafoveal RT being greater.

### 5.5 Other variables

Sex, ethnicity (including and excluding non-South Asian participants in the model) and birth (single/multiple) were not significant predictors for any parameter in either model using GA or BW. The steepest foveal slope was greater in the right eye compared to the left eye ($p<0.01$) (see SDC 8)**.** The nasal aspect of the fovea was significantly steeper ($p=0.001$) and pRT significantly thicker ($p<0.001$) compared to the temporal aspect (see SDC 8 and SDC 9) respectively.

### 5.6 Significant changes with PMA

All foveal parameters had significant dynamic mean rates of change with increasing PMA using both predictive models ($p\leq0.01$). Foveal depth (see figure 5.6), CFT (see figure 5.7) and steepest slope (see figure 5.8) all demonstrated significant non-linear changes with PMA that were modelled with a quadratic term. The change in parameters with PMA are shown dynamically in the video animation (see video 1) (https://www.dropbox.com/s/z2vo8qdl0t5blli/video%201%20.avi?dl=0) illustrating the change in the DoG model fits of ILM with increasing PMA for ROP and non-ROP groups. Particularly noteworthy is reducing foveal width in the group without ROP which is not apparent in the group with ROP.

### 5.7 Parafoveal Retina

An inverted Gaussian fitted the parafovea more often in the ROP group (75.7%) compared to the non-ROP group (55.5%) (Chi-Square test: $P=0.001$). This may also be observed in the video animation (see video 1) (https://www.dropbox.com/s/z2vo8qdl0t5blli/video%201%20.avi?dl=0) where the parafovea slopes in more towards the fovea in the ROP group, especially at early PMAs.

## 5.8 Discussion

We show that foveal width demonstrates a different trajectory of development depending on the presence or absence of retinopathy of prematurity (ROP/non-ROP) that is independent of gestational age (GA) and birth weight (BW), factors that are clearly associated with the degree of prematurity. This is evident from a highly significant interaction between presence of ROP and PMA ($p<0.001$), due to foveal width increasing in the ROP group and decreasing in the non-ROP group. Other parameters of foveal morphology show marked changes with PMA but no differences exist depending on the presence or absence of ROP when models are adjusted for GA and BW.

Yanni and colleagues (Yanni et al. 2012) studied older ex preterm children (5 to 16 years of age), including ROP, and found shallow, less steep foveae but no significant difference in foveal diameter compared to full-term born control children. However, their study had 4 preterm children with no ROP and included 15 children who had received treatment for ROP.

In contrast, our investigation of preterm infants shows a difference in foveal width between ROP and non-ROP which is more apparent at early PMA. At 32 weeks, foveal width in the ROP group is 76% of the width in the non-ROP group. After 32 weeks, foveal width increases in the ROP group with increasing PMA but decreases in the non-ROP group. Since this difference is found particularly in early PMA, foveal width may potentially differentiate between preterm infants that do not need further screening for ROP from those that do.

### *5.81 Foveal width as a potential early indicator of ROP*

Risk algorithms to identify treatment requiring ROP (type 1 ROP) are based on BW, GA and weight gain as predictive variables in multivariate logistic regression models (Binenbaum G et al. 2012). The prospective PINT ROP study (Binenbaum et al. 2011) investigated such a model in extreme low BW infants, however, one infant with severe ROP but not requiring treatment was missed. The authors highlight that factors associated with ROP in univariate analysis were not significant in multivariate analysis underlining the multifactorial nature of the risk in prematurity. The e-ROP study (Ying

et al. 2016) developed a model based on GA, weight gain, respiratory support data, and analysis of colour image findings to predict ROP requiring treatment, producing risk scores. The results showed that image criteria predicted treatment requiring ROP better than GA and that this was best at 34 weeks PMA or earlier. In our study, we analyzed image characteristics using HH-OCT on foveal morphology and GA, BW, PMA and identified foveal width as an early predictor variable independent of GA and BW. This suggests that HH-OCT of the fovea is a promising method that could be used with risk models utilizing GA, BW, weight gain and colour image findings.

*5.82 Foveal width, foveal avascular zone (FAZ) and ROP*

It has been suggested that differences in the foveal width of older children and adults with a history of ROP could be related to the size of the foveal avascular zone (FAZ) (Hammer et al. 2008). The FAZ is determined by an absence of vessels in the macula, and has been correlated with foveal shape, continuation of the inner nuclear layer (INL) at the fovea and increased foveal thickness (Yanni et al. 2012; Tick et al. 2011; Provis and Hendrickson 2008; Chui et al. 2012). Chui et al (Chui et al. 2012) studied 11 healthy adults and found that a smaller FAZ was associated with a thicker, narrower fovea. A small FAZ has also been noted in children aged between 1 and 17 years of age with a history of prematurity (Mintz-Hittner et al. 1999). Falavarjani et al (Falavarjani et al. 2017) compared the FAZ in 15 preterm children (including those with ROP) with 11 age-matched controls between 4-12 years of age using OCT angiography. They showed an abnormal FAZ in preterm children born less than 29 weeks GA. We found a significant correlation between earlier GA and increased CFT which is not influenced by diagnosis of ROP suggesting that prematurity could result in the development of a smaller FAZ independently of the diagnosis of ROP. Future studies of the inner retinal layers at the FAZ using OCT during early active development of ROP, may provide more information to explain the differences we found in foveal width between preterm infants with and without ROP.

*5.83 Foveal parameters dependant on GA and BW*

Previous studies in infants and ex preterm children including ROP, report increased CFT with ROP which is in contrast to our study, where CFT was independent of ROP. However, these conclusions are based on studies comparing preterm with full-term children (Vinekar et al. 2011), small numbers of nonROP children (Gursoy et al. 2016), treated preterm children with ROP (Maldonado et al. 2012) or retrospective data (Erol et al. 2014; Ecsedy et al. 2007; Recchia and Recchia 2007).

Our results on GA and CFT in preterm infants are in keeping with previous reports of older ex preterm children that describe an association between CFT with GA but not with diagnosis of ROP (Fieβ et al. 2017; Akerblom et al. 2011; Wang et al. 2012b; Tariq et al. 2011; Bowl et al. 2016). Tariq et al (Tariq et al. 2011) showed that both GA and BW were significant predictors for increased foveal retinal thickness. Similarly, Bowl and colleagues (Bowl et al. 2016) reported a cross-sectional analysis of RT at the foveal centre and found inverse correlation between GA and BW with total retinal thickness in preterm children with and without ROP compared with full - term born children aged between 6 to 13 years. However, by utilizing separate predictor models, we found only a relationship for GA and not for BW which is in contrast with these large studies of older preterm children. This may reflect either a change in foveal thickness between preterm birth and foveal maturity in childhood or differences in sample size.

Our finding of a greater early GA effect on CFT supports that of Wang et al (Wang et al. 2012a) who suggested that before 28 weeks GA, there is an increased likelihood of delayed migration of the inner retina away from the foveal centre with persistence of the inner retina and increased CFT. A recent investigation by Molnar et al (Molnar et al. 2017) reported a strong association between central macular thickness and GA before 27 weeks in preterm children, after adjusting for ROP and sex. We also found that GA interacts with foveal depth similar to Rosen et al (Rosen et al. 2015) who investigated foveal depth in preterm children aged 6.5 years including ROP. The correlation of increased CFT and reduced foveal depth with early GA in both preterm infants and older former preterm individuals, suggests that extreme preterm birth interferes with the normal mechanisms of inner centrifugal retina migration at the

fovea.

*5.84 Differences due to sex and ethnicity*

Adults with normal foveae show differences between race and sex (Wagner-Schuman et al. 2011), male gender being associated with increased central macular thickness in preterm children (Rosen et al. 2015). Our results present no differences in foveal dimensions between Caucasians and Non-Caucasians (including or excluding non-South Asians) , multiple / single birth infants or sex possibly because changes are not present in very early foveal development or due to insufficient numbers to reach significance.

*5.85 Asymmetry of the nasal and temporal foveal slope*

The results found that the mean foveal slope was greater in right eyes compared with left eyes. Asymmetry of the foveal slope likely reflects the greater nasal RNFL and GCL compared with temporally that is observed in developed healthy eyes (Mwanza et al. 2011). However, it is not apparent from the analysis why there should be asymmetry of slope between eyes. It is possible that lateralisation of foveal dimensions may mirror asymmetry of brain development (Neveu et al. 2008), although Huynh et al suggest that normal variations within individuals may include intraocular asymmetry, and our results could reflect this (Huynh et al. 2007).

**5.9 Limitations**

Limitations of this study include conducting our study using one horizontal scan through the central fovea without analysis of the entire volume of the fovea. Also, we did not incorporate specific systemic confounders in our analysis such as oxygen therapy, or illness with each individual, and it is known that these may relate to the severity and development of ROP. In order to adjust for the variability between the ROP and non-ROP groups for systemic factors, a larger number of participants would be needed in order to adjust for each disease category and oxygen delivery method.

A number of infants included in this study (n=19) were only successfully scanned on one visit, although 78% (n=68) were imaged ≥2 times and 49% (n=43) infants were imaged ≥3 times. To investigate changes with time more systematically it would be useful to develop a more consistent repeated scanning protocol for future studies.

We also did not incorporate FAZ measurements from fluorescein angiography in our investigation since we were primarily concerned with modelling foveal morphology using OCT. The advent of portable OCT angiography *in vivo* would further our understanding of the relationship between ROP, the FAZ and the foveal development.

### 5.10 Conclusions

Foveal width in early PMA appears to have a significant relationship with ROP when adjusting for GA and BW. Further study may determine if this has the potential to predict type 1 ROP during screening using HH-OCT. The finding that only GA significantly influences CFT, supports the view that early birth interferes with inner retinal migration at the fovea despite continuing development of the fovea. The EPICure@19 Study (Balasubramanian et al. 2018) has reported a correlation between increased retinal thickness with a reduction in best corrected visual acuity (BCVA) in adults born extremely preterm. The BCVA reduction was found to be similar in untreated ROP and nonROP, suggesting that prematurity and not presence of ROP per se, has an impact on retinal thickness and vision.

A longitudinal HH-OCT study grading foveal morphology, gestational age and visual acuity could be useful in understanding the changes that occur during visual development and in the management of children who are born preterm.

# Chapter 6 Retinal Layers at the Fovea

Chapter 6 addresses Research Aim 2 which was to investigate individual retinal layer development at the fovea with respect to PMA, GA, BW and ROP.

## 6.1 Introduction

The fovea is immature in infants and individual retinal layers become visible on HH – OCT images with increasing maturity (Maldonado et al. 2011; Dubis et al. 2012; Vajzovic et al. 2012; Lee et al. 2015; Alabduljalil et al. 2018). However, in preterm infants, foveal immaturity is further manifest by the persistence of inner retinal layers across the fovea, shallower foveal depression, and a delay in the appearance of the outer layers (Vajzovic et al. 2015).

In term born individuals, using SD-OCT, the development of the foveal retinal layers demonstrates a temporal relationship, changing with increasing chronological age. The GCL, IPL, INL and OPL all decreases from birth until 18 months of age, while the ONL, inner and outer photoreceptor segments increase until 32.4 months, 26.9 months and 45.3 months of age, respectively. The parafoveal GCL and INL increase from 18 months until 65.5 months of age while the parafoveal outer retina continues to increase until 146 months of age (Lee et al. 2015). The inner retinal thickness does not change significantly in the first 5 years after birth, and in the first 24 months, the increasing CFT is primarily due to the increasing photoreceptor layer thickness (Alabduljalil et al. 2018).

However, ex-preterm children demonstrate a disruption of this process, and have thicker foveal GCL, INL and ONL in comparison with term born individuals (Park and Oh 2012; Wang et al. 2012b; Bowl et al. 2016) with reduced retinal (Akerblom et al. 2012; Tariq et al. 2011) and disc (Park and Oh 2015) RNFL thickness. The foveal to parafovea retinal layer ratio changes from 30 to 42 weeks PMA. This reflects the gradual decrease of the inner retina at the fovea due to outward migration, and concurrent increase of the parafovea (Vajzovic et al. 2012). The outer layers are still relatively immature by 42

weeks PMA and do not yet contribute much to CFT unlike in the first 2 years after birth (Alabduljalil et al. 2018).

Although the retinal layers change with PMA, the impact of GA on individual retinal layers at the fovea with PMA measured using SD-OCT in preterm infants has been less well explored except with retrospective studies in older ex-preterm children (Wang et al. 2012b). Previously we showed that foveal depth and CFT were correlated with GA, where younger born infants develop a thicker retina at the fovea and a shallower foveal depression. This suggests that extreme prematurity interferes with foveal inner layer outward migration from birth and even after adjusting for changes with time, persists in older ex-preterm children (Akerblom et al. 2011; Tariq, Burlutsky, and Mitchell 2012; Molnar et al. 2017). This has been reported to even interfere with visual acuity (Balasubramanian et al. 2018).

It is unclear which retinal layer(s) may be significantly delayed in the inner retinal migration associated with early GA and increased CFT. In view of our results (see Chapter5, Figure 5.7, p89), it is expected that GA will be a significant predictor for individual retinal layer thickness at the fovea but it is uncertain if some layers are affected more by prematurity than others, e.g. plexiform compared to nuclear layers. This could aid understanding of the inner retinal migration process at the fovea in extreme preterm infants and Chapter 6 will explore this in greater detail.

The effect of ROP on individual retinal layers in the early neonatal period is unclear. Regressed ROP (treated and untreated) increases the nasal RNFL in ex-preterm children compared with term born children (Wang et al. 2012b) and in those with a history of severe or treated ROP (Akerblom et al. 2012) where it has been inversely correlated with ROP stage (Park and Oh 2015). Regressed ROP ex-preterm children are also reported to have thicker foveal GCL+IPL, OPL+ONL+IS and OS+RPE layers (Wang et al. 2012b).

In Chapter 5, we showed that in early PMA, foveal width was followed a significantly different time course between ROP and non-ROP (see Chapter 5, Figure 5.4, p85). In this chapter we will also explore the effect of ROP on individual retinal layers in preterm infants and discuss the results with respect to this earlier finding.

## 6.2 Methods

Individual layer thicknesses were calculated between border edges as described earlier in Chapter 4 (Methods, p57) and based on previous literature (Bagci et al. 2008; Loduca et al. 2010). Locations were measured from points on either side of the fovea in increments of 50µm, up to 1000µm nasally and temporally (Sjostrand et al. 2017).

The individual layers segmented were as follows (Chapter 4, Methods, Table 4.1 p58): RNFL, GCL, IPL, INL, OutRET (OPL+PRC) and RPE. Predictor variables included PMA, GA and BW, diagnosis (ROP, non-ROP), sex (male, female), ethnicity (Caucasian, Non-Caucasian) and multiplicity of birth (single, multiple), eye (right, left). Statistical analysis was performed as described in Chapter 4 (Methods, statistical analysis, p68) Statistical significance was considered for p values of less than 0.05. Individual retinal layers data were explored according to location (at the fovea, and nasal or temporal to fovea up to the parafovea at 1000µm).

## 6.3 Results

The general demographics have been previously described in Chapter 5 (Results, tables 5.2, 5.3, 5.4, 5.5, pp78-81). Statistical modeling for left eyes is reported. The development of individual retinal layers will be under the following sub-sections as follows:

***6.31*** reports changes in retinal layers at the fovea with PMA for two models where either GA or BW were included, respectively.

***6.32*** reports the effect of GA, BW and ROP at the fovea.

***6.33*** addresses diagnosis of ROP and foveal width at early PMA

Note the following with respect to interpretation of the results:

- Since GA and BW are closely correlated as discussed in Chapters 4 and 5, therefore GA and BW results will be reported separately.

- In order to understand and compare how individual layers change with PMA, the mean value for either GA or BW is chosen to describe and compare the changes depending on which factor is included in the model.

Hence section ***6.31*** of the Results establishes the differences between individual retinal layers at the fovea with PMA (time) for a preterm with GA or BW included in the model. The mean value of individual retinal layers with corresponding mean value of GA or BW is reported accordingly.

Section ***6.32*** will compare the differences between individual retinal layers at the fovea with respect to changing GA, or changing BW or the presence of ROP. For this comparison, a single time point is chosen for comparing the data which is at the mean PMA.

Section ***6.33*** will discuss the effect of ROP at a specific time point in early PMA (32 weeks) in order to explore the effect of ROP on foveal width as reported in Chapter 5 (see Figure 5.7 p89).

## 6.31 *Development of retinal layers at the fovea with PMA without adjustment for gestational age or birthweight*

### *6.31A without adjustment for gestational age or birthweight*

Figure 6.1 shows bivariate scatterplots with the line of best fit for CFT and individual retinal layer thickness(μm) at the fovea with respect to PMA from 30 to 42 weeks. There is a decrease in CFT, RNFL, GCL and INL, and an increase in PRC with PMA.

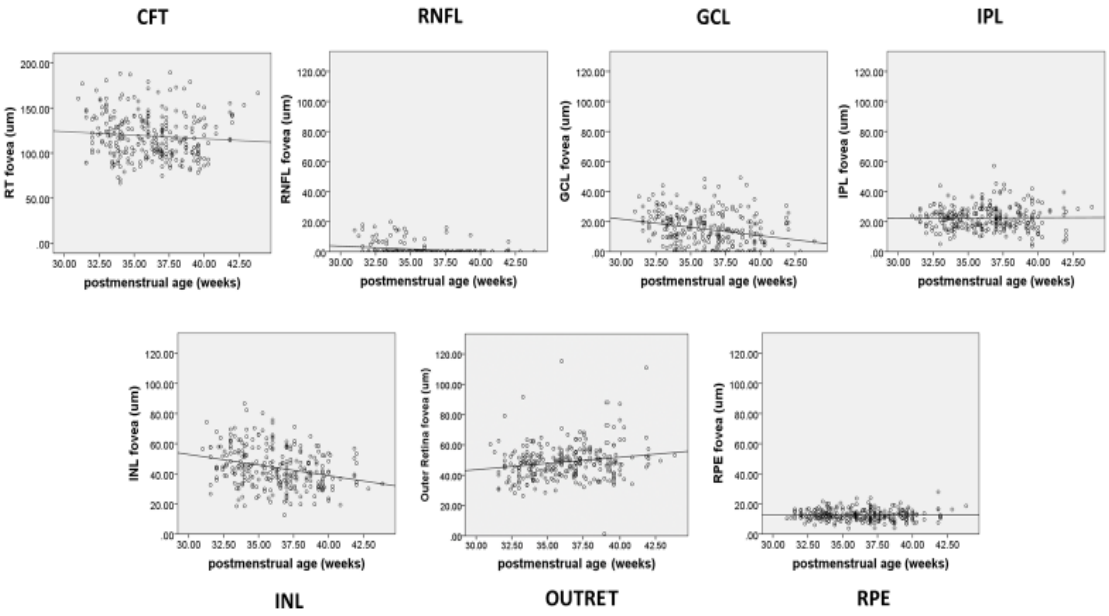


**Figure 6.1 Bivariate scatterplots of change in individual retinal layer thickness at the fovea (µm) with postmenstrual age (PMA).** A line of best fit is shown for each. *RNFL –retinal nerve fibre layer, GCL – ganglion cell layer, IPL – inner plexiform layer, INL – inner nuclear layer, OUTRET – outer retina, RPE – retinal pigment epithelium, RT – retinal thickness, CFT – central foveal RT.*

Correlation results are shown in table 6.1.

| | | RNFL | GCL | IPL | INL | OUTRET | RPE |
|---|---|---|---|---|---|---|---|
| postmenstrual age (weeks) | Pearson Correlation | -.279** | -.260** | .012 | -.280** | .181** | .003 |
| | Sig. (2-tailed) | .000 | .000 | .841 | .000 | .002 | .959 |

** Correlation is significant at the 0.01 level (2-tailed).

* Correlation is significant at the 0.05 level (2-tailed).

**Table 6.1 Correlation between individual foveal retinal layers and PMA.** *RNFL –retinal nerve fibre layer, GCL – ganglion cell layer, IPL – inner plexiform layer, INL – inner nuclear layer, OUTRET – outer retina, RPE – retinal pigment epithelium*

### *6.31B Changes in retinal layer thicknesses with PMA for preterm infants with model including gestational age*

Figure 6.2 plots the results of multivariate regression modeling illustrating the change of mean individual mean retinal layer thickness at the fovea and parafovea with increasing PMA, from 33, 35, 37 and 39 weeks.

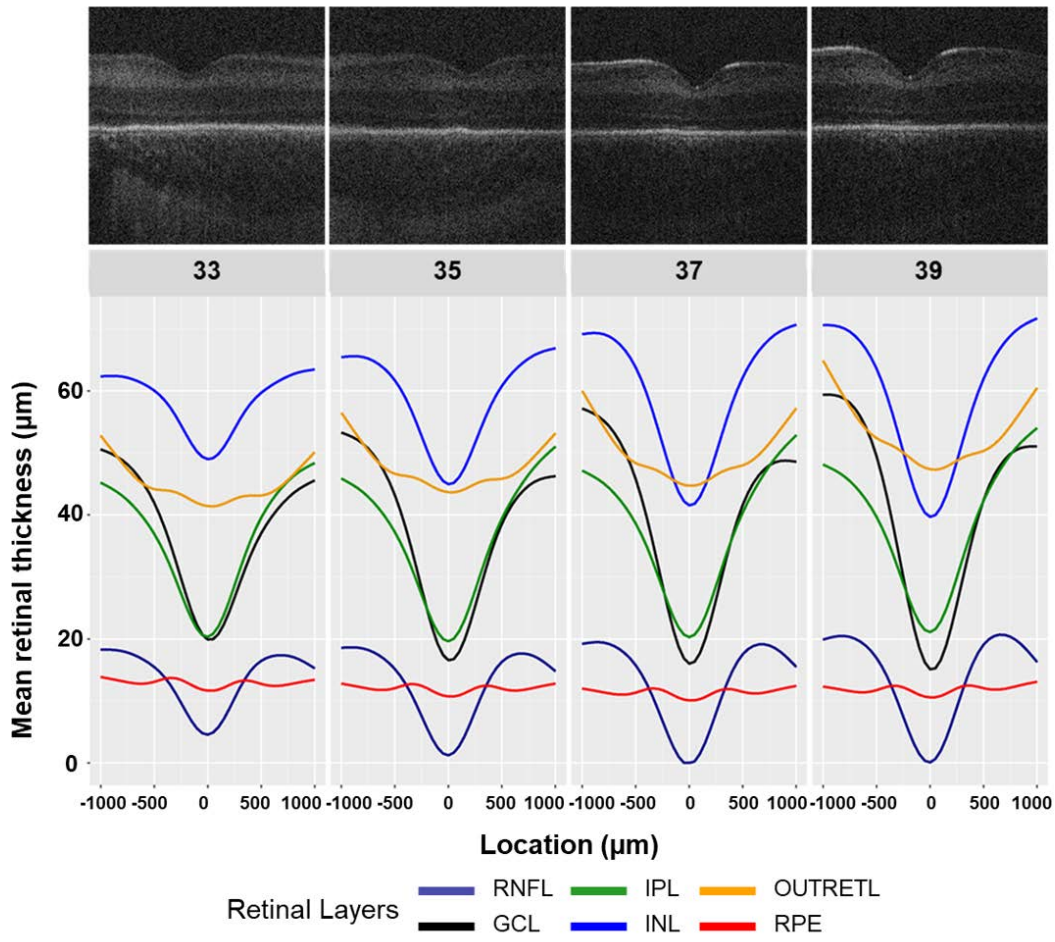


**Figure 6.2 Plot of individual mean retinal layer thickness (µm) at 33,35, 37- and 39-weeks postmenstrual age for mean gestational age 27 weeks.** Examples of original flattened longitudinal OCT images of a preterm infant are shown above. Fovea (0), nasal is negative, temporal is positive. *RNFL –retinal nerve fibre layer, GCL – ganglion cell layer, IPL – inner plexiform layer, INL – inner nuclear layer, OUTERTL – outer retinal layers, RPE – retinal pigment epithelium.*

Corresponding original flattened longitudinal HH -SD-OCT images are also shown above for illustration. From the figure it is evident that as the fovea deepens with PMA

there is a decrease of the RNFL, GCL and INL. The PRC increases at the fovea and the RPE shows marginal changes.

Table 6.2 shows the statistical results of the difference in mean foveal thickness from 33 to 39 weeks PMA for each retinal layer. All retinal layers demonstrated significant changes with PMA. However, the IPL differences were less significant in comparison with the other layers at the fovea. The outer retinal layers became thicker at the fovea with increasing PMA (yellow line on figure 6.2).

| Layer | Difference (μm) | p value |
|---|---|---|
| RNFL | -4.47 | <0.001 |
| GCL | -4.81 | <0.001 |
| IPL | 0.77 | 0.08 |
| INL | -9.31 | <0.001 |
| OUTRet | 5.94 | <0.001 |
| RPE | -1.08 | <0.001 |

**Table 6.2 Difference in mean individual retinal layer thickness at the fovea between postmenstrual ages 33 and 39 weeks with p values** for **mean gestational age** 27 weeks. *RNFL –retinal nerve fibre layer, GCL – ganglion cell layer, IPL – inner plexiform layer, INL – inner nuclear layer, OPL – outer plexiform layer, PRC – photoreceptor complex, RPE – retinal pigment epithelium.*

The differences are further illustrated in figure 6.3 with 95% confidence intervals.

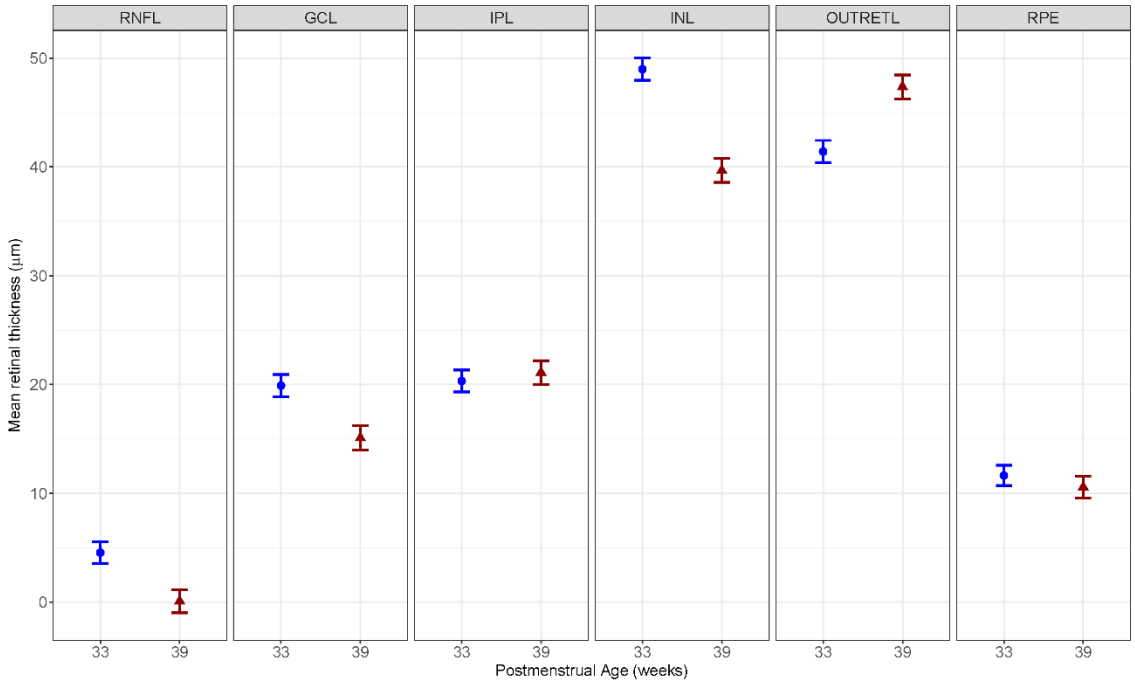


**Figure 6.3 Plot of mean individual retinal layer thickness at the fovea with 95% confidence intervals between postmenstrual age 33 and 39 weeks** for **mean gestational age** 27 weeks. *RNFL – retinal nerve fibre layer, GCL – ganglion cell layer, IPL – inner plexiform layer, INL – inner nuclear layer, OUTRETL – outer retinal layers, RPE – retinal pigment epithelium.*

The IPL and RPE show the least difference between 33 to 39 weeks PMA on figure 6.3.

### *6.31C Changes in Retinal Layer Thicknesses with PMA for preterm infants with model including birthweight*

We found that the changes in mean individual retinal layers at the fovea with postmenstrual age from 33 to 39 weeks for mean birthweight were similar to those found for the mean GA. This is shown in table 6.3.

| Layer | Difference (μm) | p value |
|---|---|---|
| RNFL | -4.69 | <0.001 |
| GCL | -5.10 | <0.001 |
| IPL | 0.81 | 0.06 |
| INL | -9.19 | <0.001 |
| OUTRet | 6.51 | <0.001 |
| RPE | -1.12 | <0.001 |

**Table 6.3 Difference in mean individual retinal layer thickness at the fovea between postmenstrual ages 33 and 39 weeks with p values** for **mean birthweight** 1000 grams. *RNFL –retinal nerve fibre layer, GCL – ganglion cell layer, IPL – inner plexiform layer, INL – inner nuclear layer, OUTRet – outer retinal layers, RPE – retinal pigment epithelium.*

There were no differences when BW was included in the model similar to when GA was included in the model (see table 6.2 earlier).

### *6.32A. The effect of gestational age (GA) on individual foveal retinal layers*

Figure 6.4 plots the results of multivariate regression modeling for individual retinal layers at the fovea and parafovea for mean PMA between 24, 26, 28- and 30-weeks GA. Corresponding original flattened longitudinal HH -SD-OCT images are shown above for illustration. The most noticeable differences at the fovea between GA 24 to GA 30 weeks occur for the INL (p=0.005).

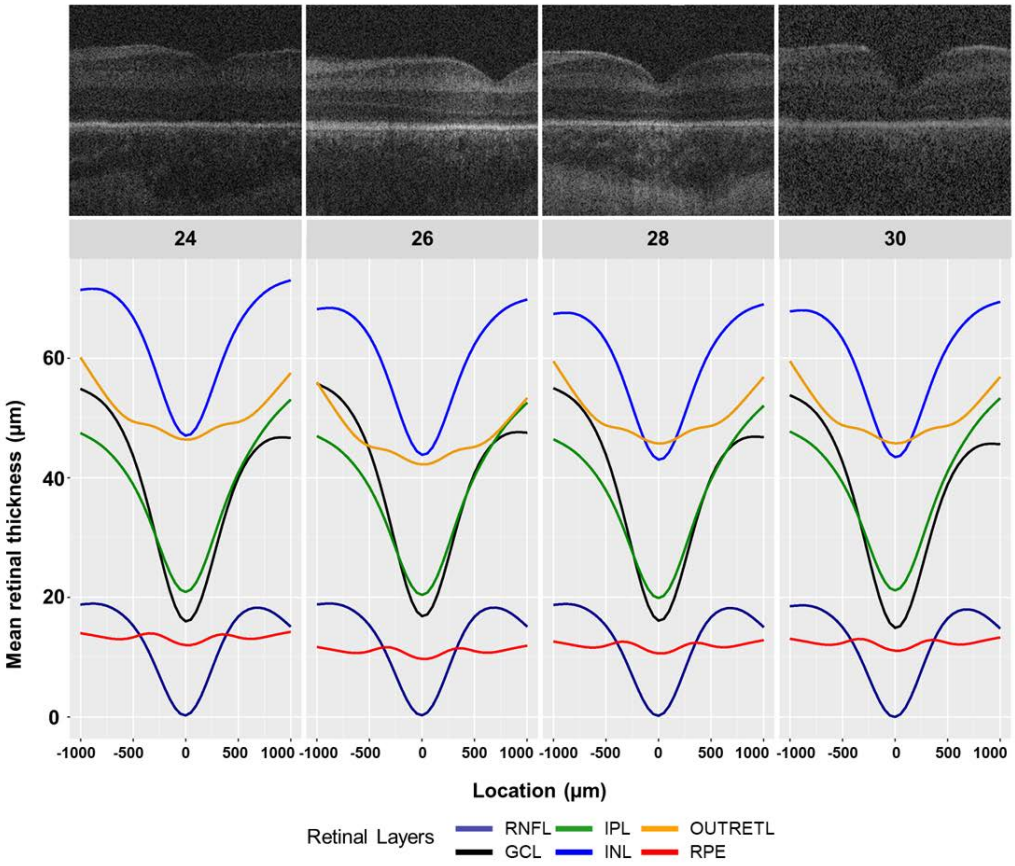


**Figure 6.4 Plot of individual mean retinal layer thickness (µm) at gestational ages 24, 26, 28 and 30 weeks** for **mean postmenstrual age** 36 weeks. Examples of corresponding original flattened OCT images are shown above. Fovea (0), nasal is negative, temporal is positive. *RNFL –retinal nerve fibre layer, GCL – ganglion cell layer, IPL – inner plexiform layer, INL – inner nuclear layer, OURETL – outer retinal layers, RPE – retinal pigment epithelium.*

Figure 6.5 further illustrates the mean values with 95% confidence intervals for individual retinal layers at the fovea between gestational age 24 and 30 weeks.

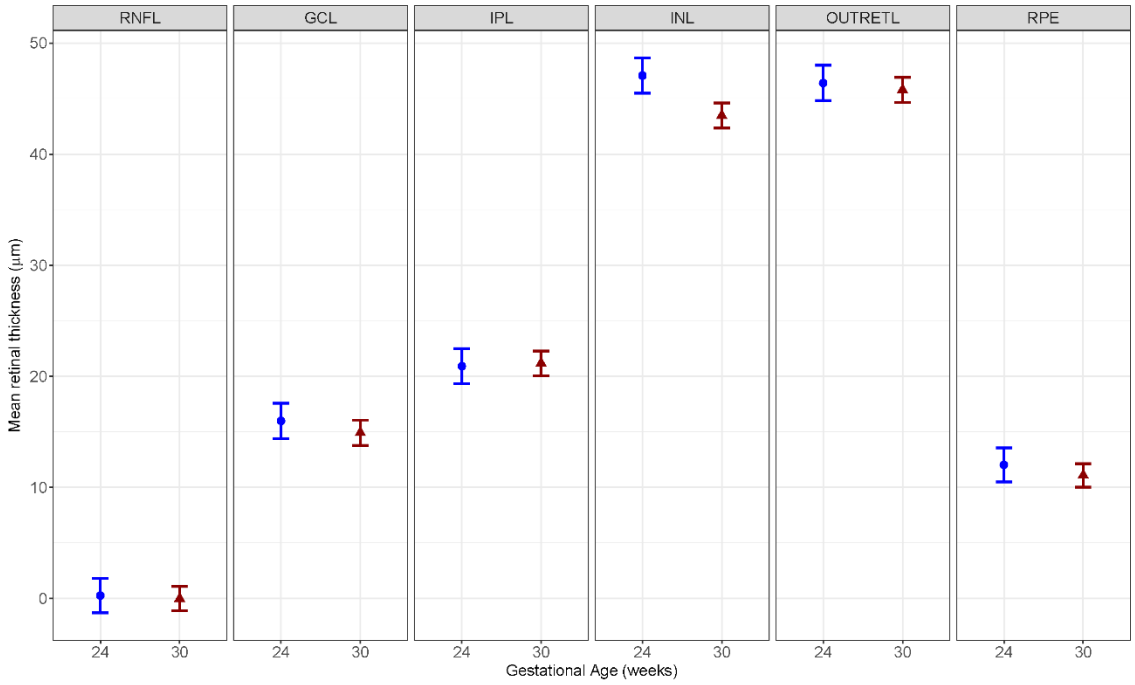


**Figure 6.5 Plot of mean individual retinal layer thickness at the fovea with 95% confidence intervals between gestational age 24 and 30 weeks** at **mean postmenstrual age** 36 weeks. *RNFL – retinal nerve fibre layer, GCL – ganglion cell layer, IPL – inner plexiform layer, INL – inner nuclear layer, OUTERTL – outer retinal layers, RPE – retinal pigment epithelium.*

The greatest difference between 24 to 30 weeks GA occurs in the INL and table 6.4 shows this is statistically significant.

| Layer | Difference (µm) | p value |
|---|---|---|
| RNFL | -0.28 | 0.75 |
| GCL | -1.07 | 0.24 |
| IPL | 0.26 | 0.78 |
| INL | -3.60 | >0.001 |
| OUTRet | -0.62 | 0.50 |
| RPE | -0.94 | 0.30 |

**Table 6.4 Results of the difference in mean individual retinal layer thickness at the fovea between gestational ages 24 to 30 weeks** with p values for **mean postmenstrual age** 36 weeks. *RNFL –retinal nerve fibre layer, GCL – ganglion cell layer, IPL – inner plexiform layer, INL – inner nuclear layer, OUTRet – outer retinal layers, RPE – retinal pigment epithelium.*

### *6.32B. The effect of birth weight on individual foveal retinal layers*

We investigated the difference between two birthweights (750 to 1500 grams) to explore the effect of BW on individual foveal retinal layers at mean PMA 36 weeks. The results are shown in table 6.5.

| Layer | Difference (µm) | p value |
|---|---|---|
| RNFL | 0.94 | 0.18 |
| GCL | 0.75 | 0.28 |
| IPL | 2.30 | 0.001 |
| INL | -4.37 | >0.001 |
| OUTRet | 2.81 | >0.001 |
| RPE | 1.02 | 0.15 |

**Table 6.5 Difference in mean individual retinal layer thickness at the fovea with increased birthweight 750 to 1500 grams** with p values for **mean PMA** 36 weeks. *RNFL –retinal nerve fibre layer, GCL – ganglion cell layer, IPL – inner plexiform layer, INL – inner nuclear layer, OUTRet – outer retinal layers, RPE – retinal pigment epithelium, PMA – postmenstrual age*

An increase in BW from 750 to 1500 grams resulted in significantly decreased foveal INL with increased Outer retina at mean PMA shown in figure 6.6.

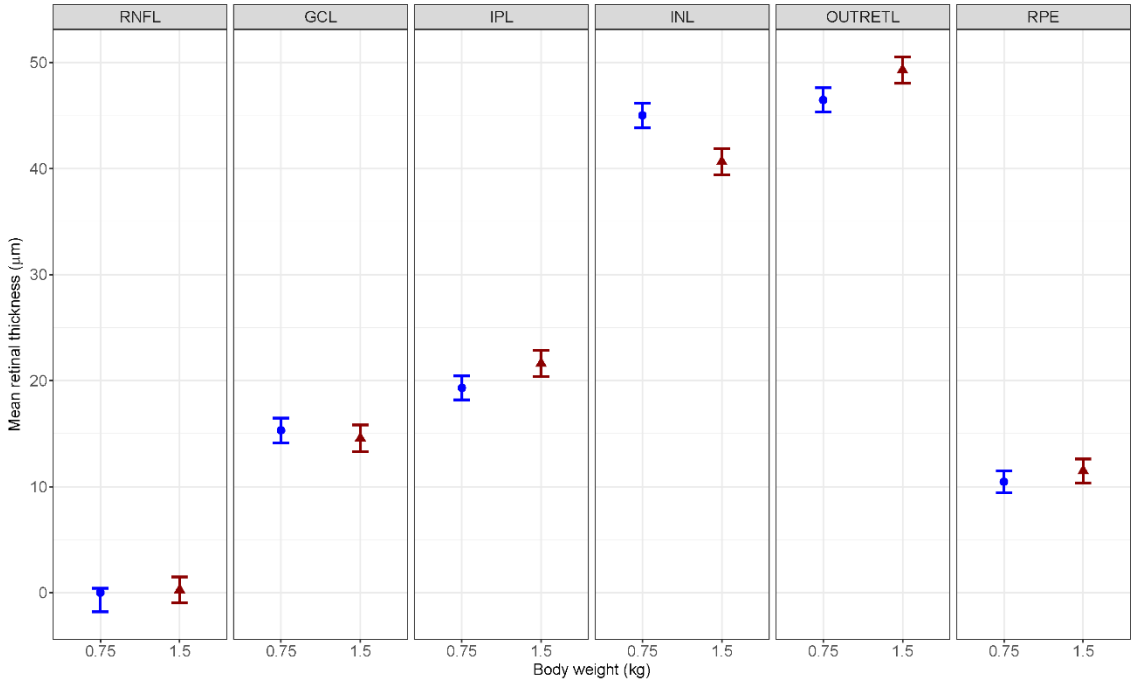


**Figure 6.6 Plot of mean individual retinal layer thickness at the fovea with 95% confidence intervals between 750- and 1500-grams birthweight** at **mean postmenstrual age** 36 weeks. *RNFL – retinal nerve fibre layer, GCL – ganglion cell layer, IPL – inner plexiform layer, INL – inner nuclear layer, OUTRet – outer retinal layers, RPE – retinal pigment epithelium.*

### *6.32C. The effect of ROP on individual foveal retinal layers at the mean PMA (36 weeks)*

In the previous chapter we reported that there was no statistically significant effect on CFT for the presence or absence of ROP. Table 6.6 shows the results of the mean difference in individual retinal layer thickness at the fovea with ROP present compared with non-ROP at mean PMA 36 weeks.

| Layer | Difference fovea (µm) | p value |
|---|---|---|
| RNFL | 1.36 | <0.001 |
| GCL | 2.69 | <0.001 |
| IPL | 3.35 | <0.001 |
| INL | -0.19 | 0.48 |
| OUTRet | 5.20 | <0.001 |
| RPE | 2.14 | <0.001 |

**Table 6.6 Difference in mean individual retinal layer thickness at the fovea when ROP is present compared with ROP not present** for **mean PMA** 36 weeks. *RNFL –retinal nerve fibre layer, GCL – ganglion cell layer, IPL – inner plexiform layer, INL – inner nuclear layer, OUTRet – outer retinal layers, RPE – retinal pigment epithelium, PMA – postmenstrual age*

All individual layers significantly increased at the fovea in the presence of ROP except the INL.

### *6.33. The effect of ROP presence at early PMA (32 weeks)*

In Chapter 5 our results showed that in early PMA (30 to 33 weeks), the mean foveal width (diameter) was greater in the absence of ROP compared with presence of ROP (see Figure 5.4, p85).

The mean foveal width (diameter) with and without ROP for PMA from 30 to 33 weeks was 1047.3 µm ± 158.2 and 1480.0 µm ± 290.1 respectively (p= 0.021). Therefore, we examined the differences between presence and absence of ROP for individual retinal layers at 500µm nasal and temporal to the fovea (foveal width 1000µm).

Figure 6.7 is a still from the video animation (see video 1) (https://www.dropbox.com/s/z2vo8qdl0t5blli/video%201%20.avi?dl=0) showing the internal limiting membrane (ILM) contour between ROP and non-ROP at 32 weeks PMA. The difference in foveal width may be seen at -500 µm nasal and 500 µm temporal to the fovea (location 0).

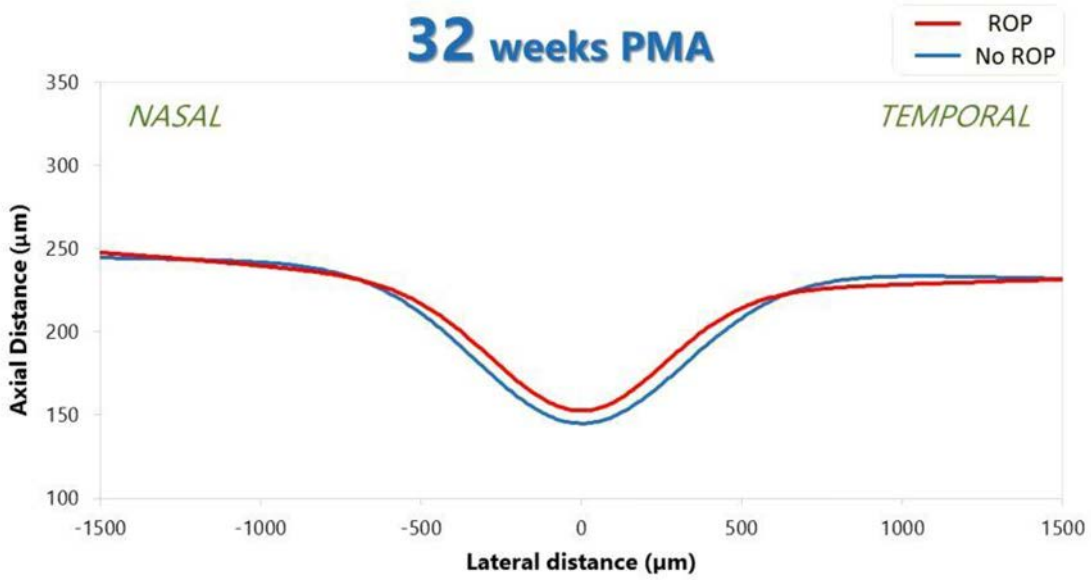


**Figure 6.7 ILM contour between ROP and non-ROP for 32 weeks PMA** (see video 1). Fovea is location 0, nasal is negative, temporal is positive. *ILM – internal limiting membrane, ROP – retinopathy of prematurity*

Table 6.7 shows the differences in mean individual retinal thickness for ROP presence compared with absence of ROP at the fovea, and at -500 µm nasal, 500 µm temporal to the fovea at PMA 32 weeks using mean GA. We found similar results when using mean BW in the model.

Figure 6.8 plots results of INL and Outer retinal layers between ROP and non-ROP at 32 weeks PMA using mean GA.

| Layer | Difference nasal 500 (μm) | p value | Difference fovea (μm) | p value | Difference temporal 500 (μm) | p value |
|---|---|---|---|---|---|---|
| RNFL | -0.38 | 0.16 | 1.36 | <0.001 | -0.55 | 0.04 |
| GCL | 0.95 | <0.001 | 2.69 | <0.001 | 0.78 | 0.04 |
| IPL | 1.62 | <0.001 | 3.35 | <0.001 | 1.44 | <0.001 |
| INL | -1.93 | <0.001 | -0.19 | 0.48 | -2.11 | <0.001 |
| OUTRet | 3.47 | <0.001 | 5.20 | <0.001 | 3.29 | <0.001 |
| RPE | 0.40 | 0.15 | 2.14 | <0.001 | 0.22 | 0.42 |

**Table 6.7 Difference in mean individual retinal layer thickness when ROP is present compared with ROP absent**: at -500 μm (nasal), 500 μm (temporal) and at the fovea for **PMA 32 weeks**. *RNFL –retinal nerve fibre layer, GCL – ganglion cell layer, IPL – inner plexiform layer, INL – inner nuclear layer, OUTRet – outer retinal layers, RPE – retinal pigment epithelium, PMA – postmenstrual age*

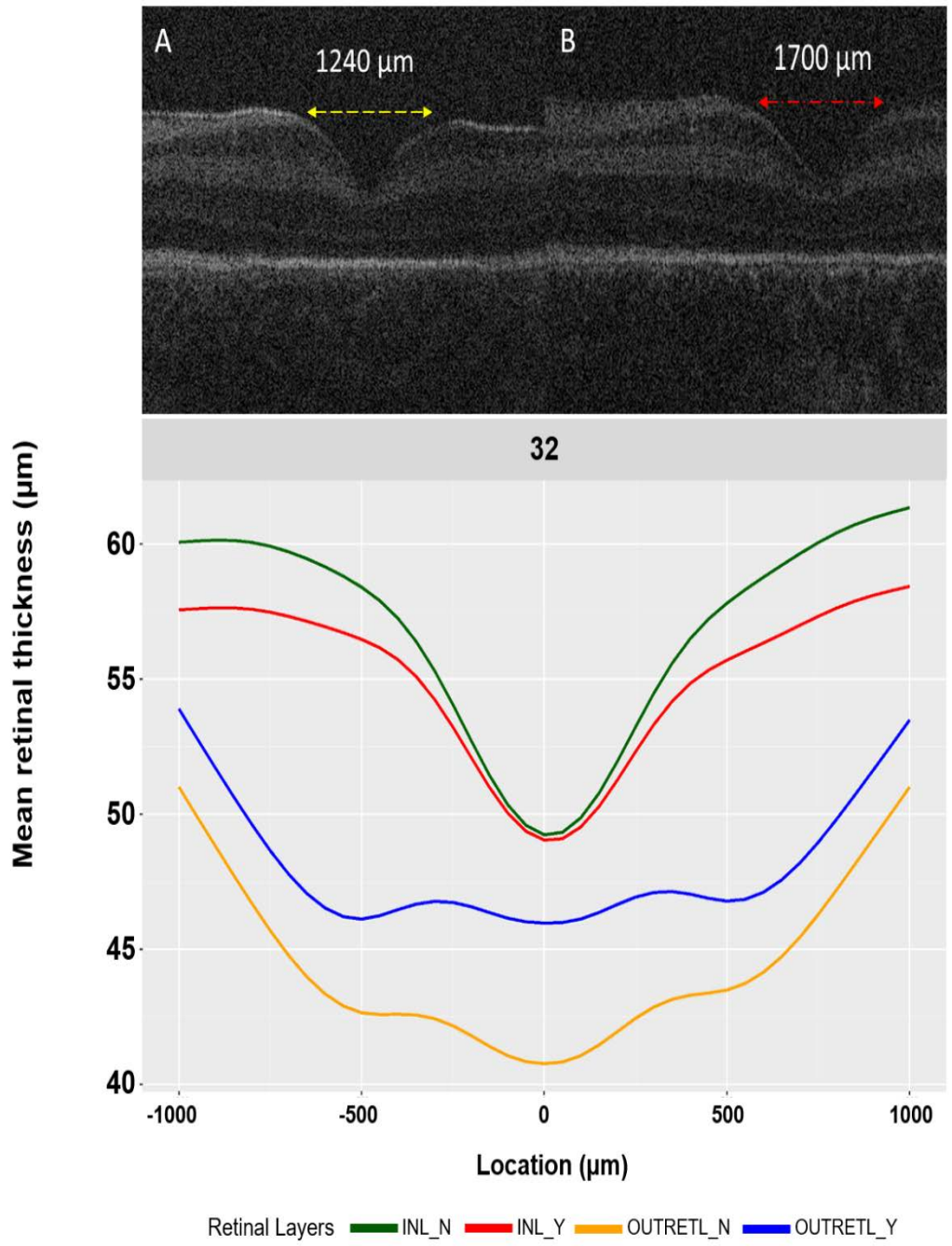


**Figure 6.8 Plot of mean retinal thickness from -1000 µm to 1000 µm between ROP and non-ROP for INL and OUTRETL** (Y, N respectively) at **PMA 32 week**. Fovea is location 0, negative is nasal, temporal is positive. Example of original flattened HH SD-OCT images of ROP (A) and non-ROP (B) infants with mean GA 27 weeks. Image measurements are not to scale. *INL – inner nuclear layer, OUTRETL – outer retinal layers, PMA – postmenstrual age, ROP – retinopathy of prematurity, HH SD-OCT – hand held spectral domain optical coherence tomography.*

Table 6.7 and figure 6.8 show that although the GCL, IPL and Outer retinal layers are all significantly increased at the fovea, and at -500 µm nasal, 500 µm temporal to the fovea, the greatest increases are in the Outer retinal layers. The INL shows a reduction at -500µm and 500µm but the INL shows no statistically significant difference between ROP and non-ROP at the fovea.

## 6.4 Discussion

### *6.41 Overall conclusions*

Using HH SD-OCT, we show that from 33 to 39 weeks postmenstrual age, significant changes are observed at the fovea in preterm infants for all individual retinal layers except the IPL.

We also show that at the mean time point of 36 weeks PMA, significant differences exist between the individual layers with respect to early or late GA, low or higher BW and presence of ROP. This is a comprehensive study separating these closely related factors in order to understand the differences in greater detail. We report for the first time, the impact of BW on individual retinal layers at the fovea in preterm infants using HH SD-OCT.

The results find that the foveal INL before 40 weeks is the layer most significantly affected by prematurity (GA and BW). It is therefore the layer most likely to result in increased CFT found with continuation of inner layers at the fovea in ex-preterm children since the INL is observed to reduce very little during childhood in this group.

In early PMA, ROP significantly affects the retinal layers between the fovea and parafovea especially the photoreceptor layers, which are increased compared to when ROP is absent. The INL nasal and temporal to the fovea is reduced with the presence of ROP. The difference in foveal width between ROP and non-ROP that we identified in early PMA, is most likely due to these changes in the outer retina and inner nuclear layers when ROP is present.

*6.42 Individual retinal layer differences at the fovea with postmenstrual age*

There are few preterm infant studies of individual retinal layers before 42 weeks PMA using SD-OCT. Vajzovic and colleagues (Vajzovic et al. 2012) correlated histology with SD-OCT in 22 premature infants subdivided into two groups according to PMA (30-32 weeks, n=8) and 33-36 weeks, n=14).

The changes in retinal layers with PMA (in weeks) are described according to phases: phase 1 (30-32), phase 2 (33-36), phase 3 (37-39) and phase 4 (40-42). Phases 3 and 4 include term born children in the analysis. Phases 1 and 2 represent the change in retinal layers with PMA up to 36 weeks for preterm infants and not beyond and stated by the authors. However, an adjustment for GA and individual retinal layers was not included in the analysis. The results of the study are shown on figure 2.2 (see Chapter 2, p33).

Nevertheless, the study shows clearly that retinal layers change according to PMA and retinal location (reported as eccentricity away from the foveal centre nasally and temporally). The changes become more marked with increasing PMA after term (phase 5, 43weeks to 23 months) and within 500µm nasal and temporal to the central fovea.

Our results plotted in Figure 6.2 support that of Vajzovic and colleagues (Vajzovic et al. 2012), where we also find that the mean foveal thicknesses of individual retinal layers change with PMA. However, a comparison between the two studies shows the approximate differences are not similar between 33 to 39 weeks PMA (phase 2 plus phase 3 of the study by Vajzovic et al. 2012 (Table 6.8).

| % difference at fovea from 33 to 39 weeks PMA | | |
|---|---|---|
| Layer | Vajzovic et al | our study |
| RNFL | -15% | -89% |
| GCL+IPL | -39% | -10% |
| INL | -63% | -19% |
| PRC +OPL | 13% | 14% |
| RPE | -1% | -9% |

**Table 6.8 Comparison of percentage change at the fovea from PMA 33 to 39 weeks between Vajzovic et al. 2012 and the current study.** *RNFL –retinal nerve fibre layer, GCL – ganglion cell layer, IPL – inner plexiform layer, INL – inner nuclear layer, OPL – outer plexiform layer, PRC – photoreceptor complex (ONL+IS+OS), RPE – retinal pigment epithelium. PMA – postmenstrual age*

In our study the RNFL decreased much more than that of the infants in the study by Vajzovic et al. 2012 while the GCL, IPL and INL decreased less. Interestingly the foveal outer retinal layers increase was similar in both studies.

The differences may reflect the sample size between the two studies (n= 22 preterm infants for the study by Vajzovic et al, compared to n=87 for this study), the inclusion of 19 term born infants at PMA 37 to 39 weeks in the study by Vajzovic and colleagues (Vajzovic et al. 2012), and the adjustment for ROP diagnosis and GA in our study.

*6.43 The effect of prematurity (GA and BW) on foveal retinal layers and relationship with central foveal thickness (CFT)*

Figures 6.4 and 6.5 illustrate the effect of changing GA on individual mean retinal layer thickness at the mean time point (PMA 36 weeks) while figure 6.6 details the effect of BW. Choosing the mean PMA allows comparisons for each individual layer between GA or BW to be better appreciated.

Figure 6.4 shows that the retinal layers at the fovea change according to GA in preterm infants. However, only the foveal INL is significantly different between preterm infants born at GA 24 weeks and older preterm infants born at 30 weeks GA. This is also strongly true of younger BW compared with heavier BW, but the changes that are seen at the fovea with BW are not limited to the INL (see Table 6.5).

We investigated the effect of prematurity on the fovea because we wished to determine which retinal layer (s) might result in the increased CFT reported widely in prematurity. In the analysis of CFT with prematurity, we found that CFT was correlated with GA but not BW (see Chapter 5, Figure 5.7 p89).

In the present analysis, GA correlated only with one retinal layer at the fovea (INL) but BW correlated with two (INL and Outer retinal layers). To understand why BW did not significantly affect CFT we hypothesized that despite the greater change in the INL with low BW (Table 6.5) compared with GA (Table 6.4), the overall CFT effect with BW would still be less than that with GA, due to changes in the outer retinal layers layers for infants with low GA.

Table 6.9 compares the percentage differences between low BW 750Kg and GA 24 weeks for the INL and the Outer retinal layers at the fovea.

| Layer | % Difference |
|---|---|
| RNFL | |
| GCL | |
| IPL | |
| INL | 121 |
| OUTRet | 453 |
| RPE | |

**Table 6.9 Differences between effect of reduced BW and early GA at the fovea** for **mean PMA** with respect to the mean individual retinal layer thicknesses that show significance. *PMA – postmenstrual age*

Table 6.9 illustrates that at the mean time point of 36 weeks PMA, although the INL is greater by 121% for low BW infants of 750 grams compared with early born infants GA 24 weeks, the Outer retinal layers are 453% less at the fovea. The overall effect for CFT is that it will be decreased in low BW infants compared with early GA infants despite the greater effect of BW on the INL than GA at the fovea. This possibly explains our earlier finding regarding CFT where only GA and not BW was significant.

Therefore, we propose that the increased CFT seen in preterm infants is secondary to an increased INL and related to earlier GA rather than low BW. This is seen at both fovea (Tariq et al. 2011) and parafovea in older ex-prem children in association with a history of early gestational ages (Wang et al. 2012b).

Since little further outward migration of the inner retinal layers occurs after preterm birth (Maldonado et al. 2011), our findings suggest that the increased CFT observed in preterm children (Bowl et al. 2016; Akerblom et al. 2011) due to continuation of the inner layers across the central fovea, is established from birth. However, Bowl and colleagues (Bowl et al. 2016) found that average GCL+ (=GCL plus IPL) and ONL+ (=ONL plus ELM) thicknesses were greater at the fovea in ex-preterms compared with term born children which is in contrast to our findings.

An increased ONL at the fovea measured using OCT in ex-preterm individuals has been reported by others (Yanni et al. 2012; Hammer et al. 2008; Wang et al. 2012b;

Sjostrand et al. 2017) while an inverse relationship between foveal ONL and CFT with increasing GA in ex-preterm children has also been described (Park and Oh 2012). However, the ONL is challenging to measure using SD-OCT in preterm infants as outlined in Chapter 4 Methods (p59), due to the variability of the presence or absence of the ELM.

Bowl et al. 2016 conducted a sub-analysis of retinal layers where foveal depth was shallow or absent (30% of the group) and labelled as macular developmental arrest (MDA). The authors found although the GCL+ was increased, the RNFL and INL+ (INL plus OPL) were also increased unlike in ex-preterm children with a foveal depression.

We did not explore foveal depth and individual foveal retinal layers and though our results also show that the foveal INL is increased in younger born preterm infants, we did not find any significant increase of RNFL at the fovea in infants before PMA 42 weeks.

Using HH SD-OCT, Vajzovic and colleagues showed that the appearance of the EZ was delayed at the fovea in preterm infants of GA less than 32 weeks when compared with term born infants when images were acquired at 40 and 39 weeks respectively (Vajzovic et al. 2015). We found no significant difference in the foveal PRC between earlier or later born preterm infants at the mean PMA (Table 6.4).

The outer retina increases in early childhood (Vajzovic et al. 2012; Lee et al. 2015) which would also increase CFT, although the increase plateaus around 24 months in term born children (Alabduljalil et al. 2018). Since the inner retina remains relatively static after birth as discussed earlier, the additional increase in CFT is mostly due to increased outer retina. It is possible therefore that with development of the retina at the fovea, and the visibility of the ONL, this layer becomes a significant component of the greater CFT seen in ex-preterm infants by age 6 years as found by Bowl and others (Bowl et al. 2016; Yanni et al. 2012; Wang et al. 2012b; Park and Oh 2012; Sjostrand et al. 2017).

Pueyo (Pueyo et al. 2015) reported no differences in the average RNFL and GCL-IPL thickness between ex-preterm and term born children, unless ex-preterm children

suffered hypoxic-ischaemic events/perinatal infections, or underwent treatment for ROP. However, in their study, the mean GA of 'early' ex-preterm children without ROP was 29 weeks (n=17) while for those with a history of ROP, GA was 27 weeks (n=10). The older gestational age and smaller numbers, suggests that an absence of differences between ex-preterm children from those born at term may not hold true for children with a history of extreme prematurity i.e. GA less than 27 weeks.

*6.44 Retinal layers at the fovea in the presence of ROP*

Section 2C of the Results shows that each measured individual retinal layer at the fovea was increased in the presence of ROP compared with the absence of ROP ($p<0.001$) except the INL. Older ex-preterm children may have reduced optic nerve RNFL in association with severe ROP (grades 3 and 4 including treated ROP) (Akerblom et al. 2012; Park and Oh 2015). However, Akerblom et al. 2012 noted that treated ROP which was included in the severe ROP category, could result in decreased RNFL from the effects of laser and 40% of analysed ex-preterm children in Park and Oh's study had received treatment for ROP.

*6.45 ROP in early PMA and the relationship with foveal width*

As discussed earlier, changes in foveal morphology result from a combination of inner retinal migration away from the foveal centre, increased retinal thickness nasal and temporal to the foveal centre and increased inward photoreceptor packing.

Consequently, foveal width and CFT decrease and foveal depth increases as does foveal slope. This dynamic change can be seen in video 1 (https://www.dropbox.com/s/z2vo8qdl0t5blli/video%201%20.avi?dl=0). Video 1 shows the increasing retinal thickness nasal and temporal to the foveal centre, as the foveal depression decreases with PMA.

In Chapter 5 (see Figure 5.7 p 89) we showed that while foveal width decreased in the absence of ROP, the opposite occurred when ROP was present. The difference in foveal width between ROP and non-ROP was greatest in early PMA when the mean

width or diameter for ROP was 1000 µm. Although the fovea is asymmetric, we investigated the underlying retinal layers with ROP diagnosis at 500µm nasal and temporal to the fovea for the purposes of analysis.

We found a significant difference between ROP and non-ROP for the mean individual retinal layer thicknesses of the INL and Outer retinal layers at 500µm nasal to the fovea. Similar differences were found temporally. The most significant layers were the outer retina which were greater in the presence of ROP compared with ROP absent. In contrast, the INL was found to be less with ROP.

The increased outer retinal layers and reduced INL in the presence of ROP (see Table 6.7) could be the reason that there are differences in foveal width between ROP and non-ROP particularly in early PMA. The outer retina does not contain retinal vasculature and therefore does not reflect vessel structure. The photoreceptor layers comprise the metabolically active component of the retina in ROP. The macula is often affected indirectly in diseases of the periphery (Bird and Bok 2018), and the increased outer retina in the foveal region may be either as a result of an accelerated growth from vascular factors released due to the peripheral retinal ischaemia or some other unknown mechanism.

It is not apparent why the INL is decreased with ROP at the parafovea but it could reflect either vascular or inflammatory Müller cell pathology. The INL is composed of bipolar, amacrine and horizontal cells and contains the bodies of Müller cells. Muller cells are known to respond to photoreceptor injury or stress (Goldman 2014; Hippert et al. 2015). Possibly the INL is responding to the increased outer retina at the same location.

Müller cells express vascular endothelial growth factor (VEGF) (Pierce et al. 1995) and the deep vascular networks are located above and below the INL while the intermediate capillary plexus component is located at the INL and IPL interface (Campbell et al. 2017; Provis 2001). Retinal ischaemia as seen in oxygen induced retinopathy (OIR) in rats, increases Müller cell expression of VEGF type A (Becker et al. 2018). Muller cell expressed VEGF is implicated in intraretinal vascularization (Bai et al. 2009) and in a vascular/avascular retinal OIR mouse model, inner retinal thickness varied according to retinal vascularity and venular width (Mezu-Ndubuisi et al. 2018).

Future study of retinal structure and vascularisation during preterm retinal development with and without ROP using SD-OCT combined with OCT angiography would aid understanding of this finding; early reports using new devices in the infant population show potential in visualisation of the deep intra-retinal plexus which currently cannot be assessed using fluorescein angiography (Campbell et al. 2017).

Our study did not investigate the retinal layer differences between ROP and non-ROP at the parafovea with increasing PMA e.g. early PMA vs late PMA to explore the changes that could explain the increasing foveal width seen with PMA when ROP is present.

### 6.6 Limitations

The limitations of the study include that we did not analyse individual retinal layer changes at the fovea with increasing PMA between various GA, or various BW, or when ROP is present; we reported only changes at the mean PMA for these variables.

Similarly, we did not explore the parafovea with PMA or the differences at the parafovea between ROP and non-ROP. These analyses would add to the findings and help to evaluate a more dynamic description of the fovea adjusting for GA, BW and ROP. An increased number of preterm infants imaged in early PMA would improve the analysis of retinal layers eccentric to the fovea since retinal layer segmentation particularly of the outer retina, is more challenging in early PMA. We also did not explore the systemic health challenges posed during the early postnatal period which as described in Chapter 5, may impact both growth in the neonatal period, and ROP.

The lack of information regarding the vasculature within the inner retina presents difficulties in correlating the inner retinal differences found between ROP and non-ROP, since disparities may represent vascular change or unrelated characteristics between the two groups.

## 6.7 Conclusion

The premature fovea demonstrates great change with postmenstrual age during the perinatal period before term birth but also with birth age, birthweight and diagnosis of ROP.

It is important to acknowledge these differences exist when assessing the foveal changes that occur in preterm infants, since the various birth ages, birthweights and diagnosis of ROP will differ within this group. The inner nuclear layer is conspicuous in the development of the fovea in prematurity and is the layer that increases CFT in extremely early born preterm infants when CFT is measured before 40 weeks PMA.

Although we did not show how each individual layer changes with time comparing early and late GA, low or high BW or ROP presence/absence, our findings are relevant for the development of the retinal layers during early childhood. This is especially useful for infants where comparisons are made between age adjusted preterm infants with term born individuals.

The highly metabolically active photoreceptor layers are especially associated with the presence of ROP and may reflect the wider changes within the ischaemic retina. Understanding the disparity between the retinal layers in foveal width measured using HH SD-OCT at early PMA between ROP and non-ROP may reveal ROP disease mechanisms. Further study of the peripheral outer retina and correlation with the deep vascular plexus located in the INL in the presence of ROP would be interesting.

# Chapter 7 Foveal Oedema

Chapter 7 discusses research aim 3 and describes the cystic intra-retinal changes observed at the fovea using HH SD-OCT imaging of preterm infants from 31-42 weeks PMA.

## 7.1 Introduction

Optical coherence tomography imaging of infants has revealed retinal details that are invisible with direct or conventional examination (Patel 2006; Chavala et al. 2009; Cabrera et al. 2012; Muni et al. 2010). A consistent feature observed in preterm infants is intra-retinal cystic change at the fovea described as cystic macular oedema (CME) visualised as hyporeflective spaces within the retina (Maldonado et al. 2011; Maldonado et al. 2012; Dubis et al. 2013; Vinekar et al. 2011; Erol et al. 2014; Gursoy et al. 2016; Vajzovic et al. 2015; Lee et al. 2011; Bondalapati et al. 2015).

Studies report that between 15% to 72% of preterm infants demonstrate CME on at least one SD-OCT imaging session from 32 to 43 weeks PMA and CME has also been found in term born infants (Vajzovic et al. 2015; Cabrera et al. 2013). It is thought that CME does not resolve before 36 weeks PMA if CME is found between 30 to 35 weeks PMA (Maldonado et al. 2012) and has disappeared in preterm infants imaged at 52 weeks PMA (Vinekar et al. 2011).

The severity of CME as measured by CFT may be associated with an increased stage of ROP (Vinekar et al. 2011; Erol et al. 2014; Gursoy et al. 2016) although others report no such association, and CME may be present before and after treatment for ROP (Dubis et al. 2013; Vogel et al. 2018; Maldonado et al. 2012; Bondalapati et al. 2015).

CME is not associated with BW, sex, ethnicity (Dubis et al. 2013; Vogel et al. 2018; Rothman, Tran-Viet, et al. 2015; Bondalapati et al. 2015) or systemic preterm neonatal risk factors such as sepsis, necrotizing enterocolitis, intraventricular hemorrhage, periventricular leukomalacia, hydrocephalus or immature lung disease (Maldonado et al. 2012; Bondalapati et al. 2015).

However, the development of the photoreceptor layer at the foveal centre by 42 weeks PMA appears delayed using SD-OCT in preterm infants found to have CME (Vajzovic et al. 2015) while reduced visual acuity and greater hyperopia is shown between preterm infants with and without CME at 3 months corrected age (Vinekar et al. 2015). Additionally, preterm infants with CME may have worse neuro-developmental speech and language outcomes in early childhood between 18 to 24 months corrected age (Rothman, Tran-Viet, et al. 2015).

Two patterns of CME have been described: loss of the foveal depression due to distortion of the foveal contour from large intra-retinal cystic spaces ('dome CME') or preservation of the foveal pit with increased INL thickening from multiple cystic spaces ('fovea CME') (Vinekar et al. 2011; Maldonado et al. 2012; Erol et al. 2014). Dome CME is not reported with the CME described in term born infants (Vajzovic et al. 2015). A summary of CME infants studies using SD-OCT is shown in Chapter 2, Table 2.1, p36.

The exact mechanism or significance of infant CME is currently unknown. Several hypotheses regarding the pathophysiology of CME (Maldonado et al. 2012; Vinekar et al. 2011; Erol et al. 2014) are based on aetiology such as a breakdown of the blood retinal barrier (BRB) (Daruich et al. 2018) or vascular retinopathies e.g. diabetes (Xia and Rizzolo 2017).

It is possible that infant CME may result from the increased levels of VEGF associated with Müller cell physiology and or from swelling of Müller cells themselves (Xin et al. 2013; Bai et al. 2009; Wang, Zhu, and Le 2015; Fine and Brucker 1981; Bringmann, Reichenbach, and Wiedemann 2004). Other hypotheses relate to the sub-retinal oedema reported in term infants (Cabrera et al. 2012) and decreased RPE density found in infants (Robb 1985) since the primary BRB is formed by tight junctions between retinal capillary endothelial cells and the RPE.

The external limiting membrane (ELM, also known as the outer limiting membrane) is a protein limiting fenestrated structure (Bunt-Milam et al. 1985) formed between the Müller cell membrane junction with that of the photoreceptor cell inner segment membrane by zonulae adherentes (Hogan, Alvarado, and Weddell 1971). The ELM also

forms part of the blood retinal barrier preventing large proteins passing to and from the retina (Omri et al. 2010). The presence or absence of the ELM may play a role in CME aetiology but has not been reported in the literature investigating preterm infants with CME.

In this chapter, the relationship between CME size with GA, BW and diagnosis of ROP will be explored, as well as the possible role of the ELM.

### 7.2 Methods

Optical coherence images were acquired and saved for analysis as described previously in General Methods Chapter 4. Images that demonstrated hyporeflective spaces within the retina at the fovea similar to that described in the literature were analysed. An example of this is shown below in Figure 7.1.

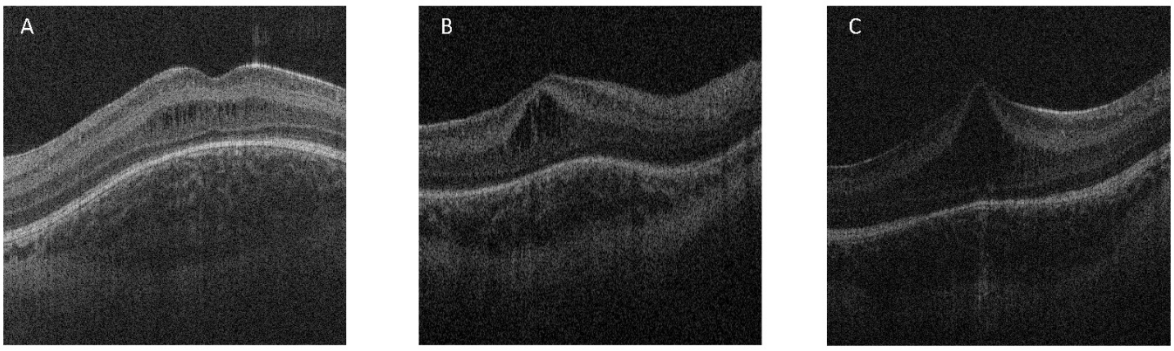


**Figure 7.1 Intra-retinal hyporeflective spaces at the fovea** observed using hand held optical spectral domain optical coherence tomography (HH SD-OCT) in 3 preterm infants. A - male infant, twin, gestational age (GA) 26 weeks, image left eye, acquired 37 weeks postmenstrual age (PMA), no retinopathy of prematurity (ROP); B - female infant, 30 weeks GA, image right eye, acquired 38 weeks PMA, ROP stage 1; C - male infant, twin, 31 weeks GA, image right eye, acquired 37 weeks PMA, no ROP.

Figure 7.1 demonstrates hyporeflective spaces in the retina of three preterm infants described in the literature as CME. Two common types of foveal CME are determined by the presence or absence of the foveal depression ('fovea CME' and 'dome CME') shown in figure 7.1 A, and 7.1B, C respectively.

The outline of the hyporeflective space was manually segmented using Image J (United States National Institutes of Health, Bethesda, MD, https://imagej.nih.gov/ij/,

downloaded on December 2013) after inspection of the image. An example is shown in Figure 7.2.

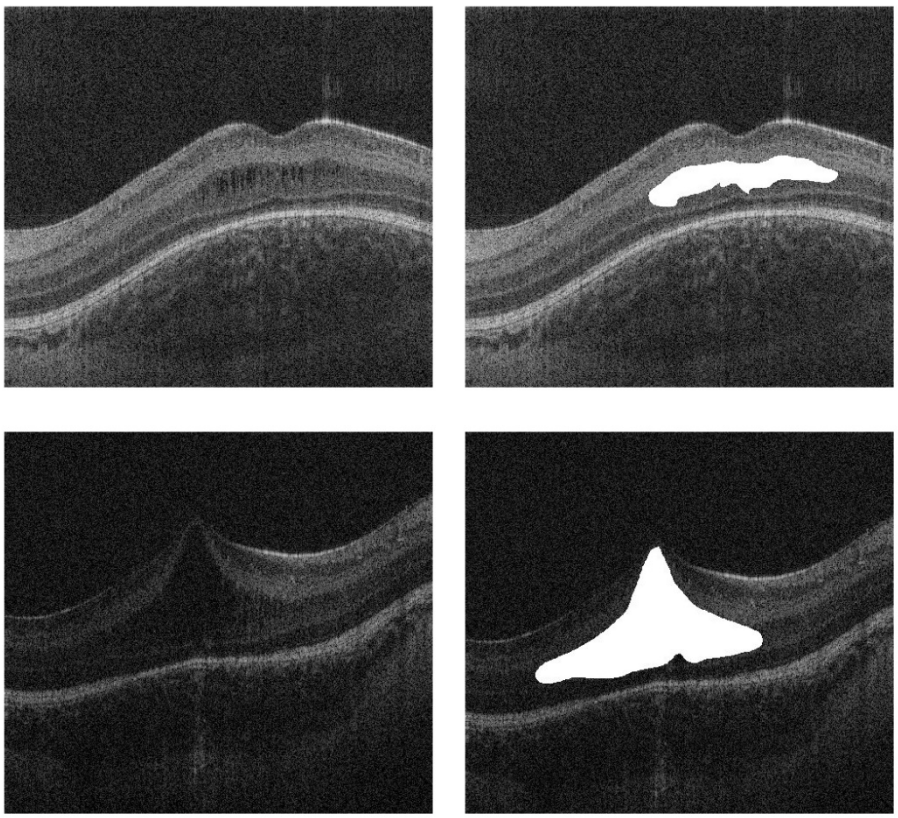

**Figure 7.2 Hand-held spectral domain optical coherence tomography image of a preterm infant**. Example of foveal hyporeflective space outline and area for analysis. Fovea CME is shown in the top panel, dome CME is shown below.

Repeated measures were taken from either or both eyes of individual infants between 1 to 2-week intervals between 31 to 44 weeks PMA. For repeated images, the foveae were matched as closely as possible when manual segmentation was undertaken, to try and delineate the affected spaces involving the fovea and surrounding retina consistently.

Data were saved as text files and a customised macro using Excel (Microsoft Windows®) was used sum up the number of white pixels in each A-scan in order to calculate thickness (CFT), width and area after incorporating an axial length correction for PMA based on previous literature (Maldonado et al. 2010). Figure 4.6 (Chapter 4,

Methods, page 60) demonstrates the ELM.

Image data were recorded according to the presence or absence of the ELM, the type of CME (dome, or fovea), diagnosis of ROP, in addition to demographic data (sex, GA, BW, right or left eye, ethnicity, multiplicity of birth). The details of data analysis have been discussed previously in Chapter 4 Methods (statistical analysis, p68).

Descriptive statistics are presented below. Chi-square tests were used to investigate the distribution between variables such as ethnicity, sex, and multiplicity of birth with CME type. Two- sample unpaired t-tests (parametric or non-parametric depending on data normality assessment) were used to estimate mean differences between GA, BW, and CME size between CME presence or absence and type. A simple linear regression model was used to investigate possible predictors of CME type. The outcome or dependent variables included: CME (presence or absence), CME type (fovea/dome), CFT, width and area. Principle predictor variables included diagnosis (presence or absence of ROP), GA or BW and presence or absence of the ELM.

## 7.3 Results

### *7.31 Descriptive statistics*

Descriptive summaries for preterm infants without CME been described previously (Results, Chapter 5) and are presented again below in Table 7.1 along with details of twenty-five infants with CME (n=9 with, n=16 without ROP) and sixty-six images suitable for analysis.

Table 7.1 shows that the total number of images was 344. CME was present in 22% of all preterm infants in the study and 19% of all images acquired that were suitable for analysis. Of the images with CME present, there was the following breakdown as follows: nonROP n=33, (16% of all nonROP images), ROP n=33, (24% of all ROP images); CME with ELM present n=17 (17% of all ELM present images) and CME with ELM absent (n=49, 49% of all ELM absent images).

The mean (± standard deviation) for GA (weeks) and BW (grams), respectively for CME absent and CME present was: 28.2 (±2.6), 29.8 (2.6) (p=0.009); 1085.7 (± 427.7), 1308.1 (±443.1), (p=0.021).

| | | CME no | CME yes |
|---|---|---|---|
| **number of infants** | | | |
| **Total 112** | | 87 | 25 (22%) |
| Male | 61 | 47 | 14 (23%) |
| Female | 51 | 40 | 11 (22%) |
| | | | |
| Caucasian | 60 | 46 | 14 (23%) |
| Non-Caucasian | 52 | 41 | 11 (21%) |
| | | | |
| Single birth | 90 | 75 | 15 (20%) |
| Multiple birth | 22 | 12 | 10 (45%)* |
| | | | |
| **Mean (±SD) GA, BW, PMA** | | | |
| GA (weeks) | | 28.2(2.6) | 29.8 (2.6) |
| BW (grams) | | 1083.2 (429.2) | 1308.1(443.1) |
| PMA (weeks) | | 36.2 (2.6) | 36.8 (2.4) |
| | | | |
| **Number of images** | | | |
| **Total 344** | | 278 (81%) | 66 (19%) |
| Right eye | 176 | 132 | 44 (25%) |
| Left eye | 168 | 146 | 22 (13%) |
| | | | |
| nonROP | 206 | 173 | 33 (16%) |
| ROP | 138 | 105 | 33 (24%) |
| | | | |
| CME fovea | | - | 32 |
| CME dome | | - | 34 |
| | | | |
| ELM absent | 244 | 195 | 49 (21%) |
| ELM present | 100 | 83 | 17 (17%) |

**Table 7.1 Participant and image characteristics including cystoid macular oedema**. *GA – gestational age, BW – birthweight, PMA – postmenstrual age, ELM – external limiting membrane, CME – cystoid macular oedema.*

### 7.4 Analysis of CME present with CME absent

*7.41 Comparison of GA and BW between CME presence or absence*

Figure 7.3 shows stacked histograms of the distribution with CME present (blue) and CME absent (green), with GA and BW.

The mean (± standard deviation) for GA (weeks) respectively for CME absent and CME present was: 28.2 (±2.6), 29.8 (2.6) (p=0.009); and for BW (grams) it was 1085.7 (± 427.7), 1308.1 (±443.1), (p=0.021), Table 7.1.

Preterm infants with CME were born later and were heavier at birth when compared with preterm infants without CME.

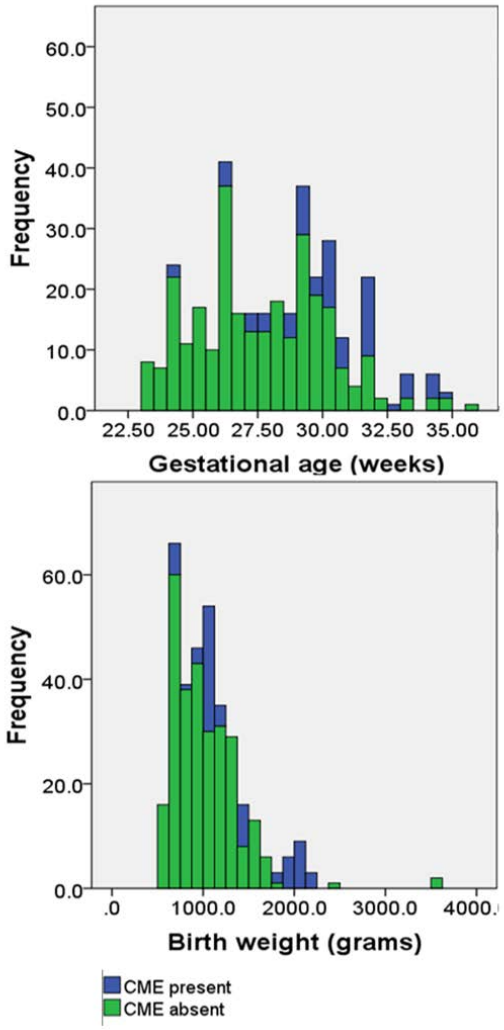


**Figure 7.3. Stacked histogram of the distribution for CME presence or absence** with gestational age and birthweight. *CME – cystoid macular oedema.*

A sub-analysis investigating differences of mean GA and mean BW between sex, ethnicity and birth multiplicity was undertaken and the results are given in table 7.2. Table 7.2 shows the mean GA and BW comparisons between CME absent and present (CME no, CME yes) for sex (males, females), ethnicity (Caucasian, Non-Caucasian), and birth multiplicity (singles, multiple).

| | **GA (± SD) weeks** | p value | **BW (± SD) grams** | p value |
|---|---|---|---|---|
| **sex** | | | | |
| males CME no | 28.5 (±2.5) | 0.08 | 1121.9 (±347.4) | 0.109 |
| males CME yes | 29.7 (±2.4) | | 1335.7 (±417.5) | |
| females CME no | 27.8 (±2.8) | 0.053 | 1043.2 (±507.5) | 0.101 |
| females CME yes | 29.9 (±3.0) | | 1270.5 (±494.2) | |
| **ethnicity** | | | | |
| caucasian CME no | 28.5 (±2.6) | 0.003 | 1090.0 (±333.1) | 0.012 |
| caucasian CME yes | 30.8 (±1.7) | | 1405.3 (±360.0) | |
| non-caucasian CME no | 27.9 (±2.7) | 0.759 | 1081.1 (±514.4) | 0.661 |
| non-caucasian CME yes | 28.5 (±3.1) | | 1175.5 (±525.2) | |
| **multiplicity** | | | | |
| Single CME no | 28.4 (±2.8) | 0.056 | 1100.9 (±457.7) | 0.062 |
| single CME yes | 30.0 (±2.7) | | 1280.6 (±369.9) | |
| multiple CME no | 27.2 (±1.6) | 0.031 | 1018.1 (±255.4) | 0.165 |
| multiple CME yes | 29.5 (±2.7) | | 1352.0 (±560.3) | |

**Table 7.2 The mean comparisons of GA and BW between sex, ethnicity and birth multiplicity** for presence and absence of CME. *GA – gestational age, BW – birthweight, PMA – postmenstrual age, CME – cystoid macular oedema.*

Although there were differences in the mean comparisons of GA for CME presence and absence between males (p=0.08), Caucasians (p=0.003), multiple births (p=0.031) and BW for Caucasians (p=0.012), statistical modeling did not find that these variables were predictors of CME presence. Similarly, no significance was found for presence or absence of ROP, stage eye laterality or presence /absence of the ELM on the presence or absence of CME.

### 7.5 Analysis of preterm infants with CME

In the CME group, the breakdown was as follows: n= 25 preterm infants; 14 males (56%) and 11 females (44%); 14 Caucasians (56%), 11 Non-Caucasians (44%); 15 singletons (60%) and 10 multiple birth infants (twins) (40%).

The number of CME images with nonROP = 44 (67%) and ROP = 22 (33%) [n= 11 stage1; n=10 stage 2; n=1 stage 3]. Fifty percent of the CME images were right eyes (n=33 respectively).

Fovea CME was present in 32 images, dome CME was present in 34 images while the ELM was present in 17 images (26%) and absent in 49 images (74%). Table 7.3 shows the number of preterm infants with CME and imaging sessions.

| Imaging sessions | Number of infants | Number of images |
|---|---|---|
| 1 | 13 | 19 |
| 2 | 8 | 25 |
| 3 | 3 | 13 |
| 5 | 1 | 9 |
| Total | 25 | 66 |

**Table 7.3 Number of imaging sessions** for preterm infants with cystoid macular oedema.

#### *7.51 Comparison of mean GA and BW between individuals with fovea CME and dome CME*

Table 7.4 shows that there were no differences in the mean GA or mean BW between individuals with fovea CME or dome CME.

| | **GA (± SD) weeks** | p value | **BW (± SD) grams** | p value |
|---|---|---|---|---|
| **CME type** | | | | |
| fovea | 29.3 (±3.2) | 0.196 | 1215.0 (±431.6) | 0.115 |
| dome | 30.6 (±1.4) | | 1469 (±454.9) | |

**Table 7.4 Comparisons of mean GA and BW for CME type** (fovea or dome). *GA – gestational age, BW – birthweight, CME – cystoid macular oedema.*

*7.52 Comparison of mean GA and BW between individuals irrespective of CME type*

The results of mean GA and mean BW comparison between sex, ethnicity and birth multiplicity are given in table 7.5. Table 7.5 shows the mean GA and BW comparisons for infants irrespective of CME type. Ethnicity was significant in the CME group, which found Caucasians with CME to be older at birth than Non-Caucasians with CME.

| | **GA (± SD) weeks** | p value | **BW (± SD) grams** | p value |
|---|---|---|---|---|
| **sex** | | | | |
| males | 29.8 (±2.5) | 0.893 | 1353.2 (±427.4) | 0.536 |
| females | 29.9 (±3.0) | | 1270.5 (±494.1) | |
| **ethnicity** | | | | |
| caucasian | 30.9 (±1.7) | 0.033 | 1427.9 (±362.5) | 0.075 |
| non-caucasian | 28.5 (±3.1) | | 1175.5 (±525.2) | |
| **multiplicity** | | | | |
| single | 30.0 (±2.8) | 0.723 | 1293.3 (±379.2) | 0.935 |
| multiple | 29.5 (±2.7) | | 1352 (±560.3) | |

**Table 7.5 Comparisons of mean GA and BW for sex, ethnicity and birth multiplicity for preterm with CME**. *GA – gestational age, BW – birthweight, CME – cystoid macular oedema.*

*7.53 Comparisons between groups depending on CME type*

Figure 7.4 shows bar charts of the percentage between fovea and dome CME for sex, ethnicity, birth multiplicity, right and left eyes, presence or absence of ROP and presence or absence of the ELM.

Pearson's Chi-Square test reported a greater percentage of dome CME between Caucasian and Non-Caucasians (79.4% vs 20.6%) than fovea CME (53.1% vs 46.9%) (p= 0.024). A difference was also found between the presence and absence of the ELM for dome CME (11.8% vs 88.2%) and fovea CME (40.6% vs 59.4%) (p= 0.007, Pearson's Chi-Square).

No difference was found between CME type and sex, multiplicity of birth, eye laterality or ROP diagnosis.

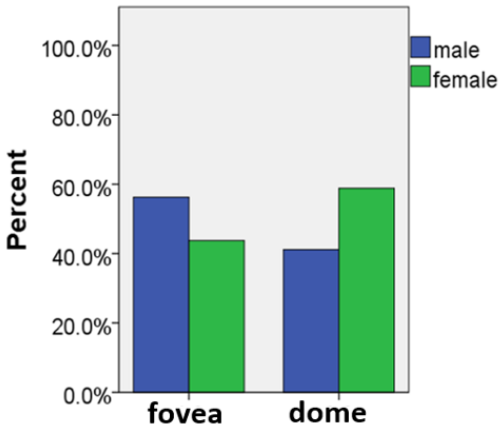


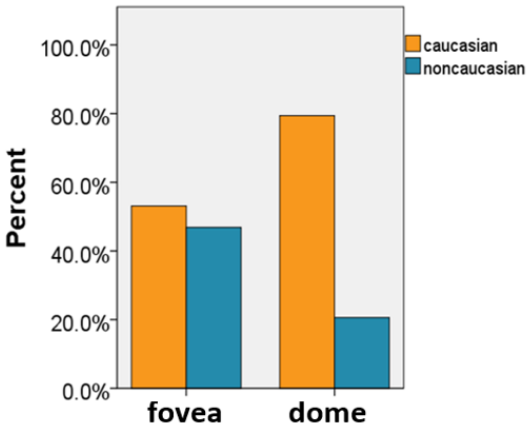


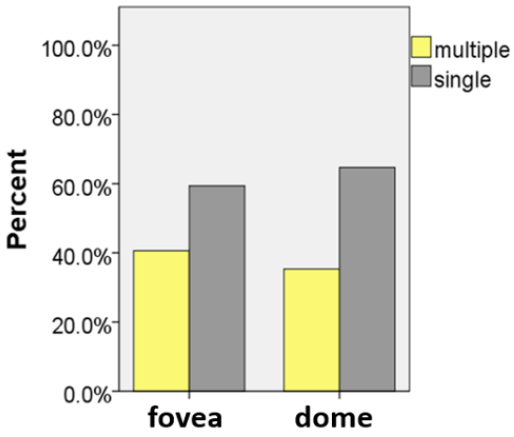


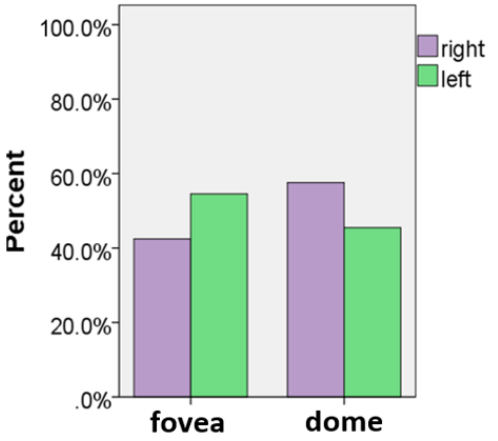


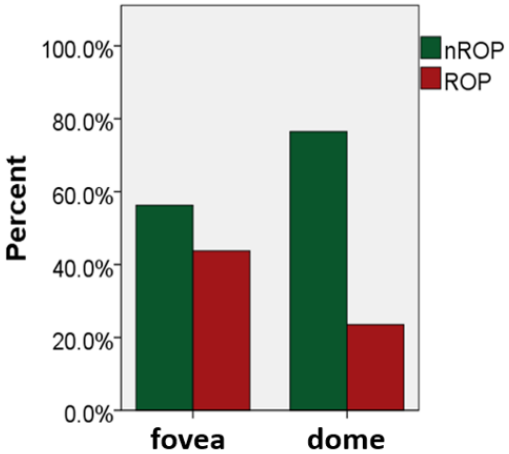


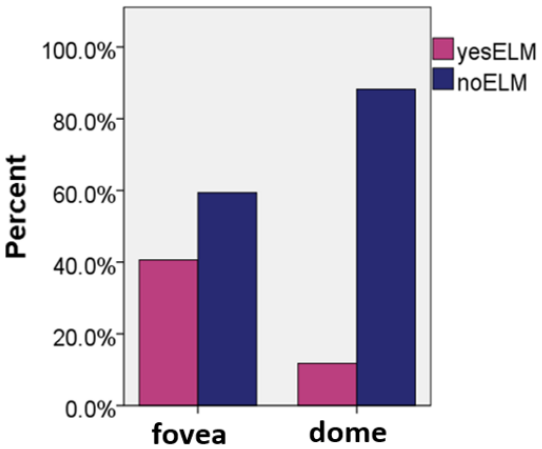

**Figure 7.4. Percentage bar charts of variables: sex, ethnicity, birth multiplicity, right /left eyes, ROP diagnosis and presence or absence of ELM** between **fovea CME and dome CME**. *CME – cystoid macular oedema, ELM – external limiting membrane, nROP – no retinopathy of prematurity*

### *7.54 CME size (CFT, width and area)*

Table 7.6 shows the mean (± standard deviation) for CFT, width and area between CME type for sex, ethnicity, birth multiplicity, laterality (right or left eye), diagnosis (nonROP or ROP) and ELM (present/not present).

| | Fovea (mean ± SD) & [CI] | | | Dome (mean ± SD) & [CI] | | |
|---|---|---|---|---|---|---|
| | **CFT (µm)** | **width (µm)** | **area (µm²)** | **CFT (µm)** | **width (µm)** | **area (µm²)** |
| **CME type** | 64.4 (±17.1) [58.2-70.5] | 2226.3 (±1123.8) [1821.1-2631.5] | 155059.1 (±109513.9) [115575.1 - 194543.1] | 128.5 (±34.2) [116.5-140.4] | 3624.5 (±1323.0) [3162.8-4086.1] | 492709.8 (±284114.7) [383577.5 -591842.0] |
| **male** | 66.2 (±15.5) [58.5-73.9] | 2311.7 (±1123.8) [1766.4-2856.9] | 165067.4 (±103885.5) [113406.3 - 216728.4] | 114.7 (±26.9) [99.2-130.3] | 3193.2 (±749.1) [2760.7-3625.7] | 365703.1 (±116296.3) [298555.6 -432850.6] |
| **female** | 62.0 (±19.3) [50.9-73.1] | 2116.5 (±1190.1) [1429.4-2803.7] | 142191.3 (±119035.8) [73462.1 - 210920.6] | 138.1 (±36.1) [121.2-155.0] | 3926.3 (±1556.7) [3197.8-4654.9] | 581614.4 (±332776.6) [425870.2 -737358.7] |
| | | | | | | |
| **caucasian** | 64.8 (±15.5) [56.8-72.7] | 2011.1 (±1069.8) [1461.1-2561.2] | 142145.5 (±97164.7) [92188.1 - 192103.0] | 128.3 (±32.9) [115.3-141.3] | 3616.4 (±1237.6) [316.4-4106.0] | 484847.1 (±267891.1) [378872.9 - 590821.3] |
| **non-caucasian** | 63.9 (±19.3) [53.2-74.6] | 2470.1 (±1169.9) [1822.2-3118.0] | 169694.5 (±123834.2) [101117.4 - 238271.6] | 129.1 (±42.0) [90.3-168.0] | 3655.5 (±1728.7) [2056.8-5254.3] | 523037.3 (±362809.6) [187494.3 - 858580.2] |
| | | | | | | |
| **single** | 61.1 (±17.1) [52.9 -69.4] | 2172.5 (±1129.9) [1627.9 - 2717.1] | 146958.4 (±110884.1) [93514.0 - 200402.8] | 131.2 (±31.7) [117.2-145.3] | 3567.5 (±1453.3) [2923.2 - 4211.9] | 495784.0 (±296986.2) [364107.7 - 627460.3] |
| **multiple** | 69.1 (±16.7) [59.0-79.2] | 2304.9 (±1156.0) [1606.3.1-3003.4] | 166898.6 (±110833.2) [99922.8 - 233874.5] | 124.4 (±39.5) [98.3-148.5] | 3728.8 (±1095.8) [3032.6 - 4425.1] | 487073.7 (±271526.6) [314553.9 - 659593.4] |
| | | | | | | |
| **right eye** | 64.9 (±16.5) [55.4 -74.4] | 1941.0 (± 1039.7) [1340.6 - 2541.3] | 136995.8 (±101572.3) [78349.7 - 195641.9] | 125.7 (±34.9) [108.9-142.5] | 3699.1 (±1537.7) [2958.0 - 4440.3] | 493980.0 (±316511.3) [341426.5 - 646533.6] |
| **left eye** | 64.0 (±18.0) [55.0 -73.0] | 2448.2 (± 1165.0) [1868.9 - 3027.6] | 169108.3 (± 116202.5) [111322.2 - 226894.5] | 132.0 (±34.3) [113.0-151.0] | 3529.9 (± 1033.9) [2957.3 - 4102.4] | 491100.8 (±247920.0) [353807.3 - 628394.3] |
| | | | | | | |
| **nonROP** | 61.5 (±13.8) [54.7 -68.4] | 2066.5 (± 957.5) [1590.3 - 2542.6] | 131916.5 (±76066.9) [94089.3 - 169743.7] | 127.2 (±31.1) [114.6-139.8] | 3521.6 (±1115.3) [3071.1 - 3972.1] | 467389.8 (±231114.6) [374040.6 - 560739.0] |
| **ROP** | 68.0 (±20.6) [56.1 - 79.9] | 2431.8 (± 1316.0) [1671.9 - 3191.6] | 184813.9 (±139060.5) [104522.7 - 265105.1] | 132.5 (±45.1) [98.4 -170.2] | 3958.8 (±1098.5) [2363.2 - 5554.4] | 574999.8 (±423861.2) [220642.9 - 929356.6] |
| | | | | | | |
| **ELM (present)** | 66.0 (±15.9) [56.4 -75.6] | 2150.1 (± 1459.9) [1267.8 - 3032.3] | 157793.6 (±135517.1) [75901.5 - 239685.7] | 101.6 (±25.6) [60.9-142.4] | 2825.5 (±682.5) [1739.4 - 3911.5] | 296188.8 (±141145.8) [71594.3 - 520783.2] |
| **ELM (absent)** | 63.3 (±18.2) [54.5 -72.0] | 2278.4 (±864.4) [1861.8 - 2695.0] | 153188.1 (±91666.6) [109006.2 - 197370.0] | 132.0 (±34.0) [119.4 - 144.7] | 3731.0 (±1357.9) [3223.9 - 4238.0] | 518912.6 (±289408.0) [410845.8 - 626979.3] |

**Table 7.6 The mean CFT (µm), width (µm) and area (µm)² between fovea CME and dome CME dome** for sex, ethnicity, birth multiplicity, right and left eyes, ROP and non-ROP and ELM presence or absence. *CME – cystoid macular oedema, CFT – central foveal thickness, ROP – retinopathy of prematurity, ELM – external limiting membrane.*

Mean comparison p values for the differences between the groups for CFT, width and area are shown in table 7.7.

| | CFT (µm) | width (µm) | area (µm²) |
|---|---|---|---|
| | p value | | |
| **CME pattern** | 0.000 | 0.000 | 0.000 |
| **sex** | 0.062 | 0.165 | 0.264 |
| **ethnicity** | 0.083 | 0.689 | 0.165 |
| **birth multiplicity** | 0.741 | 0.852 | 0.848 |
| **laterality** | 0.635 | 0.97 | 0.693 |
| **diagnosis** | 0.424 | 0.87 | 0.962 |
| **ELM** | 0.009 | 0.042 | 0.014 |

**Table 7.7 Results of mean comparison for CFT, width and area between CME type** (fovea and dome). Significance level p<0.05. *CFT – central foveal thickness, CME – cystoid macular oedema, nROP – no retinopathy of prematurity, ELM – external limiting membrane.*

Table 7.7 shows that a significant difference between CME fovea and CME dome exists for CFT, width and area, which is expected by definition (see Figure 7.2).

Fovea CME and dome CME were significantly difference in size when measured as mean CFT, width and area. In addition, the absence or presence of the ELM also affected mean CFT, width and area (Table 7.7).

Figure 7.5 illustrates that mean CFT, width and area are greater for dome CME and greater when the ELM is absent (green box plot) compared to when ELM is present (blue box plot) but only for dome CME.

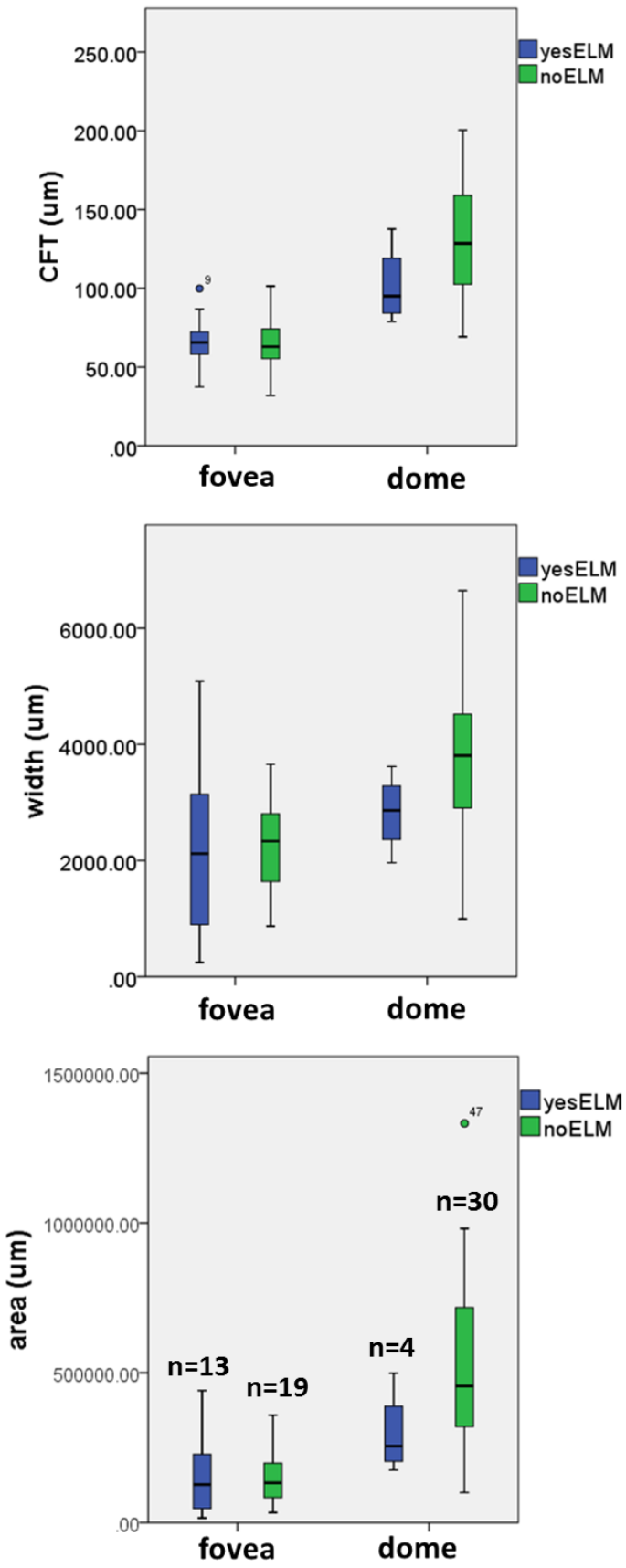


**Figure 7.5. Mean CFT, width and area for fovea CME and dome CME between presence and absence of ELM** (ELM yes, ELM no). *ELM – external limiting membrane, CFT – central foveal thickness, CME – cystoid macular oedema.*

## 7.6 Discussion

### *7.61 Overall conclusions*

Preterm infants with CME were older at birth and heavier than preterm infants without CME but neither factor was found to predict the presence of CME.

The two types of CME as defined by the presence or absence of the foveal depression (fovea CME and dome CME respectively) differed significantly in size from each other with dome CME measuring greater CFT, width and area than fovea CME.

Caucasian infants with CME were more likely to have dome CME compared with Non-Caucasians while the absence of the ELM was observed more often in dome CME.

ROP diagnosis and stage was not a significant risk factors for either the presence of CME or the type of CME.

### *7.62 Possible mechanisms of CME differences between fovea and dome type relating to Müller cells and the ELM*

Adult macular oedema is primarily pathological and histologically found in several retinal layers (GCL, ONL, INL, IPL Henlè's fibres) (Trichonas and Kaiser 2014; Tso 1982). Cystoid macular oedema (CME) in fully developed retinae is seen in conjunction with a large number of local retinal pathology and systemic disease e.g. diabetes mellitus. The exact underlying pathogenesis is unknown but a multifactorial aetiology is suspected (Yanoff et al. 1984), with disruption of the blood retinal barrier (BRB), retinal pigment epithelium and damage to Müller cells considered to be likely associations (Daruich et al. 2018; Tso 1982; Bringmann, Reichenbach, and Wiedemann 2004). Accumulation of protein results in oncotic pressure attracting water and the greatest oedema will be adjacent to where either fluid leaks e.g. near capillaries or protein builds up e.g. at the ELM).

Bilateral cystoid maculopathy has been described at postmortem examination in three infants (Trese and Foos 1980). The first was described as a black preterm infant weighing 820 gram that survived 11 days. The globe had an axial length 14.2 mm

which equates to approximately 24 weeks GA based on literature (Maldonado et al. 2010) and bilateral cystoid macular change was found in the outer nuclear layers.

The second was born to a Hispanic mother at term (axial length 16.2 mm equates to approximately 38-40 weeks gestation) and birth weight 1450 grams. The infant suffered anencephaly and the eyes demonstrated bilateral cystoid spaces involving the inner nuclear layer.

The third child was a term infant of white ethnicity with hydrocephalus, spina bifida and large eyes of axial lengths of right 21.2 mm; left 19.9mm although the corneas measured 9.8 mm horizontally and appropriate for term birth. This time the bilateral cystoid spaces were notes in the nerve fibre layer. In all three cases, Müller cells were stretched across the cavitation with the cells vertically lining the cavities described as pillars. This appearance is seen on OCT (Figures 7.1 and 7.2).

The CME observed on SD-OCT in preterm infants occurs almost exclusively in the INL (Maldonado et al. 2012) although Bondalapati et al. 2015 reported 4 preterm infants with cystic spaces involving the GCL. The INL has several cell types including Müller cells which span the entire width of the neurosensory retina, forming the internal and external (inner and outer respectively) limiting membranes (Goldman 2014).

In adults, CME appears petaloid on fluorescein angiography (FFA) due to the vertical structure of the Müller cells that become stretched as a result. However, CME on OCT without FFA leakage is also reported in adults who undergo taxane chemotherapy (Yokoe et al. 2017) and Vitamin B3 (Niacin) in the treatment of high cholesterol (Domanico et al. 2015). The underlying hypothesis is that these agents are toxic to Müller cells without disrupting the blood retinal barrier (BRB) (Millay Ophthalmol 1988). Swelling of Müller cells has been shown using electron and light microscopy in cases of macular cystoid oedema (Fine and Brucker 1981; Yanoff et al. 1984).

In preterm infants, the fibre's of Henlè are not yet mature and macular oedema was not visualised as leakage on FFA in one preterm infant of 25 weeks GA with a single cyst imaged at 49 weeks PMA (Chen et al. 2018). Since the ELM also forms part of the BRB, the CME in preterm infants could relate to the absence of the ELM at the fovea.

Figure 7.5 shows that although the numbers with ELM present and dome CME were only 4 in our cohort, the general trend suggested that that severe dome CME was more likely to be observed in infants in the absence of ELM.

*7.63 CME and disruption of the Blood Retinal Barrier (BBB)*

Higher stage of ROP has been correlated with CME (Vinekar et al. 2011; Erol et al. 2014). The current analysis was not able to identify the stage with the highest risk, and this may reflect the fewer numbers of stage 3 images in the data.

The stage of ROP as a risk factor for CME suggests that there may be disruption of the BRB, since ROP is associated with increased levels of VEGF and vascular instability (Gardner et al. 1999) but the situation is complicated by the fact that Müller cells themselves express VEGF which may promote retinal neovascularisation (Bai et al. 2009) and the development of CME. There are no animal models of CME since the fovea is a structure only present in primates, some birds and lizards, and the levels of intra-ocular or systemic VEGF in conjunction with observed CME in preterm infants has not been investigated. However FFA leak in infants who are observed to have both CME with pre-retinal neovascularisation (Chen et al. 2018) suggests disruption of the BRB.

*7.64 CME and multiple birth*

Multiple birth is commonly associated with prematurity and up to 10% of twins are born before 32 weeks GA (Blondel et al. 2002). Multiple birth preterm infants are at an increased risk of adverse outcomes such as cerebral palsy and growth delay, and are more likely to be born to older mothers (Papiernik et al. 2010).

When compared with term born infants, twins are born earlier (Lee, Cleary-Goldman, and D'Alton 2006) but in the preterm group born before 32 weeks, twin GA is either higher or similar to preterm singletons (Papiernik et al. 2010). In our study cohort (n=112 infants), the mean GA (±SD) in weeks for multiple birth and singletons was 28.1 (2.3) and 28.7 (2.8) respectively (p=0.31), and 20% of the preterm cohort were

multiple births. However, 45% of multiple births were observed to have CME (Table7.1).

Rothman et al. 2015 reported an increased likelihood of neuro developmental delay at aged 18 to 24 months for preterm infants with CME. However, the authors did not specify the proportion of multiple births in the study group nor discuss this in the analysis. It is possible therefore that their results reflect development outcomes for CME which is related to multiple birth rather than specifically with CME in preterm infants. Although we did not find multiple birth to be a predictor for the presence of CME, this could reflect the small sample size of infants with CME in our preterm cohort.

*7.65 CME and gestational age (GA)*

Although we found in our preterm group that infants with CME were older at birth and heavier than those with no CME, there no significant association between GA with CME which is supported by Vinekar et al. 2011 and Rothman et al. 2015. However, this result is in contrast with other authors who report that younger born infants are more likely to have CME (Dubis et al. 2013; Maldonado et al. 2012; Bondalapati et al. 2015; Erol et al. 2014).

*7.66 CME and ethnicity*

We observed that Caucasians with CME were more likely to have dome CME compared with Non-Caucasians with CME. Currently no association has been reported between sex or ethnicity with respect to CME in preterm infants. It is possible that the differences between Caucasians and Non-Caucasians reflect maturity of the BRB. A larger cohort of infants and further study would be useful to explore this more precisely.

### 7.7 Limitations

A limitation of the study is the small sample size of infants without the ELM and fovea CME. A larger sample size of infants with CME could also reveal more information regarding the possible differences between CME type with respect to variables such as the ELM or ethnicity.

Another limitation was the lack of data on maternal medical history especially in light of the data on multiple birth and CME. Mothers of twins for example are older and may have associated health problems or pre-pregnancy medication requirements. This might be relevant in the development of CME for this group.

### 7.8 Conclusion

CME remains an incompletely understood observation visualised using portable OCT in preterm infants. The reported risk factors for the development of CME such as presence or severity of ROP and early GA remain inconclusive. Despite limitations in sample size, a general trend towards an absence of the ELM in dome CME was suggested.

The percentage of multiple birth with CME is relevant due to the increased likelihood of multiple births in prematurity and the increasing incidence of prematurity. Longitudinal study of the relationship between CME, vision and childhood development in this group would help to understand if this relates to an adverse future outcome.

# Chapter 8 General Discussion and Conclusions

We report on the developing fovea in preterm infants, measured using HH SD-OCT during the perinatal period between 30- and 44-weeks PMA. The effect of GA, BW and diagnosis of ROP were examined during this period of foveal change to discern if differences existed secondary to severity of prematurity and presence of ROP. As such, the analysis adjusted for GA and BW separately and included data until infants underwent treatment for ROP after which they were excluded.

The aims of the study were to investigate foveal morphology (chapter 5) and explore the retinal layers at the fovea with respect to the foveal morphology analysis (chapter 6). The final aim was to describe the infants with CME in a separate analysis (chapter 7).

## 8.1 Summary of main findings

8.11 In preterm infants without CME:

1. *Foveal width* in early PMA demonstrated a different trajectory when ROP was present compared with when ROP was absent. Foveal width was narrow in ROP infants and became wider with increasing PMA. This was in contrast when ROP was absent, when the fovea was wider after birth and became narrower with increasing PMA, in line with histological descriptions (Yuodelis and Hendrickson 1986; Hendrickson and Yuodelis 1984). Furthermore, the differences in foveal width were independent of GA and BW. The analysis of individual retinal layers at early PMA investigating this finding at 500 µm nasal and temporal to the fovea identified significant differences in the outer retinal layers and INL between ROP and non-ROP; mean INL thickness was reduced but outer retinal layers were increased at these locations in the presence of ROP.

2. *Central foveal thickness (CFT)* was significantly predicted by GA but not BW or ROP. When measured at the mean PMA, earlier born infants demonstrated increased CFT compared with later born infants. Investigation of the individual retinal layers at the fovea found that the INL was significantly increased at the fovea in severe prematurity.

3. *Foveal depth* was determined by prematurity and not ROP, with early GA infants and lower BW infants showing significantly more shallow foveae in comparison with older born or heavier infants.

4. *Foveal slope* and *parafoveal retinal thickness* differed between nasal and temporal fovea being reduced in early GA and low BW. Although the individual retinal layers were not analysed at the parafovea, the asymmetry of the fovea is likely to reflect the differences in individual retinal layers at these locations particularly the retinal nerve fibre layer (RNFL) and the ganglion cell layer (GCL).

8.12 <u>In preterm infants with CME</u>:

1. CME was observed in 22% of the study cohort. Infants with CME were heavier, born later, more likely to be males, Caucasians and multiple births compared with infants without CME.

2. Two types of CME were defined according to presence or absence of the foveal depression ('fovea CME' and 'dome CME' respectively). Dome CME was more severe, with greater CFT, width and area compared with fovea CME. Caucasians with CME were more often likely to have dome CME compared with Non-Caucasians with CME. There was a trend that suggested an absence of the ELM could be important in the development of dome CME.

## 8.2 General Discussion

In humans, the fovea is a highly specialised area of the central retina usually shaped as a hollow or depression. Histological studies show that the foveal depression appears late in pregnancy during the last trimester but is not structurally mature until at least 5 years of age, with adult features found by 13 years of age (Hendrickson and Yuodelis 1984; Mann 1950; Hendrickson et al. 2012).

As a result of portable imaging technology, *in vivo* studies have revealed the enormous changes in morphology and structure undergone by the fovea from birth onwards (Lee et al. 2015; Alabduljalil et al. 2018; Dubis et al. 2012; Vajzovic et al. 2012). From these studies, variations of both shape and structure of the fovea between term and preterm infants are identified (Maldonado et al. 2011; Dubis et al. 2012; Vajzovic et al. 2012; Vajzovic et al. 2015; Dubis et al. 2013; Yanni et al. 2012).

Prematurity poses particular obstacles for normal development, and preterm children are known to experience deficits due to either immaturity in comparison with term age equivalent peers or incomplete growth (Vohr et al. 2000; Pierrat et al. 2017) . This has generated much interest on the impact of prematurity on both the structure and function through study of foveal development in this group.

Retinopathy of prematurity remains a worldwide clinical challenge (Kong et al. 2012; Quinn 2016) and affects the developing retina of prematurely born infants. Reliable objective markers of disease identification and progression remain elusive. Furthermore, the close relationship between prematurity and ROP has led to contrasting results despite a number of good studies regarding the role of ROP and prematurity on foveal development which have been outlined in the preceding chapters. In the context of this, the current study findings and conclusions will be discussed.

### *8.21 Retinopathy of Prematurity*

ROP is a vascular abnormality which results from metabolic demands placed upon an incomplete immature vascular system. The major component of the developing

retina that requires oxygen is the photoreceptor layer. The photoreceptor layer in the peripheral avascular retina is comprised of rod photoreceptors which are absent at the fovea by definition (Hendrickson and Yuodelis 1984). The cone photoreceptors of the fovea are rudimentary and the metabolic demand in ROP originates principally from the rods due to the number and location of the rods compared with the cones. However, it is important to note that differentiation of the peripheral retina lags behind the central by around 10 weeks and is not comparable until 5 months post term birth (Narayanan and Wadhwa 1998) so despite its relatively smaller size in comparison to the periphery (Provis et al. 2005), the central retina may be more highly metabolically active immediately after preterm birth and at early PMA.

We devised a method of measuring foveal parameters including width and depth based on established literature (Dubis, McAllister, and Carroll 2009; Wang et al. 2012b; Yanni et al. 2012) and accounting for the known asymmetry of the fovea in adults (Liu et al. 2016). Our study identified foveal width as a foveal morphology parameter that was significantly interactive with ROP (Chapter 5, Figure 5.4, page 85). The trajectory of foveal width with PMA was dependent on the presence or absence of ROP even after adjustment for GA and BW. Foveal width decreased from 31 to 40 weeks PMA when ROP was absent. However, when ROP was present, foveal width increased over the same time period. The contrast in foveal width was greatest in early PMA (31 to 33 weeks).

We investigated early foveal width at 32 weeks PMA further, by analysing the individual retinal layers between the fovea and parafovea at 500 µm nasal and temporal to the fovea and found differences in the outer retinal and inner nuclear layers for infants with ROP compared with those without ROP. The study group of ROP infants were mostly Stages 1 and 2 and did not contain already treated infants.

Our hypothesis is that decreased INL and increased outer retinal layers modify foveal width between ROP and non-ROP. It is not clear why this is the case, whether this reflects a generally thicker outer retinal layer in preterm infants vulnerable to developing ROP, for example a more differentiated peripheral retina

than in those without ROP (Narayanan and Wadhwa 1998; Hendrickson and Drucker 1992) or if ROP infants develop an increased outer retinal layer as a result of ischaemia and ischaemic factors in association with the disease.

*8.211 Limitations:* There were infants that did not follow the trend and the foveal width was less in ROP rather than wider than in infants without ROP. Our study group had 30 infants with ROP of which 11 were mixed with not enough longitudinal data to infer what happens to foveal width in cases where ROP regresses spontaneously or where it then develops after early PMA.

Nonetheless, the disparity between ROP and non-ROP in early PMA of a greater foveal width with ROP has the potential for use of portable OCT during screening. Our data analysis shows that this is independent of both GA and BW and could be used as an additional tool in the screening process e.g. distinguishing infants without ROP that do not require further examination from ROP infants who remain at risk.

*8.212 Future study:* A greater number of infants imaged particularly in early PMA and more longitudinal data would be important to develop this further. Improved automated layer segmentation and calculation of foveal parameters in OCT algorithms would be especially advantageous in portable OCT technology.

It would also be valuable to visualise the vasculature particularly the intermediate and deep capillary plexuses, the former within the IPL to INL interface and the latter between the INL and Outer retina. Our results found that the Outer retina is also significantly increased while the INL was decreased at 500µm from the central fovea and this could be due to changes in the plexuses. There is some evidence that each of the 3 plexuses are distinct and supply corresponding retinal layers (Nesper and Fawzi 2018). Only the superficial vascular plexus located in the ganglion cell layer, is visualised with enough clarity using fluorescein angiography, but portable OCT angiography is currently unavailable for use in preterm infants during routine ROP screening. This could elucidate the vascular abnormalities in ROP and its effect on the retinal layers that we have identified.

*8.22 Prematurity and the Fovea*

The foveal depression consists of the foveal base known as the foveola and the foveal slope or clivus, a zone of decreasing retinal thickness. Histological and OCT studies demonstrate that this is due to the outward migration of the inner foveal layers in conjunction with increased outer retina during foveal maturity. A shallow or absent depression seen on OCT is now termed foveal hypoplasia (Recchia, Carvalho-Recchia, and Trese 2002) or foveal plana (Marmor et al. 2008; Noval et al. 2014). The two terms have been used interchangeably even where vision has been normal (Thomas et al. 2011; Dolz-Marco et al. 2016; Benouaich et al. 2017) illustrating the incongruity between describing the contour of the depression alone or referring to the foveal architecture underlying the depression. A grading system of foveal hypoplasia categorising structure as a predictor of visual acuity in nystagmus patients with various pathology is described. Subjects with foveal hypoplasia associated with a history of prematurity were not included (Thomas et al. 2011). Foveal cone specialisation, necessary for good visual acuity, does not always appear to depend on the inner layers (Hendrickson et al. 2006) or foveal shape, and individuals with continuous inner layers across the central fovea can have normal visual acuity. (Marmor et al. 2008; Wilk et al. 2014; McAllister et al. 2010). Furthermore, isolated shallow foveae with increased CFT described as fovea plana have been observed in up to 3% of term born children aged between 3-17 years (Noval et al. 2014).

Developmentally mature ex-preterm children and adults demonstrate a thicker central fovea often in association with a shallower depression described as foveal hypoplasia. Although we did not explore the relationship between CFT and foveal depth, the study results demonstrated a significant difference in foveal depth between 24- and 30-weeks GA and for 600 grams BW compared with 1400 grams (see Chapter 5 figure 5.6 p88).

We also measured an increased CFT with earlier GA (see Chapter 5 Figure 5.7 p89) which is in keeping with reports in ex-preterm children after foveal development has almost completed. Our findings support those of Wang and others who

suggested that increased CFT in ex -preterm child was secondary to inner layer migration delay associated with extreme prematurity (Wang et al. 2012b; Fieβ et al. 2017; Bowl et al. 2016; Molnar et al. 2017).

However, we have now identified the INL as the inner retinal layer, and likely to be responsible for increased CFT with preterm infants showing an arrest of INL reduction at the fovea in the perinatal period.

The inner nuclear layer is composed chiefly of the cell bodies of horizontal, bipolar, amacrine cells and also Müller cells. The mechanism of inner layer reduction at the fovea which occurs in normal development is not well understood. Histology shows that outward migration of the inner retina occurs after the outer retina has already begun moving towards the foveal centre (Diaz-Araya and Provis 1992) and the two are independent. Interestingly, in our study low BW was also associated with increased foveal INL and additionally a reduced IPL and OPL which is a new finding.

The increased CFT noted in ex-preterm individuals may be associated with reduced vision and increased ganglion cell layer thickness (Balasubramanian et al. 2018). However normal visual acuity is also reported with increased CFT in prematurity (Akerblom et al. 2011).

*8.221 Limitations:* The principle changes at the fovea observed in the perinatal period using HH SD-OCT occur in the inner retina while the outer retina is still immature. The outer retina develops even when inner layers are abnormal (Hendrickson et al. 2006), with a greater proportion of foveal growth in the neonatal and postnatal childhood period. This, along with the apparent independent trajectories of inner and outer retina suggests that caution should be applied in interpreting future visual outcomes based on foveal shape and the inner retina without correlation of the outer retina.

*8.222 Future study:* While the importance of the foveal shape with respect to vision and function has been debated (Walls 1937; Weale 1966; Marmor et al. 2008; Provis et al. 2013) there is also some evidence that individual foveal morphology may influence future macular pathology (Shin et al. 2015). Therefore, expanding on

the study findings, it may be possible to develop an OCT grading system based on GA, CFT, the developing outer retina and visual acuity from longitudinal assessment of preterm infants. Utilising this when comparing with the foveal development of term born infants after birth age correction might help determine where and when the structural and functional disparities exist between preterm and term born individuals in the first 6 years of childhood.

*8.23 Foveal and Parafoveal asymmetry*

In Chapter 5 we reported asymmetry of the foveal slope, and nasal and temporal asymmetry of parafoveal retinal thickness (see Figure 5.3 p83 B. Steepest Slope of Foveal wall and C. Parafoveal Retinal Thickness (pRT); also Figure 5.8 p90 and Figure 5.9 p91).

We found a predicted difference in both slope and parafoveal thickness between GA 24, 26, 28 and 30 weeks and with BW from 600g to 1400 grams. The asymmetry likely reflects the difference between GCL and therefore RNFL distribution at the parafovea (Curcio and Allen 1990) but it remains uncertain which other layers might also demonstrate asymmetry of distribution at the parafovea using HH SD-OCT in the perinatal period.

Foveal hypoplasia with generalized RNFL and GCL thinning has been found with optic nerve hypoplasia (Anwar et al. 2011; Pilat et al. 2015) and analysis of the macular GCL and GCL-IPL is increasingly recognised as clinical utility in the assessment of optic neuropathies (Danesh-Meyer et al. 2006; Gu et al. 2014; Maldonado et al. 2015). An understanding of the asymmetry in retinal layers at the parafovea in prematurity could be additionally useful particularly in neurological assessment of preterm infants during early childhood.

A further feature in prematurity is the smaller foveal avascular zone (FAZ) (Mintz-Hittner et al. 1999; Yanni et al. 2012). The FAZ has been correlated with continuation of the INL at the fovea and reduces during the perinatal period (Provis and Hendrickson 2008). A close relationship exists between retinal neurons and

vascular endothelial growth factor (VEGF) expression which may determine angiogenesis direction (Okabe et al. 2014; Yoshikawa et al. 2016) while the distribution of astrocyte glial cells correlates with RNFL thickness (Büssow 1980). Astrocytes are sensitive to hypoxia and mediate the vascularisation process at the FAZ (Provis 2001). The effect of prematurity on the inner layers at the parafovea particularly with respect to the location of the vascular plexuses might be important in understanding the development of the FAZ.

*8.231 Limitations:* An analysis of parafoveal retinal layers was not undertaken but is planned for future investigation. The study also did not correlate the FAZ using fluorescein angiography at the fovea in preterm infants with OCT findings since modelling of the fovea using HH SD-OCT was the primary research aim.

*8.232 Future study:* RNFL reduction is reported in optic nerve studies of ex-preterm children with no clinical neurological deficit (Ruberto et al. 2014) but in preterm infants, reduced RNFL may be associated with abnormal structure on MRI and reduced cognitive ability in early childhood (Rothman, Sevilla, Mangalesh, et al. 2015). We did not find an association between GA and RNFL reduction at the fovea but we did not explore the effect of GA on the inner layers at the parafovea. Although we did not analyse MRI imaging of our infants, a follow up study to review the neuro developmental scores in our study group would be interesting. In addition, comparison of optic nerve head parameters of the study group with term born individuals (Patel et al. 2016) would also be useful since there are differences between the optic nerve of term born and preterm children (Tong et al. 2014).

*8.24 Foveal oedema (CME)*

The observation of clinically invisible cystic spaces at the fovea found using HH SD-OCT in preterm infants remains unexplained despite reports suggesting associations with ROP and younger GA. We defined CME according to the presence or absence of the fovea ('fovea CME' or 'dome CME' respectively) as reported previously (Vinekar et al. 2011; Erol et al. 2014). Dome CME had significantly

greater CFT, width and area as expected. Our analysis identified a greater proportion of Caucasians with dome CME compared to Non-Caucasians. We also found a trend towards absence of the ELM in dome CME and hypothesise that disruption or immaturity of the ELM could be a factor in the development of dome CME.

*8.241 Limitations:* The sample size was limited especially for numbers of ELM presence and dome CME making a comparison between ELM presence or absence less reliable in the dome CME group. However, our results suggest that the ELM may be an important factor in CME severity.

*8.242 Future study:* An analysis using a larger sample of preterm infants with CME investigating the ELM would be useful. In terms of mechanisms, increased spaces within the INL are likely to be secondary to Müller cell dysfunction (Goldman 2014). Studies using preterm small animal models may provide insight into cellular abnormalities within the INL since in vivo imaging technology is currently unable to visualise Müller cells.

### 8.3 Conclusions

The preterm infant fovea undergoes significant change during the perinatal period with foveal morphology and individual retinal layers being influenced by gestational age, birthweight and the presence of ROP.

Foveal width in early PMA shows a potential clinical utility in the screening of preterm infants at risk of developing ROP using HH SD-OCT and warrants further investigation.

Central foveal thickness is significantly related to early gestational age and is increased secondary to an increased foveal inner nuclear layer in earlier born infants. We report a new finding that extremely low BW also results in increased INL at the fovea and significantly affects the outer retina.

Our results suggest that the severity of prematurity in the assessment of foveal development in preterm infants and children should be considered. The grading of foveal structure accordingly could be a useful tool when comparing visual outcomes between preterm infants or with term born age equivalent children.

The integrity or maturity of ELM may be an important risk factor determining the severity of CME; further study with more participants would be beneficial in exploring this in greater detail.

# Appendices

**Appendix 1** Preterm Infants without cystoid macular oedema. Demographic Data**.**

| SN | Person ID | PMA | Eye R(1) / L(2) | Diagnosis Non ROP 1 ROP 2 | birthage (GA) | birthweight | M(1)/F(0) | multiple birth Y(1)/N (0) | Stage ROP | Caucasian Y(1)/N(0) | fov depth |
|---|---|---|---|---|---|---|---|---|---|---|---|
| 1 | 1 | 37.71 | 1 | 1 | 34.71 | 3540 | 0 | 0 | 0 | 0 | 137.49 |
| 2 | 1 | 37.71 | 2 | 1 | 34.71 | 3540 | 0 | 0 | 0 | 0 | 121.84 |
| 4 | 2 | 34.29 | 1 | 1 | 28.14 | 1170 | 1 | 0 | 0 | 1 | 63.63 |
| 7 | 2 | 34.29 | 2 | 1 | 28.14 | 1170 | 1 | 0 | 0 | 1 | 87.96 |
| 5 | 2 | 36.29 | 1 | 1 | 28.14 | 1170 | 1 | 0 | 0 | 1 | 89.41 |
| 8 | 2 | 36.29 | 2 | 1 | 28.14 | 1170 | 1 | 0 | 0 | 1 | 86.64 |
| 3 | 2 | 38.29 | 1 | 1 | 28.14 | 1170 | 1 | 0 | 0 | 1 | 101.72 |
| 6 | 2 | 38.29 | 2 | 1 | 28.14 | 1170 | 1 | 0 | 0 | 1 | 78.89 |
| 9 | 3 | 33.85 | 2 | 1 | 28.71 | 1140 | 1 | 0 | 0 | 0 | 104.64 |
| 10 | 4 | 34.14 | 1 | 1 | 29.14 | 1510 | 1 | 0 | 0 | 1 | 75.94 |
| 11 | 4 | 34.14 | 2 | 1 | 29.14 | 1510 | 1 | 0 | 0 | 1 | 85.34 |
| 14 | 5 | 35.00 | 1 | 1 | 23.43 | 635 | 0 | 0 | 0 | 1 | 92.00 |
| 19 | 5 | 35.00 | 2 | 1 | 23.43 | 635 | 0 | 0 | 0 | 1 | 83.64 |
| 15 | 5 | 36.00 | 1 | 1 | 23.43 | 635 | 0 | 0 | 0 | 1 | 104.54 |
| 16 | 5 | 36.00 | 2 | 1 | 23.43 | 635 | 0 | 0 | 0 | 1 | 84.18 |
| 12 | 5 | 38.00 | 1 | 1 | 23.43 | 635 | 0 | 0 | 0 | 1 | 118.92 |
| 17 | 5 | 38.00 | 2 | 1 | 23.43 | 635 | 0 | 0 | 0 | 1 | 112.16 |
| 13 | 5 | 40.00 | 1 | 1 | 23.43 | 635 | 0 | 0 | 0 | 1 | 117.95 |
| 18 | 5 | 40.00 | 2 | 1 | 23.43 | 635 | 0 | 0 | 0 | 1 | 100.94 |
| 20 | 6 | 36.85 | 1 | 1 | 31.71 | 1670 | 1 | 0 | 0 | 1 | 147.69 |

| SN | Person ID | PMA | Eye R(1) / L(2) | Diagnosis Non ROP 1 ROP 2 | birthage (GA) | birthweight | M(1)/F(0) | multiple birth Y(1)/N (0) | Stage ROP | Caucasian Y(1)/N(0) | fov depth |
|---|---|---|---|---|---|---|---|---|---|---|---|
| 21 | 6 | 36.85 | 2 | 1 | 31.71 | 1670 | 1 | 0 | 0 | 1 | 148.52 |
| 22 | 7 | 37.00 | 1 | 1 | 34.00 | 1210 | 1 | 0 | 0 | 1 | 165.77 |
| 23 | 7 | 37.00 | 2 | 1 | 34.00 | 1210 | 1 | 0 | 0 | 1 | 155.50 |
| 24 | 8 | 33.57 | 1 | 2 | 25.14 | 800 | 0 | 0 | 2 | 0 | 66.02 |
| 25 | 8 | 33.57 | 1 | 2 | 25.14 | 800 | 0 | 0 | 3 | 0 | 41.74 |
| 27 | 9 | 34.85 | 2 | 1 | 31.57 | 500 | 1 | 0 | 0 | 1 | 79.91 |
| 26 | 9 | 41.85 | 1 | 2 | 31.57 | 500 | 1 | 0 | 2 | 1 | 72.86 |
| 28 | 9 | 41.85 | 2 | 2 | 31.57 | 500 | 1 | 0 | 2 | 1 | 89.61 |
| 29 | 10 | 39.57 | 1 | 1 | 29.43 | 1390 | 0 | 0 | 0 | 1 | 70.04 |
| 30 | 11 | 41.85 | 1 | 1 | 29.00 | 1140 | 1 | 0 | 0 | 0 | 136.92 |
| 31 | 12 | 41.85 | 2 | 1 | 29.00 | 1120 | 1 | 0 | 0 | 0 | 99.14 |
| 32 | 13 | 34.57 | 2 | 1 | 27.43 | 1070 | 0 | 0 | 0 | 0 | 109.68 |
| 33 | 13 | 34.57 | 1 | 1 | 27.43 | 1070 | 0 | 0 | 0 | 0 | 149.62 |
| 35 | 15 | 36.00 | 1 | 2 | 26.29 | 960 | 0 | 0 | 2 | 1 | 86.36 |
| 36 | 15 | 36.00 | 2 | 2 | 26.29 | 960 | 0 | 0 | 2 | 1 | 47.09 |
| 38 | 15 | 40.00 | 2 | 2 | 26.29 | 960 | 0 | 0 | 2 | 1 | 106.30 |
| 37 | 15 | 42.00 | 1 | 2 | 26.29 | 960 | 0 | 0 | 2 | 1 | 121.68 |
| 39 | 15 | 42.00 | 2 | 2 | 26.29 | 960 | 0 | 0 | 2 | 1 | 111.22 |
| 40 | 16 | 37.57 | 2 | 1 | 29.71 | 1200 | 0 | 0 | 0 | 1 | 100.20 |
| 41 | 17 | 37.00 | 1 | 1 | 31.14 | 1170 | 1 | 0 | 0 | 1 | 114.07 |
| 42 | 17 | 37.00 | 2 | 1 | 31.14 | 1170 | 1 | 0 | 0 | 1 | 57.67 |
| 45 | 18 | 33.29 | 1 | 1 | 25.14 | 900 | 0 | 1 | 0 | 1 | 97.61 |

| SN | Person ID | PMA | Eye R(1) / L(2) | Diagnosis Non ROP 1 ROP 2 | birthage (GA) | birthweight | M(1)/F(0) | multiple birth Y(1)/N (0) | Stage ROP | Caucasian Y(1)/N(0) | fov depth |
|---|---|---|---|---|---|---|---|---|---|---|---|
| 50 | 18 | 33.29 | 2 | 1 | 25.14 | 900 | 0 | 1 | 0 | 1 | 113.79 |
| 46 | 18 | 35.29 | 1 | 2 | 25.14 | 900 | 0 | 1 | 1 | 1 | 102.81 |
| 47 | 18 | 35.29 | 2 | 2 | 25.14 | 900 | 0 | 1 | 1 | 1 | 99.70 |
| 48 | 18 | 37.29 | 2 | 2 | 25.14 | 900 | 0 | 1 | 1 | 1 | 35.39 |
| 44 | 18 | 39.29 | 1 | 1 | 25.14 | 900 | 0 | 1 | 0 | 1 | 65.80 |
| 49 | 18 | 39.29 | 2 | 1 | 25.14 | 900 | 0 | 1 | 0 | 1 | 95.58 |
| 43 | 18 | 37.29 | 1 | 2 | 26.29 | 915 | 0 | 1 | 1 | 1 | 168.83 |
| 51 | 19 | 39.14 | 1 | 1 | 26.43 | 1040 | 1 | 0 | 0 | 1 | 112.98 |
| 52 | 19 | 39.14 | 2 | 1 | 26.43 | 1040 | 1 | 0 | 0 | 1 | 109.72 |
| 54 | 20 | 36.71 | 2 | 1 | 28.43 | 740 | 1 | 0 | 0 | 0 | 103.49 |
| 53 | 20 | 38.71 | 1 | 1 | 28.43 | 740 | 1 | 0 | 0 | 0 | 115.50 |
| 55 | 20 | 38.71 | 2 | 1 | 28.43 | 740 | 1 | 0 | 0 | 0 | 101.21 |
| 57 | 21 | 35.00 | 2 | 1 | 30.85 | 1020 | 1 | 0 | 0 | 1 | 84.73 |
| 56 | 21 | 37.00 | 1 | 1 | 30.85 | 1020 | 1 | 0 | 0 | 1 | 87.46 |
| 58 | 21 | 37.00 | 2 | 1 | 30.85 | 1020 | 1 | 0 | 0 | 1 | 57.85 |
| 59 | 22 | 33.00 | 2 | 1 | 25.85 | 1205 | 0 | 0 | 0 | 0 | 61.89 |
| 60 | 23 | 31.29 | 1 | 1 | 25.71 | 880 | 1 | 0 | 0 | 0 | 49.88 |
| 61 | 24 | 36.71 | 2 | 1 | 30.57 | 1460 | 1 | 0 | 0 | 0 | 67.61 |
| 62 | 25 | 31.57 | 1 | 1 | 26.43 | 1175 | 1 | 1 | 0 | 0 | 69.55 |
| 63 | 25 | 31.57 | 2 | 2 | 26.43 | 1175 | 1 | 1 | 1 | 0 | 115.02 |
| 64 | 26 | 31.57 | 1 | 2 | 26.43 | 1175 | 1 | 1 | 1 | 0 | 112.55 |
| 65 | 26 | 39.57 | 1 | 1 | 26.43 | 1040 | 1 | 1 | 0 | 0 | 60.01 |

| SN | Person ID | PMA | Eye R(1) / L(2) | Diagnosis Non ROP 1 ROP 2 | birthage (GA) | birthweight | M(1)/F(0) | multiple birth Y(1)/N (0) | Stage ROP | Caucasian Y(1)/N(0) | fov depth |
|---|---|---|---|---|---|---|---|---|---|---|---|
| 66 | 26 | 39.57 | 2 | 1 | 26.43 | 1040 | 1 | 1 | 0 | 0 | 127.54 |
| 68 | 27 | 32.57 | 1 | 2 | 25.57 | 770 | 1 | 1 | 1 | 1 | 100.24 |
| 73 | 27 | 32.57 | 2 | 2 | 25.57 | 770 | 1 | 1 | 1 | 1 | 80.36 |
| 67 | 27 | 35.57 | 1 | 2 | 25.57 | 770 | 1 | 1 | 1 | 1 | 113.33 |
| 71 | 27 | 35.57 | 2 | 2 | 25.57 | 770 | 1 | 1 | 1 | 1 | 98.18 |
| 69 | 27 | 38.57 | 1 | 2 | 25.57 | 770 | 1 | 1 | 2 | 1 | 57.26 |
| 72 | 27 | 38.57 | 2 | 2 | 25.57 | 770 | 1 | 1 | 2 | 1 | 69.10 |
| 70 | 27 | 39.57 | 1 | 2 | 25.57 | 770 | 1 | 1 | 2 | 1 | 96.25 |
| 74 | 27 | 39.57 | 2 | 2 | 25.57 | 770 | 1 | 1 | 2 | 1 | 100.27 |
| 75 | 28 | 35.85 | 1 | 1 | 28.29 | 635 | 0 | 0 | 0 | 0 | 141.34 |
| 76 | 28 | 35.85 | 2 | 1 | 28.29 | 635 | 0 | 0 | 0 | 0 | 103.93 |
| 79 | 29 | 36.00 | 1 | 2 | 26.43 | 830 | 1 | 0 | 2 | 1 | 75.43 |
| 83 | 29 | 36.00 | 2 | 2 | 26.43 | 830 | 1 | 0 | 2 | 1 | 122.82 |
| 82 | 29 | 37.00 | 2 | 2 | 26.43 | 830 | 1 | 0 | 1 | 1 | 93.24 |
| 80 | 29 | 40.00 | 2 | 2 | 26.43 | 830 | 1 | 0 | 2 | 1 | 73.11 |
| 77 | 29 | 40.13 | 1 | 2 | 26.43 | 830 | 1 | 0 | 2 | 1 | 61.73 |
| 78 | 29 | 42.00 | 1 | 2 | 26.43 | 830 | 1 | 0 | 1 | 1 | 85.26 |
| 81 | 29 | 42.00 | 2 | 2 | 26.43 | 830 | 1 | 0 | 2 | 1 | 135.18 |
| 84 | 30 | 35.85 | 1 | 2 | 26.85 | 850 | 0 | 1 | 2 | 1 | 119.33 |
| 87 | 30 | 35.85 | 2 | 2 | 26.85 | 850 | 0 | 1 | 2 | 1 | 52.31 |
| 85 | 30 | 40.85 | 1 | 2 | 26.85 | 850 | 0 | 1 | 2 | 1 | 106.38 |
| 86 | 30 | 40.85 | 2 | 2 | 26.85 | 850 | 0 | 1 | 2 | 1 | 34.50 |

| SN | Person ID | PMA | Eye R(1) / L(2) | Diagnosis Non ROP 1 ROP 2 | birthage (GA) | birthweight | M(1)/F(0) | multiple birth Y(1)/N (0) | Stage ROP | Caucasian Y(1)/N(0) | fov depth |
|---|---|---|---|---|---|---|---|---|---|---|---|
| 89 | 31 | 33.29 | 1 | 2 | 26.29 | 915 | 0 | 1 | 2 | 0 | 109.47 |
| 92 | 31 | 33.29 | 2 | 2 | 26.29 | 915 | 0 | 1 | 2 | 0 | 80.61 |
| 88 | 31 | 36.29 | 1 | 2 | 26.29 | 915 | 0 | 1 | 2 | 0 | 121.45 |
| 93 | 31 | 36.29 | 2 | 2 | 26.29 | 915 | 0 | 1 | 2 | 0 | 95.45 |
| 90 | 31 | 37.29 | 2 | 2 | 26.29 | 915 | 0 | 1 | 2 | 0 | 157.71 |
| 91 | 31 | 38.29 | 2 | 2 | 26.29 | 915 | 0 | 1 | 3 | 0 | 96.11 |
| 94 | 32 | 33.29 | 1 | 1 | 26.29 | 885 | 1 | 1 | 0 | 0 | 82.41 |
| 95 | 32 | 37.29 | 1 | 1 | 26.29 | 885 | 1 | 1 | 0 | 0 | 118.17 |
| 96 | 32 | 37.29 | 2 | 2 | 26.29 | 885 | 1 | 1 | 1 | 0 | 105.06 |
| 97 | 32 | 39.29 | 2 | 2 | 26.29 | 885 | 1 | 1 | 2 | 0 | 67.84 |
| 100 | 33 | 33.57 | 2 | 1 | 29.14 | 1125 | 1 | 0 | 0 | 1 | 123.57 |
| 98 | 33 | 37.57 | 1 | 1 | 29.14 | 1125 | 1 | 0 | 0 | 1 | 165.77 |
| 101 | 33 | 37.57 | 2 | 1 | 29.14 | 1125 | 1 | 0 | 0 | 1 | 118.55 |
| 99 | 33 | 39.57 | 2 | 1 | 29.14 | 1125 | 1 | 0 | 0 | 1 | 169.59 |
| 102 | 34 | 33.71 | 1 | 2 | 26.43 | 745 | 1 | 0 | 1 | 0 | 40.85 |
| 103 | 34 | 33.71 | 2 | 2 | 26.43 | 745 | 1 | 0 | 1 | 0 | 115.23 |
| 104 | 35 | 33.00 | 1 | 1 | 26.43 | 900 | 1 | 1 | 0 | 1 | 34.35 |
| 108 | 35 | 33.00 | 2 | 1 | 26.43 | 900 | 1 | 1 | 0 | 1 | 118.95 |
| 105 | 35 | 35.00 | 1 | 2 | 26.43 | 900 | 1 | 1 | 2 | 1 | 100.31 |
| 106 | 35 | 38.00 | 1 | 2 | 26.43 | 900 | 1 | 1 | 2 | 1 | 93.13 |
| 107 | 35 | 39.00 | 2 | 2 | 26.43 | 900 | 1 | 1 | 2 | 1 | 136.03 |
| 109 | 36 | 37.00 | 1 | 2 | 25.00 | 720 | 1 | 0 | 2 | 1 | 106.23 |

| SN | Person ID | PMA | Eye R(1) / L(2) | Diagnosis Non ROP 1 ROP 2 | birthage (GA) | birthweight | M(1)/F(0) | multiple birth Y(1)/N (0) | Stage ROP | Caucasian Y(1)/N(0) | fov depth |
|---|---|---|---|---|---|---|---|---|---|---|---|
| 111 | 36 | 37.00 | 2 | 2 | 25.00 | 720 | 1 | 0 | 2 | 1 | 136.79 |
| 110 | 36 | 38.00 | 1 | 2 | 25.00 | 720 | 1 | 0 | 2 | 1 | 117.42 |
| 112 | 36 | 38.00 | 2 | 2 | 25.00 | 720 | 1 | 0 | 2 | 1 | 57.24 |
| 113 | 37 | 34.85 | 1 | 1 | 30.85 | 1550 | 1 | 0 | 0 | 0 | 48.53 |
| 119 | 38 | 34.57 | 2 | 2 | 23.71 | 655 | 0 | 0 | 1 | 0 | 130.01 |
| 116 | 38 | 35.57 | 1 | 2 | 23.71 | 655 | 0 | 0 | 2 | 0 | 39.71 |
| 120 | 38 | 35.57 | 2 | 2 | 23.71 | 655 | 0 | 0 | 2 | 0 | 145.71 |
| 114 | 38 | 36.57 | 1 | 2 | 23.71 | 655 | 0 | 0 | 2 | 0 | 61.72 |
| 117 | 38 | 36.57 | 2 | 2 | 23.71 | 655 | 0 | 0 | 2 | 0 | 49.27 |
| 115 | 38 | 37.57 | 1 | 2 | 23.71 | 655 | 0 | 0 | 1 | 0 | 111.73 |
| 118 | 38 | 37.57 | 2 | 2 | 23.71 | 655 | 0 | 0 | 1 | 0 | 119.61 |
| 121 | 39 | 33.57 | 1 | 1 | 30.43 | 1250 | 0 | 0 | 0 | 1 | 35.65 |
| 122 | 39 | 33.57 | 2 | 1 | 30.43 | 1250 | 0 | 0 | 0 | 1 | 58.18 |
| 123 | 40 | 37.29 | 2 | 1 | 28.29 | 1155 | 0 | 0 | 0 | 1 | 140.91 |
| 124 | 41 | 34.00 | 1 | 2 | 24.29 | 830 | 1 | 0 | 1 | 0 | 151.52 |
| 125 | 41 | 36.00 | 1 | 2 | 24.29 | 830 | 1 | 0 | 2 | 0 | 114.79 |
| 126 | 41 | 36.00 | 2 | 2 | 24.29 | 830 | 1 | 0 | 2 | 0 | 117.01 |
| 127 | 42 | 33.85 | 1 | 1 | 24.29 | 850 | 1 | 0 | 0 | 1 | 101.01 |
| 128 | 42 | 33.85 | 1 | 1 | 24.29 | 850 | 1 | 0 | 0 | 1 | 78.99 |
| 129 | 43 | 33.57 | 2 | 1 | 29.71 | 915 | 0 | 0 | 0 | 0 | 46.84 |
| 130 | 44 | 38.71 | 1 | 1 | 29.00 | 660 | 0 | 0 | 0 | 0 | 90.32 |
| 131 | 44 | 38.71 | 2 | 1 | 29.00 | 660 | 0 | 0 | 0 | 0 | 86.20 |

| SN | Person ID | PMA | Eye R(1) / L(2) | Diagnosis Non ROP 1 ROP 2 | birthage (GA) | birthweight | M(1)/F(0) | multiple birth Y(1)/N (0) | Stage ROP | Caucasian Y(1)/N(0) | fov depth |
|---|---|---|---|---|---|---|---|---|---|---|---|
| 137 | 45 | 32.43 | 2 | 1 | 24.14 | 730 | 0 | 0 | 0 | 0 | 76.42 |
| 135 | 45 | 34.43 | 2 | 2 | 24.14 | 730 | 0 | 0 | 2 | 0 | 184.02 |
| 133 | 45 | 35.43 | 1 | 2 | 24.14 | 730 | 0 | 0 | 2 | 0 | 171.23 |
| 136 | 45 | 35.43 | 2 | 2 | 24.14 | 730 | 0 | 0 | 2 | 0 | 98.97 |
| 132 | 45 | 36.43 | 1 | 2 | 24.14 | 730 | 0 | 0 | 2 | 0 | 155.78 |
| 134 | 45 | 36.43 | 2 | 2 | 24.14 | 730 | 0 | 0 | 2 | 0 | 176.28 |
| 139 | 46 | 32.57 | 2 | 1 | 25.43 | 740 | 1 | 0 | 0 | 0 | 41.95 |
| 140 | 46 | 34.57 | 2 | 1 | 25.43 | 740 | 1 | 0 | 0 | 0 | 59.52 |
| 138 | 46 | 36.57 | 1 | 1 | 25.43 | 740 | 1 | 0 | 0 | 0 | 77.50 |
| 141 | 46 | 36.57 | 2 | 1 | 25.43 | 740 | 1 | 0 | 0 | 0 | 86.18 |
| 142 | 47 | 34.29 | 1 | 1 | 30.43 | 1100 | 0 | 0 | 0 | 1 | 84.48 |
| 145 | 48 | 32.43 | 1 | 1 | 27.00 | 1100 | 1 | 0 | 0 | 1 | 70.82 |
| 148 | 48 | 32.43 | 2 | 1 | 27.00 | 1100 | 1 | 0 | 0 | 1 | 63.07 |
| 144 | 48 | 34.43 | 1 | 1 | 27.00 | 1100 | 1 | 0 | 0 | 1 | 83.61 |
| 150 | 48 | 34.43 | 2 | 1 | 27.00 | 1100 | 1 | 0 | 0 | 1 | 74.86 |
| 146 | 48 | 36.43 | 1 | 1 | 27.00 | 1100 | 1 | 0 | 0 | 1 | 89.76 |
| 147 | 48 | 36.43 | 2 | 1 | 27.00 | 1100 | 1 | 0 | 0 | 1 | 96.03 |
| 143 | 48 | 38.43 | 1 | 1 | 27.00 | 1100 | 1 | 0 | 0 | 1 | 93.71 |
| 149 | 48 | 38.43 | 2 | 1 | 27.00 | 1100 | 1 | 0 | 0 | 1 | 55.77 |
| 151 | 49 | 32.00 | 1 | 1 | 29.00 | 1360 | 0 | 1 | 0 | 1 | 105.66 |
| 153 | 49 | 32.00 | 2 | 1 | 29.00 | 1360 | 0 | 1 | 0 | 1 | 95.78 |
| 154 | 49 | 34.00 | 2 | 1 | 29.00 | 1360 | 0 | 1 | 0 | 1 | 141.52 |

| SN | Person ID | PMA | Eye R(1) / L(2) | Diagnosis Non ROP 1 ROP 2 | birthage (GA) | birthweight | M(1)/F(0) | multiple birth Y(1)/N (0) | Stage ROP | Caucasian Y(1)/N(0) | fov depth |
|---|---|---|---|---|---|---|---|---|---|---|---|
| 152 | 49 | 36.00 | 1 | 1 | 29.00 | 1360 | 0 | 1 | 0 | 1 | 95.18 |
| 155 | 49 | 36.00 | 2 | 1 | 29.00 | 1360 | 0 | 1 | 0 | 1 | 111.27 |
| 156 | 50 | 32.00 | 1 | 1 | 29.00 | 1330 | 0 | 1 | 0 | 1 | 151.34 |
| 159 | 50 | 32.00 | 2 | 1 | 29.00 | 1330 | 0 | 1 | 0 | 1 | 156.79 |
| 157 | 50 | 34.00 | 1 | 1 | 29.00 | 1330 | 0 | 1 | 0 | 1 | 168.36 |
| 160 | 50 | 34.00 | 2 | 1 | 29.00 | 1330 | 0 | 1 | 0 | 1 | 80.80 |
| 158 | 50 | 36.00 | 1 | 1 | 29.00 | 1330 | 0 | 1 | 0 | 1 | 120.04 |
| 162 | 51 | 37.71 | 2 | 1 | 28.71 | 910 | 1 | 1 | 0 | 1 | 143.89 |
| 161 | 51 | 39.71 | 1 | 1 | 28.71 | 910 | 1 | 1 | 0 | 1 | 126.09 |
| 163 | 52 | 34.71 | 1 | 1 | 28.57 | 1135 | 1 | 1 | 0 | 1 | 154.17 |
| 164 | 52 | 36.71 | 1 | 1 | 28.57 | 1135 | 1 | 1 | 0 | 1 | 136.91 |
| 165 | 52 | 38.71 | 2 | 1 | 28.57 | 1135 | 1 | 1 | 0 | 1 | 146.99 |
| 168 | 53 | 32.14 | 2 | 1 | 27.00 | 720 | 0 | 0 | 0 | 1 | 69.22 |
| 166 | 53 | 34.14 | 1 | 1 | 27.00 | 720 | 0 | 0 | 0 | 1 | 98.26 |
| 167 | 53 | 34.14 | 2 | 1 | 27.00 | 720 | 0 | 0 | 0 | 1 | 113.79 |
| 170 | 54 | 33.00 | 1 | 2 | 24.14 | 685 | 0 | 0 | 2 | 0 | 151.54 |
| 171 | 54 | 33.00 | 2 | 2 | 24.14 | 685 | 0 | 0 | 2 | 0 | 156.01 |
| 169 | 54 | 34.00 | 1 | 2 | 24.14 | 685 | 0 | 0 | 2 | 0 | 132.19 |
| 173 | 55 | 32.71 | 1 | 2 | 24.00 | 600 | 0 | 0 | 2 | 1 | 126.37 |
| 176 | 55 | 32.71 | 2 | 2 | 24.00 | 600 | 0 | 0 | 2 | 1 | 142.58 |
| 174 | 55 | 33.71 | 1 | 2 | 24.00 | 600 | 0 | 0 | 2 | 1 | 102.99 |

| SN | Person ID | PMA | Eye R(1) / L(2) | Diagnosis Non ROP 1 ROP 2 | birthage (GA) | birthweight | M(1)/F(0) | multiple birth Y(1)/N (0) | Stage ROP | Caucasian Y(1)/N(0) | fov depth |
|---|---|---|---|---|---|---|---|---|---|---|---|
| 172 | 55 | 35.71 | 1 | 2 | 24.00 | 600 | 0 | 0 | 2 | 1 | 109.53 |
| 175 | 55 | 35.71 | 2 | 2 | 24.00 | 600 | 0 | 0 | 2 | 1 | 152.23 |
| 177 | 56 | 33.85 | 2 | 1 | 28.57 | 840 | 0 | 0 | 0 | 1 | 83.99 |
| 178 | 56 | 42.85 | 2 | 2 | 28.57 | 840 | 0 | 0 | 2 | 1 | 146.47 |
| 179 | 56 | 43.85 | 2 | 2 | 28.57 | 840 | 0 | 0 | 2 | 1 | 132.32 |
| 180 | 57 | 32.00 | 1 | 2 | 27.57 | 955 | 1 | 0 | 1 | 0 | 122.17 |
| 182 | 58 | 32.00 | 1 | 1 | 27.57 | 710 | 1 | 1 | 0 | 0 | 77.31 |
| 183 | 58 | 34.00 | 2 | 1 | 27.57 | 710 | 1 | 1 | 0 | 0 | 99.24 |
| 181 | 58 | 40.00 | 1 | 1 | 27.57 | 710 | 1 | 1 | 0 | 0 | 41.76 |
| 184 | 58 | 40.00 | 2 | 1 | 27.57 | 710 | 1 | 1 | 0 | 0 | 101.50 |
| 187 | 59 | 34.14 | 2 | 1 | 28.85 | 1085 | 1 | 0 | 0 | 0 | 64.33 |
| 185 | 59 | 39.14 | 1 | 2 | 28.85 | 1085 | 1 | 0 | 3 | 0 | 115.18 |
| 186 | 59 | 39.14 | 2 | 2 | 28.85 | 1085 | 1 | 0 | 3 | 0 | 110.22 |
| 188 | 60 | 34.00 | 1 | 1 | 31.00 | 1310 | 0 | 0 | 0 | 0 | 98.92 |
| 189 | 60 | 34.00 | 2 | 1 | 31.00 | 1310 | 0 | 0 | 0 | 0 | 97.00 |
| 190 | 61 | 38.57 | 1 | 1 | 30.71 | 1310 | 0 | 0 | 0 | 0 | 100.21 |
| 191 | 61 | 38.57 | 2 | 1 | 30.71 | 1310 | 0 | 0 | 0 | 0 | 94.74 |
| 192 | 62 | 32.71 | 1 | 1 | 27.71 | 1180 | 1 | 0 | 0 | 0 | 138.46 |
| 195 | 62 | 32.71 | 2 | 1 | 27.71 | 1180 | 1 | 0 | 0 | 0 | 104.47 |
| 193 | 62 | 37.71 | 1 | 1 | 27.71 | 1180 | 1 | 0 | 0 | 0 | 149.85 |
| 196 | 62 | 37.71 | 2 | 1 | 27.71 | 1180 | 1 | 0 | 0 | 0 | 174.27 |
| 194 | 62 | 39.71 | 1 | 1 | 27.71 | 1180 | 1 | 0 | 0 | 0 | 173.78 |

| SN | Person ID | PMA | Eye R(1) / L(2) | Diagnosis Non ROP 1 ROP 2 | birthAge (GA) | birthweight | M(1)/F(0) | multiple birth Y(1)/N (0) | Stage ROP | Caucasian Y(1)/N(0) | fov depth |
|---|---|---|---|---|---|---|---|---|---|---|---|
| 197 | 62 | 39.71 | 2 | 1 | 27.71 | 1180 | 1 | 0 | 0 | 0 | 161.30 |
| 198 | 63 | 33.14 | 1 | 1 | 29.29 | 1540 | 1 | 0 | 0 | 1 | 92.68 |
| 199 | 63 | 33.14 | 2 | 1 | 29.29 | 1540 | 1 | 0 | 0 | 1 | 123.96 |
| 200 | 64 | 33.00 | 1 | 1 | 27.71 | 975 | 0 | 0 | 0 | 1 | 51.14 |
| 201 | 64 | 33.00 | 2 | 1 | 27.71 | 975 | 0 | 0 | 0 | 1 | 46.67 |
| 202 | 65 | 37.00 | 2 | 1 | 35.71 | 2430 | 1 | 0 | 0 | 0 | 78.09 |
| 203 | 66 | 31.57 | 1 | 1 | 28.29 | 1600 | 0 | 0 | 0 | 1 | 36.34 |
| 206 | 66 | 31.57 | 2 | 1 | 28.29 | 1600 | 0 | 0 | 0 | 1 | 133.57 |
| 204 | 66 | 33.57 | 1 | 1 | 28.29 | 1600 | 0 | 0 | 0 | 1 | 42.09 |
| 205 | 66 | 33.57 | 2 | 1 | 28.29 | 1600 | 0 | 0 | 0 | 1 | 37.36 |
| 207 | 67 | 37.57 | 1 | 2 | 24.85 | 690 | 1 | 0 | 2 | 1 | 143.88 |
| 208 | 67 | 37.57 | 2 | 2 | 24.85 | 690 | 1 | 0 | 2 | 1 | 113.37 |
| 209 | 68 | 35.57 | 1 | 1 | 30.29 | 1750 | 1 | 0 | 0 | 1 | 142.10 |
| 210 | 69 | 33.43 | 2 | 1 | 29.85 | 795 | 0 | 0 | 0 | 0 | 83.21 |
| 211 | 70 | 38.43 | 2 | 1 | 30.43 | 1385 | 0 | 0 | 0 | 0 | 129.07 |
| 212 | 71 | 37.29 | 1 | 2 | 24.29 | 650 | 0 | 0 | 1 | 0 | 99.43 |
| 216 | 72 | 32.29 | 2 | 2 | 26.57 | 1020 | 1 | 0 | 1 | 0 | 111.72 |
| 217 | 72 | 32.29 | 2 | 2 | 26.57 | 1020 | 1 | 0 | 1 | 0 | 121.36 |
| 213 | 72 | 34.29 | 1 | 2 | 26.57 | 1020 | 1 | 0 | 1 | 0 | 110.11 |
| 214 | 72 | 35.29 | 1 | 2 | 26.57 | 1020 | 1 | 0 | 2 | 0 | 106.98 |
| 215 | 72 | 37.29 | 1 | 1 | 26.57 | 1020 | 1 | 0 | 0 | 0 | 112.69 |
| 218 | 72 | 37.29 | 2 | 2 | 26.57 | 1020 | 1 | 0 | 2 | 0 | 139.26 |

| SN | Person ID | PMA | Eye R(1) / L(2) | Diagnosis Non ROP 1 ROP 2 | birthAge (GA) | birthweight | M(1)/F(0) | multiple birth Y(1)/N (0) | Stage ROP | Caucasian Y(1)/N(0) | fov depth |
|---|---|---|---|---|---|---|---|---|---|---|---|
| 219 | 73 | 33.29 | 1 | 1 | 29.57 | 890 | 1 | 0 | 0 | 0 | 87.63 |
| 222 | 73 | 33.29 | 2 | 1 | 29.57 | 890 | 1 | 0 | 0 | 0 | 67.29 |
| 220 | 73 | 35.29 | 1 | 1 | 29.57 | 890 | 1 | 0 | 0 | 0 | 61.53 |
| 223 | 73 | 35.29 | 2 | 1 | 29.57 | 890 | 1 | 0 | 0 | 0 | 78.37 |
| 221 | 73 | 39.29 | 1 | 1 | 29.57 | 890 | 1 | 0 | 0 | 0 | 46.16 |
| 224 | 73 | 39.29 | 2 | 1 | 29.57 | 890 | 1 | 0 | 0 | 0 | 52.75 |
| 228 | 74 | 31.00 | 2 | 2 | 26.71 | 617 | 0 | 0 | 1 | 1 | 134.40 |
| 225 | 74 | 33.00 | 1 | 1 | 26.71 | 617 | 0 | 0 | 0 | 1 | 70.78 |
| 229 | 74 | 33.00 | 2 | 1 | 26.71 | 617 | 0 | 0 | 0 | 1 | 56.43 |
| 226 | 74 | 34.00 | 1 | 1 | 26.71 | 617 | 0 | 0 | 0 | 1 | 54.96 |
| 227 | 74 | 37.00 | 1 | 2 | 26.71 | 617 | 0 | 0 | 2 | 1 | 146.61 |
| 230 | 74 | 37.00 | 2 | 2 | 26.71 | 617 | 0 | 0 | 2 | 1 | 151.16 |
| 231 | 75 | 38.71 | 1 | 1 | 33.14 | 1420 | 1 | 0 | 0 | 1 | 69.39 |
| 232 | 75 | 38.71 | 2 | 1 | 33.14 | 1420 | 1 | 0 | 0 | 1 | 132.90 |
| 233 | 76 | 39.57 | 1 | 1 | 29.57 | 1350 | 1 | 1 | 0 | 0 | 129.64 |
| 234 | 76 | 39.57 | 2 | 1 | 29.57 | 1350 | 1 | 1 | 0 | 0 | 107.87 |
| 235 | 76 | 40.29 | 2 | 1 | 29.57 | 1350 | 1 | 1 | 0 | 0 | 107.45 |
| 236 | 77 | 39.57 | 1 | 2 | 29.57 | 1370 | 0 | 1 | 2 | 0 | 152.59 |
| 238 | 77 | 39.57 | 2 | 2 | 29.57 | 1370 | 0 | 1 | 2 | 0 | 136.77 |
| 237 | 77 | 40.29 | 1 | 2 | 29.57 | 1370 | 0 | 1 | 3 | 0 | 142.68 |
| 239 | 77 | 40.29 | 2 | 2 | 29.57 | 1370 | 0 | 1 | 3 | 0 | 156.82 |
| 240 | 78 | 34.00 | 1 | 1 | 24.71 | 685 | 0 | 0 | 0 | 0 | 136.07 |

| SN | Person ID | PMA | Eye R(1) / L(2) | Diagnosis Non ROP 1 ROP 2 | birthAge (GA) | birthweight | M(1)/F(0) | multiple birth Y(1)/N (0) | Stage ROP | Caucasian Y(1)/N(0) | fov depth |
|---|---|---|---|---|---|---|---|---|---|---|---|
| 244 | 78 | 34.00 | 2 | 1 | 24.71 | 685 | 0 | 0 | 0 | 0 | 115.67 |
| 241 | 78 | 37.00 | 1 | 1 | 24.71 | 685 | 0 | 0 | 0 | 0 | 108.22 |
| 245 | 78 | 37.00 | 2 | 1 | 24.71 | 685 | 0 | 0 | 0 | 0 | 105.05 |
| 242 | 78 | 38.00 | 1 | 1 | 24.71 | 685 | 0 | 0 | 0 | 0 | 94.60 |
| 246 | 78 | 38.00 | 2 | 1 | 24.71 | 685 | 0 | 0 | 0 | 0 | 135.47 |
| 243 | 78 | 39.00 | 1 | 1 | 24.71 | 685 | 0 | 0 | 0 | 0 | 134.29 |
| 247 | 78 | 39.00 | 2 | 1 | 24.71 | 685 | 0 | 0 | 0 | 0 | 113.10 |
| 251 | 79 | 33.85 | 2 | 2 | 30.14 | 865 | 0 | 0 | 2 | 1 | 144.09 |
| 252 | 79 | 33.85 | 2 | 2 | 30.14 | 865 | 0 | 0 | 2 | 1 | 131.71 |
| 249 | 79 | 34.85 | 1 | 2 | 30.14 | 865 | 0 | 0 | 2 | 1 | 106.85 |
| 254 | 79 | 34.85 | 2 | 2 | 30.14 | 865 | 0 | 0 | 2 | 1 | 93.63 |
| 250 | 79 | 35.85 | 1 | 2 | 30.14 | 865 | 0 | 0 | 2 | 1 | 127.98 |
| 255 | 79 | 35.85 | 2 | 2 | 30.14 | 865 | 0 | 0 | 2 | 1 | 80.49 |
| 248 | 79 | 36.85 | 1 | 2 | 30.14 | 865 | 0 | 0 | 2 | 1 | 116.50 |
| 253 | 79 | 36.85 | 2 | 2 | 30.14 | 865 | 0 | 0 | 2 | 1 | 89.23 |
| 256 | 80 | 35.57 | 1 | 2 | 24.71 | 735 | 0 | 0 | 2 | 0 | 94.48 |
| 257 | 81 | 33.43 | 1 | 1 | 29.29 | 1270 | 1 | 0 | 0 | 1 | 123.84 |
| 259 | 81 | 33.43 | 2 | 1 | 29.29 | 1270 | 1 | 0 | 0 | 1 | 91.95 |
| 258 | 81 | 35.43 | 1 | 1 | 29.29 | 1270 | 1 | 0 | 0 | 1 | 128.77 |
| 260 | 81 | 35.43 | 2 | 1 | 29.29 | 1270 | 1 | 0 | 0 | 1 | 123.95 |
| 262 | 82 | 34.57 | 1 | 1 | 30.29 | 1545 | 1 | 0 | 0 | 1 | 86.69 |
| 264 | 82 | 34.57 | 2 | 1 | 30.29 | 1545 | 1 | 0 | 0 | 1 | 104.78 |

| SN | Person ID | PMA | Eye R(1) / L(2) | Diagnosis Non ROP 1 ROP 2 | birthAge (GA) | birthweight | M(1)/F(0) | multiple birth Y(1)/N (0) | Stage ROP | Caucasian Y(1)/N(0) | fov depth |
|---|---|---|---|---|---|---|---|---|---|---|---|
| 261 | 82 | 36.57 | 1 | 1 | 30.29 | 1545 | 1 | 0 | 0 | 1 | 120.75 |
| 263 | 82 | 36.57 | 2 | 1 | 30.29 | 1545 | 1 | 0 | 0 | 1 | 92.02 |
| 266 | 83 | 37.29 | 1 | 1 | 31.57 | 1730 | 0 | 0 | 0 | 1 | 64.47 |
| 267 | 83 | 37.29 | 2 | 1 | 31.57 | 1730 | 0 | 0 | 0 | 1 | 81.38 |
| 265 | 83 | 39.29 | 1 | 1 | 31.57 | 1730 | 0 | 0 | 0 | 1 | 112.42 |
| 268 | 83 | 39.29 | 2 | 1 | 31.57 | 1730 | 0 | 0 | 0 | 1 | 86.45 |
| 270 | 84 | 35.00 | 2 | 1 | 29.71 | 1420 | 1 | 0 | 0 | 1 | 58.50 |
| 269 | 84 | 37.00 | 1 | 1 | 29.71 | 1420 | 1 | 0 | 0 | 1 | 62.69 |
| 271 | 84 | 37.00 | 2 | 1 | 29.71 | 1420 | 1 | 0 | 0 | 1 | 32.49 |
| 272 | 85 | 36.00 | 1 | 1 | 28.14 | 985 | 1 | 0 | 0 | 0 | 76.79 |
| 273 | 85 | 36.00 | 2 | 1 | 28.14 | 985 | 1 | 0 | 0 | 0 | 52.01 |
| 274 | 86 | 37.00 | 1 | 1 | 29.43 | 1280 | 1 | 0 | 0 | 1 | 66.48 |
| 275 | 86 | 37.00 | 2 | 1 | 29.43 | 1280 | 1 | 0 | 0 | 1 | 61.34 |
| 276 | 87 | 33.85 | 1 | 2 | 24.43 | 555 | 0 | 1 | 2 | 1 | 173.11 |
| 277 | 87 | 33.85 | 2 | 2 | 24.43 | 555 | 0 | 1 | 2 | 1 | 206.02 |
| 278 | 88 | 39.57 | 1 | 1 | 32.43 | 1045 | 0 | 0 | 0 | 1 | 34.74 |
| 279 | 88 | 39.57 | 2 | 1 | 32.43 | 1045 | 0 | 0 | 0 | 1 | 48.64 |

**Appendix 2** Supplementary Data Foveal Morphology

| Person ID | width_all | width_n | width_t | fov depth | area_all | area_n | area_t | slope_n | slope_t | xslope_n | xslope_t | xSD_n | xSD_t | RT+RPE | RT | max_n | max_t | RT1000_n | RT1000_t |
|---|---|---|---|---|---|---|---|---|---|---|---|---|---|---|---|---|---|---|---|
| 1 | 1520.00 | 760.00 | 760.00 | 137.49 | 99276.84 | 49638.42 | 49638.42 | 0.29 | 0.29 | 320.00 | 320.00 | 560.00 | 560.00 | 125.62 | 111.70 | 265.32 | 265.32 | 250.88 | 248.26 |
| 1 | 1400.00 | 600.00 | 800.00 | 121.84 | 76743.10 | 36220.32 | 40522.78 | 0.34 | 0.24 | 250.00 | 340.00 | 440.00 | 600.00 | 127.20 | 112.87 | 268.40 | 256.73 | 257.82 | 242.35 |
| 2 | 1220.00 | 500.00 | 720.00 | 88.78 | 47807.91 | 22441.44 | 25366.48 | 0.29 | 0.21 | 210.00 | 310.00 | 370.00 | 540.00 | 135.43 | 123.29 | 239.65 | 249.96 | 225.80 | 231.34 |
| 2 | 1320.00 | 520.00 | 800.00 | 63.63 | 36629.18 | 17540.04 | 19089.14 | 0.20 | 0.14 | 220.00 | 340.00 | 380.00 | 600.00 | 138.48 | 127.75 | 232.98 | 217.06 | 208.50 | 204.70 |
| 2 | 1240.00 | 560.00 | 680.00 | 89.41 | 53744.72 | 26589.75 | 27154.97 | 0.24 | 0.20 | 240.00 | 290.00 | 420.00 | 500.00 | 131.16 | 121.87 | 250.90 | 239.38 | 223.51 | 219.58 |
| 2 | 1120.00 | 430.00 | 690.00 | 78.89 | 39003.13 | 19212.57 | 19790.56 | 0.28 | 0.22 | 190.00 | 300.00 | 320.00 | 510.00 | 133.58 | 122.23 | 256.49 | 247.60 | 228.05 | 229.34 |
| 2 | 1320.00 | 660.00 | 660.00 | 87.96 | 58633.73 | 29316.87 | 29316.87 | 0.20 | 0.20 | 290.00 | 290.00 | 490.00 | 490.00 | 120.29 | 108.43 | 237.05 | 237.05 | 206.70 | 209.02 |
| 2 | 1320.00 | 620.00 | 700.00 | 86.64 | 56319.68 | 28064.03 | 28255.65 | 0.22 | 0.18 | 270.00 | 300.00 | 460.00 | 520.00 | 130.66 | 117.24 | 245.36 | 222.43 | 216.50 | 207.54 |
| 3 | 1410.00 | 740.00 | 670.00 | 104.64 | 71719.93 | 36755.15 | 34964.78 | 0.23 | 0.23 | 320.00 | 280.00 | 550.00 | 490.00 | 129.34 | 117.53 | 254.46 | 233.90 | 235.69 | 220.82 |
| 4 | 1820.00 | 890.00 | 930.00 | 75.98 | 67397.11 | 33623.18 | 33773.93 | 0.13 | 0.12 | 380.00 | 390.00 | 660.00 | 690.00 | 155.28 | 138.62 | 237.22 | 232.49 | 218.61 | 212.87 |
| 4 | 1800.00 | 900.00 | 900.00 | 85.34 | 77405.07 | 38702.54 | 38702.54 | 0.14 | 0.14 | 390.00 | 390.00 | 670.00 | 670.00 | 142.46 | 129.00 | 245.87 | 245.87 | 216.25 | 219.76 |
| 5 | 1580.00 | 820.00 | 760.00 | 118.92 | 88508.59 | 45873.69 | 42634.89 | 0.23 | 0.25 | 350.00 | 310.00 | 610.00 | 560.00 | 168.91 | 156.72 | 295.21 | 287.58 | 283.29 | 270.33 |
| 5 | 1580.00 | 800.00 | 780.00 | 117.95 | 89068.22 | 45313.43 | 43754.79 | 0.24 | 0.23 | 340.00 | 320.00 | 590.00 | 570.00 | 168.67 | 159.29 | 296.27 | 282.46 | 283.42 | 268.79 |
| 5 | 1520.00 | 780.00 | 740.00 | 92.00 | 66344.04 | 33563.26 | 32780.78 | 0.19 | 0.19 | 320.00 | 310.00 | 570.00 | 540.00 | 173.30 | 157.22 | 268.64 | 265.41 | 256.56 | 247.86 |
| 5 | 1320.00 | 480.00 | 840.00 | 80.47 | 42156.75 | 19348.70 | 22808.04 | 0.27 | 0.20 | 210.00 | 340.00 | 360.00 | 610.00 | 168.74 | 157.30 | 273.97 | 275.01 | 256.24 | 262.20 |
| 5 | 1040.00 | 570.00 | 470.00 | 84.18 | 42268.84 | 21604.83 | 20664.00 | 0.25 | 0.26 | 250.00 | 200.00 | 420.00 | 350.00 | 158.59 | 149.30 | 279.34 | 244.45 | 253.65 | 231.53 |
| 5 | 1160.00 | 580.00 | 580.00 | 112.16 | 64551.69 | 32233.66 | 32318.02 | 0.30 | 0.28 | 250.00 | 250.00 | 430.00 | 430.00 | 152.35 | 140.76 | 281.16 | 275.52 | 260.94 | 259.78 |
| 5 | 1280.00 | 790.00 | 490.00 | 97.50 | 52175.54 | 28098.58 | 24076.96 | 0.25 | 0.32 | 340.00 | 210.00 | 580.00 | 360.00 | 160.49 | 149.47 | 295.45 | 269.65 | 279.08 | 257.99 |
| 5 | 1410.00 | 830.00 | 580.00 | 83.64 | 51592.85 | 27771.25 | 23821.60 | 0.19 | 0.22 | 350.00 | 250.00 | 610.00 | 430.00 | 163.03 | 152.28 | 268.01 | 249.95 | 252.68 | 235.93 |
| 6 | 1340.00 | 670.00 | 670.00 | 147.69 | 98241.80 | 49120.90 | 49120.90 | 0.33 | 0.33 | 290.00 | 290.00 | 500.00 | 500.00 | 117.74 | 110.26 | 283.91 | 283.91 | 267.36 | 267.41 |
| 6 | 1510.00 | 720.00 | 790.00 | 148.52 | 108870.08 | 53200.82 | 55669.26 | 0.34 | 0.27 | 310.00 | 340.00 | 540.00 | 590.00 | 129.77 | 114.72 | 296.22 | 291.96 | 282.48 | 269.74 |
| 7 | 1350.00 | 620.00 | 730.00 | 165.77 | 106677.80 | 52013.13 | 54664.67 | 0.43 | 0.34 | 260.00 | 310.00 | 460.00 | 540.00 | 128.62 | 113.59 | 313.21 | 302.33 | 296.48 | 289.65 |
| 7 | 1530.00 | 750.00 | 780.00 | 155.50 | 115146.81 | 57711.68 | 57435.13 | 0.31 | 0.32 | 320.00 | 330.00 | 560.00 | 570.00 | 149.86 | 139.70 | 309.26 | 311.68 | 296.85 | 303.41 |
| 8 | 1080.00 | 540.00 | 540.00 | 79.91 | 43439.15 | 21719.58 | 21719.58 | 0.22 | 0.22 | 240.00 | 240.00 | 400.00 | 400.00 | 123.84 | 110.21 | 241.58 | 241.58 | 213.43 | 209.73 |
| 8 | 920.00 | 460.00 | 460.00 | 70.04 | 32655.96 | 16327.98 | 16327.98 | 0.22 | 0.22 | 200.00 | 200.00 | 340.00 | 340.00 | 122.16 | 110.90 | 251.95 | 251.95 | 203.16 | 205.73 |
| 9 | 1750.00 | 870.00 | 880.00 | 136.92 | 114563.63 | 57277.93 | 57285.70 | 0.27 | 0.22 | 370.00 | 370.00 | 640.00 | 650.00 | 146.69 | 128.16 | 301.09 | 272.02 | 286.77 | 258.61 |

| Person ID | width_all | width_n | width_t | fov depth | area_all | area_n | area_t | slope_n | slope_t | xslope_n | xslope_t | xSD_n | xSD_t | RT+RPE | RT | max_n | max_t | RT1000_n | RT1000_t |
|---|---|---|---|---|---|---|---|---|---|---|---|---|---|---|---|---|---|---|---|
| 9 | 1860.00 | 930.00 | 930.00 | 101.41 | 89465.11 | 44828.06 | 44637.06 | 0.19 | 0.16 | 390.00 | 380.00 | 690.00 | 680.00 | 146.33 | 134.95 | 258.84 | 239.53 | 246.67 | 228.27 |
| 9 | 1860.00 | 930.00 | 930.00 | 110.87 | 98854.17 | 49528.43 | 49325.75 | 0.21 | 0.17 | 390.00 | 390.00 | 690.00 | 690.00 | 159.98 | 152.54 | 286.06 | 260.61 | 273.89 | 247.27 |
| 10 | 1350.00 | 770.00 | 580.00 | 149.62 | 93910.08 | 48839.24 | 45070.84 | 0.34 | 0.38 | 330.00 | 250.00 | 570.00 | 430.00 | 127.82 | 117.53 | 327.10 | 283.13 | 302.98 | 269.87 |
| 11 | 1370.00 | 720.00 | 650.00 | 100.20 | 66375.61 | 34029.81 | 32345.80 | 0.22 | 0.23 | 310.00 | 270.00 | 540.00 | 480.00 | 188.74 | 172.06 | 300.11 | 290.24 | 285.30 | 271.99 |
| 12 | 1340.00 | 670.00 | 670.00 | 114.07 | 75732.07 | 37547.86 | 38184.21 | 0.25 | 0.26 | 290.00 | 290.00 | 490.00 | 500.00 | 146.50 | 130.13 | 265.66 | 287.29 | 253.48 | 261.94 |
| 13 | 1380.00 | 690.00 | 690.00 | 57.67 | 41031.65 | 20490.78 | 20540.87 | 0.12 | 0.11 | 310.00 | 310.00 | 520.00 | 520.00 | 176.83 | 166.66 | 266.20 | 262.06 | 237.46 | 228.13 |
| 13 | 3420.00 | 940.00 | 2480.00 | 67.19 | 57608.37 | 24005.29 | 33603.08 | 0.13 | 0.08 | 410.00 | 450.00 | 700.00 | 730.00 | 168.14 | 151.70 | 269.07 | 253.89 | 239.57 | 219.83 |

**Appendix 3** Preterm Infants with cystoid macular oedema (CME). Demographic Data.

| SN | person ID | PMA | GA | BW | M(1) F(2) | Single (2) multiple (1) | eye R(1) L(2) | diagnosis nROP(1) ROP(2) | stage ROP | Caucasian (1) no(2) | elm y(1) n(2) | fovea(1) dome(2) | axial length | Correction (Corr) | X res Corr | thickness | width | area | SD |
|---|---|---|---|---|---|---|---|---|---|---|---|---|---|---|---|---|---|---|---|
| 1 | 1 | 37.3 | 27.14 | 640 | 2 | 1 | 1 | 2 | 1 | 2 | 1 | 1 | 16.33 | 0.6815526 | 13.63 | 61.29 | 1090.48 | 66835.77 | 18.95 |
| 2 | 1 | 37.3 | 27.14 | 640 | 2 | 1 | 2 | 2 | 1 | 2 | 1 | 1 | 16.33 | 0.6815526 | 13.63 | 72.36 | 1172.27 | 84828.76 | 20.21 |
| 3 | 2 | 37.1 | 31.71 | 2050 | 1 | 1 | 1 | 1 | 0 | 1 | 1 | 2 | 16.301875 | 0.6803788 | 13.61 | 137.69 | 3619.61 | 498396.49 | 80.53 |
| 4 | 2 | 39.1 | 31.71 | 2050 | 1 | 1 | 1 | 1 | 0 | 1 | 2 | 2 | 16.676875 | 0.6960298 | 13.92 | 136.34 | 4287.54 | 584564.84 | 72.21 |
| 5 | 2 | 39.1 | 31.71 | 2050 | 1 | 1 | 2 | 1 | 0 | 1 | 2 | 2 | 16.676875 | 0.6960298 | 13.92 | 156.94 | 3006.85 | 471908.23 | 77.12 |
| 6 | 2 | 41.1 | 31.71 | 2050 | 1 | 1 | 1 | 1 | 0 | 1 | 2 | 2 | 17.006675 | 0.7097944 | 14.20 | 86.08 | 1689.31 | 145411.33 | 35.88 |
| 7 | 2 | 41.1 | 31.71 | 2050 | 1 | 1 | 2 | 1 | 0 | 1 | 2 | 2 | 17.006675 | 0.7097944 | 14.20 | 102.55 | 2768.20 | 283872.35 | 41.34 |
| 8 | 3 | 35.9 | 33.14 | 1380 | 2 | 2 | 2 | 2 | 1 | 2 | 2 | 1 | 16.064 | 0.6704508 | 13.41 | 59.56 | 2923.17 | 174102.65 | 17.31 |
| 10 | 4 | 37.6 | 26.43 | 1175 | 1 | 1 | 2 | 1 | 0 | 2 | 1 | 1 | 16.3825 | 0.6837437 | 13.67 | 65.60 | 3022.15 | 198263.80 | 16.10 |
| 11 | 5 | 35.9 | 30.43 | 1090 | 2 | 2 | 1 | 1 | 0 | 1 | 2 | 1 | 16.064 | 0.6704508 | 13.41 | 69.83 | 2333.17 | 162935.62 | 12.96 |
| 12 | 5 | 35.9 | 30.43 | 1090 | 2 | 2 | 2 | 1 | 0 | 1 | 2 | 1 | 16.064 | 0.6704508 | 13.41 | 62.93 | 2681.80 | 168760.50 | 14.23 |
| 13 | 5 | 36.9 | 30.43 | 1090 | 2 | 2 | 1 | 2 | 1 | 1 | 2 | 1 | 16.2475 | 0.6781093 | 13.56 | 101.32 | 3539.73 | 358660.17 | 26.95 |
| 14 | 5 | 36.9 | 30.43 | 1090 | 2 | 2 | 2 | 2 | 1 | 1 | 2 | 1 | 16.2475 | 0.6781093 | 13.56 | 69.84 | 1898.71 | 132605.64 | 18.62 |
| 15 | 5 | 38.9 | 30.43 | 1090 | 2 | 2 | 1 | 2 | 1 | 1 | 2 | 2 | 16.6225 | 0.6937604 | 13.88 | 119.74 | 1637.27 | 196040.05 | 51.87 |
| 16 | 5 | 38.9 | 30.43 | 1090 | 2 | 2 | 2 | 2 | 1 | 1 | 2 | 2 | 16.6225 | 0.6937604 | 13.88 | 94.39 | 1776.03 | 167634.72 | 38.30 |
| 17 | 5 | 40.9 | 30.43 | 1090 | 2 | 2 | 1 | 2 | 2 | 1 | 2 | 2 | 16.9639 | 0.7080092 | 14.16 | 124.92 | 2902.84 | 362613.98 | 61.59 |
| 18 | 5 | 42.9 | 30.43 | 1090 | 2 | 2 | 1 | 2 | 2 | 1 | 1 | 1 | 17.2589 | 0.7203214 | 14.41 | 48.46 | 893.20 | 43288.43 | 17.11 |
| 19 | 5 | 42.9 | 30.43 | 1090 | 2 | 2 | 2 | 2 | 2 | 1 | 1 | 1 | 17.2589 | 0.7203214 | 14.41 | 37.38 | 849.98 | 31774.82 | 11.96 |
| 21 | 6 | 37.6 | 33 | 1135 | 2 | 2 | 1 | 2 | 2 | 1 | 2 | 2 | 16.3825 | 0.6837437 | 13.67 | 200.47 | 6645.99 | 1332348.52 | 167.62 |
| 24 | 6 | 41.6 | 33 | 1135 | 2 | 2 | 1 | 2 | 2 | 1 | 2 | 2 | 17.0701 | 0.7124416 | 14.25 | 139.33 | 6340.73 | 883484.54 | 90.66 |
| 25 | 6 | 41.6 | 33 | 1135 | 2 | 2 | 2 | 2 | 2 | 1 | 2 | 2 | 17.0701 | 0.7124416 | 14.25 | 193.33 | 4673.62 | 903558.29 | 114.73 |

| SN | person ID | PMA | GA | BW | M(1) F(2) | Single (2) multiple (1) | eye R(1) L(2) | diagnosis nROP(1) ROP(2) | stage ROP | Caucasian (1) no(2) | elm y(1) n(2) | fovea(1) dome(2) | axial length | Correction (Corr) | X res Corr | thickness | width | area | SD |
|---|---|---|---|---|---|---|---|---|---|---|---|---|---|---|---|---|---|---|---|
| 26 | 7 | 36.9 | 34 | 2040 | 2 | 1 | 1 | 1 | 0 | 2 | 2 | 1 | 16.2475 | 0.6781093 | 13.56 | 73.77 | 1234.16 | 91040.25 | 32.98 |
| 27 | 7 | 36.9 | 34 | 2040 | 2 | 1 | 2 | 1 | 0 | 2 | 2 | 1 | 16.2475 | 0.6781093 | 13.56 | 53.64 | 1546.09 | 82935.49 | 10.15 |
| 28 | 7 | 38.9 | 34 | 2040 | 2 | 1 | 1 | 1 | 0 | 2 | 1 | 2 | 16.6225 | 0.6937604 | 13.88 | 78.81 | 2955.42 | 232903.70 | 52.78 |
| 29 | 7 | 38.9 | 34 | 2040 | 2 | 1 | 2 | 1 | 0 | 2 | 2 | 1 | 16.6225 | 0.6937604 | 13.88 | 31.89 | 2622.41 | 83617.56 | 10.86 |
| 30 | 8 | 37.4 | 31.57 | 1950 | 1 | 2 | 1 | 1 | 0 | 1 | 2 | 2 | 16.35625 | 0.6826482 | 13.65 | 145.77 | 2457.53 | 358242.83 | 86.18 |
| 31 | 8 | 37.4 | 31.57 | 1950 | 1 | 2 | 2 | 1 | 0 | 1 | 2 | 2 | 16.35625 | 0.6826482 | 13.65 | 132.20 | 3399.59 | 449433.71 | 74.00 |
| 32 | 8 | 39.4 | 31.57 | 1950 | 1 | 2 | 1 | 1 | 0 | 1 | 2 | 2 | 16.73125 | 0.6982992 | 13.97 | 139.57 | 2290.42 | 319664.64 | 73.50 |
| 33 | 8 | 39.4 | 31.57 | 1950 | 1 | 2 | 2 | 1 | 0 | 1 | 1 | 2 | 16.73125 | 0.6982992 | 13.97 | 100.47 | 2765.27 | 277833.72 | 63.83 |
| 34 | 8 | 41.4 | 31.57 | 1950 | 1 | 2 | 1 | 1 | 0 | 1 | 2 | 1 | 17.04945 | 0.7115797 | 14.23 | 59.38 | 1707.79 | 101408.65 | 22.18 |
| 35 | 9 | 39.6 | 30.29 | 1750 | 1 | 2 | 1 | 1 | 0 | 1 | 2 | 1 | 16.7575 | 0.6993948 | 13.99 | 38.71 | 867.25 | 33570.95 | 11.17 |
| 36 | 9 | 39.6 | 30.29 | 1750 | 1 | 2 | 2 | 1 | 0 | 1 | 1 | 1 | 16.7575 | 0.6993948 | 13.99 | 54.77 | 853.26 | 46730.76 | 15.95 |
| 37 | 10 | 38 | 27.57 | 955 | 1 | 1 | 2 | 2 | 1 | 2 | 2 | 1 | 16.463125 | 0.6871087 | 13.74 | 81.01 | 3394.32 | 274964.42 | 15.01 |
| 38 | 10 | 40 | 27.57 | 955 | 1 | 1 | 1 | 2 | 1 | 2 | 2 | 1 | 16.838125 | 0.7027598 | 14.06 | 81.25 | 3654.35 | 296913.21 | 27.52 |
| 39 | 10 | 40 | 27.57 | 955 | 1 | 1 | 2 | 2 | 1 | 2 | 1 | 1 | 16.838125 | 0.7027598 | 14.06 | 99.83 | 3851.12 | 384448.97 | 28.85 |
| 40 | 11 | 35.4 | 28.71 | 1070 | 2 | 2 | 1 | 1 | 0 | 1 | 2 | 2 | 15.99575 | 0.6676023 | 13.35 | 165.56 | 4593.10 | 760425.67 | 86.73 |
| 41 | 11 | 35.4 | 28.71 | 1070 | 2 | 2 | 2 | 1 | 0 | 1 | 2 | 2 | 15.99575 | 0.6676023 | 13.35 | 168.21 | 4179.19 | 702969.15 | 65.37 |
| 42 | 11 | 37.4 | 28.71 | 1070 | 2 | 2 | 1 | 1 | 0 | 1 | 2 | 2 | 16.35625 | 0.6826482 | 13.65 | 149.60 | 5106.21 | 763899.68 | 74.57 |
| 43 | 11 | 37.4 | 28.71 | 1070 | 2 | 2 | 2 | 1 | 0 | 1 | 2 | 2 | 16.35625 | 0.6826482 | 13.65 | 158.94 | 3549.77 | 564184.13 | 80.68 |
| 44 | 12 | 34.7 | 30.85 | 1100 | 1 | 1 | 1 | 1 | 0 | 1 | 2 | 2 | 15.87875 | 0.6627191 | 13.25 | 82.32 | 4175.13 | 343712.64 | 51.62 |
| 45 | 12 | 34.7 | 30.85 | 1100 | 1 | 1 | 2 | 1 | 0 | 1 | 2 | 2 | 15.87875 | 0.6627191 | 13.25 | 115.29 | 3830.52 | 441625.41 | 59.85 |
| 46 | 13 | 39.3 | 34.57 | 1380 | 1 | 2 | 2 | 1 | 0 | 1 | 1 | 1 | 16.705 | 0.6972037 | 13.94 | 68.45 | 3444.19 | 235766.39 | 27.29 |
| 47 | 14 | 35.7 | 26.43 | 745 | 1 | 2 | 1 | 2 | 2 | 2 | 2 | 1 | 16.04125 | 0.6695013 | 13.39 | 59.57 | 1941.55 | 115657.68 | 15.99 |
| 48 | 14 | 35.7 | 26.43 | 745 | 1 | 2 | 2 | 2 | 2 | 2 | 2 | 1 | 16.04125 | 0.6695013 | 13.39 | 35.24 | 1566.63 | 55209.75 | 9.38 |

| SN | person ID | PMA | GA | BW | M(1) F(2) | Single (2) multiple (1) | eye R(1) L(2) | diagnosis nROP(1) ROP(2) | stage ROP | Caucasian (1) no(2) | elm y(1) n(2) | fovea(1) dome(2) | axial length | Correction (Corr) | X res Corr | thickness | width | area | SD |
|---|---|---|---|---|---|---|---|---|---|---|---|---|---|---|---|---|---|---|---|
| 49 | 15 | 32.3 | 29.29 | 1490 | 1 | 2 | 1 | 1 | 0 | 1 | 2 | 2 | 15.4855 | 0.6463063 | 12.93 | 94.51 | 3877.84 | 366502.23 | 42.91 |
| 50 | 15 | 32.3 | 29.29 | 1490 | 1 | 2 | 2 | 1 | 0 | 1 | 2 | 2 | 15.4855 | 0.6463063 | 12.93 | 107.28 | 3322.01 | 356388.83 | 53.67 |
| 51 | 16 | 34.9 | 30.85 | 1080 | 1 | 1 | 1 | 2 | 1 | 1 | 2 | 2 | 15.851125 | 0.6615662 | 13.23 | 69.14 | 3215.21 | 222286.23 | 29.26 |
| 52 | 16 | 34.9 | 30.85 | 1080 | 1 | 1 | 2 | 1 | 0 | 1 | 2 | 1 | 15.9015 | 0.6636686 | 13.27 | 74.61 | 3411.26 | 254530.19 | 23.89 |
| 53 | 16 | 35.9 | 30.85 | 1080 | 1 | 1 | 2 | 1 | 0 | 1 | 2 | 1 | 16.064 | 0.6704508 | 13.41 | 82.40 | 2534.30 | 208826.64 | 30.45 |
| 54 | 17 | 42 | 29 | 1380 | 1 | 1 | 1 | 1 | 0 | 1 | 1 | 1 | 17.133525 | 0.7150887 | 14.30 | 62.40 | 243.13 | 15171.32 | 21.87 |
| 55 | 18 | 37.6 | 27.43 | 1070 | 2 | 2 | 1 | 1 | 0 | 2 | 2 | 1 | 16.3825 | 0.6837437 | 13.67 | 38.83 | 1764.06 | 68494.71 | 14.64 |
| 56 | 19 | 34.7 | 29.29 | 1090 | 1 | 2 | 1 | 1 | 0 | 1 | 1 | 1 | 15.87875 | 0.6627191 | 13.25 | 69.90 | 2120.70 | 148237.01 | 11.55 |
| 57 | 19 | 36.7 | 29.29 | 1090 | 1 | 2 | 1 | 1 | 0 | 1 | 1 | 1 | 16.22125 | 0.6770138 | 13.54 | 72.54 | 3141.34 | 227866.59 | 18.26 |
| 58 | 19 | 37.7 | 29.29 | 1090 | 1 | 2 | 2 | 1 | 0 | 1 | 2 | 1 | 16.40875 | 0.6848393 | 13.70 | 56.93 | 1027.26 | 58479.80 | 19.17 |
| 59 | 20 | 33.3 | 29.71 | 1485 | 2 | 2 | 2 | 1 | 0 | 1 | 2 | 2 | 15.648 | 0.6530885 | 13.06 | 99.20 | 3226.26 | 320034.25 | 41.45 |
| 60 | 20 | 35.3 | 29.71 | 1485 | 2 | 2 | 1 | 1 | 0 | 1 | 2 | 2 | 15.973 | 0.6666528 | 13.33 | 121.97 | 3786.59 | 461846.36 | 67.32 |
| 61 | 20 | 35.3 | 29.71 | 1485 | 2 | 2 | 2 | 1 | 0 | 1 | 2 | 2 | 15.973 | 0.6666528 | 13.33 | 122.12 | 4519.91 | 551988.48 | 81.19 |
| 62 | 21 | 38.4 | 24.17 | 730 | 2 | 2 | 2 | 2 | 2 | 2 | 1 | 1 | 16.54375 | 0.6904737 | 13.81 | 86.74 | 5081.89 | 440798.41 | 19.41 |
| 63 | 21 | 42.4 | 24.17 | 730 | 2 | 2 | 1 | 2 | 3 | 2 | 2 | 2 | 17.19695 | 0.7177358 | 14.35 | 118.79 | 4478.67 | 532031.72 | 64.66 |
| 64 | 22 | 34.7 | 26.14 | 860 | 1 | 1 | 2 | 2 | 2 | 2 | 1 | 1 | 15.87875 | 0.6627191 | 13.25 | 58.21 | 2186.97 | 127305.69 | 10.30 |
| 65 | 23 | 39.3 | 31.71 | 2240 | 2 | 1 | 1 | 1 | 0 | 2 | 2 | 2 | 16.705 | 0.6972037 | 13.94 | 176.08 | 5229.03 | 920743.90 | 143.17 |
| 66 | 23 | 39.3 | 31.71 | 2240 | 2 | 1 | 2 | 1 | 0 | 2 | 2 | 2 | 16.705 | 0.6972037 | 13.94 | 174.64 | 5619.46 | 981383.89 | 133.57 |
| 67 | 23 | 41.3 | 31.71 | 2240 | 2 | 1 | 2 | 1 | 0 | 2 | 2 | 2 | 17.0288 | 0.7107179 | 14.21 | 165.09 | 4349.59 | 718075.21 | 119.01 |
| 68 | 24 | 33.4 | 32.85 | 1940 | 1 | 2 | 1 | 1 | 0 | 1 | 2 | 1 | 15.67075 | 0.654038 | 13.08 | 71.10 | 2642.31 | 187860.64 | 23.75 |
| 69 | 25 | 41.3 | 29 | 1095 | 2 | 2 | 1 | 1 | 0 | 2 | 2 | 2 | 17.0288 | 0.7107179 | 14.21 | 101.01 | 995.01 | 100501.19 | 34.19 |
| 70 | 25 | 41.3 | 29 | 1095 | 2 | 2 | 2 | 1 | 0 | 2 | 1 | 2 | 17.0288 | 0.7107179 | 14.21 | 89.53 | 1961.58 | 175621.23 | 48.64 |

**Appendix 4** Supplementary Data Foveal Oedema.

| SN | person ID | PMA | GA | BW | M(1) F(2) | Single (2) multiple (1) | eye R(1) L(2) | diagnosis nROP(1) ROP(2) | stage ROP | Caucasian (1) no(2) | elm y(1) n(2) | fovea (1) dome (2) | axial length | **Correction (Corr)** | X res Corr | thickness | width | area | SD |
|---|---|---|---|---|---|---|---|---|---|---|---|---|---|---|---|---|---|---|---|
| 1 | 1 | 37.3 | 27.14 | 640 | 2 | 1 | 1 | 2 | 1 | 2 | 1 | 1 | 16.33 | 0.6815526 | 13.63 | 61.29 | 1090.48 | 66835.77 | 18.95 |
| 2 | 1 | 37.3 | 27.14 | 640 | 2 | 1 | 2 | 2 | 1 | 2 | 1 | 1 | 16.33 | 0.6815526 | 13.63 | 72.36 | 1172.27 | 84828.76 | 20.21 |
| 3 | 2 | 37.1 | 31.71 | 2050 | 1 | 1 | 1 | 1 | 0 | 1 | 1 | 2 | 16.301875 | 0.6803788 | 13.61 | 137.69 | 3619.61 | 498396.49 | 80.53 |
| 4 | 2 | 39.1 | 31.71 | 2050 | 1 | 1 | 1 | 1 | 0 | 1 | 2 | 2 | 16.676875 | 0.6960298 | 13.92 | 136.34 | 4287.54 | 584564.84 | 72.21 |
| 5 | 2 | 39.1 | 31.71 | 2050 | 1 | 1 | 2 | 1 | 0 | 1 | 2 | 2 | 16.676875 | 0.6960298 | 13.92 | 156.94 | 3006.85 | 471908.23 | 77.12 |
| 6 | 2 | 41.1 | 31.71 | 2050 | 1 | 1 | 1 | 1 | 0 | 1 | 2 | 2 | 17.006675 | 0.7097944 | 14.20 | 86.08 | 1689.31 | 145411.33 | 35.88 |
| 7 | 2 | 41.1 | 31.71 | 2050 | 1 | 1 | 2 | 1 | 0 | 1 | 2 | 2 | 17.006675 | 0.7097944 | 14.20 | 102.55 | 2768.20 | 283872.35 | 41.34 |
| 8 | 3 | 35.9 | 33.14 | 1380 | 2 | 2 | 2 | 2 | 1 | 2 | 2 | 1 | 16.064 | 0.6704508 | 13.41 | 59.56 | 2923.17 | 174102.65 | 17.31 |
| 10 | 4 | 37.6 | 26.43 | 1175 | 1 | 1 | 2 | 1 | 0 | 2 | 1 | 1 | 16.3825 | 0.6837437 | 13.67 | 65.60 | 3022.15 | 198263.80 | 16.10 |
| 11 | 5 | 35.9 | 30.43 | 1090 | 2 | 2 | 1 | 1 | 0 | 1 | 2 | 1 | 16.064 | 0.6704508 | 13.41 | 69.83 | 2333.17 | 162935.62 | 12.96 |
| 12 | 5 | 35.9 | 30.43 | 1090 | 2 | 2 | 2 | 1 | 0 | 1 | 2 | 1 | 16.064 | 0.6704508 | 13.41 | 62.93 | 2681.80 | 168760.50 | 14.23 |
| 13 | 5 | 36.9 | 30.43 | 1090 | 2 | 2 | 1 | 2 | 1 | 1 | 2 | 1 | 16.2475 | 0.6781093 | 13.56 | 101.32 | 3539.73 | 358660.17 | 26.95 |
| 14 | 5 | 36.9 | 30.43 | 1090 | 2 | 2 | 2 | 2 | 1 | 1 | 2 | 1 | 16.2475 | 0.6781093 | 13.56 | 69.84 | 1898.71 | 132605.64 | 18.62 |
| 15 | 5 | 38.9 | 30.43 | 1090 | 2 | 2 | 1 | 2 | 1 | 1 | 2 | 2 | 16.6225 | 0.6937604 | 13.88 | 119.74 | 1637.27 | 196040.05 | 51.87 |
| 16 | 5 | 38.9 | 30.43 | 1090 | 2 | 2 | 2 | 2 | 1 | 1 | 2 | 2 | 16.6225 | 0.6937604 | 13.88 | 94.39 | 1776.03 | 167634.72 | 38.30 |
| 17 | 5 | 40.9 | 30.43 | 1090 | 2 | 2 | 1 | 2 | 2 | 1 | 2 | 2 | 16.9639 | 0.7080092 | 14.16 | 124.92 | 2902.84 | 362613.98 | 61.59 |
| 18 | 5 | 42.9 | 30.43 | 1090 | 2 | 2 | 1 | 2 | 2 | 1 | 1 | 1 | 17.2589 | 0.7203214 | 14.41 | 48.46 | 893.20 | 43288.43 | 17.11 |
| 19 | 5 | 42.9 | 30.43 | 1090 | 2 | 2 | 2 | 2 | 2 | 1 | 1 | 1 | 17.2589 | 0.7203214 | 14.41 | 37.38 | 849.98 | 31774.82 | 11.96 |
| 21 | 6 | 37.6 | 33 | 1135 | 2 | 2 | 1 | 2 | 2 | 1 | 2 | 2 | 16.3825 | 0.6837437 | 13.67 | 200.47 | 6645.99 | 1332348.52 | 167.62 |
| 24 | 6 | 41.6 | 33 | 1135 | 2 | 2 | 1 | 2 | 2 | 1 | 2 | 2 | 17.0701 | 0.7124416 | 14.25 | 139.33 | 6340.73 | 883484.54 | 90.66 |
| 25 | 6 | 41.6 | 33 | 1135 | 2 | 2 | 2 | 2 | 2 | 1 | 2 | 2 | 17.0701 | 0.7124416 | 14.25 | 193.33 | 4673.62 | 903558.29 | 114.73 |

| SN | person ID | PMA | GA | BW | M(1) F(2) | Single (2) multiple (1) | eye R(1) L(2) | diagnosis nROP(1) ROP(2) | stage ROP | Caucasian (1) no(2) | elm y(1) n(2) | fovea (1) dome (2) | axial length | **Correction (Corr)** | X res Corr | thickness | width | area | SD |
|---|---|---|---|---|---|---|---|---|---|---|---|---|---|---|---|---|---|---|---|
| 26 | 7 | 36.9 | 34 | 2040 | 2 | 1 | 1 | 1 | 0 | 2 | 2 | 1 | 16.2475 | 0.6781093 | 13.56 | 73.77 | 1234.16 | 91040.25 | 32.98 |
| 27 | 7 | 36.9 | 34 | 2040 | 2 | 1 | 2 | 1 | 0 | 2 | 2 | 1 | 16.2475 | 0.6781093 | 13.56 | 53.64 | 1546.09 | 82935.49 | 10.15 |
| 28 | 7 | 38.9 | 34 | 2040 | 2 | 1 | 1 | 1 | 0 | 2 | 1 | 2 | 16.6225 | 0.6937604 | 13.88 | 78.81 | 2955.42 | 232903.70 | 52.78 |
| 29 | 7 | 38.9 | 34 | 2040 | 2 | 1 | 2 | 1 | 0 | 2 | 2 | 1 | 16.6225 | 0.6937604 | 13.88 | 31.89 | 2622.41 | 83617.56 | 10.86 |
| 30 | 8 | 37.4 | 31.57 | 1950 | 1 | 2 | 1 | 1 | 0 | 1 | 2 | 2 | 16.35625 | 0.6826482 | 13.65 | 145.77 | 2457.53 | 358242.83 | 86.18 |
| 31 | 8 | 37.4 | 31.57 | 1950 | 1 | 2 | 2 | 1 | 0 | 1 | 2 | 2 | 16.35625 | 0.6826482 | 13.65 | 132.20 | 3399.59 | 449433.71 | 74.00 |
| 32 | 8 | 39.4 | 31.57 | 1950 | 1 | 2 | 1 | 1 | 0 | 1 | 2 | 2 | 16.73125 | 0.6982992 | 13.97 | 139.57 | 2290.42 | 319664.64 | 73.50 |
| 33 | 8 | 39.4 | 31.57 | 1950 | 1 | 2 | 2 | 1 | 0 | 1 | 1 | 2 | 16.73125 | 0.6982992 | 13.97 | 100.47 | 2765.27 | 277833.72 | 63.83 |
| 34 | 8 | 41.4 | 31.57 | 1950 | 1 | 2 | 1 | 1 | 0 | 1 | 2 | 1 | 17.04945 | 0.7115797 | 14.23 | 59.38 | 1707.79 | 101408.65 | 22.18 |
| 35 | 9 | 39.6 | 30.29 | 1750 | 1 | 2 | 1 | 1 | 0 | 1 | 2 | 1 | 16.7575 | 0.6993948 | 13.99 | 38.71 | 867.25 | 33570.95 | 11.17 |
| 36 | 9 | 39.6 | 30.29 | 1750 | 1 | 2 | 2 | 1 | 0 | 1 | 1 | 1 | 16.7575 | 0.6993948 | 13.99 | 54.77 | 853.26 | 46730.76 | 15.95 |
| 37 | 10 | 38 | 27.57 | 955 | 1 | 1 | 2 | 2 | 1 | 2 | 2 | 1 | 16.463125 | 0.6871087 | 13.74 | 81.01 | 3394.32 | 274964.42 | 15.01 |
| 38 | 10 | 40 | 27.57 | 955 | 1 | 1 | 1 | 2 | 1 | 2 | 2 | 1 | 16.838125 | 0.7027598 | 14.06 | 81.25 | 3654.35 | 296913.21 | 27.52 |
| 39 | 10 | 40 | 27.57 | 955 | 1 | 1 | 2 | 2 | 1 | 2 | 1 | 1 | 16.838125 | 0.7027598 | 14.06 | 99.83 | 3851.12 | 384448.97 | 28.85 |
| 40 | 11 | 35.4 | 28.71 | 1070 | 2 | 2 | 1 | 1 | 0 | 1 | 2 | 2 | 15.99575 | 0.6676023 | 13.35 | 165.56 | 4593.10 | 760425.67 | 86.73 |
| 41 | 11 | 35.4 | 28.71 | 1070 | 2 | 2 | 2 | 1 | 0 | 1 | 2 | 2 | 15.99575 | 0.6676023 | 13.35 | 168.21 | 4179.19 | 702969.15 | 65.37 |
| 42 | 11 | 37.4 | 28.71 | 1070 | 2 | 2 | 1 | 1 | 0 | 1 | 2 | 2 | 16.35625 | 0.6826482 | 13.65 | 149.60 | 5106.21 | 763899.68 | 74.57 |
| 43 | 11 | 37.4 | 28.71 | 1070 | 2 | 2 | 2 | 1 | 0 | 1 | 2 | 2 | 16.35625 | 0.6826482 | 13.65 | 158.94 | 3549.77 | 564184.13 | 80.68 |
| 44 | 12 | 34.7 | 30.85 | 1100 | 1 | 1 | 1 | 1 | 0 | 1 | 2 | 2 | 15.87875 | 0.6627191 | 13.25 | 82.32 | 4175.13 | 343712.64 | 51.62 |
| 45 | 12 | 34.7 | 30.85 | 1100 | 1 | 1 | 2 | 1 | 0 | 1 | 2 | 2 | 15.87875 | 0.6627191 | 13.25 | 115.29 | 3830.52 | 441625.41 | 59.85 |
| 46 | 13 | 39.3 | 34.57 | 1380 | 1 | 2 | 2 | 1 | 0 | 1 | 1 | 1 | 16.705 | 0.6972037 | 13.94 | 68.45 | 3444.19 | 235766.39 | 27.29 |
| 47 | 14 | 35.7 | 26.43 | 745 | 1 | 2 | 1 | 2 | 2 | 2 | 2 | 1 | 16.04125 | 0.6695013 | 13.39 | 59.57 | 1941.55 | 115657.68 | 15.99 |

| SN | person ID | PMA | GA | BW | M(1) F(2) | Single (2) multiple (1) | eye R(1) L(2) | diagnosis nROP(1) ROP(2) | stage ROP | Caucasian (1) no(2) | elm y(1) n(2) | fovea (1) dome (2) | axial length | **Correction (Corr)** | X res Corr | thickness | width | area | SD |
|---|---|---|---|---|---|---|---|---|---|---|---|---|---|---|---|---|---|---|---|
| 48 | 14 | 35.7 | 26.43 | 745 | 1 | 2 | 2 | 2 | 2 | 2 | 2 | 1 | 16.04125 | 0.6695013 | 13.39 | 35.24 | 1566.63 | 55209.75 | 9.38 |
| 49 | 15 | 32.3 | 29.29 | 1490 | 1 | 2 | 1 | 1 | 0 | 1 | 2 | 2 | 15.4855 | 0.6463063 | 12.93 | 94.51 | 3877.84 | 366502.23 | 42.91 |
| 50 | 15 | 32.3 | 29.29 | 1490 | 1 | 2 | 2 | 1 | 0 | 1 | 2 | 2 | 15.4855 | 0.6463063 | 12.93 | 107.28 | 3322.01 | 356388.83 | 53.67 |
| 51 | 16 | 34.9 | 30.85 | 1080 | 1 | 1 | 1 | 2 | 1 | 1 | 2 | 2 | 15.851125 | 0.6615662 | 13.23 | 69.14 | 3215.21 | 222286.23 | 29.26 |
| 52 | 16 | 34.9 | 30.85 | 1080 | 1 | 1 | 2 | 1 | 0 | 1 | 2 | 1 | 15.9015 | 0.6636686 | 13.27 | 74.61 | 3411.26 | 254530.19 | 23.89 |
| 53 | 16 | 35.9 | 30.85 | 1080 | 1 | 1 | 2 | 1 | 0 | 1 | 2 | 1 | 16.064 | 0.6704508 | 13.41 | 82.40 | 2534.30 | 208826.64 | 30.45 |
| 54 | 17 | 42 | 29 | 1380 | 1 | 1 | 1 | 1 | 0 | 1 | 1 | 1 | 17.133525 | 0.7150887 | 14.30 | 62.40 | 243.13 | 15171.32 | 21.87 |
| 55 | 18 | 37.6 | 27.43 | 1070 | 2 | 2 | 1 | 1 | 0 | 2 | 2 | 1 | 16.3825 | 0.6837437 | 13.67 | 38.83 | 1764.06 | 68494.71 | 14.64 |
| 56 | 19 | 34.7 | 29.29 | 1090 | 1 | 2 | 1 | 1 | 0 | 1 | 1 | 1 | 15.87875 | 0.6627191 | 13.25 | 69.90 | 2120.70 | 148237.01 | 11.55 |
| 57 | 19 | 36.7 | 29.29 | 1090 | 1 | 2 | 1 | 1 | 0 | 1 | 1 | 1 | 16.22125 | 0.6770138 | 13.54 | 72.54 | 3141.34 | 227866.59 | 18.26 |
| 58 | 19 | 37.7 | 29.29 | 1090 | 1 | 2 | 2 | 1 | 0 | 1 | 2 | 1 | 16.40875 | 0.6848393 | 13.70 | 56.93 | 1027.26 | 58479.80 | 19.17 |
| 59 | 20 | 33.3 | 29.71 | 1485 | 2 | 2 | 2 | 1 | 0 | 1 | 2 | 2 | 15.648 | 0.6530885 | 13.06 | 99.20 | 3226.26 | 320034.25 | 41.45 |
| 60 | 20 | 35.3 | 29.71 | 1485 | 2 | 2 | 1 | 1 | 0 | 1 | 2 | 2 | 15.973 | 0.6666528 | 13.33 | 121.97 | 3786.59 | 461846.36 | 67.32 |
| 61 | 20 | 35.3 | 29.71 | 1485 | 2 | 2 | 2 | 1 | 0 | 1 | 2 | 2 | 15.973 | 0.6666528 | 13.33 | 122.12 | 4519.91 | 551988.48 | 81.19 |
| 62 | 21 | 38.4 | 24.17 | 730 | 2 | 2 | 2 | 2 | 2 | 2 | 1 | 1 | 16.54375 | 0.6904737 | 13.81 | 86.74 | 5081.89 | 440798.41 | 19.41 |
| 63 | 21 | 42.4 | 24.17 | 730 | 2 | 2 | 1 | 2 | 3 | 2 | 2 | 2 | 17.19695 | 0.7177358 | 14.35 | 118.79 | 4478.67 | 532031.72 | 64.66 |
| 64 | 22 | 34.7 | 26.14 | 860 | 1 | 1 | 2 | 2 | 2 | 2 | 1 | 1 | 15.87875 | 0.6627191 | 13.25 | 58.21 | 2186.97 | 127305.69 | 10.30 |
| 65 | 23 | 39.3 | 31.71 | 2240 | 2 | 1 | 1 | 1 | 0 | 2 | 2 | 2 | 16.705 | 0.6972037 | 13.94 | 176.08 | 5229.03 | 920743.90 | 143.17 |
| 66 | 23 | 39.3 | 31.71 | 2240 | 2 | 1 | 2 | 1 | 0 | 2 | 2 | 2 | 16.705 | 0.6972037 | 13.94 | 174.64 | 5619.46 | 981383.89 | 133.57 |
| 67 | 23 | 41.3 | 31.71 | 2240 | 2 | 1 | 2 | 1 | 0 | 2 | 2 | 2 | 17.0288 | 0.7107179 | 14.21 | 165.09 | 4349.59 | 718075.21 | 119.01 |
| 68 | 24 | 33.4 | 32.85 | 1940 | 1 | 2 | 1 | 1 | 0 | 1 | 2 | 1 | 15.67075 | 0.654038 | 13.08 | 71.10 | 2642.31 | 187860.64 | 23.75 |
| 69 | 25 | 41.3 | 29 | 1095 | 2 | 2 | 1 | 1 | 0 | 2 | 2 | 2 | 17.0288 | 0.7107179 | 14.21 | 101.01 | 995.01 | 100501.19 | 34.19 |

| SN | person ID | PMA | GA | BW | M(1) F(2) | Single (2) multiple (1) | eye R(1) L(2) | diagnosis nROP(1) ROP(2) | stage ROP | Caucasian (1) no(2) | elm y(1) n(2) | fovea (1) dome (2) | axial length | **Correction (Corr)** | X res Corr | thickness | width | area | SD |
|---|---|---|---|---|---|---|---|---|---|---|---|---|---|---|---|---|---|---|---|
| 70 | 25 | 41.3 | 29 | 1095 | 2 | 2 | 2 | 1 | 0 | 2 | 1 | 2 | 17.0288 | 0.7107179 | 14.21 | 89.53 | 1961.58 | 175621.23 | 48.64 |

# Bibliography


Akerblom, H., G. Holmstrom, U. Eriksson, and E. Larsson. 2012. 'Retinal nerve fibre layer thickness in school-aged prematurely-born children compared to children born at term', *Br J Ophthalmol*, 96: 956-60.

Akerblom, H., E. Larsson, U. Eriksson, and G. Holmstrom. 2011. 'Central macular thickness is correlated with gestational age at birth in prematurely born children', *Br J Ophthalmol*, 95: 799-803.

Alabduljalil, T., CA. Westall, A. Reginald, S. Farsui, S. J. Chui, A. Arshavsky, C A. Toth, and W-C. Lam. 2018. 'Demonstration of anatomical development of the human macula within the first 5 years of life using handheld OCT.', *Int Ophthalmol*, June: 1-10.

Anwar, S., S. Mohammad, B. Elahi, and I. Gottlob. 2011. "Optic nerve hypoplasia in association with foveal hypoplasia." In *ARVO*. Fort Lauderdale, Florida USA: Invest Ophthalmol Vis Sci. .

Aralikatti, AK., A. Mitra, AK. Dennistoun, MS. Haque, Ewer AK., and L. Butler. 2010. 'Is ethnicity a risk factor for severe retinopathy of prematurity?', *Arch Dis Child Fetal Neonatal Ed*, 95: F174-F76.

Bach, L., and R. Seefelder. 1914. *Atlas zur Entwicklungsgeschichte Des Manschlichen Auges.* (W Engelmann.: Leipzig).

Bagci, A. M., M. Shahidi, R. Ansari, M. Blair, N. P. Blair, and R. Zelkha. 2008. 'Thickness profiles of retinal layers by optical coherence tomography image segmentation', *Am J Ophthalmol*, 146: 679-87.

Bai, Y., J. X. Ma, J. Guo, J. Wang, M. Zhu, Y. Chen, and Y. Z. Le. 2009. 'Muller cell-derived VEGF is a significant contributor to retinal neovascularization', *J Pathol*, 219: 446-54.

Balasubramanian, S., J. Beckmann, H. Mehta, S. R. Sadda, K. Chanwimol, M. Nassisi, I. Tsui, N. Marlow, and S. Jain. 2018. 'Relationship between Retinal Thickness Profiles and Visual Outcomes in Young Adults Born Extremely Preterm: The EPICure@19 Study', *Ophthalmology*, article in press: 1-6.

Barber, AN. 1955. *Embryology of the Human Eye.* (The CV Mosby Company: St Louis.).

Barishak, YR. 2001. *Embryology of the Eye and Its Adnexa.* (Karger: Basel, Switzerland.).

Basu, M. 2002. 'Gaussian-based edge-detection methods-a survey', *IEEE Transactions on Systems, Man and Cybernetics, Part C (Applications and Reviews)*, 32: 252-60.

Becker, S., H. Wang, A. B. Simmons, T. Suwanmanee, G. J. Stoddard, T. Kafri, and M. E. Hartnett. 2018. 'Targeted Knockdown of Overexpressed VEGFA or VEGF164 in Muller cells maintains retinal function by triggering different signaling mechanisms', *Sci Rep*, 8: 2003.

Benouaich, X., L. Mahieu, F. Matonti, and V. Soler. 2017. 'Persistence of foveal capillary plexi in a case of foveal plana evident on OCT angiography.', *J Fr Ophtalmol.*, 40: 4-7.

Bidaut-Garnier, M., C. Schwartz, M. Puyraveau, M. Montard, B. Delbosc, and M. Saleh. 2014. 'Choroidal thickness measurement in children using optical coherence tomography.', *Retina*, 34: 768-74.

Binenbaum G, Ying G. S, Quinn G, Huang JH, Dreiseitl S, Antigua J, Foroughi N, and Abbasi S. 2012. 'The CHOP Postnatal Weight Gain, Birth Weight, and

Gestational Age Retinopathy of Prematurity Risk Model.', *Arch Ophthalmol*, 130: 1560-65.

Binenbaum, G., G. S. Ying, G. E. Quinn, S. Dreiseitl, K. Karp, R. S. Roberts, H. Kirpalani, and Group Premature Infants in Need of Transfusion Study. 2011. 'A clinical prediction model to stratify retinopathy of prematurity risk using postnatal weight gain', *Pediatrics*, 127: e607-14.

Bird, A. C., and D. Bok. 2018. 'Why the macula?', *Eye (Lond)*, 32: 858-62.

Biten, H., T. K. Redd, C. Moleta, J. P. Campbell, S. Ostmo, K. Jonas, R. V. P. Chan, M. F. Chiang, Imaging, and Consortium Informatics in Retinopathy of Prematurity Research. 2018. 'Diagnostic Accuracy of Ophthalmoscopy vs Telemedicine in Examinations for Retinopathy of Prematurity', *JAMA Ophthalmol*, 136: 498-504.

Blencowe, H., J. E. Lawn, T. Vazquez, A. Fielder, and C. Gilbert. 2013. 'Preterm-associated visual impairment and estimates of retinopathy of prematurity at regional and global levels for 2010', *Pediatr Res*, 74 Suppl 1: 35-49.

Blencowe, Hannah, Simon Cousens, Mikkel Z. Oestergaard, Doris Chou, Ann-Beth Moller, Rajesh Narwal, Alma Adler, Claudia Vera Garcia, Sarah Rohde, Lale Say, and Joy E. Lawn. 2012. 'National, regional, and worldwide estimates of preterm birth rates in the year 2010 with time trends since 1990 for selected countries: a systematic analysis and implications', *The Lancet*, 379: 2162-72.

Blondel, B., M.D. Kogan, G.R. Alexander, N. Dattani, M.S. Kramer, A. Macfarlane, and S.W. Wen. 2002. 'The impact of increasing number of multiple births on the rates of preterm birth and low birthweight: An international study.', *Am J Public Health*, 92: 1323-30.

Bondalapati, S., RW. Milam Jr, N. Ulrich, and M. T. Cabrera. 2015. 'The characteristics and short-term refractive error outcomes of cystoid macular edema in premature neonates as detected by spectral-domain optical coherence tomography.', *Ophthalmic Surg Lasers Imaging Retina*, 46: 806-12.

Bowl, W., K. Stieger, M. Bokun, S. Schweinfurth, K. Holve, M. Andrassi-Darida, and B. Lorenz. 2016. 'OCT-Based Macular Structure-Function Correlation in Dependence on Birth Weight and Gestational Age-the Giessen Long-Term ROP Study', *Invest Ophthalmol Vis Sci*, 57: OCT235-41.

Bringmann, A., A. Reichenbach, and P. Wiedemann. 2004. 'Pathomechanisms of Cystoid Macular Edema', *Ophthalmic Res*, 36: 241-49.

Bunt-Milam, AH., JC. Saari, IB Klock, and GG. Garwin. 1985. 'Zonulae Adherentes Pore Size in the External Limiting Membrane of the Rabbit Retina.', *Invest Ophthalmol Vis Sci*, 26: 1377-80.

Büssow, H. 1980. 'The Astrocytes in the Retina and Optic Nerve Head of Mammals: A Special Glia for the Ganglion Cell Axons.', *Cell Tissue Res.*, 206: 367-78.

Cabrera, M. T., R. S. Maldonado, C. A. Toth, R. V. O'Connell, B. B. Chen, S. J. Chiu, S. Farsiu, D. K. Wallace, S. S. Stinnett, G. M. Panayotti, G. K. Swamy, and S. F. Freedman. 2012. 'Subfoveal fluid in healthy full-term newborns observed by handheld spectral-domain optical coherence tomography', *Am J Ophthalmol*, 153: 167-75 e3.

Cabrera, M. T., O'Connell R V, C A. Toth, RS. Maldonado, Tran-Viet D, MJ. Allingham, S. J. Chui, Farsiu S, G. M. Panayotti, G. K. Swamy, and S. Freedman. 2013. 'Macular findings in healthy full-term Hispanic newborns observed by hand-held

spectral-domainoptical coherence tomography.', *Ophthalmic Surg Lasers Imaging Retina*, 44: 448-54.

Campbell, J. P., E. Nudleman, J. Yang, O. Tan, R. V. P. Chan, M. F. Chiang, D. Huang, and G. Liu. 2017. 'Handheld Optical Coherence Tomography Angiography and Ultra-Wide-Field Optical Coherence Tomography in Retinopathy of Prematurity', *JAMA Ophthalmol*, 135: 977-81.

Chavala, S. H., S. Farsiu, R. Maldonado, D. K. Wallace, S. F. Freedman, and C. A. Toth. 2009. 'Insights into advanced retinopathy of prematurity using handheld spectral domain optical coherence tomography imaging', *Ophthalmology*, 116: 2448-56.

Chen, T. C., B. Cense, J. W. Miller, P. A. Rubin, D. G. Deschler, E. S. Gragoudas, and J. F. de Boer. 2006. 'Histologic correlation of in vivo optical coherence tomography images of the human retina', *Am J Ophthalmol*, 141: 1165-8.

Chen, X., S. Mangalesh, D. Tran-Viet, S. F. Freedman, L. Vajzovic, and C. A. Toth. 2018. 'Fluorescein Angiographic Characteristics of Macular Edema During Infancy', *JAMA Ophthalmol*, 136: 538-42.

Chiang, M. F., L. Jiang, R. Gelman, YE. Du, and JT. Flynn. 2007. 'Interexpert agreement of Plus Disease diagnosis in Retinopathy of Prematurity.', *Arch Ophthalmol*, 125: 875-80.

Chui, T. Y., Z. Zhong, H. Song, and S. A. Burns. 2012. 'Foveal avascular zone and its relationship to foveal pit shape', *Optom Vis Sci*, 89: 602-10.

City Council, Leicester 2012. "Diversity and Migration." In.

Council, Leicester City. 2011. 'Population comparison between England & Leicester Census 2011'. https://www.leicester.gov.uk/media/177362/comparison-of-2011-census-findings.pdf.

Curcio, C. A., and K. A. Allen. 1990. 'Topography of Ganglion Cells in Human Retina.', *J Comp. Neurol.*, 300: 5-25.

Curcio, C. A., K. R. Sloan Jr, O. Packer, A. E. Hendrickson, and R.E. Kalina. 1987. 'Distribution of cones in human and monkey retina: individual variability and radial asymmetry.', *Science.*, 236: 579-82.

Danesh-Meyer, H. V., S. C. Carroll, R. Foroozan, P. J. Savino, J. Fan, Y. Jiang, and S. Vander Hoorn. 2006. 'Relationship between retinal nerve fiber layer and visual field sensitivity as measured by optical coherence tomography in chiasmal compression', *Invest Ophthalmol Vis Sci*, 47: 4827-35.

Daruich, A., A. Matet, A. Moulin, L. Kowalczuk, M. Nicolas, A. Sellam, P. R. Rothschild, S. Omri, E. Gelize, L. Jonet, K. Delaunay, Y. De Kozak, M. Berdugo, M. Zhao, P. Crisanti, and F. Behar-Cohen. 2018. 'Mechanisms of macular edema: Beyond the surface', *Prog Retin Eye Res*, 63: 20-68.

Diaz-Araya, C., and JM. Provis. 1992. 'Evidence of photoreceptor migration during early foveal development: A qualitative analysis of human fetal retinae.', *Vis Neurosci*, 8.

do Lago, A., L. Matieli, M. Gomes, N. T. Baba, M. E. Farah, R. Belfort Jnr, and N. S. Bueno de Moraes. 2007. 'Stratus optical coherence tomography findings in patients with retinopathy of prematurity.', *Arq Bras Oftalmol.*, 70: 19-21.

Dolz-Marco, R., N. Phasukkijwatana, D. Sarraf, and K. B. Freund. 2016. 'Optical Coherence Tomography Angiography in Fovea Plana', *Ophthalmic Surg Lasers Imaging Retina*, 47: 670-3.

Domanico, D., F. Verboschi, S. Altimari, L. Zompatori, and EM. Vingolo. 2015. 'Ocular Effects of Niacin: A review of the Literature.', *Med Hypothesis Discov Innov Ophthamol.*, 4: 64-71.

Dowdeswell, H. J., A. M. Slater, J. Broomhall, and J. Tripp. 1995. 'Visual deficits in children born at less than 32 weeks' gestation with and without major ocular pathology and cerebral damage.', *Br. J. Ophthalmol.*, 79: 447-52.

Drexler, W., and J. G. Fujimoto. 2008. 'State-of-the-art retinal optical coherence tomography', *Prog Retin Eye Res*, 27: 45-88.

Drexler, W., U. Morgner, RK. Ghanta, FX. Kartner, J. S. Schuman, and J. G. Fujimoto. 2001. 'Ultra high-resolution ophthalmic optical coherence tomography.', *Nature Medicine*, 7: 502-07.

Dubis, A. M., D. M. Costakos, C. D. Subramaniam, P. Godara, W. J. Wirostko, J. Carroll, and J M. Provis. 2012. 'Evaluation of Normal Human Foveal Development using Optical Coherence Tomography and Histologic Examination.', *Arch Ophthalmol*, 130: 1291-300.

Dubis, A. M., J. T. McAllister, and J. Carroll. 2009. 'Reconstructing foveal pit morphology from optical coherence tomography imaging', *Br J Ophthalmol*, 93: 1223-7.

Dubis, A. M., C. D. Subramaniam, P. Godara, J. Carroll, and D. M. Costakos. 2013. 'Subclinical macular findings in infants screened for retinopathy of prematurity with spectral-domain optical coherence tomography', *Ophthalmology*, 120: 1665-71.

Ecsedy, M., A. Szamosi, C. Karko, L. Zubovics, B. Varsanyi, J. Nemeth, and Z. Recsan. 2007. 'A comparison of macular structure imaged by optical coherence tomography in preterm and full-term children', *Invest Ophthalmol Vis Sci*, 48: 5207-11.

Erol, M. K., D.T. Coban, O. Ozdemir, B. Dogan, O. Tunay, and M. Bulut. 2016. 'Choroidal Thickness in Infants with Retinopathy of Prematurity.', *Retina*, 36: 1191-8.

Erol, M. K., O. Ozdemir, D. Turgut Coban, A. B. Bilgin, B. Dogan, E. Sogutlu Sari, and D. Toslak. 2014. 'Macular findings obtained by spectral domain optical coherence tomography in retinopathy of prematurity', *J Ophthalmol*, 2014: 468653.

ETROP, Early Treatment for Retinopathy of Prematurity Cooperative Group. 2003. 'Revised Indications for the Treatment of Retinopathy of Prematurity.', *Arch Ophthalmol*, 121: 1684-96.

Falavarjani, KG., NA. Iafe, FG. Velez, SD. Schwartz, SR. Sadda, D. Sarraf, and I. Tsui. 2017. 'Optical Coherence Tomography Angiography of the Fovea in Children Born Preterm.', *Retina*, 37: 2289-94.

Fielder, A., H. Blencowe, A. O'Connor, and C. Gilbert. 2015. 'Impact of retinopathy of prematurity on ocular structures and visual functions', *Arch Dis Child Fetal Neonatal Ed*, 100: F179-84.

Fieβ, A., J. Janz, A. K. Schuster, R. Kolb-Keerl, M. Knuf, B. Kirchhof, P. S. Muether, and J. Bauer. 2017. 'Macular morphology in former preterm and full-term infants aged 4 to 10 years', *Graefes Arch Clin Exp Ophthalmol*, 255: 1433-42.

Fine, BS., and AJ. Brucker. 1981. 'Macular Edema and Cystoid Macular Edema', *Am J Ophthalmol*, 92: 466-81.

Friling, R., R. Axer-Siegel, Z. Hersocovici, D. Weinberger, L. Sirota, and M. Snir. 2007. 'Retinopathy of prematurity in assisted versus natural conception and singleton versus multiple births', *Ophthalmology*, 114: 321-4.

Fujimoto, J. G., C. Pitris, S.A. Boppart, and M.E. Brezinski. 2000. 'Optical Coherence Tomography: An Emerging Technology for Biomedial Imaging and Optical Biopsy.', *Neoplasia*, 2: 9-25.

Fulton, A. B., R. M. Hansen, A. Moskowitz, and J. D. Akula. 2009. 'The neurovascular retina in retinopathy of prematurity', *Prog Retin Eye Res*, 28: 452-82.

Gallo, J. E., G. Holmstrom, U. Kugelberg, B. Hedquist, and G. Lennerstrand. 1991. 'Regressed retinopathy of prematurity and its sequelae in children aged 5-10years.', *Br. J. Ophthalmol.*, 75: 527-31.

Gardner, TW., DA. Antonetti, AJ. Barber, E. Lieth, JA. Tarbell, and The Penn State Retina Research Group. 1999. 'The molecular structure and function o fthe inner blood-retinal barrier.', *Doc Ophthalmol*, 97: 229-37.

Gergely, K., and A. Gerinec. 2010. 'Retinopathy of prematurity - epidemics, incidence, prevalence, blindness.', *Bratisl Lek Listy.*, 111: 514-17.

Gilbert, C. 2008. 'Retinopathy of prematurity: a global perspective of the epidemics, population of babies at risk and implications for control', *Early Hum Dev*, 84: 77-82.

Gilbert, C., A. Fielder, L. Gordillo, G. Quinn, R. Semiglia, P. Visintin, A. Zin, and N. O. R. O. P. Group International. 2005. 'Characteristics of infants with severe retinopathy of prematurity in countries with low, moderate, and high levels of development: implications for screening programs', *Pediatrics*, 115: e518-25.

Goldman, D. 2014. 'Muller glial cell reprogramming and retina regeneration', *Nat Rev Neurosci*, 15: 431-42.

Gu, S., N. Glaug, A. Cnaan, R. J. Packer, and R. A. Avery. 2014. 'Ganglion cell layer-inner plexiform layer thickness and vision loss in young children with optic pathway gliomas', *Invest Ophthalmol Vis Sci*, 55: 1402-8.

Gunn, D. J., D. W. Cartwright, and G. A. Gole. 2012. 'Incidence of retinopathy of prematurity in extremely premature infants over an 18-year period', *Clin Exp Ophthalmol*, 40: 93-9.

Gursoy, H., M. D. Bilgec, N. Erol, H. Basmak, and E. Colak. 2016. 'The macular findings on spectral-domain optical coherence tomography in premature infants with or without retinopathy of prematurity', *Int Ophthalmol*, 36: 591-600.

Hammer, D. X., N. V. Iftimia, R. D. Ferguson, C. E. Bigelow, T. E. Ustun, A. M. Barnaby, and A. B. Fulton. 2008. 'Foveal fine structure in retinopathy of prematurity: an adaptive optics Fourier domain optical coherence tomography study', *Invest Ophthalmol Vis Sci*, 49: 2061-70.

Hellgren, K. M., K. Tornqvist, P. G. Jakobsson, P. Lundgren, B. Carlsson, K. Kallen, F. Serenius, A. Hellstrom, and G. Holmstrom. 2016. 'Ophthalmologic Outcome of Extremely Preterm Infants at 6.5 Years of Age: Extremely Preterm Infants in Sweden Study (EXPRESS)', *JAMA Ophthalmol*.

Hellstrom, A., A. L. Hard, E. Engstrom, A. Niklasson, E. Andersson, L. Smith, and C. Lofqvist. 2009. 'Early weight gain predicts retinopathy in preterm infants: new, simple, efficient approach to screening', *Pediatrics*, 123: e638-45.

Hendrickson, A., K. Bumsted-O'Brien, R. Natoli, V. Ramamurthy, D. Possin, and J. M. Provis. 2008. 'Rod photoreceptor differentiation in fetal and infant human retina', *Exp. Eye. Res.*, 87: 415-26.
Hendrickson, A., H. Djajadi, A. Erickson, and D. Possin. 2006. 'Development of the human retina in the absence of ganglion cells', *Exp Eye Res*, 83: 920-31.
Hendrickson, A., and D. Drucker. 1992. 'The development of parafoveal and mid-peripheral human retina.', *Behav. Brain Res.*, 49: 21-31.
Hendrickson, A., D. Possin, L. Vajzovic, and C. A. Toth. 2012. 'Histologic development of the human fovea from midgestation to maturity', *Am. J. Ophthalmol.*, 154: 767-78 e2.
Hendrickson, Anita E., and Cristine Yuodelis. 1984. 'The Morphological Development of the Human Fovea', *Ophthalmology*, 91: 603-12.
Hippert, C., A. B. Graca, A. C. Barber, E. L. West, A. J. Smith, R. R. Ali, and R. A. Pearson. 2015. 'Muller glia activation in response to inherited retinal degeneration is highly varied and disease-specific', *PLoS One*, 10: e0120415.
Hogan, MJ., JA. Alvarado, and JE. Weddell. 1971. 'The Retina.' in, *Histology of the Human Eye. An Atlas and Textbook.* (WB Saunders.: Philadelphia).
Holmstrom, G. E., K. Kallen, A. Hellstrom, P. G. Jakobsson, F. Serenius, K. Stjernqvist, and K. Tornqvist. 2014. 'Ophthalmologic outcome at 30 months' corrected age of a prospective Swedish cohort of children born before 27 weeks of gestation: the extremely preterm infants in sweden study', *JAMA Ophthalmol*, 132: 182-9.
Holmstrom, G., and E. Larsson. 2008. 'Long-term follow-up of visual functions in prematurely born children--a prospective population-based study up to 10 years of age', *J AAPOS*, 12: 157-62.
Husain, S. M., A. K. Sinha, C. Bunce, P. Arora, W. Lopez, K. S. Mun, M. A. Reddy, and G. G. Adams. 2013. 'Relationships between maternal ethnicity, gestational age, birth weight, weight gain, and severe retinopathy of prematurity', *J Pediatr*, 163: 67-72.
Huynh, S. C., X. Y. Wang, G. Burlutsky, and P. Mitchell. 2007. 'Symmetry of optical coherence tomography retinal measurements in young children', *Am J Ophthalmol*, 143: 518-20.
ICROP. 2005. 'International Committee for the Classification of Retinopathy of Prematurity. The International Classification of Retinopathy of Prematurity Revisited.', *Arch Ophthalmol*, 123: 991-99.
Ingemarsson, I. 2003. 'Gender aspects of preterm birth', *BJOG: An International Journal of Obstetrics and Gynaecology*, 110: 34-38.
Isenberg, S. J. 1986. 'Macular development in the premature infant.', *Am J Ophthalmol*: 74-80.
Jayadev, C., A. Vinekar, S. Mangalesh, M. K. Kummelil, A. K. Kumar, V. Kemmanu, M. Sivakumar, P. Mahendradas, K. Avadhani, N. Bauer, C. A. Webers, and B. Shetty. 2017. 'Foveal Layer Morphology Detected on Spectral Domain Optical Coherence Tomography and its Correlation with Visual Acuity in Asian Indian Premature Infants in their First Year of Life', *Curr Eye Res*, 42: 789-95.
Johnson, AT., FL. Kretzer, MN. Hittner, PA. Glazebrook, CD. Bridges, and DM. Lam. 1985. 'Development of the subretinal space in the preterm human eye: ultrastructural and immunocytochemical studies.', *J Comp Neurol*, 233: 497-505.

Joshi, M. M., M. T. Trese, and A. Capone, Jr. 2006. 'Optical coherence tomography findings in stage 4A retinopathy of prematurity: a theory for visual variability', *Ophthalmology*, 113: 657-60.

Kafieh, R., H. Rabbani, and S. Kermani. 2013. ' A Review of Algorithms for Segmentation of Optical Coherence Tomography from Retina.', *J Med Signals Sens*, 3: 45-60.

Kenward, MG., and JH. Roger. 1997. 'Smal Sample Inference for Fixed Effects from Restricted Maximum Likelihood.', *Biometrics*, 53: 983-97.

Klufas, M. A., S. N. Patel, M. C. Ryan, M. Patel Gupta, K. E. Jonas, S. Ostmo, M. A. Martinez-Castellanos, A. M. Berrocal, M. F. Chiang, and R. V. Chan. 2015. 'Influence of Fluorescein Angiography on the Diagnosis and Management of Retinopathy of Prematurity', *Ophthalmology*, 122: 1601-8.

Kong, L., M. Fry, M. Al-Samarraie, C. Gilbert, and P. G. Steinkuller. 2012. 'An update on progress and the changing epidemiology of causes of childhood blindness worldwide', *J AAPOS*, 16: 501-7.

Larsson, E. K., A. C. Rydberg, and G. E. Holmstrom. 2005. 'A Population-Based Study on the Visual Outcome in 10-Year-Old Preterm and Full-Term Children.', *Arch. Ophthalmol.*, 123: 825-32.

Lee, A. C., R. S. Maldonado, N. Sarin, R. V. O'Connell, D. K. Wallace, S. F. Freedman, M. Cotten, and C. A. Toth. 2011. 'Macular features from spectral-domain optical coherence tomography as an adjunct to indirect ophthalmoscopy in retinopathy of prematurity', *Retina*, 31: 1470-82.

Lee, H., R. Purohit, A. Patel, E. Papageorgiou, V. Sheth, G. Maconachie, A. Pilat, R. J. McLean, F. A. Proudlock, and I. Gottlob. 2015. 'In Vivo Foveal Development Using Optical Coherence Tomography', *Invest Ophthalmol Vis Sci*, 56: 4537-45.

Lee, H., V. Sheth, M. Bibi, G. Maconachie, A. Patel, R. J. McLean, M. Michaelides, M. G. Thomas, F. A. Proudlock, and I. Gottlob. 2013. 'Potential of handheld optical coherence tomography to determine cause of infantile nystagmus in children by using foveal morphology', *Ophthalmology*, 120: 2714-24.

Lee, K. M., J. H. Kim, and Y. S. Yu. 2010. 'Idiopathic maculopathy in eyes with regressed retinopathy of prematurity', *Graefes Arch Clin Exp Ophthalmol*, 248: 1097-103.

Lee, YM., J. Cleary-Goldman, and ME. D'Alton. 2006. 'The Impact of Multiple Gestations on Late Preterm (Near-Term) Births.', *Clin Perinatol*, 33: 777-92.

Lin, Y. C., Y. J. Lin, and C. H. Lin. 2011. 'Growth and neurodevelopmental outcomes of extremely low birth weight infants: a single center's experience', *Pediatr Neonatol*, 52: 342-8.

Linberg, K. A., and S. K. Fisher. 2009. 'A burst of differentiation in the outer posterior retina of the eleven-week human fetus: An ultrastructural study', *Vis. Neurosci.*, 5: 43-60.

Liu, L., W. Marsh-Tootle, E. N. Harb, W. Hou, Q. Zhang, H. A. Anderson, T. T. Norton, K. K. Weise, J. E. Gwiazda, L. Hyman, and Comet Group. 2016. 'A sloped piecemeal Gaussian model for characterising foveal pit shape', *Ophthalmic Physiol Opt*, 36: 615-31.

Loduca, A. L., C. Zhang, R. Zelkha, and M. Shahidi. 2010. 'Thickness mapping of retinal layers by spectral-domain optical coherence tomography', *Am J Ophthalmol*, 150: 849-55.

Lofqvist, C., E. Anderson, J. Sigurdsson, E. Engstrom, A-L. Hard, A. Niklasson, LEH. Smith, and A. Hellstrom. 2006. 'Longitudinal Postnatal Weight and Insulin-Like Growth Factor I Measurements in the Prediction of Retinopathy of Prematurity. ', *Arch Ophthalmol*, 124: 1711-18.

Madan, A., J. E. Jan, and W. V. Good. 2005. 'Visual development in preterm infants', *Dev Med Child Neurol*, 47: 276-80.

Malan AF, Higgs SC. 1975. 'Gestational age assessment in infants of very low birthweight.', *Arch Dis Child*, 50: 322-24.

Maldonado, R. S., J. A. Izatt, N. Sarin, D. K. Wallace, S. Freedman, C. M. Cotten, and C. A. Toth. 2010. 'Optimizing hand-held spectral domain optical coherence tomography imaging for neonates, infants, and children', *Invest Ophthalmol Vis Sci*, 51: 2678-85.

Maldonado, R. S., R. O'Connell, S. B. Ascher, N. Sarin, S. F. Freedman, D. K. Wallace, S. J. Chiu, S. Farsiu, M. Cotten, and C. A. Toth. 2012. 'Spectral-domain optical coherence tomographic assessment of severity of cystoid macular edema in retinopathy of prematurity', *Arch Ophthalmol*, 130: 569-78.

Maldonado, R. S., R. V. O'Connell, N. Sarin, S. F. Freedman, D. K. Wallace, C. M. Cotten, K. P. Winter, S. Stinnett, S. J. Chiu, J. A. Izatt, S. Farsiu, and C. A. Toth. 2011. 'Dynamics of human foveal development after premature birth', *Ophthalmology*, 118: 2315-25.

Maldonado, R. S., E. Yuan, D. Tran-Viet, A. L. Rothman, A. Y. Tong, D. K. Wallace, S. F. Freedman, and C. A. Toth. 2014. 'Three-dimensional assessment of vascular and perivascular characteristics in subjects with retinopathy of prematurity', *Ophthalmology*, 121: 1289-96.

Maldonado, R.S., P. Mettu, M. El-Dairi, and M. T. Bhatti. 2015. 'The application of optical coherence tomography in neurologic diseases.', *Neurol Clin Pract.*, 5: 460-69.

Mann, C. J. 2003. 'Observational research methods. Research design II: cohort, cross sectional, and case-control studies', *Emergency Medicine Journal*, 20: 54-60.

Mann, I. 1950. *Development of the Human Eye.* (Grune & Stratton Inc: New York.).

Marmor, M. F., S. S. Choi, R. J. Zawadzki, and J. S. Werner. 2008. 'Visual insignificance of the foveal pit: reassessment of foveal hypoplasia as fovea plana', *Arch Ophthalmol*, 126: 907-13.

Mathes, T., and D. Pieper. 2017. 'Clarifying the distinction between case series and cohort studies in systematic reviews of comparative studies: potential impact on body of evidence and workload', *BMC Med Res Methodol*, 17: 107.

McAllister, J. T., A. M. Dubis, D. M. Tait, S. Ostler, J. Rha, K. E. Stepien, C. G. Summers, and J. Carroll. 2010. 'Arrested development: high-resolution imaging of foveal morphology in albinism', *Vision Res*, 50: 810-7.

Mezu-Ndubuisi, O. J., T. Adams, L. K. Taylor, A. Nwaba, and J. Eickhoff. 2018. 'Simultaneous assessment of aberrant retinal vascularization, thickness, and function in an in vivo mouse oxygen-induced retinopathy model', *Eye (Lond)*.

Mintz-Hittner, Helen A., Donna M. Knight-Nanan, Dale R. Satriano, and Frank L. Kretzer. 1999. 'A small foveal avascular zone may be an historic mark of prematurity', *Ophthalmology*, 106: 1409-13.

Molnar, AEC., RM. Rosen, M. Nilsson, EKB. Larsson, GE. Holmstrom, and KM. Hellgren. 2017. 'Central Macular Thickness in 6.5-year-old Children Born Extremely

Preterm is strongly associated with Gestational Age even when adjusted for risk factors.', *Retina*, 37: 2281-88.

Moore, B. A., I. Yoo, L. P. Tyrrell, B. Benes, and E. Fernandez-Juricic. 2016. 'FOVEA: a new program to standardize the measurement of foveal pit morphology', *PeerJ*, 4: e1785.

Moren, T. A., R. V. O'Connell, S. J. Chui, S. Farsui, M. T. Cabrera, R. S. Maldonado, D. Tran-Viet, S. F. Freedman, D. K. Wallace, and C. A. Toth. 2013. 'Choroid Development and Feasibility of Choroidal Imaging in the Preterm and Term Infants Utilizing SD-OCT.', *Invest. Ophthalmol. Vis. Sci.*, 54: 4140-47.

Muni, RH., RP. Kohly, AC. Charonis, and TC. Lee. 2010. 'Retinoschisis detected with handheld spectral-comain optical coherence tomography in neonates with advanced retinopathy of prematurity.', *Arch Ophthalmol*, 128: 57-62.

Mwanza, J. C., M. K. Durbin, D. L. Budenz, C. A. Girkin, C. K. Leung, J. M. Liebmann, J. H. Peace, J. S. Werner, G. Wollstein, and O. C. T. Normative Database Study Group Cirrus. 2011. 'Profile and predictors of normal ganglion cell-inner plexiform layer thickness measured with frequency-domain optical coherence tomography', *Invest Ophthalmol Vis Sci*, 52: 7872-9.

Nag, T. C., and S. Wadhwa. 2006. 'Morphological and Neurochemical Development of the Human Neural Retina', *Neuroembryology and Aging*, 4: 19-30.

Narayanan, K., and S. Wadhwa. 1998. 'Photoreceptor Morphogenesis in the Human Retina: A Scanning Electron Microscopic Study.', *Anat. Rec.*, 252: 133-39.

Nesmith, B., A. Gupta, T. Strange, Y. Schaal, and S. Schaal. 2014. 'Mathematical analysis of the normal anatomy of the aging fovea', *Invest Ophthalmol Vis Sci*, 55: 5962-6.

Nesper, P. L., and A. A. Fawzi. 2018. 'Human Parafoveal Capillary Vascular Anatomy and Connectivity Revealed by Optical Coherence Tomography Angiography', *Invest Ophthalmol Vis Sci*, 59: 3858-67.

Neveu, M. M., E. von dem Hagen, A. B. Morland, and G. Jeffery. 2008. 'The fovea regulates symmetrical development of the visual cortex', *J Comp Neurol*, 506: 791-800.

Ng, EY., B. Lannigan, and M. O'Keefe. 2006. 'Fundus Fluorescein Angiography in the Screening for and Management of Retinopathy of Prematurity.', *J Pediatr Ophthalmol Strabismus*, 43: 85-90.

Noval, S., S. F. Freedman, S. Asrani, and M. A. El-Dairi. 2014. 'Incidence of fovea plana in normal children', *J AAPOS*, 18: 471-5.

O'Brien, K. M., D. Schulte, and A E. Hendrickson. 2003. 'Expression of photoreceptor-associated molecules during human fetal eye development', *Mol Vis.*, 9: 401-09.

O'Connor, A., T. Stephenson, A. Johnson, M. J. Tobin, M. J. Moseley, S. Ratib, Y. Ng, and A. R. Fielder. 2002. 'Long-term Ophthalmic Outcome of Low Birth Weight Children with and without Retinopathy of Prematurity.', *Pediatrics*, 109: 12-18.

Okabe, K., S. Kobayashi, T. Yamada, T. Kurihara, I. Tai-Nagara, T. Miyamoto, Y. S. Mukouyama, T. N. Sato, T. Suda, M. Ema, and Y. Kubota. 2014. 'Neurons limit angiogenesis by titrating VEGF in retina', *Cell*, 159: 584-96.

Omri, S., B. Omri, M. Savoldelli, L. Jonet, B. Thillaye-Goldenberg, G. Thuret, P. Gain, JC. Jeanny, P. Cristanti, and F. Behar-Cohen. 2010. 'The outer limiting membrane (OLM) revisited: clinical implications', *Clin Ophthalmol*, 4: 183-95.

Osterberg, G. 1935. *Topography of the Layer of Rods and Cones in the Human Retina.* (WA Spuhr: Copenhagen).

Papiernik, E., J. Zeitlin, D. Delmas, B. Blondel, W. Kunzel, M. Cuttini, T. Weber, S. Petrou, L. Gortner, L. Kollee, E. S. Draper, and Mosaic Group. 2010. 'Differences in outcome between twins and singletons born very preterm: results from a population-based European cohort', *Hum Reprod*, 25: 1035-43.

Park, K. A., and S. Y. Oh. 2012. 'Analysis of spectral-domain optical coherence tomography in preterm children: retinal layer thickness and choroidal thickness profiles', *Invest Ophthalmol Vis Sci*, 53: 7201-7.

———. 2015. 'Retinal nerve fiber layer thickness in prematurity is correlated with stage of retinopathy of prematurity', *Eye (Lond)*, 29: 1594-602.

Pascolini, D., and S. P. Mariotti. 2012. 'Global estimates of visual impairment: 2010', *Br J Ophthalmol*, 96: 614-8.

Patel, A., R. Purohit, H. Lee, V. Sheth, G. Maconachie, E. Papageorgiou, R. J. McLean, I. Gottlob, and F. A. Proudlock. 2016. 'Optic Nerve Head Development in Healthy Infants and Children Using Handheld Spectral-Domain Optical Coherence Tomography', *Ophthalmology*, 123: 2147-57.

Patel, C. K. 2006. 'Optical coherence tomography in the management of acute retinopathy of prematurity', *Am J Ophthalmol*, 141: 582-4.

Patel, C. K., T. H. Fung, M. M. Muqit, D. J. Mordant, J. Brett, L. Smith, and E. Adams. 2013. 'Non-contact ultra-widefield imaging of retinopathy of prematurity using the Optos dual wavelength scanning laser ophthalmoscope', *Eye (Lond)*, 27: 589-96.

Pierce, EA., RL. Avery, ED. Foley, LP. Aiello, and LEH. Smith. 1995. 'Vascular endothelial growth factor/vascular permeability factor expression in a mouse model of retinal neovascularization.', *Proc Natl Acad Sci U S A*, 92: 905-09.

Pierrat, V., L. Marchand-Martin, C. Arnaud, M. Kaminski, M. Resche-Rigon, C. Lebeaux, F. Bodeau-Livinec, A. S. Morgan, F. Goffinet, S. Marret, P. Y. Ancel, and Epipage-writing group. 2017. 'Neurodevelopmental outcome at 2 years for preterm children born at 22 to 34 weeks' gestation in France in 2011: EPIPAGE-2 cohort study', *BMJ*, 358: j3448.

Pilat, A., D. Sibley, R. J. McLean, F. A. Proudlock, and I. Gottlob. 2015. 'High-Resolution Imaging of the Optic Nerve and Retina in Optic Nerve Hypoplasia', *Ophthalmology*, 122: 1330-9.

Polyak, SL. 1941. 'Chapter XV Regional Subdivision of the Retina; Yellow Spot and the Central Fovea.' in, *The Retina* (University of Chicago Press: Chicago).

Pons, M. E., and E. Garcia-Valenzuela. 2005. 'Redefining the limit of the outer retina in optical coherence tomography scans', *Ophthalmology*, 112: 1079-85.

Provis, J M., CM. Diaz, and B Dreher. 1998. 'Ontogeny of the Primate Fovea: A central issue in retinal development.', *Prog in Neurobiol*, 54: 549-81.

Provis, J M., and A E. Hendrickson. 2008. 'The Foveal Avascular Region of Developing Human Retina.', *Arch Ophthalmol*, 126: 507-11.

Provis, J., Penfold P. L., E. E. Cornish, Sandercoe T. M., and Madigan M. C. 2005. 'Anatomy and development of the macula: specialisation and vulnerability to macular degeneration.', *Clin. Exp. Optom.*, 88: 269-81.

Provis, J. M. 2001. 'Development of the Primate Retinal Vasculature.', *Prog. Ret. Eye Res.*, 20: 799-821.

Provis, J. M., A. M. Dubis, T. Maddess, and J. Carroll. 2013. 'Adaptation of the central retina for high acuity vision: cones, the fovea and the avascular zone', *Prog Retin Eye Res*, 35: 63-81.

Pueyo, V., I. Gonzalez, I. Altemir, T. Perez, G. Gomez, E. Prieto, and D. Oros. 2015. 'Microstructural changes in the retina related to prematurity', *Am J Ophthalmol*, 159: 797-802.

Quinn, G. E. 2016. 'Retinopathy of prematurity blindness worldwide: phenotypes in the third epidemic', *Eye Brain*, 8: 31-36.

Quinn, G. E., C. Barr, D. Bremer, R. Fellows, A. Gong, R. Hoffman, M. X. Repka, J. Shepard, R. M. Siatkowski, K. Wade, and G. S. Ying. 2016. 'Changes in Course of Retinopathy of Prematurity from 1986 to 2013: Comparison of Three Studies in the United States', *Ophthalmology*, 123: 1595-600.

Raju, T. N. 2013. 'Moderately preterm, late preterm and early term infants: research needs', *Clin Perinatol*, 40: 791-7.

RCOG, Royal College of Obstetrics & Gynaecologists. 2014. 'Perinatal Management of Pregnant Women at the Threshold of Infant Viability– the Obstetric Perspective.', Accessed 12.10.18. https://www.rcog.org.uk/en/guidelines-research-services/guidelines/sip41/.

RCOphth, Royal College of Ophthalmologists., Royal College of Paediatrics and Child Health. RCPCH, and British Association of Perinatal Medicine & Bliss BAPM. 2008. "Guideline for the Screening and Treatment of Retinopathy of Prematurity " In. United Kingdom.

Recchia, F. M., and C. C. Recchia. 2007. 'Foveal Dysplasia Evident by Optical Coherence Tomography in Patients with a History of Retinopathy of Prematurity.', *Retina*, 27: 1221-26.

Recchia, FM., CA. Carvalho-Recchia, and M. Trese. 2002. 'Optical Coherence Tomography in the Diagnosis of Foveal Hypoplasia.', *Arch Ophthalmol*, 120: 1587-88.

Robb, RM. 1985. 'Regional changes in retinal pigment epithelial cell density during ocular development.', *Invest Ophthalmol Vis Sci*, 26: 614-20.

Robinson, R., and M. O'Keefe. 1993. 'Follow-up study on premature infants with and without retinopathy of prematurity.', *Br J Ophthalmol*, 77: 91-94.

Rosen, R., J. Sjostrand, M. Nilsson, and K. Hellgren. 2015. 'A methodological approach for evaluation of foveal immaturity after extremely preterm birth.', *Ophthalmic Physiol Opt*, 35: 433-51.

Rothman, A. L., M. B. Sevilla, S. F. Freedman, A. Y. Tong, V. Tai, D. Tran-Viet, S. Farsiu, C. A. Toth, and M. A. El-Dairi. 2015. 'Assessment of retinal nerve fiber layer thickness in healthy, full-term neonates', *Am J Ophthalmol*, 159: 803-11.

Rothman, A. L., M. B. Sevilla, S. Mangalesh, K. E. Gustafson, L. Edwards, C. M. Cotten, J. S. Shimony, C. E. Pizoli, M. A. El-Dairi, S. F. Freedman, and C. A. Toth. 2015. 'Thinner Retinal Nerve Fiber Layer in Very Preterm Versus Term Infants and Relationship to Brain Anatomy and Neurodevelopment', *Am J Ophthalmol*, 160: 1296-308 e2.

Rothman, A. L., D. Tran-Viet, K. E. Gustafson, R. F. Goldstein, M. G. Maguire, V. Tai, N. Sarin, A. Y. Tong, J. Huang, L. Kupper, C. M. Cotten, S. F. Freedman, and C. A. Toth. 2015. 'Poorer neurodevelopmental outcomes associated with cystoid

macular edema identified in preterm infants in the intensive care nursery', *Ophthalmology*, 122: 610-9.
Ruberto, Giulio., R. Angeli, C. Tinelli, PE. Bianchi, and G. Milano. 2014. 'Morphologic and Functional Analysis of the Optic Nerve in Premature and Term Children With OCT, HRT, and pVEP: A 10-Year Resurvey.', *Invest Ophthalmol Vis Sci*, 55: 2367-75.
Scheibe, P., A. Lazareva, U. D. Braumann, A. Reichenbach, P. Wiedemann, M. Francke, and F. G. Rauscher. 2014. 'Parametric model for the 3D reconstruction of individual fovea shape from OCT data', *Exp Eye Res*, 119: 19-26.
Scheibe, P., M. T. Zocher, M. Francke, and F. G. Rauscher. 2016. 'Analysis of foveal characteristics and their asymmetries in the normal population.', *Exp Eye Res*, 148: 1-11.
Schmitt, JM. 1999. 'Optical Coherence Tomography (OCT): A Review.', *IEEE Journal of Selected Topics in Quantum Electronics*, 5: 1205-15.
Sebris, S. L., Dobson V., and Hartmann E. E. 1984. 'Assessment and prediction of visual acuity in 3- to 4-year-old children born prior to term.', *Hum Neurobiol*, 3: 87-92.
Shin, J. Y., Y. K. Chu, Y. T. Hong, O. W. Kwon, and S. H. Byeon. 2015. 'Determination of macular hole size in relation to individual variabilities of fovea morphology', *Eye (Lond)*, 29: 1051-9.
Siatkowski, R. M., W. V. Good, C. G. Summers, G. E. Quinn, and B. Tung. 2013. 'Clinical characteristics of children with severe visual impairment but favorable retinal structural outcomes from the Early Treatment for Retinopathy of Prematurity (ETROP) study', *J AAPOS*, 17: 129-34.
Sjostrand, J., R. Rosen, M. Nilsson, and Z. Popovic. 2017. 'Arrested Foveal Development in Preterm Eyes: Thickening of the Outer Nuclear Layer and Structural Redistribution Within the Fovea', *Invest Ophthalmol Vis Sci*, 58: 4948-58.
Slidsborg, C., J. L. Forman, A. R. Fielder, S. Crafoord, K. Baggesen, R. Bangsgaard, H. C. Fledelius, G. Greisen, and M. la Cour. 2012. 'Experts do not agree when to treat retinopathy of prematurity based on plus disease', *Br J Ophthalmol*, 96: 549-53.
Smith, L. K., E. S. Draper, B. N. Manktelow, J. S. Dorling, and D. J. Field. 2007. 'Socioeconomic inequalities in very preterm birth rates', *Arch Dis Child Fetal Neonatal Ed*, 92: F11-4.
Spaide, R. F., and C. A. Curcio. 2011. 'Anatomical correlates to the bands seen in the outer retina by optical coherence tomography. Literature Review and Model.', *Retina.*, 31: 1609-19.
Spaide, R. F., H. Koizumi, and M. C. Pozzoni. 2008. 'Enhanced depth imaging spectral-domain optical coherence tomography', *Am J Ophthalmol*, 146: 496-500.
Spong, C. Y. 2013. 'Defining "term" pregnancy: recommendations from the Defining "Term" Pregnancy Workgroup', *JAMA*, 309: 2445-6.
Srinivasan, V. J., B. K. Monson, M. Wojtkowski, R. A. Bilonick, I. Gorczynska, R. Chen, J. S. Duker, J. S. Schuman, and J. G. Fujimoto. 2008. 'Characterization of outer retinal morphology with high-speed, ultrahigh-resolution optical coherence tomography', *Invest Ophthalmol Vis Sci*, 49: 1571-9.
Statistics, Office for National. 2012. "Census result shows increase in population of the East Midlands." In.
Staurenghi, G., S. Sadda, U. Chakravarthy, R. F. Spaide, and Panel International Nomenclature for Optical Coherence Tomography. 2014. 'Proposed lexicon for

anatomic landmarks in normal posterior segment spectral-domain optical coherence tomography: the IN*OCT consensus', *Ophthalmology*, 121: 1572-8.
Tariq, Y. M., G. Burlutsky, and P. Mitchell. 2012. 'Macular parameters and prematurity: A spectral domain coherence tomography study', *J AAPOS*, 16: 382-5.
Tariq, Y. M., A. Pai, H. Li, S. Afsari, G. A. Gole, G. Burlutsky, and P. Mitchell. 2011. 'Association of birth parameters with OCT measured macular and retinal nerve fiber layer thickness', *Invest Ophthalmol Vis Sci*, 52: 1709-15.
Thomas, M. G., A. Kumar, S. Mohammad, F. A. Proudlock, E. C. Engle, C. Andrews, W. M. Chan, S. Thomas, and I. Gottlob. 2011. 'Structural grading of foveal hypoplasia using spectral-domain optical coherence tomography a predictor of visual acuity?', *Ophthalmology*, 118: 1653-60.
Tick, S., F. Rossant, I. Ghorbel, A. Gaudric, J-A. Sahel, P. Chaumet-Riffaud, and M. Paques. 2011. 'Foveal Shape and Structure in a Normal Population.', *Invest. Ophthalmol. Vis. Sci.*, 52: 5105-10.
Tong, A. Y., M. El-Dairi, R. S. Maldonado, A. L. Rothman, E. L. Yuan, S. S. Stinnett, L. Kupper, C. M. Cotten, K. E. Gustafson, R. F. Goldstein, S. F. Freedman, and C. A. Toth. 2014. 'Evaluation of optic nerve development in preterm and term infants using handheld spectral-domain optical coherence tomography', *Ophthalmology*, 121: 1818-26.
Toth, C A., DG. Narayan, SA. Boppart, Michael R. Hee, J. G. Fujimoto, R. Birngruber, CP. Cain, CD. DiCarlo, and P. Roach. 1997. 'A comparison of retinal morphology viewed by optical coherence tomography and by light microscopy.', *Arch Ophthalmol*, 115: 1425-28.
Trese, MT., and RY. Foos. 1980. 'Infantile cystoid maculopathy.', *Br J Ophthalmol*, 64: 2016-210.
Trichonas, G., and P. K. Kaiser. 2014. 'Optical coherence tomography imaging of macular oedema', *Br J Ophthalmol*, 98 Suppl 2: ii24-9.
Tso, MOM. 1982. 'Pathology of Cystoid Macular Edema', *Ophthalmol.*, 89: 902-15.
Vajzovic, L., A E. Hendrickson, R V. O'Connell, L A. Clark, D. Tran-Viet, D. Possin, S J. Chiu, S. Farsiu, and C A. Toth. 2012. 'Maturation of the human fovea: correlation of spectral-domain optical coherence tomography findings with histology', *Am. J. Ophthalmol.*, 154: 779-89 e2.
Vajzovic, L., A. L. Rothman, D. Tran-Viet, M. T. Cabrera, S. F. Freedman, and C. A. Toth. 2015. 'Delay in retinal photoreceptor development in very preterm compared to term infants', *Invest Ophthalmol Vis Sci*, 56: 908-13.
Villegas, V. M., H. Capo, K. Cavuoto, C. A. McKeown, and A. M. Berrocal. 2014. 'Foveal structure-function correlation in children with history of retinopathy of prematurity', *Am J Ophthalmol*, 158: 508-12 e2.
Vinekar, A., K. Avadhani, M. Sivakumar, P. Mahendradas, M. Kurian, S. Braganza, R. Shetty, and B. K. Shetty. 2011. 'Understanding clinically undetected macular changes in early retinopathy of prematurity on spectral domain optical coherence tomography', *Invest Ophthalmol Vis Sci*, 52: 5183-8.
Vinekar, A., S. Mangalesh, C. Jayadev, N. Bauer, S. Munusamy, V. Kemmanu, M. Kurian, P. Mahendradas, K. Avadhani, and B. Shetty. 2015. 'Macular edema in Asian Indian premature infants with retinopathy of prematurity: Impact on visual acuity and refractive status after 1-year', *Indian J Ophthalmol*, 63: 432-7.

Vogel, R. N., M. Strampe, O. E. Fagbemi, A. Visotcky, S. Tarima, J. Carroll, and D. M. Costakos. 2018. 'Foveal Development in Infants Treated with Bevacizumab or Laser Photocoagulation for Retinopathy of Prematurity', *Ophthalmology*, 125: 444-52.

Vohr, B. R., L. L. Wright, A. M. Dusick, L. Mele, J. Verter, J. J. Steichen, N. P. Simon, D. C. Wilson, S. Broyles, C. R. Bauer, V. Delaney-Black, K. A. Yolton, B. E. Fleisher, L. A. Papile, and M. D. Kaplan. 2000. 'Neurodevelopmental and Functional Outcomes of Extremely Low Birth Weight Infants in the National Institute of Child Health and Human Development Neonatal Research Network, 1993-1994', *Pediatrics*, 105: 1216-26.

Wagner-Schuman, M., A. M. Dubis, R. N. Nordgren, Y. Lei, D. Odell, H. Chiao, E. Weh, W. Fischer, Y. Sulai, A. Dubra, and J. Carroll. 2011. 'Race- and sex-related differences in retinal thickness and foveal pit morphology', *Invest Ophthalmol Vis Sci*, 52: 625-34.

Wallace, D. K., G. E. Quinn, S. F. Freedman, and M. F. Chiang. 2008. 'Agreement among pediatric ophthalmologists in diagnosing plus and pre-plus disease in retinopathy of prematurity', *J AAPOS*, 12: 352-6.

Walls, G. L. 1937. 'Significance of the Foveal Depression.', *Arch Ophthalmol.*, 18: 912-19.

Walsh, M. C., E. F. Bell, S. Kandefer, S. Saha, W. A. Carlo, T. D'Angio C, A. R. Laptook, P. J. Sanchez, B. J. Stoll, S. Shankaran, K. P. Van Meurs, N. Cook, R. D. Higgins, A. Das, N. S. Newman, K. Schibler, B. Schmidt, C. M. Cotten, B. B. Poindexter, K. L. Watterberg, and W. E. Truog. 2017. 'Neonatal outcomes of moderately preterm infants compared to extremely preterm infants', *Pediatr Res*, 82: 297-304.

Wang, J. J., M. Zhu, and Y. Z. Le. 2015. 'Functions of Muller cell-derived vascular endothelial growth factor in diabetic retinopathy', *World J Diabetes*, 6: 726-33.

Wang, J., R. Spencer, J. N. Leffler, and E. E. Birch. 2012a. 'Characteristics of peripapillary retinal nerve fiber layer in preterm children', *Am J Ophthalmol*, 153: 850-55 e1.

Wang, J., S. Spencer, J. N. Leffler, and E. E. Birch. 2012b. 'Critical period for foveal fine structure in children with regressed retinopathy of prematurity.', *Retina*, 32: 330-39.

Weale, R. A. 1966. 'Why does the human Retina possess a Fovea?', *Nature*, 212: 255-56.

Wilk, M. A., J. T. McAllister, R. F. Cooper, A. M. Dubis, T. N. Patitucci, P. Summerfelt, J. L. Anderson, K. E. Stepien, D. M. Costakos, T. B. Connor, Jr., W. J. Wirostko, P. W. Chiang, A. Dubra, C. A. Curcio, M. H. Brilliant, C. G. Summers, and J. Carroll. 2014. 'Relationship between foveal cone specialization and pit morphology in albinism', *Invest Ophthalmol Vis Sci*, 55: 4186-98.

World Health Organization. 2018. 'Preterm birth', Accessed February. www.who.int/mediacentre/factsheets/fs363/en. .

World Health Organization, Expert Committee. 1970. "The Prevention of Perinatal Mortality and Morbidity." In *Technical Report Series*, 22-23. World Health Organization.

Wu, W. C., R. I. Lin, C. P. Shih, N. K. Wang, Y. P. Chen, A. N. Chao, K. J. Chen, T. L. Chen, Y. S. Hwang, C. C. Lai, C. Y. Huang, and S. Tsai. 2012. 'Visual acuity, optical

components, and macular abnormalities in patients with a history of retinopathy of prematurity', *Ophthalmology*, 119: 1907-16.
Xia, T., and L. J. Rizzolo. 2017. 'Effects of diabetic retinopathy on the barrier functions of the retinal pigment epithelium', *Vision Res*, 139: 72-81.
Xiao, M., and A. Hendrickson. 2000. 'Spatial and Temporal Expression of Short, Long/Medium, or Both Opsins in Human Fetal Cones.', *J. Comp. Neurol.*, 425: 545-59.
Xin, X., M. Rodrigues, M. Umapathi, F. Kashiwabuchi, T. Ma, S. Babapoor-Farrokhran, S. Wang, J. Hu, I. Bhutto, D. S. Welsbie, E. J. Duh, J. T. Handa, C. G. Eberhart, G. Lutty, G. L. Semenza, S. Montaner, and A. Sodhi. 2013. 'Hypoxic retinal Muller cells promote vascular permeability by HIF-1-dependent up-regulation of angiopoietin-like 4', *Proc Natl Acad Sci U S A*, 110: E3425-34.
Yamada, E., and T. Ishikawa. 1965. 'Some observations on the submicroscopic morphogenesis of the human retina.' in JW. Rohen (ed.), *The Structure of the Eye II. Symposium* (FK Schattauer-Verlag Stuttgart.).
Yanni, S. E., J. Wang, M. Chan, J. Carroll, S. Farsiu, J. N. Leffler, R. Spencer, and E. E. Birch. 2012. 'Foveal avascular zone and foveal pit formation after preterm birth', *Br J Ophthalmol*, 96: 961-6.
Yanni, S. E., J. Wang, C. S. Cheng, K. I. Locke, Y. Wen, D. G. Birch, and E. E. Birch. 2013. 'Normative reference ranges for the retinal nerve fiber layer, macula, and retinal layer thicknesses in children', *Am J Ophthalmol*, 155: 354-60 e1.
Yanoff, M., BS. Fine, AJ. Brucker, and RC. Eagle. 1984. 'Pathology of Human Cystoid Macular Edema', *Surv Ophthalmol*, 28(Suppl): 505-11.
Ying, G. S., D. VanderVeen, E. Daniel, G. E. Quinn, A. Baumritter, and Group Telemedicine Approaches to Evaluating Acute-Phase Retinopathy of Prematurity Cooperative. 2016. 'Risk Score for Predicting Treatment-Requiring Retinopathy of Prematurity (ROP) in the Telemedicine Approaches to Evaluating Acute-Phase ROP Study', *Ophthalmology*, 123: 2176-82.
Yokoe, T., I. Fukada, K. Kobayashi, T. Shibayama, Y. Miyagi, A. Yoshida, T. Iwase, S. Ohno, and Y. Ito. 2017. 'Cystoid Macular Edema during Treatment with Paclitaxel and Bevacizumab in a Patient with Metastatic Breast Cancer: A Case Report and Literature Review', *Case Rep Oncol*, 10: 605-12.
Yoshikawa, Y., T. Yamada, I. Tai-Nagara, K. Okabe, Y. Kitagawa, M. Ema, and Y. Kubota. 2016. 'Developmental regression of hyaloid vasculature is triggered by neurons', *J Exp Med*, 213: 1175-83.
Yuodelis, C., and A. Hendrickson. 1986. 'A Qualitative and Quantitative Analysis of the Human Fovea during Development.', *Vision Res*, 26: 847-55.
Zepeda-Romero, L. C., A. A. Oregon-Miranda, D. S. Lizarraga-Barron, O. Gutierrez-Camarena, A. Meza-Anguiano, and J. A. Gutierrez-Padilla. 2013. 'Early retinopathy of prematurity findings identified with fluorescein angiography', *Graefes Arch Clin Exp Ophthalmol*, 251: 2093-7.